IDENTIFICATION OF *CIS* AND *TRANS* FACTORS THAT REGULATE GENETIC STABILITY IN *SACCHAROMYCES CEREVISIAE*

James Dominic Cauwood

A thesis submitted in fulfillment of the

requirements for the degree of

Doctor of Philosophy

University College London

May 2009

Declaration

I, James Dominic Cauwood, confirm that the work presented in this thesis is my own. Where information has been derived from other sources, I confirm that this has been indicated in the thesis.

James Cauwood
May 2009

Abstract

The genome of an organism is not uniformly mutagenic. The overall aim of this project was to identify *cis* and *trans* factors that may contribute to such differential mutagenic activities within the genome using *Saccharomyces cerevisiae*.

A well-characterised recombination reporter construct, *hisG-URA3-hisG*, was separately introduced into five different locations of chromosome III. Each locus had differing features with respect to their replication dynamics: three replication termination sites, two of which coincided with "*R*eplication *S*low *Z*ones" (RSZ; Cha and Kleckner, 2002), one replication origin and a region of no discernable feature. Fluctuation analysis was used to assess the rate of *URA3* inactivation at each locus. First, the effects of temperature, a replication inhibitor hydroxyurea, and ploidy were assessed. Significant differences in mutation rates existed in diploid strains heterozygous for the construct in these conditions, but not in respective haploids.

The effects of inactivating various genes known to be involved in genome stability were also examined. Elimination of an essential signal transduction protein, Mec1p, or a DNA helicase required for efficient replication, Rrm3p, led to an increase in mutation rates only in diploid strains. No statistically significant effect was seen when a *top2* temperature-sensitive allele was used in either haploids or diploids. In general, no *cis* effect was observed in any of these mutant backgrounds.

The nature of genetic alterations associated with *URA3* inactivation was also determined by Southern analysis for the five loci. The analysis revealed that the nature of genetic alteration is regulated in a *cis* manner, as *URA3* inactivation was either exclusively *via* recombination or by small changes depending on the location of the reporter construct.

These findings reveal some unexpected ways in which *cis* and *trans* factors may regulate mutagenic events in budding yeast. These will be discussed in context of eukaryotic genome instability in general.

Contents

List of figures

List of tables

Abbreviations

χ^2	Chi square
5-FOA	5'-fluoroorotic acid monohydrate
Amp	ampicillin
APH	aphidicolin
ARS	Autonomously Replicating Sequence
ATM	Ataxia-Telangiectasia Mutated
ATR	Ataxia-Telangiectasia and Rad3 related
Cal	calyculin A
CFS	common fragile site
Chr	chromosome
CIP	calf intestinal phosphatase
CL	confidence limit
Class I	(mutation) inactivation (of *URA3*) *via* point mutations, or small insertions or deletions
Class II	(mutation) inactivation (of *URA3*) *via* large deletions of ChrIII, or loss of the entire chromosome
Class III	(mutation) inactivation (of *URA3*) *via* a "pop-out" event
DNA	deoxyribonucleic acid
dNTP	deoxyribonucleotide
DSB	double strand break
E.	*Escherichia*
FA	Fanconi anaemia
FS	fragile site
GCR	gross chromosomal rearrangement
gDNA	genomic DNA
h	hour
hisG	subunit of bacterial ATP phosphoribosyltransferase
HRR	homologous recombination repair
Hsp	heat-shock protein
HU	hydroxyurea

JDCY	James D Cauwood Yeast (strain designation number)
k	kilo (10^3)
kb	kilobase
KOAc	potassium acetate
LB	Luria-Bertani (bacterial media)
LiAc	lithium acetate
LTR	long terminal repeat
m	milli (10^{-3})
μ	micro (10^{-6})
M	mega (10^6)
min	minute(s)
n	nano (10^{-9})
NHEJ	non-homologous end joining
OD	optical density
P	probability
PCR	polymerase chain reaction
PFGE	pulsed-field gel electrophoresis
PIKK	phosphatidyl inositol 3-kinase-like serine/threonine protein kinase
rDNA	ribosomal DNA
RE	restriction enzyme
RFS	rare fragile site
RNase	ribonuclease A
RNR	ribonucleotide reductase
RSZ	replication slow zone
R-T	room temperature
s	second(s)
S.	*Saccharomyces*
SCE	sister chromatid exchange
SMC	structural maintenance of chromosome
SPM	sporulation media
ss	single stranded
TE	Tris-EDTA
ts	temperature-sensitive (gene)
U	unit

UV	ultraviolet
V	volt(s)
v/v	volume by volume
w/v	weight by volume
WT	wild type
YPD	yeast extract, peptone, dextrose media (non-selective media)
YPG	yeast extract, peptone, glycerol (non-fermentable carbon source media)

Chapter 1.

Introduction

1.1 Preface

The genome of an organism is not uniformly susceptible to genetic alterations. Hotspots for different types of mutations exist, including single base pair changes, small insertions and/or deletions, and gross chromosomal aberrations resulting from recombination events. The reasons for such differential mutagenic potentials remain elusive, yet it is well documented that genomic instability can be potentially deleterious to an organism, resulting in cell death or cancer.

The overall aim of this project was to examine potential DNA sequences and/or key proteins involved in DNA metabolism that modulate such mutagenic activities. To this end, mutagenic events associated with five different loci along ChrIII of the budding yeast *Saccharomyces cerevisiae* were examined in various genetic backgrounds. The five loci included an active replication origin, three replication termination sites (two of which occur within yeast fragile sites), and a locus of no discernible feature. Effects of inactivating Mec1p, a homologue of ATR involved in genome stability, topoisomerase II, and Rrm3p (a replicative helicase) were assessed, as well as those of temperature and ploidy. Presented below is a brief summary of mammalian fragile sites and conditions that regulate their expression, followed by a more detailed review on "Replication Slow Zones", the budding yeast fragile site, and various conditions implicated in its stability.

1.2 Mammalian Fragile Sites

Mammalian fragile sites (FSs) are specific loci that form gaps or breaks on metaphase chromosomes following partial inhibition of DNA synthesis. Human FSs are classed into two main categories: "rare" and "common".

Rare FSs (RFS) are seen in less than 5% of individuals and are inherited in a Mendelian manner (Kremer *et al*., 1991; Sutherland *et al*., 1998). One of the most well documented RFSs is FRAXA, which is responsible for fragile X syndrome, the most common inherited form of mental retardation (Jacobs *et al*., 1980; Turner *et al*., 1978). Many reports have contributed to the finding that expansion of a specific trinucleotide repeat within the FMR1 gene is a mutational mechanism in fragile X syndrome (Fu *et al*., 1991; Oberle *et al*., 1991; Verkerk *et al*., 1991). Partial inhibition of DNA replication leads to expansion of the microsatellite repeat (Sutherland *et al*., 1977, 1979; Glover *et al*., 1981), leading to altered protein metabolism within cells that are the direct cause of the observed phenotypes (Gu *et al*., 1996; Kremer *et al*., 1991; Verkerk *et al*., 1991). RFSs are subdivided into three main groups based on which conditions the FS is expressed in. All share a common mechanism, however, in that expansion of nucleotide repeats following certain forms of replication stress at a specific locus results in disruption of gene expression, and disease (Ashley and Warren, 1995). Continuing studies have now identified many other genetic disorders associated with RFS expression (reviewed in Gatchel and Zoghbi, 2005). RFSs will not be discussed in detail in this thesis, but are reviewed in detail elsewhere (Gatchel and Zoghbi, 2005; Sutherland, 2003).

Common FSs (CFSs) are the largest class of FSs, and are seen in all individuals. CFSs are specific loci that exhibit gaps and/or breaks in metaphase chromosomes following partial inhibition of DNA synthesis. Most appear as a single-chromatid gap or break, although sometimes breaks on both chromatids occur. Like RFSs, CFSs are typically stable in cultured human cells grown under normal growth conditions. Unlike RFSs, however, CFSs are a normal component of chromosome structure; not the result of the expansion of nucleotide repeats. The majority of CFSs are expressed reproducibly at specific loci following treatment of low doses of

aphidicolin (APH), an inhibitor of DNA polymerases that competes with incorporation of deoxyribonucleotides (dNTPs) into newly replicating DNA (Krokan *et al*., 1981; Glover *et al*., 1984). Treatment of cell cultures with the thymidine analogue bromodeoxyuridine (BrdU), or the cytidine analogue 5-azacytidine, also result in chromosomal breakages at specific loci that are also considered to be CFSs, but these have been less well documented and not characterised at the molecular level (reviewed in Sutherland and Baker, 2003).

Genetic instability at CFSs in cultured cells is well documented. Apart from the cytogenetic expression of gaps or breaks in metaphase chromosomes, CFSs also exhibit a number of markers indicative of genetic instability at the DNA level. Following APH treatment, CFSs are hotspots for sister chromatid exchange (SCE: the exchange of homologous stretches of DNA sequence between sister chromatids), as the majority of CFS breaks are associated with an SCE (Glover and Stein, 1987). Increased rates of SCE are associated with a high frequency of translocations and deletion breakpoints in many tumours (Hecht and Glover, 1984; Hecht and Sutherland, 1984; Le Beau and Rowley, 1984; Yunis and Soreng, 1984). CFSs are also preferred sites of translocations and deletions, integration of foreign DNA (Popescu and DiPaulo, 1989; Rassool *et al*., 1991; Smith *et al*., 1992; Mishmar *et al*., 1998), and have been implicated in intrachromosomal gene amplification events in cancer cells (Kuo *et al*., 1994; Coquelle *et al*., 1997; Cliby *et al*., 1998).

Numerous reports have shown that CFSs are sites of frequent chromosome breakage and rearrangements in cancer cells (reviewed in Huebner and Croce, 2001). The most common rearrangements observed at CFSs are one or more large deletions of DNA within the CFS region, resulting in inactivation of the associated gene(s). Often these genes are large, spanning megabases of DNA. The CFS FRA3B, for instance, extends over 500kb within the 1.5Mb FHIT gene, which is inactivated by deletion of large sequences within coding sequences (Ohta *et al*., 1996; Boldog *et al*., 1997; Wilke *et al*., 1996). Recently, submicroscopic deletions of 100s of kilobases of DNA were found within the FHIT gene following replication stress induced by APH treatment, mimicking those found in tumours and tumour cell lines (Durkin *et al*., 2008). There is ample evidence that FHIT is a tumour suppressor gene

(Siprashvili *et al*., 1997; Zanesi *et al*., 2001), and homozygous genomic deletions within FHIT have been observed in a large number of human cancers and cancer cell lines, including lung, breast, gastric, cervical, and oesophageal carcinomas (reviewed in Arlt *et al*., 2006). Also, it has been suggested that the variety of deletions that occur within FRA3B in tumour cell lines is evidence of ongoing instability in CFS regions (Corbin *et al*., 2002).

At present there are over 89 reported APH-induced CFSs in the human genome (Arlt *et al*., 2006; Denison *et al*., 2003). APH-induced FS expression forms the basis of defining most CFS loci. The specific number is dependent upon two variables, however: the dose of APH used and the individual concerned. The number of FSs expressed increases with increasing doses of APH until replication ceases altogether, and not all CFSs form breaks at the same frequency amongst different individuals (Denison *et al*., 2003). The exact number of APH-induced CFSs is therefore a matter of debate and open to interpretation. Despite these discrepancies, however, gaps and breaks at a small number of loci are reproducible and represent the majority of all observed CFSs. FRA3B, for instance, is the most "fragile" site in the genome, and was also the first CFS to be cloned (Boldog *et al*., 1997; Ohta *et al*., 1996; Wilke *et al*., 1994). FRA3B and another "fragile" CFS, FRA16D, are consistently the most sensitive sites to chromosomal breakage in the presence of APH (Glover *et al*., 1984).

CFSs are conserved throughout mammalian evolution. Orthologs of humans CFSs have been identified in a number of mammalian species, including primates, cats, dogs, pigs, horses, cows, and laboratory rats and mice (Elder and Robinson, 1989; Ruiz-Herrera *et al*., 2004; Smeets and van de Klundert, 1990; Soulie and De Grouchy, 1981; Stone *et al*., 1991, 1993; Yang and Long, 1993). Extensive studies have been carried out in mice, where at least eight mice CFSs have human CFS orthologs, with associated gene loci (Durkin and Glover, 2007, and references cited therein). Additionally, CFSs may extend to lower eukaryotes such as yeast, as "*R*eplication *S*low *Z*ones" (RSZ) in *Saccharomyces cerevisiae* are analogous in behaviour to CFSs (Cha and Kleckner, 2002; see Section 1.4). Also, recombination between retrotransposons in yeast (particularly between Ty elements) is a source of

genomic rearrangements (Dunham *et al*., 2002; Roeder and Fink, 1980): Ty elements arranged head-on may mimic FSs, as they are preferred sites of DSBs under conditions of replicative stress (Lemoine *et al*., 2005). Therefore, both mammalian and yeast genomes exhibit loci that are sensitive to replication-stress.

The conservation of CFSs both within and across species may seem paradoxical given that these loci are prone to genetic instability and rearrangements. As these are potentially detrimental to organisms, they may have been selected against throughout evolution. The fact that FSs occur across a range of phyla would suggest that they serve a conserved purpose, however. What this purpose is not clear. It may be that CFSs are tolerated as a necessary consequence of higher order chromatin structure, or, conversely, that FSs actively play a role in chromatin metabolism, signalling to the cell that DNA replication in late-replicating regions is complete before the rest of the cell cycle can proceed.

1.3 Conditions that lead to mammalian CFS expression

1.3.1 Perturbation of DNA replication

CFSs can be expressed by a number of different conditions and/or chemical agents. Cells subjected to folate or thymidylate stress, when grown in folate-deficient medium or treatment with inhibitors of the folate biosynthesis pathway, for instance, induce expression of CFSs at low levels, presumably by modulating the cellular pool of nucleotides (Glover, 1981). Other replication-inhibiting drugs such as hydroxyurea (HU) are less specific in inducing FS expression, in that the sites of breakage are not consistent between different experiments, and are most likely a result of a differing inhibitory mechanism (see Section 1.4.1.2). Induction of CFSs is most efficient, however, when cell cultures are grown in low doses of APH.

A feature of both rare and common FSs is that they are late replicating. The delayed replication in RFSs is likely due to the expanded nucleotide repeats forming secondary structures such as hairpins and cruciform structures that impede progression of the replication fork machinery (Gacy *et al*., 1995; Hewett *et al*., 1998). Impeded progression of the DNA replication machinery is also evident in

CFSs, even though initiation of replication in these regions proceeds correctly (Hellman *et al*., 2000; Palakodeti *et al*., 2004). As replication through CFSs is slow, and is sometimes not fully completed even by G_2 phase of the cell cycle in FRA3B following APH treatment (Le Beau *et al*., 1998), chromosome gaps and breaks could arise in metaphase cells in these regions due to unreplicated DNA breaking as a consequence of mechanical forces imposed by, for instance, the spindle apparatus separating sister chromatids during anaphase (Thrower and Bloom, 2001). The late-replicating DNA at CFSs is therefore particularly sensitive to further delay resulting from DNA replication inhibitors such as APH, and chromosomal breakage is caused by preferential inhibition of DNA replication at these sites (Glover *et al*., 1984). Late-replicating regions do not specifically define a CFS, however, as other regions of the genome exist that replicate late yet do not form chromosomal breaks.

The underlying molecular basis for stalled replication following replication stress is not entirely understood, but likely relates to the late replication that occurs at CFSs, and the genetic sequences within. As mentioned above, expansion of nucleotide repeats does not occur in CFSs. This is not to say, however, that *cis* sequences are not important factors in modulating genetic stability within these regions. Some CFSs contain relatively high numbers of AT-rich sequences, including long stretches of interrupted AT microsatellite sequences (Arlt *et al*., 2002; Boldog *et al*., 1997; Mishmar *et al*., 1998; Ried *et al*., 2000; Shiraishi *et al*., 2001) and also contain high numbers of flexibility peaks (Ferber *et al*., 2004; Limongi *et al*., 2003). Flexibility peaks are sequence of particularly flexible DNA, calculated from deviations of twist angle between stacked bases in the DNA helix (Mishmar *et al*., 1998), and are also present within RFSs (Zlotorynski *et al*., 2003).

Although there is no evidence for the expansion of AT-repeats in CFSs, these sequences have the potential to form hairpin and cruciform structures that could lead to replication fork arrest, like the situation seen in microsatellite expansions of RFSs (Jackson *et al*., 2003). Indeed, deletions of specific sequences within CFSs are able to prevent the induction of breaks in some tumour cell lines (Arlt *et al*., 2002), although this is not evident for all CFSs (Corbin *et al*., 2002). Together, these results

suggest that deletion of sequences within CFSs reduces, but not eliminates, expression of metaphase chromosomal gaps or breaks after replication stress.

FSs are regions that often fail to compact properly for mitosis (Sutherland, 2003). As described above, CFSs replicate very late in S-phase and, after inhibition of replication, are sometimes not fully replicated by even the G_2/M transition in cell cycles (Le Beau *et al*., 1998). If cell cycle arrest does not occur by this transition, unreplicated ssDNA in these regions give rise to the cytogenetic gaps in metaphase chromosomes observed in CFSs.

A study by El Achkar *et al*. (2005) postulated that the relationships linking replication to chromatin condensation along CFSs might be pivotal to their stability. Calyculin A (Cal) triggers chromosome condensation at any phase of the cell cycle (Kanda *et al*., 1999; Alsbeih and Raaphorst, 1999), but does not markedly impair DNA replication (El Achkar *et al*., 2005). Cal treatment of human cell lines induces chromosome breaks at specific sites, the vast majority of which co-localise with CFSs induced by APH. Most of these sites lie at the interface of early and late replicating chromosome bands. Additionally, completion of replication-associated chromatin reorganisation occurs throughout the entire G_2 phase after unperturbed DNA replication. This may well explain why cells treated with Cal at G_2 cannot properly condense their chromosomes.

1.3.2 ATR inactivation

ATR (*A*taxia-*T*elangiectasia and *R*ad3 Related) and ATM (Ataxia-*T*elangiectasia *M*utated) are members of the PIKK family, a family of phosphoinositide 3-kinase-like serine-threonine kinases that is conserved across phyla such as fission and budding yeast, *Drosophila melanogaster*, *Caenorhabditis elegans* and mammals (Hunter, 1995; Zakian, 1995; Tibbetts *et al*., 2000). Both are large, chromosome-bound signal transduction proteins involved in DNA replication, DNA repair and recombination (Abraham, 2001; Zhou and Elledge, 2000). Depending on the type of DNA damage, sensor proteins signal to ATR and/or ATM (Lydall and Weinert, 1995; Lowndes and Murguia, 2000), which in turn phosphorylate target proteins

such as p53, Cdc25A and Cdc25C (Caspari, 2000; Mailand *et al*., 2000; Lakin and Jackson, 1999) to delay the cell cycle, a process called the DNA damage checkpoint (reviewed in Lowndes and Murguia, 2000; Elledge, 1996). In addition to this checkpoint role, downstream kinases also modulate DNA repair and can trigger apoptosis (Lowe *et al*., 1993; Clarke *et al*., 1993; Xu and Baltimore, 1996; Rich *et al*., 2000; Hirao *et al*., 2000).

ATR and ATM act in distinct but partially overlapping pathways in response to specific types of DNA damage during S-phase (Abraham, 2001; Durocher and Jackson, 2001). ATM is activated by DSBs resulting from ionising radiation, for instance (Pincheira *et al*., 2001), whilst ATR is required for checkpoint responses after treatment of cells with UV light and agents that block replication fork progression, such as HU, APH, (Cliby *et al*., 1998; Cortez *et al*., 2001) and another condition known to impair S-phase progression, hypoxia (Goda *et al*., 2003; Hammond *et al*., 2002, 2004). ATR-deficient cells treated with high concentrations of HU or APH exhibit extreme levels of chromosome fragmentation (Nghiem *et al*., 2001). The current understanding is that ATM is required for checkpoint activation in response to DSBs whilst ATR is required to respond to replicative stress.

Casper *et al*. (2002) found that expression of FSs was elevated when ATR, but not ATM, was inhibited in human cell cultures following treatment with APH. Breaks or gaps on metaphase chromosomes were not random, and instead occurred preferentially at known CFSs. Additionally, expression of CFSs such as FRA3B and FRA16D were observed even in the absence of treatment with APH in ATR-deficient cell lines. These results suggest that ATR is required for CFS stability even during unperturbed replication, and that some level of replication stalling occurs normally within these regions. Additionally, other studies have demonstrated that ATR plays a central role in stabilising stalled replication forks (Brown and Baltimore, 2003; Cliby *et al*., 1998; Cortez *et al*., 2001; Nghiem *et al*., 2001). As discussed below, expression of FSs increases when stalled replication forks are not stabilised following replication stress (Musio *et al*., 2005).

Cell lines cultured from individuals with Seckel syndrome, who have a hypomorphic mutation in ATR (O'Driscoll *et al*., 2003), show dose-responsive increases of FS expression when treated with APH (Casper *et al*., 2004). Seckel syndrome is a rare genetic disorder, and individuals with this disease show phenotypes of dwarfism, mental retardation and distinctive facial features (Seckel, 1960). This is the first human genetic disorder shown to have increased susceptibility to CFS instability.

1.3.3 DNA damage checkpoint proteins

Inactivation of ATR induces breaks and gaps at CFSs even in the absence of DNA replication inhibitors. Since ATR is intimately involved in DNA damage checkpoint responses, numerous studies have focused on other proteins of the intra-S and G_2/M checkpoint mechanisms as candidates that could modulate CFS stability.

BRCA1 (*BR*east *CA*ncer *1*) and CHK1 (*CH*eckpoint *K*inase *1*) are two primary downstream targets of ATR and ATM phosphorylation in response to DNA damage (Cortez *et al*., 1999; Gatei *et al*., 2001; Tibbetts *et al*., 2000; Zhao and Piwnica-Worms, 2001). BRCA1 encodes a nuclear phosphoprotein and plays a key role in the G_2/M checkpoint. It acts as a tumour suppressor: mutations in this gene are responsible for approximately 40% of inherited breast cancers and more than 80% of inherited ovarian cancers. CHK1 is an evolutionarily conserved checkpoint kinase that acts as a central regulator of cell-cycle checkpoint delays in S- and G_2-phases of the cell cycle (Liu et *al*., 2000; Takai *et al*., 2000; Bartek and Lukas, 2003), and acts downstream of BRCA1 following activation by ATM or ATR, caused by ionising radiation or stalled replication forks, respectively.

Mice and human cells deficient for BRCA1 (Arlt *et al*., 2004) or CHK1 (Durkin *et al*., 2006) have elevated chromosome breaks specifically at CFSs following treatment with low doses of APH. BRCA1 functions in the induction of the G_2/M checkpoint after APH-induced replication stalling: this checkpoint function is involved in FS stability since FSs are recognised by this checkpoint. Additionally, the Fanconi anaemia (FA) proteins interact with BRCA1 and BRCA2 in a common pathway (Garcia-Higuera *et al*., 1999; Taniguchi *et al*., 2002). Disruption to the FA

pathway leads to an increase in APH-induced chromosome gaps and breaks and instability specifically at CFSs (Howlett *et al*., 2005). FA is a rare autosomal and X-linked recessive disorder characterised by specific developmental abnormalities, haematological defects and increased susceptibility to cancer (Grompe and D'Andrea, 2001; Joenje and Patel, 2001).

In eukaryotes, members of the *S*tructural *M*aintenance of *C*hromosome (SMC) family of ATPases play important roles in chromosome condensation, sister chromatid cohesion, and DNA repair (Losada and Hirano, 2005). SMC1 forms a heterodimer with SMC3 to form the core of the cohesion complex and is a component of the DNA damage response, being a direct target of ATM phosphorylation after ionising radiation (Kitagawa *et al*., 2004; Kim *et al*., 2002; Yazdi *et al*., 2002). The SMC1/SMC3 heterodimer promotes the repair of gaps and deletions (Jessberger *et al*., 1993; Strunnikov and Jessberger, 1999) and cohesin complex is required for postreplicative DSBs repair in *S. cerevisiae* (Sjogren and Nasmyth, 2001). Inhibition of SMC1 in human cell lines promotes chromosomal fragility specifically at CFSs following treatment with APH. It was also found that SMC1 protein is phosphorylated by an ATR-dependent, ATM-independent manner following exposure to APH (Musio *et al*., 2005).

Together, these findings highlight the importance of members of the DNA damage checkpoints and associated repair pathways in maintaining genetic stability at CFSs following inhibition of DNA replication.

1.3.4 Repair of fragile sites

The homologous recombination repair (HRR) pathway plays a major role in responding to DSBs and stalled or collapsed replication forks during S- or G_2-phase when the sister chromatid is present. Glover and Stein (1987) reported that 70% of all gaps or breaks at FRA3B after induction by APH had an associated SCE, suggesting a role for HRR in the repair of lesions at CFSs. Another report also showed that after replication stress induced by APH treatment, a key component of the HRR pathway (RAD51) co-localises with DSBs found at CFSs. Additionally,

however, components of the non-homologous end joining (NHEJ) repair pathway also co-localise to these loci (Schwartz *et al*., 2005). These findings suggest that DSBs formed at CFSs may require HRR for their repair.

1.4 RSZs are budding yeast fragile sites

In the absence of Mec1p function DNA replication forks stall prior to chromosome breakage. These breaks occur within specific 10kb regions of the genome, in regular alternation with active replication origins (*ARS*s; *A*utonomously *R*eplicating *S*equence), except that no break region occurs between the origins that flank the centromere. These breaks occur at the G_2/M transition in mitotic cell cycles. Replication fork movement through these regions is intrinsically slow, even in WT cells, and were therefore named "Replication Slow Zones" (Cha and Kleckner, 2002). These RSZs do not correlate with known *cis* DNA sequences such as meiotic DSB hotspots, cohesin binding sites or DNase hypersensitivity sites (Blat and Kleckner, 1999; Borde *et al*., 1999).

Since DSBs, caused by X-rays or site-specific nucleases, efficiently stimulate mitotic recombination (Paques and Haber, 1999), it is possible that these RSZs would be hotspots for mitotic exchange, especially in cells with low levels of Mec1p.

Studies have shown that sequences within mammalian CFSs are typically AT-rich and contain higher numbers of flexibility peaks compared to those found in other regions of DNA (see above). Although RSZs are genetically determined (Cha and Kleckner, 2002), specific genetic sequences or chromosomal features common to all RSZs have not yet been identified. Nevertheless, high-throughout microarray analysis of chromosome replication showed correlation between mapped RSZs and rates of slow fork progression within chromosome III (ChrIII) under conditions lacking physiological stress (Raghuraman *et al*., 2001).
In summary, the similarities between RSZs and CFSs described above suggest that yeast RSZs may serve as a model for mammalian fragile sites.

1.4.1 Conditions that regulate RSZ expression

1.4.1.1 MEC1

The *Saccharomyces cerevisiae* gene *MEC1* (*M*itosis *E*ntry *C*heckpoint) is the homolog of mammalian ATR (Kato and Ogawa, 1994; Weinert *et al*., 1994). Mec1p, like ATR, is an essential phosphoinositide 3-kinase-related protein kinase involved in DNA replication, repair and meiotic recombination. Strains with *mec1* mutations have multiple phenotypes in addition to their sensitivity to DNA damaging agents including: (1) defective regulation of nucleotide pools (Zhao *et al*., 1998), (2) defective meiotic checkpoints and regulation of recombination (Kato and Ogawa, 1994; Lydall *et al*., 1996; Grushcow *et al*., 1999), (3) loss of telomeric silencing (Craven and Petes, 2000), (4) inability to redistribute silencing proteins from the telomeres to the sites of DSBs (McAinsh *et al*., 1999; Mills *et al*., 1999), (5) deficiency in regulating the firing of DNA replication origins in response to reduced nucleotide pools (Santocanale and Diffley, 1998), (6) reduced ability to prevent collapse of DNA replication forks stalled due to DNA damage (Tercero and Diffley, 2001), and (7) accumulated small single-stranded DNA synthesis intermediates (Merrill and Holm, 1999). At least some of these phenotypes are likely to reflect the reduced/absence of Mec1p protein kinase activity, since a number of proteins involved in DNA replication and DNA repair, such as Rad53p (Sanchez *et al*., 1996) are phosphorylated in a Mec1p- and/or Tel1p-dependent manner (Lowndes and Murguia, 2000).

As mentioned above, inactivation of Mec1p leads to chromosome breakage at RSZs, the budding yeast fragile sites.

1.4.1.2 HU

In yeast, synthesis of dNTPs depends on the multiprotein complex ribonucleotide reductase (RNR; Thelander and Reichard, 1979). RNR catalyses the conversion of all four precursor ribonucleotide diphosphates into their deoxy-forms (Elledge *et al*., 1993; Jordan and Reichard, 1998; Eklund *et al*., 2001; Stubbe *et al*., 2001) and is regulated by multiple mechanisms (Reichard, 1988; Nordlund and Reichard, 2006;

Mathews, 2006). The eukaryotic RNR is a tetrameric complex of two large regulatory subunits and two small subunits that house the di-iron centre tyrosyl radical essential for catalysis (Voegtli *et al*., 2001).

HU is an inhibitor of DNA synthesis in most organisms – from viruses to yeast to humans – by affecting RNR function (Timson, 1975). It is a non-competitive inhibitor that irreversibly inhibits the protein without remaining bound to it (Krakoff *et al*., 1968). Specifically, HU binds with high affinity to the non-haem iron subunit that contains the free radical of the enzyme essential for reduction of NTPs to dNTPs (Atkin *et al*., 1973; Giles, 2007). Inhibition of RNR leads to a decrease in dNTPs (Koc *et al*., 2004), slowing the progression of DNA replication forks during duplication of the genome (Santocanale and Diffley, 1998; Vassilev and Russev, 1984).

In tumour cell lines, rats, and bacterial and tissue cultures the effect of HU is rapidly reversible once the drug has been removed from the growth media. This reversible effect in living cells may be due to the enzyme being rapidly replenished (Gale *et al*., 1964[a,b]; Krakoff *et al*., 1964). HU does not, however, affect mRNA or protein synthesis (Giles, 2007).

HU induces many effects in yeast, such as mitotic crossing-over, mitotic gene conversion, intrachromosomal recombination (Zimmermann, 1971; Ferguson, 1990; Galli and Schiestl, 1995), deletions, chromosome loss (Mayer *et al*., 1986; Galli and Schiestl, 1996), as well as meiotic recombination (Simchen *et al*., 1976). A study by Barbera and Petes (2006), for instance, saw a 38-fold increase in reciprocal crossovers when W303a strains were treated with 100mM HU.

1.4.1.3 TOP2

The topology of DNA is altered depending on the needs of the cell. These changes are required during several cellular processes such as replication, transcription, recombination, and chromatin remodelling (Berger, 1998[a]). During quiescent times, for instance, non-transcribed regions of the genome are highly compacted, whilst

genes and regulatory sequences are in an open, easily accessible configuration for transcription. Topoisomerases are essential for these processes, catalysing the interconversion between topological states of DNA by introducing temporary single- or double strand breaks (DSBs) in the DNA. In addition, these enzymes fine-tune the steady-state level of DNA supercoiling both to facilitate protein interactions with the DNA and to prevent excessive supercoiling, which is deleterious.

There are two main classes of DNA topoisomerases: type I enzymes (of which there are two subgroups, IA and IB) break and rejoin one DNA strand at a time, while type II enzymes (also Type IIA and IIB) cleave and rejoin a pair of complementary strands. Type IA topoisomerases relax only negatively supercoiled DNA, whilst type IB enzymes relax both positively and negatively supercoiled DNA. Type IIA and IIB topoisomerases share similar structure and mechanisms, relaxing both positive and negative supercoils in DNA, in an active process requiring the hydrolysis of ATP (Berger, 1998[b]). Both strands of one DNA double helix are cut, the unbroken strand is passed through the created gap, and then the cut strand is reannealed.

Yeast *TOP2* codes for the Type II topoisomerase, Top2p (Wang *et al*., 1996, and references cited therein). Top2p is an essential protein that is highly conserved, with homologues in *C. elegans*, *Drosophila melanogaster* and humans (Strumberg *et al*., 1999). It is required for chromatin dis/assembly, chromatin remodelling at centromeres, DNA strand elongation during DNA replication, reciprocal meiotic recombination and regulation of mitotic recombination (Klein *et al*., 1992, Goto and Wang, 1984, Wang, 1996; Roca, 1995).

A temperature-sensitive (*ts*) *top2* strain shows multiple abnormalities in *S. cerevisiae*, including an inability to complete mitotic and meiotic division owing to a defect in chromosome segregation, and hyper-recombination within the repetitive rDNA gene cluster (Jensen *et al*., 1996). Also, *S. cerevisiae* strains with either a null mutation in the *TOP1* gene or a *ts* mutation in the *TOP2* gene grown at a semi-permissive temperature show 50- to 200-fold higher frequencies of mitotic recombination in rDNA relative to WT controls. Suppression of recombination at another tandem array (*CUP1* locus), at a simple *HIS4* duplication, or amongst

dispersed repeats (*MAT* and *HML* or *HMR*) is not elevated, however, in *top1* or *top2* mutants (Christman *et al*., 1988).

Two studies of *Xenopus laevis* egg extracts found that APH uncouples the replicative polymerases from the helicase/topoisomerase complex (Pacek *et al*., 2006; Walter and Newport, 2000). If the helicase complex continues to unwind DNA after stalling within CFSs, long tracts of single stranded (ss) DNA arise that can potentially form secondary structures in the AT-rich sequences, thus destabilising replication and leading to breaks: a hypothesis originally proposed by Arlt *et al*. (2006). Indeed, treatment of human cell cultures with inhibitors of topoisomerase I reduces APH-induced CFS expression (Arlt and Glover, *unpublished results*). These results suggest that uncoupling of polymerase-helicase activity may be a key initial event in CFS instability after perturbation of replication.

Analagous to these results, inactivation of Top2p function *via* use of a *top2-ts* allele (*top2-1*) at the non-permissive temperature suppressed DSB formation within RSZs in a *mec1-ts* background, yet cell viability was not restored (Nadia Hashash, *unpublished results*). This raised the possibility that Top2p catalyses chromosome breakages at RSZs. Also, a study by Bermejo *et al*. (2007) found that Top2p localises at several locations within ChrIII, some of which map near to RSZs.

1.4.1.4 RRM3

S. cerevisiae Rrm3p is a member of the Pif1 family of DNA helicases, a family that is highly conserved from yeast to humans (Zhou *et al*., 2002, Boulé and Zakian, 2006). It is a 5'-to-3' DNA helicase, and its absence results in replication fork pausing at multiple (~1400) sites within the yeast genome. Rrm3p is required to promote fork progression through non-histone protein-DNA complexes found at all of these sites, acting catalytically via the hydrolysis of ATP (Torres *et al*., 2004). A large fraction (~900) of these sites are in the rDNA on ChrXII (Ivessa et al., 2000), which contains ~100-200 tandem copies of the 9.1kb rDNA repeat (Skryabin *et al*., 1984, Warner, 1989), with each repeat having six Rrm3p-dependent sites (Ivessa *et al*., 2003). The remaining Rrm3p-dependent sites are found within telomeres and

subtelomeric DNA (Ivessa *et al*., 2000, 2002), at tRNA genes, inactive replication origins, centromeres and the silent mating-type loci (Ivessa *et al*., 2003). In *rrm3Δ* cells, the natural slowing of replication forks through telomeres and internal tracts of $C_{1-3}A/TG_{1-3}$ telomeric DNA is increased (Ivessa *et al*., 2002). In addition, forks slow as they move through multiple sites in subtelomeric DNA, including inactive replication origins. None of these sites cause detectable fork slowing in WT cells.
Recent studies have shown that Rrm3p has a more global role in DNA replication. An *rrm3* strain showed a significant delay in replication of yeast chromosomes VI, XII and XIV, including in chromosomal regions containing no known Rrm3p-dependent sites. The authors reasoned that, although not every chromosome was thoroughly tested, Rrm3p is most likely required for the timely replication of most, if not all, yeast chromosomes. Rrm3p was also shown to be a component of the replisome, interacting with the catalytic subunit of DNA polymerase ε and moving with the replication fork, rather than being recruited to its sites of action (Azvolinsky *et al*., 2006).

The role of Rrm3p in promoting replication fork progression contributes to genomic integrity. Broken replication forks are found within rDNA, subtelomeric DNA and tRNA genes in *rrm3* strains (Ivessa *et al*., 2000, 2002, 2003), triggering a checkpoint response and promoting recombination. Levels of recombination increase ~10-fold in the rDNA in *rrm3Δ* cells (Ivessa *et al*., 2000), and even more so (>100-fold, Keil and McWilliams, 1993) between other naturally-occurring tandem repeats such as the *CUP1* array, which is composed of 10-15 repeats 2.0kb in length within ChrVIII (Fogel and Welch, 1982). Recombination is also increased in subtelomeric Y' elements (Ivessa *et al*., 2002), within tRNA-rich regions (Ivessa *et al*., 2003; Admire *et al*., 2006) and between plasmid-borne RNA polymerase II-transcribed genes (Prado and Aguilera, 2005). Even though recombination is increased in *rrm3* cells, however, the recombination rate is still sufficiently low that recombination should affect the behaviour of only a small number of chromosomes. For example, the rate of interchromosomal recombination in *rrm3* cells in a tRNA-rich 184-kb interval on ChrVII was only 1.5×10^{-5} events/cell/generation in a study by Ivessa *et al*. (2003), compared to the WT basal rate of 0.4×10^{-5} events/cell/generation. Keil and McWilliams (1993) earlier proposed that, as mitotic and meiotic recombination is

not affected in *rrm3Δ* cells in regions that do not contain tandem repeats, Rrm3p is only needed to repress recombination between naturally occurring direct repeats.

Work in my lab has found that DSBs are not formed at RSZs in a *mec1-4 rrm3Δ* double mutant. Viability at the non-permissive temperature was not fully restored but was improved compared to a *mec1-4* single mutant. It was later found that *rrm3Δ* restored Sml1p cycling in the *mec1-ts* strain, and that suppression of *mec1-ts* defects were dependent upon Tel1p function (Nadia Hashash, *unpublished results*). Taken together, these considerations suggest that suppression of *mec1-ts*-induced DSBs by *rrm3Δ* is via Tel1p-dependent degradation of Sml1p.

1.5 Mutation assays

1.5.1 Direct-repeat reporter construct: hisG-URA3-hisG

The *hisG-URA3-hisG* cassette was chosen to assess the rates of mitotic recombination within yeast strains for this thesis. The *hisG-URA3-hisG* construct was originally created as a "reusable" means to disrupt gene function within yeast strains. The construct consists of a functional *URA3* gene flanked by two identical 1.1kb bacterial sequences arranged in the same orientation. *URA3* encodes orotidine-5'phosphate decarboxylase, an enzyme that is required for the biosynthesis of uracil (Umezu *et al*., 1971), whilst *hisG* is a subunit of bacterial ATP phosphoribosyltransferase that catalyses the first step in the biosynthesis of histidine (Kronenberg *et al*., 1975). The construct can be transformed easily into vegetatively growing cells, inserting into genomic DNA *via* homologous recombination without any deleterious effect to the cell. It was reasoned that placing *URA3* between two direct repeat sequences would strongly favour the "pop-out" event upon selection for 5-Fluoroorotic acid- (5-FOA-) resistance in *URA3* strains (Figure 1.1): Ura3p converts 5-FOA into the toxic compound 5-fluorouracil. The complete loss of *URA3* would then allow another round of gene disruption using the *URA3* marker again. Indeed, studies have confirmed that the majority of *ura3* derivatives from *hisG-URA3-hisG* integrants acquire 5-FOA-resistance by the pop-out event (Alani *et al*., 1987).

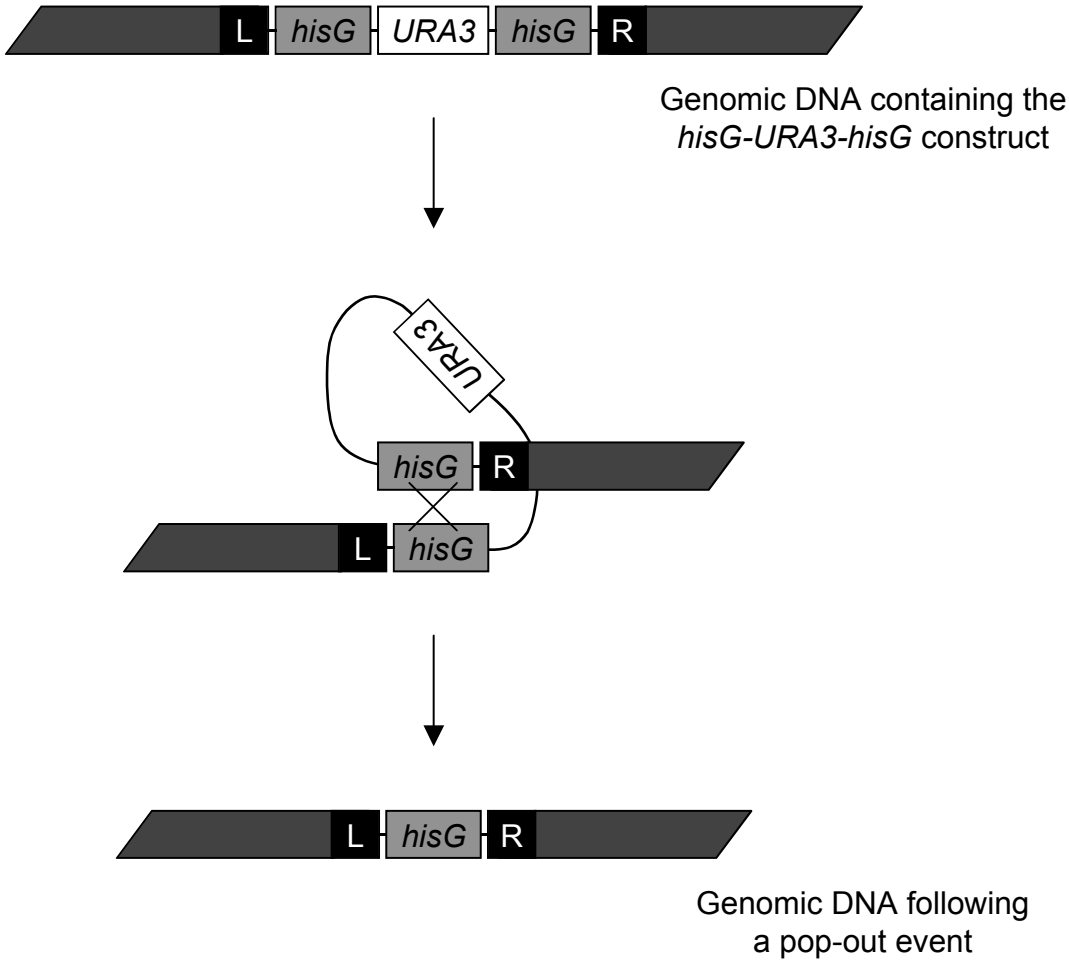

Figure 1.1. Pop-out event within the *hisG-URA3-hisG* construct.

Recombination between the *hisG* repeats of the construct results in a "pop-out" event. One repeat and the *URA3* gene are "lost," leaving one remaining *hisG* gene in the genomic DNA.

1.5.2 Types of mutation that can be scored

There is more than one way in which *URA3* function in the *hisG-URA3-hisG* cassette can be inactivated. These include, as well as the pop-out event discussed above, (1) small genetic changes such as point mutations, small insertions and/or deletions, and frame-shift errors, (2) loss of the entire region/chromosome containing the construct, (3) translocations that inactivate the gene due to loss of sequence, and (4) ectopic recombination (Figure 1.2).

Southern blot analysis and/or PCR-based strategies of *ura3* colonies are able to easily distinguish between large chromosomal changes (such as pop-out events) and small changes (such as point mutations or frameshift errors within the *URA3* gene) that have led to its inactivation. For instance, a frameshift mutation would produce the same banding pattern as that produced by *hisG-URA3-hisG* strains with functional *URA3*, as the difference at the genetic level would not be detectable by Southern blot analysis. Larger chromosomal changes that have led to inactivation of *URA3*, such as pop-out events or loss of the entire region/chromosome containing the construct, would result in a different, readily identifiable banding pattern by the same analysis (Figure 1.3).

1.5.3 Previously reported mutation rates of direct-repeat recombination

In Alani *et al.'s* (1987) paper describing the creation of *hisG-URA3-hisG*, the construct was targeted to replace the *TRP1* gene (ChrIV). The rate of *URA3* inactivation within WT strains was 2×10^{-5} events/cell/generation. Southern blot analysis was used to analyse a proportion of the *ura3* colonies produced, and showed the expected banding pattern that would result from a deletion of the *URA3* gene and one of the *hisG* sequences: pop-out events.

Two other studies of note used similar constructs to study rates of direct-repeat recombination in yeast mitotic cell cycles. Zhang *et al*. (2006) for instance, used a *leu2-URA3-leu2* construct inserted into an intergenic region of ChrV in S228C yeast strains, and found the rate of *URA3* inactivation to be $1.1 \pm 0.4 \times 10^{-5}$

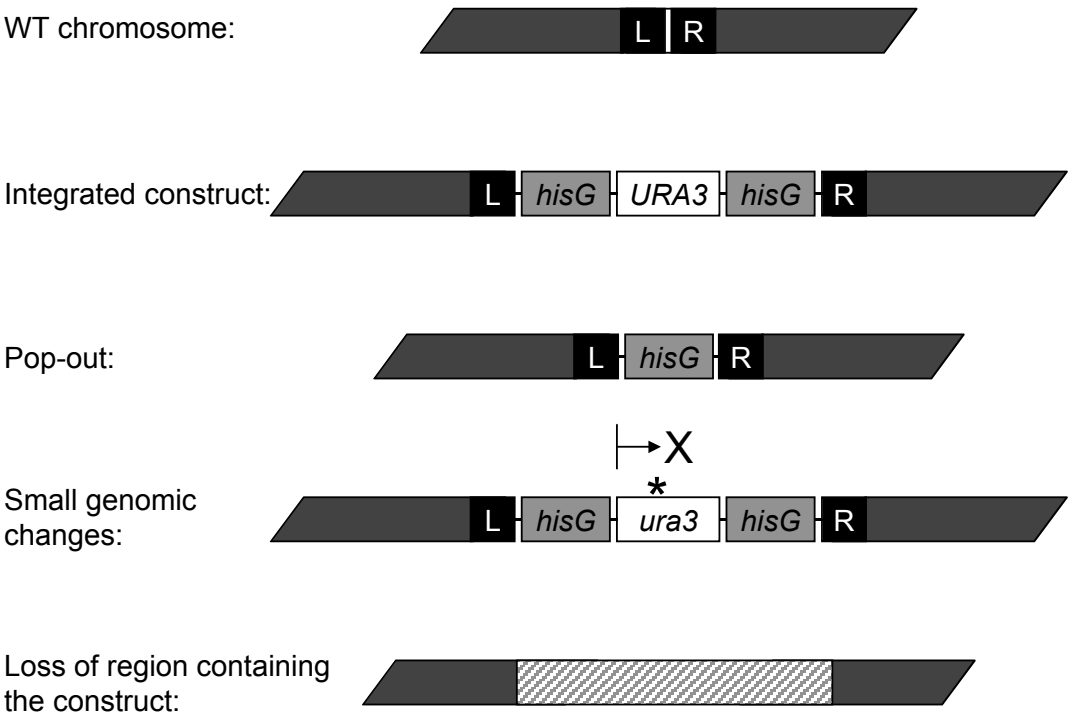

Figure 1.2. Types of mutation that can result in *URA3* inactivation.

URA3 within the *hisG-URA3-hisG* reporter construct can be inactivated by various means. Pop-out events can occur from HRR pathways (see text). Small genomic changes, such as small insertions or frameshift mutations (*) can inactivate *URA3* by preventing and/or erroneous transcription of the coding region. Large, gross chromosomal changes, such as translocations to ectopic regions or loss of the entire chromosome containing the reporter construct also lead to *URA3* inactivation. The latter cases are more likely to be detected in diploids where the potential loss of essential genes is tolerated. "L" and "R" represent genomic DNA flanking the insertion site of the construct.

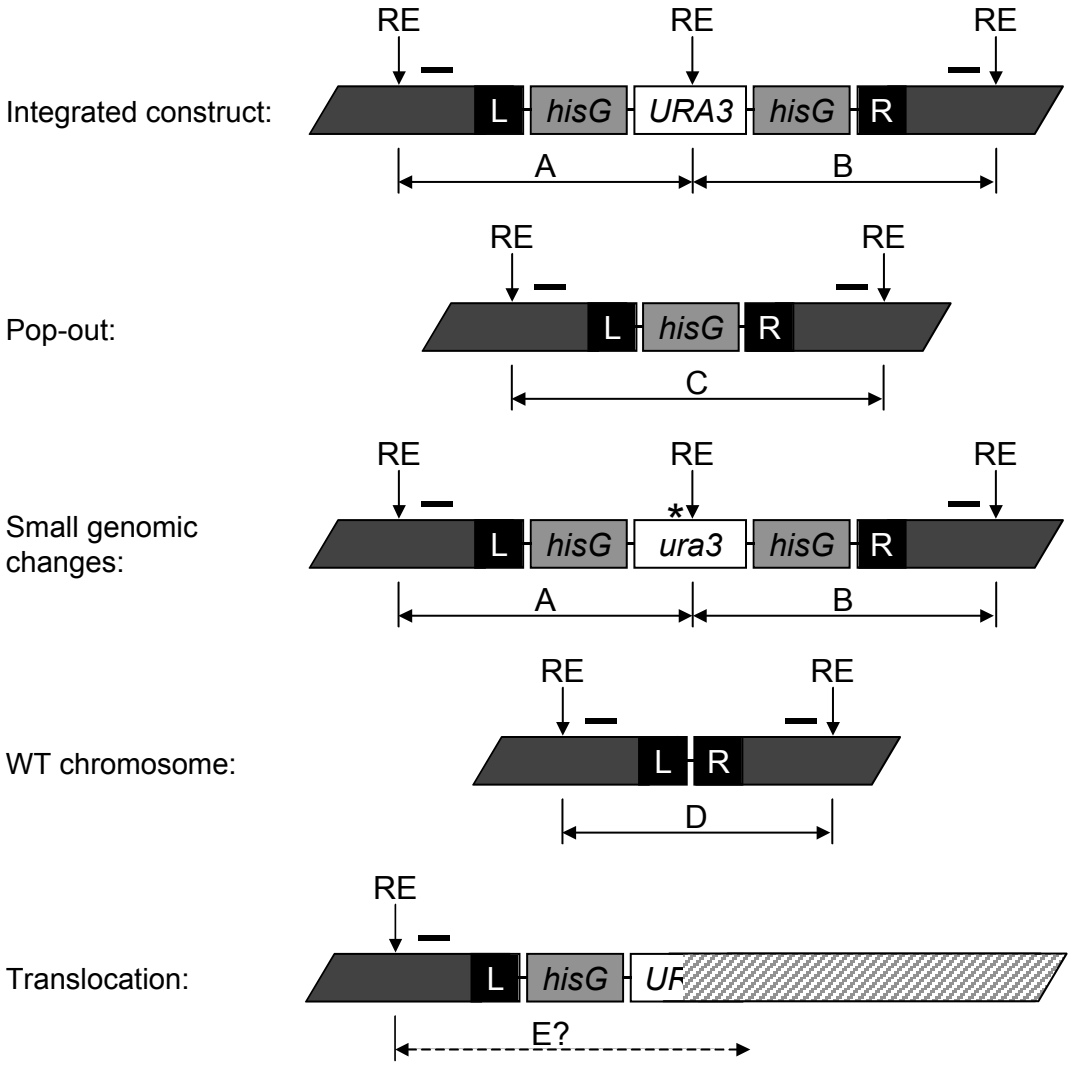

Figure 1.3. Types of mutational events resulting in *URA3* inactivation that can be detected by Southern blot analysis.

Restriction enzyme (RE) digestion followed by Southern blot analysis using two probes both sides of the reporter construct (dashed lines) will result in detection of two fragments if cutting occurs both in genomic DNA and within the construct itself. This will result in two bands, A and B, which can be easily distinguished from one band (C) resulting from pop-out events. Similarly, if only small changes have occurred that led to *URA3* inactivation, such as point mutations or small insertions or deletions within the gene (*), the migrating bands will be similar in size to those in the original *URA3* strains. If the chromosome or region containing the reporter construct is lost, no detectable signal will be present. In the diploid state, a fragment from the WT chromosome will be detected in all cases (D). Unexpected translocations, such as in the last example, will also not be detected by this preliminary analysis.

events/cell/generation in WT strains grown in non-selective conditions. The ± valuein this case was the standard deviation between three independent analyses. Instead of pop-out events being the cause of inactivation of the *URA3* gene, however, all of these events were due to small changes within the *URA3* gene, such as small insertions and/or deletions. A study by Thomas and Rothstein (1989) found the measure of *URA3* inactivation to be 2.0 x 10^{-5} events/cell/generation using a *gal10-URA3-gal10* construct inserted into intergenic regions of ChrII. All of these mutagenic events were due to pop-out events. Note that although the mutation rates are similar among the three studies mentioned above, the incidence of pop-out event differed dramatically depending on the experimental system.

1.6 Factors that regulate mutagenesis

1.6.1 DNA replication

The role(s) of DNA replication in regulating genomic stability have already been addressed with respect to mammalian rare and common FSs. CFSs are late-replicating, and ssDNA in unreplicated regions resulting from replication stress have been shown to lead to cytogenetic gaps and breaks on metaphase chromosomes, as well as submicroscopic deletions in cancer cell lines (Durkin *et al*., 2008). Genetic sequences, such as microsatellite expansions in RFSs, and AT-rich sequences in CFSs, can form secondary structures such as hairpins and cruciforms that impede DNA replication. Also, the fact that members of intact DNA damage checkpoint pathways are required to maintain stability within FSs, even in the absence of replication stress, highlights the importance of DNA replication and FS stability.

In two recent yeast studies, inhibition of replication resulted in genetic instability at the chromosomal level. Lemoine *et al*. (2005) found that a 10-fold decrease in the levels of WT DNA polymerase α lead to elevated frequencies of chromosome translocations and chromosome loss at preferred sites. One of these preferred sites of translocation was accurately mapped within ChrIII, and contained two retrotransposons (Ty1 elements) arranged head-to-head.

S. cerevisiae has five distinct retrotransposon families, Ty1 through Ty5. Retrotransposons are similar to retroviruses, replicating through reverse transcription of an mRNA intermediate (Boeke and Chapman, 1991). The resulting cDNA integrates into new sites within the genome and can influence genome evolution by generating mutations in coding or transcriptional control sequences. Overall, retrotransposon sequences constitute more than 3.1% of the yeast genome. Ty1 elements (of which there are two distinct subtypes, Ty1 and Ty1') are the most common, with 32 full-length element insertions identified in the sequenced genome (Kim *et al*., 1998). The 5.9kb Ty1 elements are flanked by 330bp *L*ong *T*erminal *R*epeat (LTR) sequences (delta elements) in direct orientation. Several studies have shown that chromosomal translocations, deletions and inversions can result from recombination events occurring between Ty elements or between solo delta elements (Roeder and Fink, 1980; Dunham *et al*., 2002 are just two examples).

Lemoine *et al*. (2005) found that the pair of Ty elements arranged head-to-head was a preferred site of chromosomal arrangements when DNA replication was inhibited. Recombination events occurred between Ty elements on non-homologous chromosomes, leading to translocations. Disruption of the site substantially reduced the rate of chromosomal translocations in the same conditions. The authors concluded that the region with Ty elements arranged head-to-head is an analogous situation to FSs observed in mammalian chromosomes when replication is perturbed.

Another group studied chromosomal instability in a haploid strain containing an additional, genetically marked ChrVII (Admire *et al*., 2006). Cell with unstable chromosomes occurred at a very low rate (~1 in 10^6 cells) in unperturbed WT cells, which was elevated (~1 in 10^3) in cells where DNA replication was inhibited by HU treatment, in an *rrm3* background, and in strain backgrounds defective for replication checkpoint genes such as *mec1* or *rad9* (Rad9p is a checkpoint protein that has several roles in the cell cycle and is required to maintain genomic stability [Weinert and Hartwell, 1990; Klein, 2001]). Translocations occurred at several sites within the reporter chromosome, and one specific site was accurately mapped where the majority of translocations occurred. This site contained multiple tRNA genes that stall replication forks in *rad9* cells (Admire *et al*., 2006). Ongoing instability

occurred within this region until the translocations became unstable or the region/chromosome containing the tRNA genes were lost. When deleted, the overall rates of chromosomal instability decreased. These results imply that replication forks stall at specific sites, and, in the absence of intact replication checkpoints, lead to fork collapse that ultimately result in genetic instability.

1.6.2 Ploidy

Many studies on chromosomal rearrangements in yeast have been carried out in haploids, whilst only a relatively small number have focused on spontaneous chromosomal rearrangements in the diploid state (such as Hiraoka *et al*., 2000; Fasullo *et al*., 2001; Klein, 2001).

One recent study assessed the role of ploidy on the rate of *URA2* prototrophic revertants formed from *ura2* strains, where the *URA2* allele had been inactivated by multiple point mutations (Tourrette *et al*., 2007). The formation of *URA2* revertants resulting after non-selective growth conditions was assessed in isogenic haploid and diploid strains. In haploids, *URA2* prototrophic revertants arose by three different means: deletion of the region containing the point mutations; duplication of the essential coding sequence under control of a resident promoter after integration at an ectopic site; or insertion of a Ty1 element that led to the formation of WT *URA2* (Roelants *et al*., 1995). In diploid *URA2* revertant strains numerous chromosomal rearrangements occurred that were not observed in the haploid strains, several of which would be lethal at the haploid level. A large, 130kb-long deletion occurred bearing 10 essential genes, for instance, which only occurred in diploid strains.

When the rate of formation of *URA2* prototrophic strains was assessed, it was 19-fold lower in diploid strains than in haploid strains. This was a surprising result, since in diploids the number of chromosomal reshaping opportunities is higher, they show a greater tolerance for genomic rearrangements, and are therefore able to withstand events that are potentially lethal in haploids. A large proportion (~40%) of revertants selected for in diploids, for instance, would be lethal at the haploid level. Also of note was that no Ty1 elements were found to be involved in the uracil

prototrophy recovery because the retrotransposition process is almost abolished at the diploid level (Errede *et al*., 1980; Company and Errede, 1987). The decrease in mutation rate in diploids compared to haploids may have been partly attributable to this fact alone, since ~40% of the revertants selected for in haploids contained a Ty1 insertion. Also, repair of DSBs in diploids was more accurate than in haploids. As there was a second copy of the *ura2* allele in the diploid strains that could be used for repair purposes, accurate repair using this as a template would not lead to the formation of prototrophic revertants, resulting in a lower mutation rate.

The greater opportunities that exist for chromosomal rearrangements in diploids are also evident in another study. Haploid and diploid strains were grown under four different growth conditions, and it was found that diploid strains were more adaptable to new growth conditions than their respective isogenic haploid strains due to beneficial mutations that are only accessible to diploids (Thompson *et al*., 2006).

Although these two studies are obviously not exhaustive in their analysis of the effects of ploidy on mutation rates, they highlight a number of potential differences between haploid and diploid strains. There are numerous opportunities within diploids for genomic rearrangements, some of which do not occur, and others of which would be genetically inviable, at the haploid level. Some yeast cell systems designed for studying chromosomal rearrangements with different selection schemes show that Ty1 elements are involved in triggering these events (Hiraoka *et al*., 2000; Dunham *et al*., 2002; Umezu *et al*., 2002; Lemoine *et al*., 2005). The fact that none of these Ty sequences have ever been observed in Tourrette *et al*.'s (2007) studies suggests that several possible mechanisms may lead to spontaneous chromosomal rearrangements in diploid cells, such as the involvement of short repetitive DNA sequences being preferred sites for translocations. Despite the large opportunity for genomic rearrangements, however, the rate of mutation in diploids is not necessarily higher than those found in haploids.

1.6.3 Recombination

The reports described above detail chromosomal translocations that can occur in both haploid and diploid strains. Past studies that have used the *hisG-URA3-hisG* cassette or similar reporter constructs have shown the *URA3* allele to be inactivated by pop-out events, by small insertions or deletions within the gene, and by chromosomal translocations (Alani *et al*, 1987; Thomas and Rothstein, 1989; Zhang *et al*., 2006). These events are the result of single strand annealing (SSA) or gap repair, both part of the HRR pathways.

SSA is an efficient mechanism of DNA DSB repair, and is dependent on the presence of two homologous sequences in direct orientation flanking the site of a DSB (Nickoloff *et al*., 1989; Ray *et al*., 1988; Rudin and Haber, 1988; Fishman-Lobell *et al*., 1992). Repair occurs intrachromosomally and results in the deletion of the sequences between the direct repeats flanking the DSB and also one of the repeats (Lin *et al*., 1990; Fishman-Lobell *et al*., 1992). DNA is resected by a 5'-to-3' exonuclease on each side of the DSB until the flanking regions of homology are exposed, leaving 3'-ended single-stranded tails. Annealing can then take place between the complementary sequences located on opposite sides of the DSB; this is followed by nucleolytic removal of any remaining tails, DNA synthesis to fill in the gaps, and ligation (Figure 1.4). SSA occurs efficiently even when the flanking homologous regions are separated by as much as 15kb or when the extent of shared homology of the flanking regions is only a few hundred base pairs (Sugawara and Haber, 1992; Fishman-Lobell *et al*., 1992). SSA is not a minor pathway in yeast: when a DSB is created in a region that can be repaired either by intrachromosomal gene conversion or by SSA, more than two-thirds of the events occur by SSA (Fishman-Lobell *et al*., 1992), regardless of the endonuclease used to initiate the DSB (Plessis *et al*., 1992). Another study found that when two constructs containing direct repeats were introduced into two different chromosomes, half of all repair events of simultaneously-induced DSBs located between the homologous flanking sequences were repaired by SSA whilst the remaining repair events occurred by interchromosomal recombination, resulting in the formation of a pair of reciprocal translocations (Haber and Leung, 1996). Therefore, although SSA is an efficient

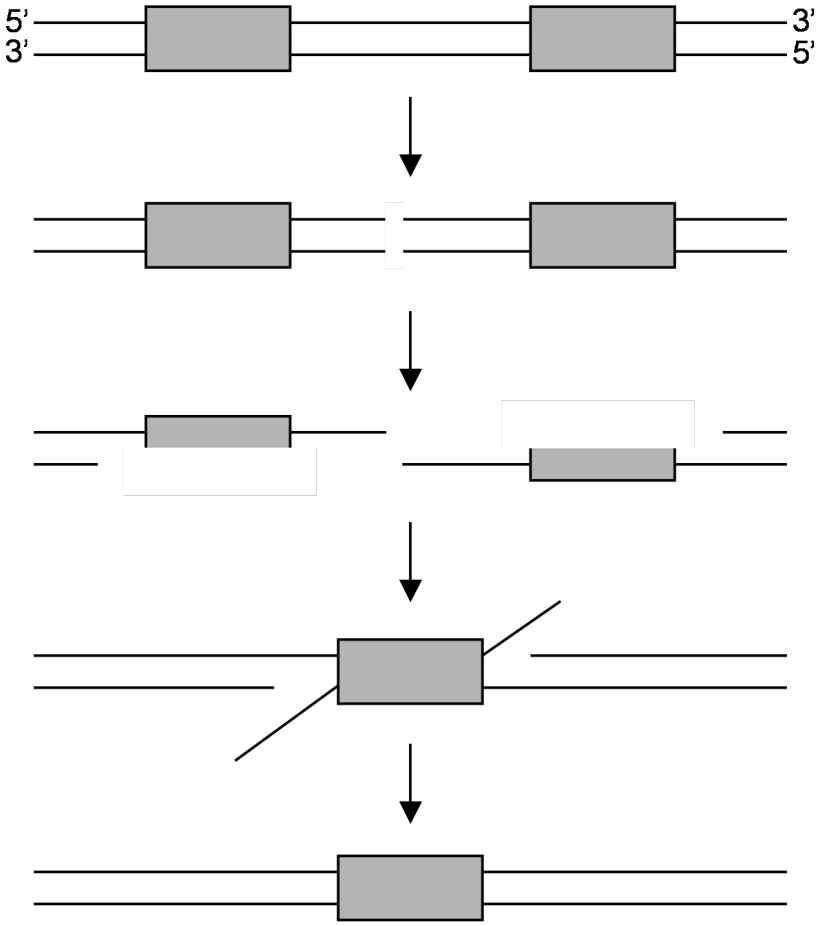

Figure 1.4. SSA results in deletion of one direct repeat and intervening sequence.

A DSB that occurs in a unique sequence between two flanking homologous sequences (grey boxes) can be repaired by SSA. After the initial DSB event, resection of DNA by an exonuclease occurs in a 5'-to-3' direction until complementary sequences are exposed, leaving 3'-ended single tails. The complementary sequences anneal, DNA tails are cleaved, and DNA synthesis fills in any gaps. A DNA ligase is then recruited in the last stage of repair to join the strands, leaving one intact repeat. In the case of the *hisG-URA3-hisG* reporter construct used in this thesis, SSA results in deletion of *URA3* and one *hisG* repeat.

repair mechanism in response to DSBs initiated between direct repeats, recombination between other sites that also contain the same regions of homology can be used just as efficiently.

Gap repair of DSBs was first proposed by Szostak *et al*. (1983). After a DSB event, broken DNA ends are resected to form a double stranded gap. Ends invade a homologous region of DNA and prime DNA synthesis by using the undamaged allele as a template for repair. Recombination intermediates can be resolved as a reciprocal exchange (crossover) or non-reciprocal transfer of information from one allele to another (gene conversion; Figure 1.1 is an example of this). Common to both gap repair and SSA is that repair at break sites occurs with high fidelity, since long stretches of sequence homology are often involved. SSA is always a non-conservative mechanism, since repair always leads to the deletion of sequences between homologous regions. HRR can also achieve deletion of one direct repeat and the intervening sequence, however. Deletions can occur, for instance, from unequal SCE, unequal sister chromatid gene conversion (Maloney and Fogel, 1987; Rothstein *et al*., 1987) or mispairing of the replication fork (Lovett *et al*., 1993). Deletion of the sequences between the direct repeats can therefore be achieved through multiple mechanisms. All of these processes are indicative of a DSB and its consequential repair. If the rates of deletion are elevated at certain regions within the genome, this is indicative of increased genomic instability at the specific locus concerned.

1.6.4 Temperature

Organisms have evolved to function optimally at certain growth conditions. One such important condition is temperature, which can affect many diverse metabolic processes within a cell. Organisms have developed strategies for tolerating high temperatures, such as the induction of *H*eat-*s*hock *p*roteins (Hsp) in yeast that play important roles in helping cells cope with the toxic effects of high temperatures (Parsell and Lindquist, 1993). Hsp70 and Hsp90, for example, are essential proteins required for growth at all temperatures that bind to unfolded proteins, maintain them in a soluble state, and prevent aggregation (reviewed in Saibil, 2008).

Proteins are not the only molecules affected by temperature. Past studies have shown that living cells exposed to elevated temperatures incur several different types of DNA damage, including depurination, deamination of cytosine, destruction of deoxyribose residues (Lindahl and Nyberg, 1972), DNA strand breaks and DNA degradation (Bridges *et al*., 1969; Woodcock and Grigg, 1972; Gomez and Sinskey, 1973). Elevated temperatures may also produce some types of DNA damage similar to that produced by ionising radiation (Bridges *et al*., 1969; Evans and Parry, 1972).

Since elevated temperatures induce DNA damage, they may also lead to an increase in genetic alterations. Several studies have demonstrated that elevated temperatures result in increases in mutation rate in both prokaryotes and eukaryotes. Evans and Parry (1975), for instance, found increased frequencies of mitotic crossing-over at the *ade2* locus at both 37˚C and 52˚C. The frequency of mitotic gene conversion at the *trp5* and *his4* loci also increased at these temperatures. In meiosis, the recombination frequency of many chromosomal regions appeared to be independent of temperature in a study by Johnston and Mortimer (1967). Additionally, although different temperatures have routinely been used in order to study the effects of temperature-sensitive alleles on mutation rates, no recent study exists that describes the temperature-specific effects on mitotic recombination (or mutation) rates.

1.7 Project aims

Comparisons of known mutational hotspots to RSZs do not provide convincing evidence that they are inherently more mutagenic than other regions. As described above, sites of chromosomal instability in *S. cerevisiae* have been associated with clusters of tRNA genes and Ty1 elements arranged head-to-head in conditions of replication stress. These features are not generally associated with RSZs, since only two out of six RSZs on ChrIII map to transposition hotspots, and clusters of tRNA genes are only associated with one RSZ (see Figure 3.1, page 76). Additionally, mammalian CFSs often contain tracts of interrupted AT-rich sequences, yet no correlation with RSZs and AT-rich sequences exists.

The primary aims of the work presented in this thesis were to address several questions regarding genome structure and genome stability. Do levels of mitotic recombination vary at different locations? Specifically, are RSZs more mutagenic than other regions within the same chromosome? Are levels of mitotic recombination modulated by such "*cis*" factors, and do "*trans*" factors, such as lack of certain proteins, ploidy, or temperature have any effect?

In order to address these questions the *hisG-URA3-hisG* reporter construct was inserted into five different loci within ChrIII. Two loci within known RSZs were chosen, along with three other loci that served as comparisons to assess any *cis* specific effects on mutation rate. To identify relevant trans-regulators, the effects of ploidy, temperature, as well as inactivating selected proteins (Mec1p, Top2p and Rrm3p) were then assessed. Results of these analyses, as well as their implications regarding genome stability are presented.

Chapter 2.

Materials and Methods

2.1 Commonly used buffers, reagents and solutions

Most chemicals and reagents used in this work were analytical grade. Commonly used aqueous buffers and solutions are listed in Table 2.1.

2.2 Bacterial techniques

Escherichia coli (*E. coli*) DH10B (*F- mcrA [mrr-hsdRMS-mcrBC] 80lacZM15 lacX74 recA1 endA1 ara139 [ara, leu]7697 galU galK – rpsL [StrR] nupG*) was used for all bacteriological work.

2.2.1 E. coli media and growth conditions

E. coli cells were grown in Luria-Bertani broth (LB; 1% [w/v] bacto-tryptone, 0.5% [w/v] yeast extract, 1% [w/v] NaCl [pH 7.5]) with the addition of 100μg/mL ampicillin for plasmid selection. Liquid cultures were grown in at 37˚C in a gyratory shaker (New Brunswick Scientific) at 250rpm. For solid LB media, 1.5% [w/v] Difco agar was added and the plates incubated overnight at 37˚C.

2.2.2 Preparation of competent E. coli

A single, fresh colony of DH10B cells (Invitrogen) was inoculated into 5mL LB in a 125mL conical flask and incubated for 2h at 37˚C at 300rpm. This starter culture was added to 100mL fresh LB media and shaken for a further 2-3h until an OD_{600nm} of 0.5 was achieved. Cells were harvested by centrifuging for 5min at 2200rpm in a Sorvall Legend RT centrifuge at room temperature (R-T). The cell pellet was resuspended in 40mL RFI solution (30mM potassium acetate [pH 6.9], 50mM $MnCl_2$, 100mM KCl,

10mM $CaCl_2$, 15% [v/v] glycerol) and left on ice for 30 min. Cells were centrifuged for 5min at 2200 rpm in a Sorvall Legend RT centrifuge at 4˚C, resuspended in 4mL RFII solution (10mM Na-MOPS [pH 7.0], 75mM $CaCl_2$, 10mM KCl, 15% [v/v] glycerol) and stored in 200µL aliquots at -80˚C.

2.2.3 Transformation of E. coli

Frozen *E. coli* competent cells for transformation were thawed at 37˚C before use. Usually 1µg of DNA was mixed with 100µL of competent cells and kept on ice for a minimum of 20min. Cells were heat-shocked for 1.5min at 42˚C, and then allowed to recover by adding 500µL LB and incubating for 1h at 37˚C in a hot block. Cells were then plated directly onto LB-Amp plates and incubated overnight at 37˚C.

2.3 Plasmids

All plasmids used in this study are listed in Table 2.4. Plasmid maps of pRSC081 and pNKY51 are shown below in Figure 2.1.

2.4 Yeast techniques

2.4.1 Strains

All strains used in this study were isogenic with SK1, except for alterations introduced by transformation or by crosses with isogenic strains. The progenitor SK1 strain has the markers *MAT**a***, *ho::LYS2* or *ho::hisG, ura3, lys2, leu2::hisG*, and are listed in Table 2.2.

Figure 2.1. pRSC081 and pNKY51.

Relevant RE sites are shown. Plasmids are not drawn to scale. *TEM1* encodes the *β*-lactamase that confers resistance to ampicillin in *E. coli* strains. MCS, multiple cloning site.

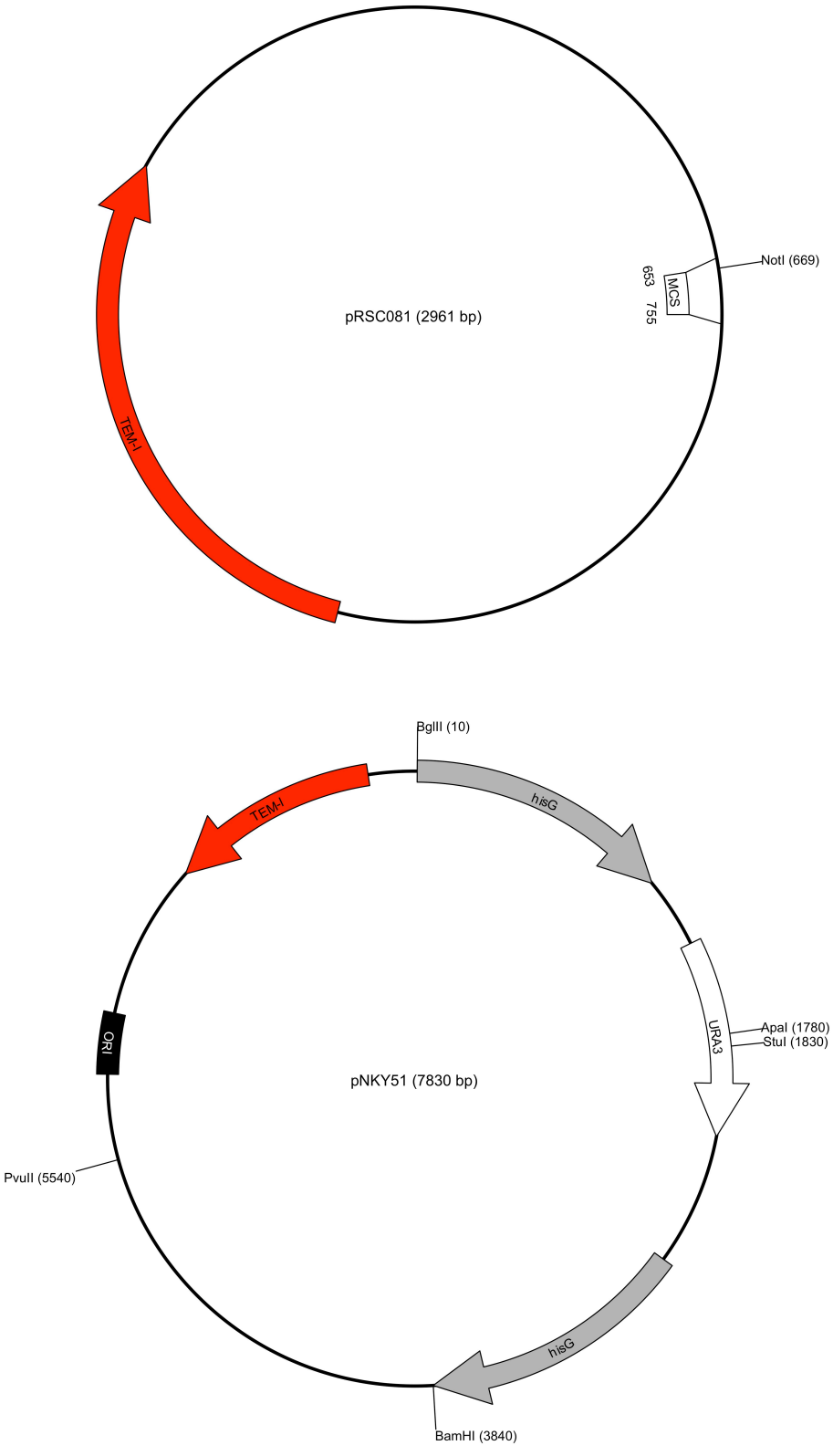

2.4.2 Yeast culture conditions

Cells were routinely grown in complete medium (YPD: 1% yeast extract, 2% Bacto peptone, 2% glucose) at the indicated temperature at 175rpm in a gyratory shaker (New Brunswick). For solid media, 2% Difco agar was added and the plates incubated at the indicated temperature.

For selection purposes, synthetic drop out agar plates (0.67% yeast nitrogen base, 2% Difco agar, 2% glucose) with the appropriate (40µg/mL) amino acid supplements were used. Diploid strains were sporulated on SPM plates (*s*porulation *p*late *m*edium: 1% potassium acetate, 2% Bacto agar). For selective growth of kanamycin- or hygromycin-resistant strains, 200µg/mL geneticin sulphate (G-418, Invitrogen), or 100µg/mL concentration hygromycin, respectively, was added to YPD agar. To prevent petite cell colony formation, cells were grown on YPG plates that used 3% glycerol instead of glucose as the carbon source. For the selection of *ura3* mutants, 1mg/mL 5-Fluoroorotic Acid (5-fluorouracil-6-carboxylic acid monohydrate; 5-FOA, Apollo) was added to minimal media agar plates (0.67% yeast nitrogen base, 2% glucose, 3% Bacto agar) containing 40µg/mL arginine, histidine, leucine, lysine and uracil. Bacto agar, Bacto peptone and Bacto yeast extract were from Becton Dickinson.

Cells were stored for short periods of time at 4˚C on appropriate agar plates. For long-term storage, strains were grown on non-selective media plates for two days, suspended in connelation media and stored in 1.8mL 20% glycerol at -80˚C.

2.4.3 Transformation of S. cerevisiae

Cells from a single colony of relevant genotype were inoculated into non-selective media and grown until an OD_{600nm} of 0.5-1.0 (approximately 1-2 $x10^7$ cells/mL) was achieved. For each transformation, 15mL of culture was used. Cells were harvested by centrifuging for 2min at 2200rpm in a Sorvall Legend RT centrifuge at room temperature (R-T); then washed once with sterile water. The pellet was resuspended in 1mL of 1x TE (pH 7.6), 0.1M lithium acetate (LiAc) solution and transferred to a

fresh microfuge tube. Cells were then centrifuged once again for 15s at 13,000rpm on a desktop microcentrifuge at R-T, aspirated and resuspended in 80µL 1x TE, 0.1M LiAc solution. To this cell suspension was added 25µL herring sperm DNA (2mg/mL, phenol extracted and sheared), 700µL 1x TE [pH 7.6], 40% polyethylene glycol (PEG, Sigma), 0.1M LiAc solution and DNA to transform the cells with (1µg for plasmid DNA, up to 10µg for linear DNA). The tube was vortexed vigorously until the cell pellet was completely mixed, then incubated for 30min at 30˚C. Cells were heat-shocked for 20min at 42˚C, collected by centrifuging for 5-10s at 13,000 rpm on a desktop microcentrifuge at R-T, and washed twice with sterile water. The cell pellet was resuspended in 450µL sterile water, 150µL plated onto appropriate selection media and cells incubated at 30˚C.

2.4.4 Growth analysis (spot test)

Indicated yeast strains were grown to mid-log phase and diluted to a cell density corresponding to an OD_{600nm} of 0.3. Ten-fold serial dilutions of each culture were spotted (3.0µL per spot) onto specified agar plates and incubated for 3-5 days at the indicated temperature(s).

2.4.5 Kinetics of commitment to inviability among temperature sensitive (ts) mutants

Indicated *ts* yeast strains were grown for 2 days on non-selective media and then inoculated into 5mL rich medium. Cultures were then incubated at 23˚C for 1.5h, shifted to the restrictive temperature of 37˚C (t=0) and 1mL samples taken at regular intervals. Serial dilutions were performed so that 50-200 cells were typically plated onto non-selective agar plates. Cells were incubated at 23˚C due to their temperature sensitivity.

2.4.6 Tetrad dissection

Diploid strains were incubated overnight on SPM plates at 30˚C, mixed in spheroplasting buffer (SCE, 1mg/mL 100T zymolyase) and then incubated for 1h at

30˚C. Tetrads were dissected on non-selective medium and incubated at the appropriate temperature.

2.5 DNA methods

2.5.1 Extraction of plasmid DNA

Colonies from overnight incubations were picked from agar plates, inoculated into 2mL LB-Amp medium in 10mL tubes and incubated overnight at 37˚C at 300rpm on a gyratory rotor. DNA was purified from these cells using a Biolab miniprep kit, as per the manufacturer's instructions, and eluted into 100μL 1x TE [pH 7.6].

2.5.2 Isolation of yeast chromosomal DNA

S. cerevisiae chromosomal DNA was extracted and purified using a method adapted from that of Fujimura and Sakuma (1993) Briefly, cells from which DNA was to be extracted were incubated overnight at 30˚C in 2mL non-selective medium (ts strains were incubated at 23˚C) until they reached a minimum OD_{600nm} of 5.0. Cells were harvested by centrifuging for 2min at 2200rpm in a Sorvall Legend RT centrifuge at R-T. The supernatant was discarded and the pellets washed once with water before being centrifuged once again. Pellets were resuspended in 500μL genomic DNA (gDNA) extract buffer (50mM Tris-HCl [pH 7.6], 20mM EDTA, 1% SDS) and transferred to a 2.0mL ribolyser tube. Glass beads (0.5mm diameter, BioSpec) were added to a level just above the liquid meniscus, and cells lysed 5 times for 10s at 4.0m/s speed on a Hybaid ribolyser), with minute on ice between each one. A 1.8mL screw-cap tube was placed in the bottom of a 15mL Falcon tube. A hole was made in the bottom of the ribolyser tube using a hot needle and this tube placed on top of the screw-cap tube. The supernatant was subsequently collected by centrifuging for 30s at 2200rpm in a Sorvall Legend RT centrifuge at R-T. Tubes were briefly vortexed, incubated for 10min at 70˚C in a hot block, then 200μL 5M potassium acetate (Fisher Scientific) and 150μL 5M NaCl were added. Tubes were placed on ice for a minimum of 20min, and then centrifuged for 20min at 13,000 rpm in a desktop microcentrifuge at 4˚C. The supernatant was transferred to a fresh microfuge tube and mixed with 1/3 volume 30% (w/v) PEG-6000 (Sigma) and placed on ice for a

minimum of 10min. DNA was harvested by centrifuging for 10min at 13,000 rpm in a desktop microcentrifuge at 4˚C. Pellets were resuspended in 40μL 1x TE buffer (10mM Tris-HCl [pH 7.6], 1mM EDTA). RNA was removed by adding 4μL RNase A (10mg/mL,) to the suspension and incubating for 35 min at 37˚C. Finally, tubes were incubated overnight at 4˚C to ensure the DNA pellet had fully resuspended into the TE buffer.

2.5.3 Purification of DNA

DNA was purified from restriction endonuclease (RE) digests and/or PCR amplifications using a "DNA purification system" (Wizard), as per manufacturer's instructions. DNA was eluted in 50μL 1x TE [pH 7.6].

2.5.4 Polymerase chain reaction (PCR)

Primers were designed using the Saccharomyces Genome Database (*http://www.yeastgenome.org/*). Oligonucleotides were synthesised at Eurogentec and supplied at 100μM concentration. All primers used in this study are listed in Table 2.3.

Genomic DNA amplifications for cloning and probe construction were performed using the "Thermoprime Plus DNA Polymerase system" (ABgene) with the following conditions; 1x Taq polymerase reaction buffer. 1.5mM Mg^{2+}, 0.2mM each of dATP, dCTP, dGTP and dTTP, 100pmol of each single-stranded oligonucleotide primer, 5U of Taq polymerase and DNA template as specified for each individual PCR reaction, in a total volume of 100μL. The PCR reaction mixture was subjected to the following temperature cycle in a 200μL PCR tube using a thermal cycler (T3 Thermocycler^{TM}; Biometra): 94˚C/5min, followed by 30 cycles of 94˚C/30s, 58˚C/30s and 72˚C/1 min and finally 72˚C for 5 min. "Hot-start PCR" was used for each reaction. Reaction products were analysed by RE digestion and agarose gel electrophoresis.

2.5.5 Restriction endonucleases and DNA-modifying enzymes

DNA was incubated with the 40U of indicated RE in the appropriate RE buffer at 37˚C. REs were supplied from Roche or New England Biolabs (NEB). Genomic DNA digestions for Southern blot analysis were incubated overnight, whilst RE digestion of plasmids or PCR products were incubated for a maximum of 2.5h. Calf intestinal phosphatase (CIP; Roche) was added to the reaction mixture of plasmid vector DNA after 1.5h incubation of the RE digest.

2.5.6 DNA ligations

DNA fragments were ligated using T4 DNA ligase (NEB) in a total volume of 20μL reaction mixture containing: 1x T4 DNA ligase buffer (50mM Tris-HCl [pH 7.5], 10mM $MgCl_2$, 10mM DTT, 1mM ATP, 25μg/mL bovine serum albumin; NEB) and 3U T4 DNA ligase (Promega). The ligation mixture was incubated for 1h at R-T or overnight at 18˚C, and 10μL used for transformation of *E. coli*.

2.5.7 Agarose gel electrophoresis of DNA

Agarose gels were prepared on Owl horizontal slab minigel apparatus (8.3 x 7cm; 50mL gel volume, or 14.9 x 14cm; 150mL gel volume). Agarose (0.7% electrophoresis grade, Invitrogen) was dissolved in electrophoresis buffer (1x TBE), and gels cast with a well-forming comb in place. DNA loading buffer was added to samples prior to loading into the pre-cast wells. Electrophoresis buffer was added to cover the gels by 2-3mm, and 2-5μL of ethidium bromide (10mg/mL; Life Technologies) was added in the buffer prior to running the gel. Small gels (50mL gel volume) were run at 80V constant voltage (6V/cm), large gels (150mL volume) at 110V constant voltage (5V/cm), for 1.5-2.0h. A 1kb DNA ladder (Invitrogen) was used for size estimation of DNA fragments.

2.5.8 Pulsed-field gel electrophoresis (PFGE)

Genomic DNA samples were prepared in low melting point agarose plugs (adapted from Louis & Haber, 1990 and Border *et al*., 1999). Briefly, cells were inoculated into 3-5 mL YPD in 15mL falcon tubes and incubated overnight at 30˚C (*ts* strains at 23˚C). Cells were harvested by centrifuging for 2min at 2200rpm in a Sorvall Legend RT centrifuge at R-T. Pellets were resuspended in 1mL ice-cold 50mM EDTA and liquid transferred to new 1.5mL microfuge tubes. Cells were centrifuged for 10s at 13,000rpm in a desktop microcentrifuge at R-T, washed once more in 1mL ice-cold 50mM EDTA, resuspended in 50µL 50mM EDTA and kept on ice. Fifty microlitres of "solution 1" (SCE [1M sorbitol, 0.1M sodium citrate, 60mM EDTA], 50µL/mL β-mercaptoethanol, 1mg/mL 100T zymolyase) and 150µL of LMP agarose mix (1% LMP agarose, 0.125M EDTA) were added for each 0.03g of cells, mixed by careful pipetting and dispensed into dry plug formers. Once set, plugs were incubated in "solution 2" (0.45M EDTA, 10mM Tris-HCl [pH 7.4], 7.5% β-mercaptoethanol, 10µg/mL RNase A) for a minimum of 2h at 37˚C. Tubes were chilled on ice for 10min, aspirated and subsequently incubated overnight in "solution 3" (0.25M EDTA, 10mMTris-HCl [pH 7.4], 1% sarkosyl). Solution 3 was removed and plugs stored in storage buffer (50mM EDTA, 50% glycerol) at –20˚C. One third to one half of a plug was used for analysis. Electrophoresis was performed for 16h at 190V with 90s pulses, followed by 16h with 60s pulses, in 1x TBE at 10˚C on a CHEF-DR III System (BioRad).

2.5.9 Detection and photography of DNA agarose and pulse-field gels

DNA gels were exposed to short wave ultraviolet light (254nm) transilluminator and photographed using a "BioDoc-It" system (UVP).

2.5.10 Southern blot analysis

2.5.10.1 Transfer

Genomic DNA was digested with the appropriate RE and then electrophoresed on a 0.7% 1x TBE agarose gel. DNA was depurinated by submerging the gel in 0.25M

HCl for 15min. Gels were then rinsed twice in dH_2O and denatured in 0.4N NaOH for 30min. Blotting apparatus was set up as described in Maniatis *et al.*, (1989) and DNA transferred onto Amersham Hybond™-XL membranes (GE Healthcare) overnight. Blots were neutralised in 50mM "phosphate buffer" (0.28M $NaH_2PO_4.H_2O$, 0.71M Na_2HPO_4) and immediately hybridised or stored at 4˚C.

2.5.10.2 Hybridisation

Transferred blots were rinsed for a minimum of 15min in 50mM phosphate buffer. Hybridisation tubes were kept at 65˚C and prepared with two 10min washes: one with 50mM phosphate buffer followed with one in "prehybridisation buffer" (7% SDS, 0.5M phosphate buffer, 1mM EDTA). Blots were placed in the tubes with fresh prehybridisation buffer. Hybridisation probes were prepared by PCR amplification of genomic DNA and radioactively labelled using the "Prime-It RmT Random Primer Labeling Kit" (Stratagene) as per manufacturer's instructions, using α-^{32}P-dCTP (GE Healthcare). The probe was denatured by incubating at >98˚C for 2min, added to fresh prehybridisation buffer in the tubes and blots hybridised overnight. The following day blots were washed 3 times for 20min in "wash buffer" (1% SDS, 40mM phosphate buffer, 1mM EDTA) at 65˚C, blot-dried with paper towels and then covered with Saran wrap. Signals detection and visualization were carried out using a phosphoimager.

Table 2.1. Commonly used buffers and solutions.

Buffer/ solution	*Constituents*[a]
DNA loading buffer (5x)	0.2% bromophenol blue, 30% glycerol in water
PCR buffer	20mM Tris [pH 8.4], 50mM KCl
Phosphate buffer	0.28M sodium phosphate monobasic monohydrate, 0.71M di-sodium hydrogen orthophosphate anhydrous
PFGE storage buffer	50% glycerol, 50mM EDTA
DNA buffer	50mM Tris-HCl [pH 7.6], 1% SDS, 20mM EDTA
TAE	40mM Tris-acetate, 1mM EDTA
TBE	90mM Tris-phosphate, 2mM EDTA
TE [pH 7.6]	10mM Tris-HCl [pH 7.6], 1mM EDTA [pH 8.0]

[a] Buffers and solutions are listed at the normal working concentration (1x), unless specified. All percentages are given as [w/v].

Table 2.2. Yeast strains used in this study.

[a] All haploid and diploid strains are isogenic to either RCY2549 (MAT**a**, *ho::LYS2* or *ho::hisG, ura3*, *lys2*, *leu2::hisG*) or RCY2458 (*ho::LYS2/"* or *ho::LYS2/ho::hisG* or *ho::hisG/", ura3/", lys2/", leu2::hisG/"*).

[b] All haploid strains are *MAT**a*** unless stated otherwise

Strain	*Relevant genotype*[a]	*Source*
<u>*Haploids*</u>[b]		
JDCY228	*ChrIII-139k::hisG-URA3-hisG*	This study
JDCY230	*ChrIII-139k::hisG-URA3-hisG*	This study
JDCY232	*ChrIII-230k::hisG-URA3-hisG*	This study
JDCY233	*ChrIII-230k::hisG-URA3-hisG*	This study
JDCY235	*ChrIII-242k::hisG-URA3-hisG*	This study
JDCY237	*ChrIII-242k::hisG-URA3-hisG*	This study
JDCY239	*ChrIII-216k::hisG-URA3-hisG*	This study
JDCY243	*ChrIII-216k::hisG-URA3-hisG*	This study
JDCY291	*mec1Δ::LEU2, sml1Δ::HphMx4, ChrIII-242k::hisG-URA3-hisG*	This study
JDCY293	*sml1Δ::HphMx4, ChrIII-242k::hisG-URA3-hisG*	This study
JDCY297	*arg4N, rrm3Δ:: HphMx4, ChrIII-139k::hisG-URA3-hisG*	This study

JDCY298	*arg4N, rrm3Δ:: HphMx4, ChrIII-242k::hisG-URA3-hisG*	This study
JDCY300	*arg4N, rrm3Δ:: HphMx4, ChrIII-230k::hisG-URA3-hisG*	This study
JDCY303	*arg4N, rrm3Δ:: HphMx4, ChrIII-139k::hisG-URA3-hisG*	This study
JDCY305	*mec1Δ::LEU2, arg4NΔ::mec1-40-KanMX4, ChrIII-230k::hisG-URA3-hisG*	This study
JDCY306	*arg4N, rrm3Δ:: HphMx4, ChrIII-216k::hisG-URA3-hisG*	This study
JDCY307	*rrm3Δ::HphMx4, ChrIII-216k::hisG-URA3-hisG*	This study
JDCY326	*mec1Δ::LEU2, arg4NΔ::mec1-40-KanMX4, ChrIII-242k::hisG-URA3-hisG*	This study
JDCY328	*mec1Δ::LEU2, arg4NΔ::mec1-40-KanMX4, ChrIII-139k::hisG-URA3-hisG*	This study
JDCY329	*sml1Δ::HphMx4, ChrIII-230k::hisG-URA3-hisG*	This study
JDCY331	*sml1Δ::HphMx4, mec1Δ::LEU2, ChrIII-230k::hisG-URA3-hisG*	This study
JDCY333	*sml1Δ::HphMx4, ChrIII-139k::hisG-URA3-hisG*	This study
JDCY335	*sml1Δ::HphMx4, mec1Δ::LEU2, ChrIII-139k::hisG-URA3-hisG*	This study
JDCY337	*sml1Δ::HphMx4, mec1Δ::LEU2, ChrIII-230k::hisG-URA3-hisG*	This study
JDCY338	*sml1Δ::HphMx4, ChrIII-230k::hisG-URA3-hisG*	This study
JDCY341	*sml1Δ::HphMx4, mec1Δ::LEU2, ChrIII-139k::hisG-URA3-hisG*	This study
JDCY344	*sml1Δ::HphMx4, ChrIII-139k::hisG-URA3-hisG*	This study
JDCY345	*rrm3Δ::HphMx4, ChrIII-230k::hisG-URA3-hisG*	This study
JDCY346	*arg4N, rrm3Δ::HphMx4, ChrIII-230k::hisG-URA3-hisG*	This study
JDCY348	*sml1Δ::HphMx4, mec1Δ::LEU2, ChrIII-242k::hisG-URA3-hisG*	This study

JDCY350	*sml1Δ::HphMx4, ChrIII-242k::hisG-URA3-hisG*	This study
JDCY351	*mec1Δ::LEU2, arg4NΔ::mec1-40-KanMX4, ChrIII-230k::hisG-URA3-hisG*	This study
JDCY353	*sml1Δ::HphMx4, mec1Δ::LEU2, ChrIII-216k::hisG-URA3-hisG*	This study
JDCY355	*sml1Δ::HphMx4, ChrIII-216k::hisG-URA3-hisG*	This study
JDCY357	*sml1Δ::HphMx4, ChrIII-216k::hisG-URA3-hisG*	This study
JDCY359	*sml1Δ::HphMx4, mec1Δ::LEU2, ChrIII-216k::hisG-URA3-hisG*	This study
JDCY360	*mec1Δ::LEU2, arg4NΔ::mec1-40-KanMX4, ChrIII-216k::hisG-URA3-hisG*	This study
JDCY362	*mec1Δ::LEU2, arg4NΔ::mec1-40-KanMX4, ChrIII-216k::hisG-URA3-hisG*	This study
JDCY378	*TOP2::top2-1, ChrIII-216k::hisG-URA3-hisG*	This study
JDCY380	*TOP2::top2-1, ChrIII-216k::hisG-URA3-hisG*	This study
JDCY382	*TOP2::top2-1, ChrIII-242k::hisG-URA3-hisG*	This study
JDCY384	*TOP2::top2-1, ChrIII-230k::hisG-URA3-hisG*	This study
JDCY385	*TOP2::top2-1, ChrIII-230k::hisG-URA3-hisG*	This study
JDCY388	*TOP2::top2-1, ChrIII-139k::hisG-URA3-hisG*	This study
JDCY390	*TOP2::top2-1, ChrIII-139k::hisG-URA3-hisG*	This study
JDCY399	*mec1Δ::LEU2, arg4NΔ::mec1-40-KanMX4, ChrIII-242k::hisG-URA3-hisG*	This study
JDCY415	*TOP2::top2-1, ChrIII-242k::hisG-URA3-hisG*	This study
JDCY463	*ChrIII-53k::hisG-URA3-hisG*	This study
JDCY465	*ChrIII-53k::hisG-URA3-hisG*	This study

JDCY478	*sml1Δ::HphMx4, mec1Δ::LEU2, ChrIII-53k::hisG-URA3-hisG*	This study
JDCY479	*sml1Δ::HphMx4, ChrIII-53k::hisG-URA3-hisG*	This study
JDCY480	*rrm3Δ::HphMx4, ChrIII-53k::hisG-URA3-hisG*	This study
JDCY481	*rrm3Δ::HphMx4, ChrIII-53k::hisG-URA3-hisG*	This study
JDCY482	*TOP2::top2-1, ChrIII-53k::hisG-URA3-hisG*	This study
JDCY483	*TOP2::top2-1, ChrIII-53k::hisG-URA3-hisG*	This study
JDCY484	*mec1Δ::LEU2, arg4NΔ::mec1-40-KanMX4, ChrIII-53k::hisG-URA3-hisG*	This study
JDCY493	*mec1Δ::LEU2, arg4NΔ::mec1-40-KanMX4, ChrIII-139k::hisG-URA3-hisG*	This study
JDCY495	*mec1Δ::LEU2, arg4NΔ::mec1-40-KanMX4, ChrIII-53k::hisG-URA3-hisG*	This study
JDCY498	*sml1Δ::HphMx4, ChrIII-53k::hisG-URA3-hisG*	This study
JDCY499	*sml1Δ::HphMx4, mec1Δ::LEU2, ChrIII-53k::hisG-URA3-hisG*	This study
JDCY517	*ChrIII-230k::hisG-URA3-hisG*	This study
JDCY521	*ChrIII-236k::hisG-URA3-hisG*	This study
NHY30	*TOP2::top2-1*	Cha lab
RCY426	*mec1Δ::LEU2, ade2::LK, his4x, arg4NΔ::mec1-40-KanMX4*	Cha lab
RCY427	*mec1Δ::LEU2, ade2::LK, his4x, arg4NΔ::mec1-40-KanMX4, MATα*	Cha lab
RCY2459	*ho::LYS2, ura3, lys2, leu2::hisG*	Cha lab
RCY2460	*ho::LYS2, ura3, lys2, leu2::hisG, MATα*	Cha lab

Diploids[c]		
JDCY179	*his4B::LEU2*/+, *ChrIII-139k::hisG-URA3-hisG*/+	This study
JDCY181	*his4B::LEU2*/+, *ChrIII-139k::hisG-URA3-hisG*/+	This study
JDCY185	*his4B::LEU2*/+, *ChrIII-230k::hisG-URA3-hisG*/+	This study
JDCY187	*his4B::LEU2*/+, *ChrIII-230k::hisG-URA3-hisG*/+	This study
JDCY189	*his4B::LEU2*/+, *ChrIII-242k::hisG-URA3-hisG*/+	This study
JDCY191	*his4B::LEU2*/+, *ChrIII-242k::hisG-URA3-hisG*/+	This study
JDCY199	*his4B::LEU2*/+, *ChrIII-216k::hisG-URA3-hisG*/+	This study
JDCY203	*his4B::LEU2*/+, *ChrIII-216k::hisG-URA3-hisG*/+	This study
JDCY309	*ade2::LK*/+, *his4x*/+, *arg4NΔ::mec1-40-KanMX4/", ChrIII-230k::hisG-URA3-hisG/"*	This study
JDCY311	*his4B*/+, *sml1Δ::HphMx4/", mec1Δ::LEU2/", ChrIII-242k::hisG-URA3-hisG*/+	This study
JDCY312	*sml1Δ::HphMx4/", ChrIII-242k::hisG-URA3-hisG*/+	This study
JDCY315	*his4X*/+, *arg4N/", rrm3Δ::HphMx4/", ChrIII-242k::hisG-URA3-hisG*	This study
JDCY316	*his4X*/+, *arg4N/", rrm3Δ::HphMx4/", ChrIII-230k::hisG-URA3-hisG*	This study
JDCY364	*sml1Δ::HphMx4/", ChrIII-230k::hisG-URA3-hisG*/+	This study
JDCY365	*sml1Δ::HphMx4/", ChrIII-139k::hisG-URA3-hisG*/+	This study
JDCY366	*sml1Δ::HphMx4/", ChrIII-230k::hisG-URA3-hisG*/+	This study
JDCY367	*sml1Δ::HphMx4/", ChrIII-139k::hisG-URA3-hisG*/+	This study
JDCY368	*his4B*/+, *sml1Δ::HphMx4/", mec1Δ::LEU2/", ChrIII-139k::hisG-URA3-hisG*/+	This study

JDCY369	*ade2::LK/+, his4x/+, mec1Δ::LEU2/", arg4NΔ::mec1-40-KanMX4/", ChrIII-139k::hisG-URA3-hisG/+*	This study
JDCY370	*ade2::LK/+, his4x/+, mec1Δ::LEU2/", arg4NΔ::mec1-40-KanMX4/", ChrIII-242k::hisG-URA3-hisG/+*	This study
JDCY374	*his4B/+, sml1Δ::HphMx4/", mec1Δ::LEU2/", ChrIII-139k::hisG-URA3-hisG/+*	This study
JDCY375	*his4B/+, sml1Δ::HphMx4/", mec1Δ::LEU2/", ChrIII-139k::hisG-URA3-hisG/+*	This study
JDCY376	*sml1Δ::HphMx4/", ChrIII-242k::hisG-URA3-hisG/+*	This study
JDCY391	*ade2::LK/+, his4x/+, mec1Δ::LEU2/", arg4NΔ::mec1-40-KanMX4/", ChrIII-230k::hisG-URA3-hisG/+*	This study
JDCY392	*ade2::LK/+, his4x/+, mec1Δ::LEU2/", arg4NΔ::mec1-40-KanMX4/", ChrIII-216k::hisG-URA3-hisG/+*	This study
JDCY393	*ade2::LK/+, his4x/+, mec1Δ::LEU2/", arg4NΔ::mec1-40-KanMX4/", ChrIII-216k::hisG-URA3-hisG/+*	This study
JDCY394	*his4B/+, sml1Δ::HphMx4/", mec1Δ::LEU2/", ChrIII-242k::hisG-URA3-hisG/+*	This study
JDCY395	*his4B/+, sml1Δ::HphMx4/", mec1Δ::LEU2/", ChrIII-216k::hisG-URA3-hisG/+*	This study
JDCY396	*his4B/+, sml1Δ::HphMx4/", mec1Δ::LEU2/", ChrIII-216k::hisG-URA3-hisG/+*	This study
JDCY397	*sml1Δ::HphMx4/", ChrIII-216k::hisG-URA3-hisG/+*	This study
JDCY398	*sml1Δ::HphMx4/", ChrIII-216k::hisG-URA3-hisG/+*	This study
JDCY400	*his4X/+, arg4N/+, rrm3Δ::HphMx4/", ChrIII-230k::hisG-URA3-hisG/+*	This study
JDCY401	*his4x/+, top2-1/", ChrIII-139k::hisG-URA3-hisG/+*	This study
JDCY402	*his4x/+, top2-1/", ChrIII-255k::hisG-URA3-hisG/+*	This study
JDCY403	*his4x/+, top2-1/", ChrIII-230k::hisG-URA3-hisG/+*	This study
JDCY404	*his4x/+, top2-1/", ChrIII-216k::hisG-URA3-hisG/+*	This study

JDCY406	*his4X/+, arg4N/", rrm3Δ::HphMx4/", ChrIII-216k::hisG-URA3-hisG/+*	This study
JDCY407	*his4X/+, arg4N/", rrm3Δ::HphMx4/", ChrIII-139k::hisG-URA3-hisG/+*	This study
JDCY408	*his4X/+, arg4N/+, rrm3Δ::HphMx4/", ChrIII-216k::hisG-URA3-hisG/+*	This study
JDCY409	*his4x/+, top2-1/", ChrIII-139k::hisG-URA3-hisG/+*	This study
JDCY410	*his4x/+, top2-1/", ChrIII-242k::hisG-URA3-hisG/+*	This study
JDCY411	*arg4N/", rrm3Δ::HphMx4/", ChrIII-230k::hisG-URA3-hisG/+*	This study
JDCY416	*his4X/+, top2-1/", ChrIII-242k::hisG-URA3-hisG/+*	This study
JDCY417	*his4X/+, top2-1/", ChrIII-216k::hisG-URA3-hisG/+*	This study
JDCY427	*his4B/+, sml1Δ::HphMx4/", mec1Δ::LEU2/", ChrIII-230k::hisG-URA3-hisG/+*	This study
JDCY429	*his4X/+, arg4N/", rrm3Δ::HphMx4/", ChrIII-139k::hisG-URA3-hisG/+*	This study
JDCY444	*ade2::LK/+, his4x/+, mec1Δ::LEU2/", arg4NΔ::mec1-40-KanMX4/", ChrIII-242k::hisG-URA3-hisG/+*	This study
JDCY469	*ChrIII-53k::hisG-URA3-hisG/+*	This study
JDCY477	*ChrIII-53k::hisG-URA3-hisG/+*	This study
JDCY486	*his4B/+, sml1Δ::HphMx4/", mec1Δ::LEU2/", ChrIII-53k::hisG-URA3-hisG/+*	This study
JDCY487	*sml1Δ::HphMx4/", ChrIII-53k::hisG-URA3-hisG/+*	This study
JDCY488	*ade2::LK/+, his4x/+, mec1Δ::LEU2/", arg4NΔ::mec1-40-KanMX4/", ChrIII-53k::hisG-URA3-hisG/+*	This study
JDCY489	*his4x/+, TOP2::top2-1/", ChrIII-53k::hisG-URA3-hisG/+*	This study
JDCY490	*his4x/+, TOP2::top2-1/", ChrIII-53k::hisG-URA3-hisG/+*	This study
JDCY491	*his4X/+, arg4N/+, rrm3Δ::HphMx4/", ChrIII-53k::hisG-URA3-hisG/+*	This study

JDCY492	*his4X/+, arg4N/+, rrm3Δ::HphMx4/", ChrIII-53k::hisG-URA3-hisG/+*	This study
JDCY499	*sml1Δ::HphMx4/", mec1Δ::LEU2/", ChrIII-53k::hisG-URA3-hisG/+*	This study
JDCY501	*ade2::LK/+, his4x/+, mec1Δ::LEU2/", arg4N::mec1-40-KanMX4/", ChrIII-53k::hisG-URA3-hisG/+*	This study
JDCY502	*ade2::LK/+, his4x/+, mec1Δ::LEU2/", arg4N::mec1-40-KanMX4/", ChrIII-139k::hisG-URA3-hisG/+*	This study
JDCY503	*sml1Δ::HphMx4/", ChrIII-53k::hisG-URA3-hisG/+*	This study
JDCY524	*his4B::LEU2/+, ChrIII-230k::hisG-URA3-hisG/+*	This study
JDCY526	*his4B::LEU2/+, ChrIII-230k::hisG-URA3-hisG/+*	This study
RCY681	*ade2::LK, his4x, arg4N, mec1-4-URA3*	Cha lab

Table 2.3. Oligonucleotides used in this study.

Primer	*Sequence (5'-3')*	*Use*
53k_F1	GGG GCG GCC GCA AGG TGC ACT TGA AGA TTG C	Strain construction
53k_R1	AGA GTG CAT GCA GAT CTA TGT ATC AGT AAT TTA GTG AGC	Strain construction
53k_F2	TAC ATA GAT CTG CAT GCA CTC TAA AGG AGC TGG GC	Strain construction
53k_R2	GGG GCG GCC GCG TCG ACA GTT CTC TCA AGG	Strain construction
139k_F1	GGG GCG GCC GCT CAG TAT ATA ATG ATC TTT TGC	Strain construction
139k_R1	TTA TAG CAT GCA GAT CTG TTT TGT AAG AAA TTA TAC TTC C	Strain construction
139k_F2	AAA ACA GAT CTG CAT GCT ATA ACA AGA TCG TCT AAG TAA C	Strain construction
139k_R2	GGG GCG GCC GCC GTA CGT TAG TGA AAC ATC C	Strain construction
216k_F1	GGG GCG GCC GCG ATG GTT TTT CTC TTG GTG G	Strain construction
216k_R1	AGA GTG CAT GCA GAT CTT TCA TTC TAA GAA AGA AGG AGC	Strain construction
216k_F2	ATG AAA GAT CTG CAT GCA CTC TTG GCA GAC TCC TTG	Strain construction
216k_R2	GGG GCG GCC GCT CTT AGT AGA GAG CTG GAG G	Strain construction
230k_F1	GGG GCG GCC GCA ATA CTG CAA ATA CCA AAT ACC	Strain construction
230k_R1	TAG CGG CAT GCA GAT CTA ATT ATA CAA TAG ACA AGA CC	Strain construction
230k_F2	TAA TTA GAT CTG CAT GCC GCT AGT ATT TGT TTT GCA TTG	Strain construction
230k_R2	GGG GCG GCC GCT TAC GGA CGA AAT ACA AAT GC	Strain construction

242k_F1	GGG GCG GCC GCA CAC AAA CTT CCT CAA GTG G	Strain construction
242k_R1	CTG TGG CAT GCA GAT CTA ACG CTT CAA GTA ACC TAC G	Strain construction
242k_F2	GCG TTA GAT CTG CAT GCC ACA GTT CTC ATT TAC ACT G	Strain construction
242k_R2	GGG GCG GCC GCG TAC TGT TGA ACA AAG GTG C	Strain construction
hisG_FC1	ACA TGG TCA GCA GCG AAA CC	Probe for Southern analysis
145_RC1	TCT CCA GTT GGG GAA CTT GC	Probe for Southern analysis
210_RC1	ACA AGT ACA CGG GTT CGA CC	Probe for Southern analysis
225_RC1	TTA TCA CCC TCG TCT TCG CC	Probe for Southern analysis
53k_LF	CAA TTA GAC ATG CTG CTT GC	Probe for Southern analysis
53k_LR	GGC TTT GTG TAA GTC GTC G	Probe for Southern analysis
53k_RF	TGT CTA CGA TTT CAG TGG G	Probe for Southern analysis
53k_RR	TTA TCT GCA GGG TTT GAT GC	Probe for Southern analysis
242k_LF	GAA GGG ATT GAT TCA GAA GC	Probe for Southern analysis
242k_LR	CAG CAT TAT CCA CAA GTA CC	Probe for Southern analysis
242k_RF	TGT GCA AGA GTG AGC TAC C	Probe for Southern analysis
242k_RR	TCT GGT TCA ACG CAC TTG G	Probe for Southern analysis
PRS3_F1	ATC AGA ATA CTC TTC GGA GG	+ve control for Colony PCR
PRS3_R1	TTT CCT TAC ACC ATC CTT GG	+ve control for Colony PCR
C_PCR_URA3_F1	TGT CGA AAG CTA CAT ATA AGG	Colony PCR

C_PCR_URA3_R1	TCT CAA ATA TGC TTC CCA GC	Colony PCR
C_PCR_hisG_F1	CTG TTC TGG GAA ACC ATG G	Colony PCR
C_PCR_hisG_R1	TGC ATA GCT ATG CGT AAA CG	Colony PCR
139k_C_PCR_F1	TCG AGA GGA TAA GGC TAG C	Colony PCR
139k_C_PCR_R1	TTG CAA GAG GAA CGA TAA CC	Colony PCR
216k_C_PCR_F1	TCT TCT TTA CTG GGA GTT CC	Colony PCR
216k_C_PCR_R1	TAC AAC GAT CCT AAA CAG CG	Colony PCR
230k_C_PCR_F1	ATA GTA CGA AAC TAT ACA CC	Colony PCR
230k_C_PCR_R1	CAG CGT AAT AAT GTG GTA GC	Colony PCR
242k_C_PCR_F1	TGC AAC CAA CTA GAA TCA GG	Colony PCR
242k_C_PCR_R1	TCA ACT GGA AAT GCT TTC CC	Colony PCR

Table 2.4. Plasmids used in this study.

"L" and "R" are 500bp genomic fragments that flank the integration point, used for homologous recombination of the transformation cassette (ie. pJDCX-hUh) into the DNA: see Section 3.2, page 77. Amp^R: ampicillin-resistance.

Plasmid name	*Relevant features*	*Use*	*Reference/ Source*
pRSC081	Amp^R	Contains polyclonal site	Cha lab
pNKY51	*hisG-URA3-hisG*	*URA3* marker cassette	Alani *et al*. (1987)
pJDC53	Amp^R, 53kb L-R	53kb L-R DNA cloned into pRSC081	This study
pJDC139	Amp^R, 139kb L-R	139kb L-R DNA cloned into pRSC081	This study
pJDC216	Amp^R, 216kb L-R	216kb L-R DNA cloned into pRSC081	This study
pJDC230	Amp^R, 230kb L-R	230kb L-R DNA cloned into pRSC081	This study
pJDC242	Amp^R, 242kb L-R	242kb L-R DNA cloned into pRSC081	This study
pJDC53-hUh	Amp^R, 53kb L-R, *hisG-URA3-hisG*	*hisG-URA3-hisG* cloned into pJDC53	This study
pJDC139-hUh	Amp^R, 139kb L-R, *hisG-URA3-hisG*	*hisG-URA3-hisG* cloned into pJDC139	This study
pJDC216-hUh	Amp^R, 216kb L-R, *hisG-URA3-hisG*	*hisG-URA3-hisG* cloned into pJDC216	This study
pJDC230-hUh	Amp^R, 230kb L-R, *hisG-URA3-hisG*	*hisG-URA3-hisG* cloned into pJDC230	This study
pJDC242-hUh	Amp^R, 242kb L-R, *hisG-URA3-hisG*	*hisG-URA3-hisG* cloned into pJDC242	This study

Table 2.5. Suppliers of chemicals, reagents and equipment.

Supplier	*Full name and location*
Apollo	Apollo Scientific Ltd, Bradbury, Stockport, UK
BD	Becton, Dickinson and Co, Sparks, MD 21152, USA
Biorad	Biorad Laboratories, Hercules, CA, USA
Difco	Difco Laboratories, Detroit, MI, USA
Fisher Scientific	Fisher Scientific UK Ltd, Loughborough, UK
GE Healthcare	GE Healthcare Life Sciences, Buckinghamshire, UK
Invitrogen	Invitrogen Life Technologies, Carlsbad, CA, USA
Kodak	Eastman Kodak Company, Rochester, NY, USA
Life Technologies	Life Technologies Inc, MD, USA
Microsoft	Microsoft Corporation, USA
Millipore	Millipore Corporation, Bedford, MA, USA
NEB	New England Biolabs Inc, MA, USA
Promega	Promega Corporation, Madison, WI, USA
Roche	Roche Diagnostics GmbH, Mannheim, Germany
Sigma	Sigma Chemical Company, St. Louis, MO, USA

Chapter 3.

Yeast strain construction

3.1 Locations chosen for addressing potential *cis*-effects on mutagenesis

The aim of this thesis was to identify *cis* sequences and *trans*-acting factors that contribute to genetic instability within the genome of the budding yeast, *S. cerevisiae*. As one of the specific aims was to study potential genomic instability within RSZs, and RSZs have only been accurately mapped in ChrIII, this chromosome was chosen for study. Figure 3.1 shows that all six RSZs in ChrIII occur at or near to a replication termination site, but only two co-localise with retrotransposons. One RSZ from each class was therefore chosen to test if the presence of a retrotransposon affected the rate of mutation. The first location to be targeted, 53kb from the left telomere of ChrIII, is within both a replication termination region and a RSZ. The second locus, 139kb, is also within a RSZ and replication termination region but also has a Ty2 type retrotransposon 4kb downstream of its location. In comparison, the closest retrotransposon-like elements to the 53kb locus are a Ty5-1 element 2.5kb from the beginning of ChrIII, and the same Ty2 nearest the 139kb locus, 93kb away. Two tRNA genes are also in close proximity to the 139kb region: one is 2kb upstream and the other is 5kb downstream. No tRNA genes are close to the 53kb region.

The 53kb and 139kb loci are associated with replication termination sites as well as RSZs. To examine if replication termination alone contributes to genetic instability, a known termination site not within a RSZ or near to Ty elements was chosen (216kb). It might be predicted that mutagenesis at this locus will be higher than non-termination regions, since prokaryotic replication termination sites are known recombination hotspots (Bierne *et al*., 1991; Nishitani *et al*., 1993; Louarn *et al*., 1994; Horiuchi *et al*., 1995).

A

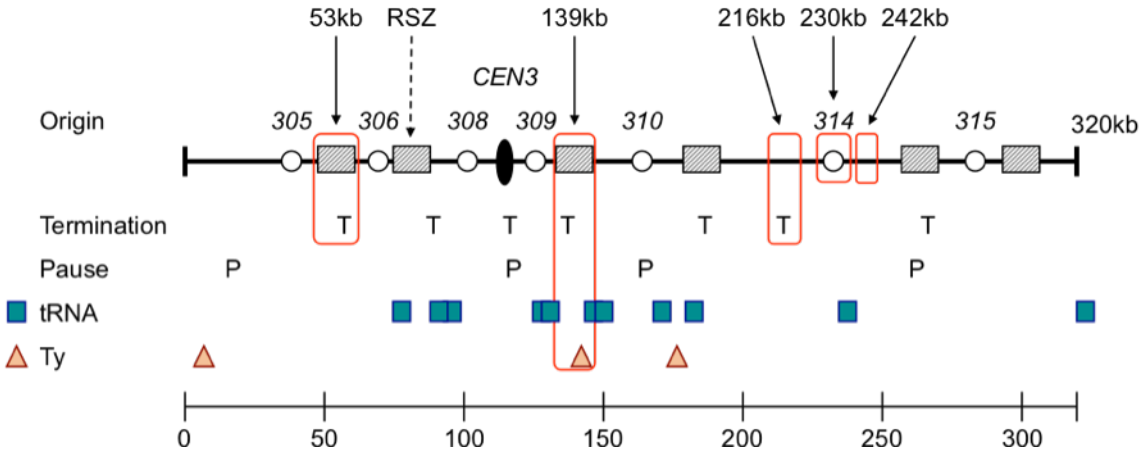

B

Distance from left telomere (kb)[§]	Notable features[a]				
	RSZ	Replication Termination	Ty element	Replication Origin	tRNA
53	√	√	-	-	-
139	√	√	√	-	√
216	-	√	-	-	-
230	-	-	-	√	√
242	-	-	-	-	-

Figure 3.1. Locations within ChrIII tested for the rate of *URA3* inactivation.

(A) Locations to be tested and their associated chromosomal features are outlined in red. The numbers along the top represent the distance in kb the five locations are from the left telomere (as is the bar along the bottom). Grey boxes represent RSZs, open circles replication origins, and the filled-in oval, the centromere. Abbreviations used are: T or Termination, DNA replication termination site; P or Pause, replication fork pause site; Ty, Ty element. Relevant features are not drawn to scale.

(B) [§]Distances shown are calculated using the strain data for S228C in the Saccharomyces Genome Database™ (www.yeastgenome.org) and SK1 strain information published by Baudat & Nicolas (1997). Actual distances from the left telomere of ChrIII in SK1 are 52.5, 138.5, 215.5, 230.0 and 241.5kb, respectively, to the nearest 0.5kb. [a]All locations were checked to ensure the regions studied contained the specified chromosomal feature(s) in the SK1 strain.

The DNA replication origin *ARS314* (*ARS315* in S228C) is a highly active origin, used in more than 90% of cell cycles (Poloumienko *et al*., 2001). To see if the close proximity of a very efficient origin affected mutation rates, the 230kb region, less than 0.5kb away from the origin, was chosen for study. Of note is that a tRNA-Ser gene is only 2.5kb downstream of this location.

Finally, the 242kb region was chosen to examine mutation rates of a region where no known discernable features are present.

3.2 Strain construction

In order to study mutation rates at each of the five loci the *hisG-URA3-hisG* reporter construct was chosen for integration into DNA at the five locations described above (Figure 3.1). As detailed in the Introduction (Section 1.5.1), this artificial construct was originally created as a "reusable" means to disrupt gene function within yeast strains. It was reasoned that placing *URA3* between two direct repeat sequences would strongly favour the "pop-out" event upon selection for 5-FOA-resistance (Figure 1.1, page 38). The complete loss of *URA3* would then allow another round of gene disruption using the *URA3* marker again. Indeed, studies have confirmed that the majority of *ura3* derivatives from *hisG-URA3-hisG* integrants acquired 5-FOA-resistance by the pop-out event (Alani *et al*., 1987).

In order to insert the *hisG-URA3-hisG* construct into the DNA, a "transformation cassette" was created for each specific location. The step-by-step procedure used to create these is described in Figure 3.2. As *S. cerevisiae* can repair DNA by homologous recombination, this was utilised to insert the transformation cassette specific for each location into genomic DNA (Figure 3.3). This homologous recombination-based approach used to insert the intended fragment of DNA into specific genomic DNA loci is very efficient and has been used extensively by other labs (Schneider *et al*., 1995 and references cited therein). Technical details of each step are described in detail below.

Figure 3.2. Strategy for creating insertion cassettes.

(A) Primer design and PCR amplification. All primers are ~20nt in size with unique tail sequences. The tails of F1 and R2 contain a *Not*I restriction site at the 5' end, along with an additional three guanine nucleotides at the outer ends of the sequence to aid cutting in later restriction steps. F2 and R1 tails complement each other: they contain a *Bgl*II and *Sph*I restriction site, with an additional 5nt complementary to the 5' end of the R sequence and 5nt complementary to the 3' end of the L sequence, respectively. L and R genomic fragments are separately PCR-amplified from each of the five locations of interest. (B) L and R are joined in a subsequent PCR-amplification using the F1 and R2 primers to produce LR, approximately 1kb in size. (C) This fusion product is ligated into the *Not*I site of pRSC081 to produce pJDCX, where "X" is 53, 139, 216, 230 or 242. (D) The *hisG-URA3-hisG* construct is cut from pNKY51 using the *Bam*HI and *Bgl*II REs, and then ligated into the *Bgl*II site of pJDCX to generate pJDCX-hUh, as shown in (E). This plasmid contains the insertion cassette needed to create strains used for fluctuation analysis. Abbreviations used for restriction sites are: N, *Not*I; B, *Bam*HI; Bg, *Bgl*II, L, Left; R, Right; Fn, forward primer n; Rn, reverse primer n.

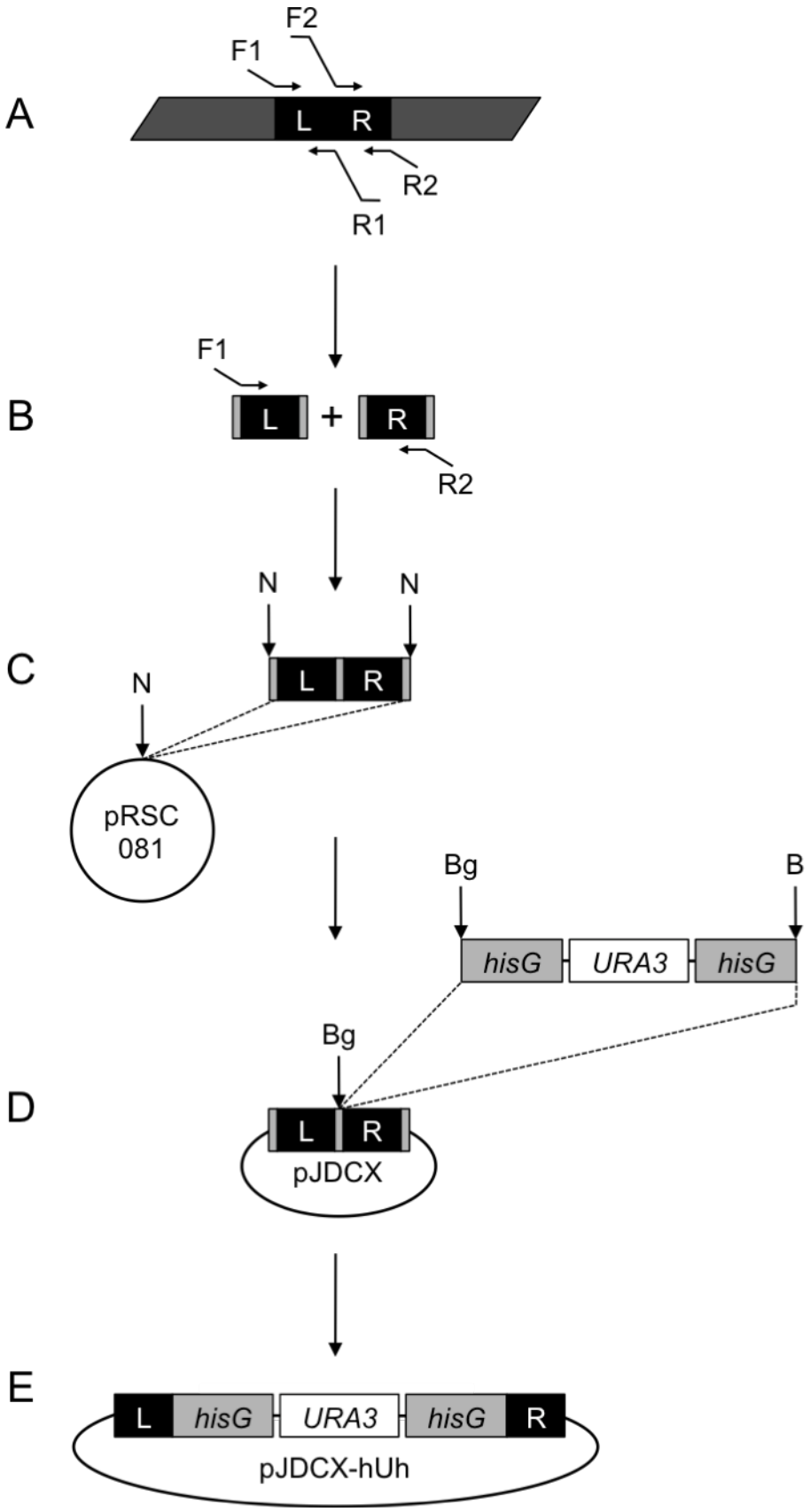

Figure 3.2. Strategy for creating insertion cassettes.

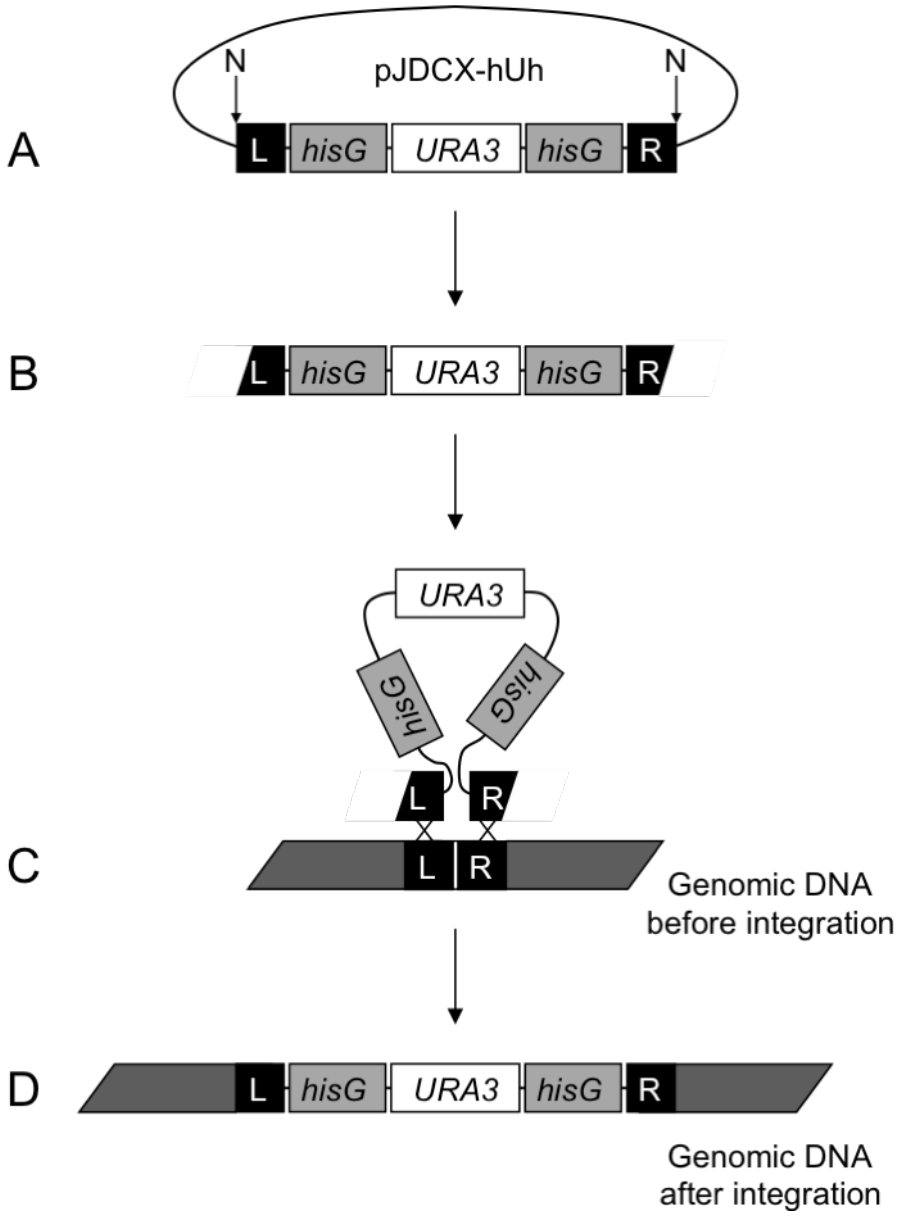

Figure 3.3. Integration of the *hisG-URA3-hisG* construct into genomic DNA *via* homologous recombination.

(A and B) The *Not*I fragment containing the *hisG-URA3-hisG* cassette is cut and gel purified. (C) Following introduction of the fragment into suitable haploid yeast cells *via* transformation, the L and R sequences within the cassette pair with their homologous sequences in the genome and initiate homologous recombination, which results in integration of the *hisG-URA3-hisG* construct between the L and R sequences in the genomic DNA, (D). Transformants are selected on plates lacking uracil, and correct integrants are identified by Southern blot analysis (see Figures 3.4-3.8). N: *Not*I restriction site.

3.2.1 Construction of hisG-URA3-hisG integration cassettes for assessing cis-effects on mutagenesis

In order to minimise any potential disruption to gene function the *hisG-URA3-hisG* construct was targeted to intergenic regions. Schneider *et al*. (1995) used a similar construct (*HA-URA3-HA*) and method to tag the 3' end of genes of interest. They found that if their construct integrated near the 3' end of a gene it inactivated the target gene in all cases examined. To minimise the likelihood of an essential gene being inactivated in the strains used in this thesis, non-essential genes were selected either side of the insertion point. Approximately 500bp of DNA was chosen either side of this point for the flanking sequences used to initiate recombination. This size was chosen as this gave a high percent likelihood (≥80%) that the transformation cassette would recombine at its specific intended location, rather than at an ectopic one. In general, smaller sequences reduce the efficiency of transformation, whilst larger sequences would not increase the efficiency significantly over that already achievable using 500bp. It was also ensured that no loss of DNA sequence occurred at the midpoint.

All of the following steps are summarised in Figure 3.2. First, the 500bp genomic fragments required for each transformation cassette were amplified from genomic DNA isolated from a WT strain. Primers specific to each location were used in a standard PCR reaction to make the "L" and "R" 500bp sequences. Conditions required to PCR amplify these fragments were optimised, and resulted in the successful production of all ten L and R fragments. The L and R fragments were then joined together by a second PCR step, using the F1 and R2 primers. This produced five products of the correct size. These first two steps had therefore created genomic fragments approximately 1kb in size with a *Bgl*II restriction site in the middle, and new *Not*I RE sites at either end. This 1kb sequence was then ligated into a plasmid vector.

Next, the *hisG-URA3-hisG* cassette was ligated separately into each plasmid at the *Bgl*II restriction site between the L and R sequences. This therefore produced five unique plasmids that contained the transformation cassette specific for each location

of interest in ChrIII. These plasmids were cut with *Not*I to produce DSB ends and were then used to separately transform WT haploid yeast cells. It was ensured that none of the *URA3* transformants were petite; otherwise slow-growing cells could affect cell counts used for estimating the rate of *URA3* loss.

3.2.2 Correct integration of the hisG-URA3-hisG construct was confirmed by Southern blot analysis

Correct integration of each *hisG-URA3-hisG* construct was initially tested by a PCR-based approach. Unfortunately this produced either many non-specific products, or no PCR product at all (data not shown). PCR amplification was attempted under fourteen different conditions: Mg^{2+} concentration was varied from 0.5-2.5mM; the amount of primer used varied from 50-150pmol; the annealing temperature was set from 58-68˚C; the template DNA used was changed and new primers were used. In no case, however, was a correctly sized PCR product achieved. This approach was therefore abandoned and instead Southern blot analysis was used to confirm that the construct had integrated at the correct location for each region of interest.

Figures 3.4–3.8 show the location of relevant RE sites used for Southern blot analysis and the expected and observed banding pattern following integration of the *hisG-URA3-hisG* cassette into the five different locations. Specific details for each location are mentioned in the accompanying figure legends. All of the constructs inserted correctly into haploid genomic DNA, as shown by the size shift from WT ChrIII to the expected sizes in the *URA3* transformants (columns 3 and 4), with two notable exceptions being for the 230kb and 242kb loci. The 230kb strains showed a non-specific band that migrated at ~7kb. As this was also present within the untransformed parental WT strains, however, this was not due to the construct inserting at an ectopic location. For the 242kb locus, the expected sizes of the migrating bands within the transformed strains were 5.1kb and 5.3kb. The Southern blot analysis revealed, however, that the bands migrated at 5.1kb (as expected) and at ~3.7kb, much smaller than the expected 5.3kb. More than 20 independent transformants were analysed, and none resulted in the expected banding pattern. The *hisG-URA3-hisG* construct could not have been truncated, as the 3.7kb band

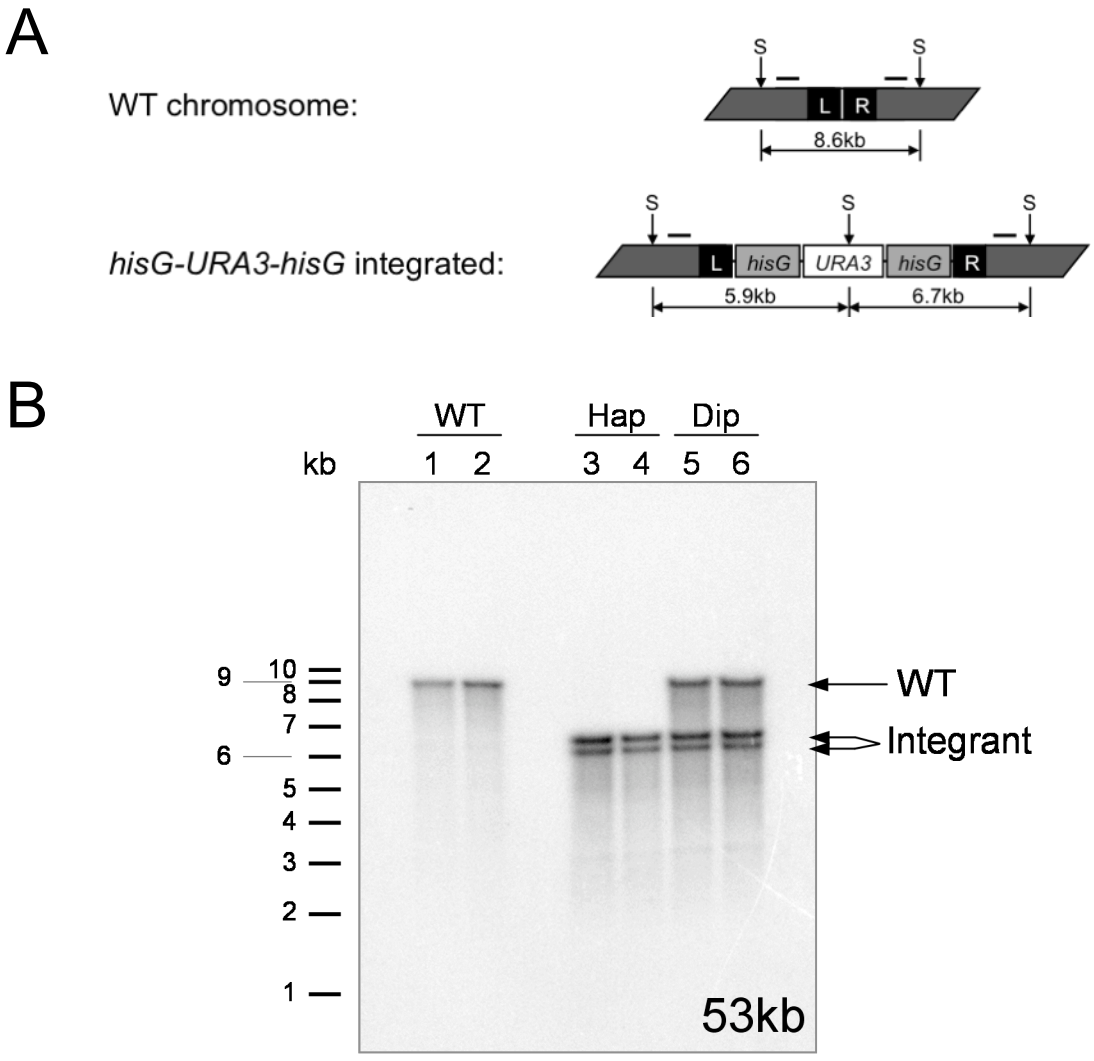

Figure 3.4. Integration of *hisG-URA3-hisG* at the 53kb locus.

(A) Schematic presentation of DNA structures resolved using probes upstream and downstream (dashed lines) of the integration site. The upper cartoon shows the genomic DNA before insertion of the construct, whilst the lower one shows an integrated *hisG-URA3-hisG* construct. "L" and "R" are the ~500bp sequences that flank the insertion point. Dashed lines indicate the position of 0.5kb probes used for the analysis. Vertical arrows mark relevant RE sites: S, *Stu*I. Drawings are not to scale.

(B) Southern blot analysis. Both the upstream and the downstream probes are used in the same blot to generate the image above. 1-2, WT haploid and diploid strains, respectively, lacking the *hisG-URA3-hisG* construct; 3-4, haploid strains containing an integrated construct; 5-6, diploid strains heterozygous for the construct, derived from a cross of the haploid strains (lanes 3 and 4) with a WT strain. Known sizes of DNA markers (in kb) are shown on the left hand side and are approximate only.

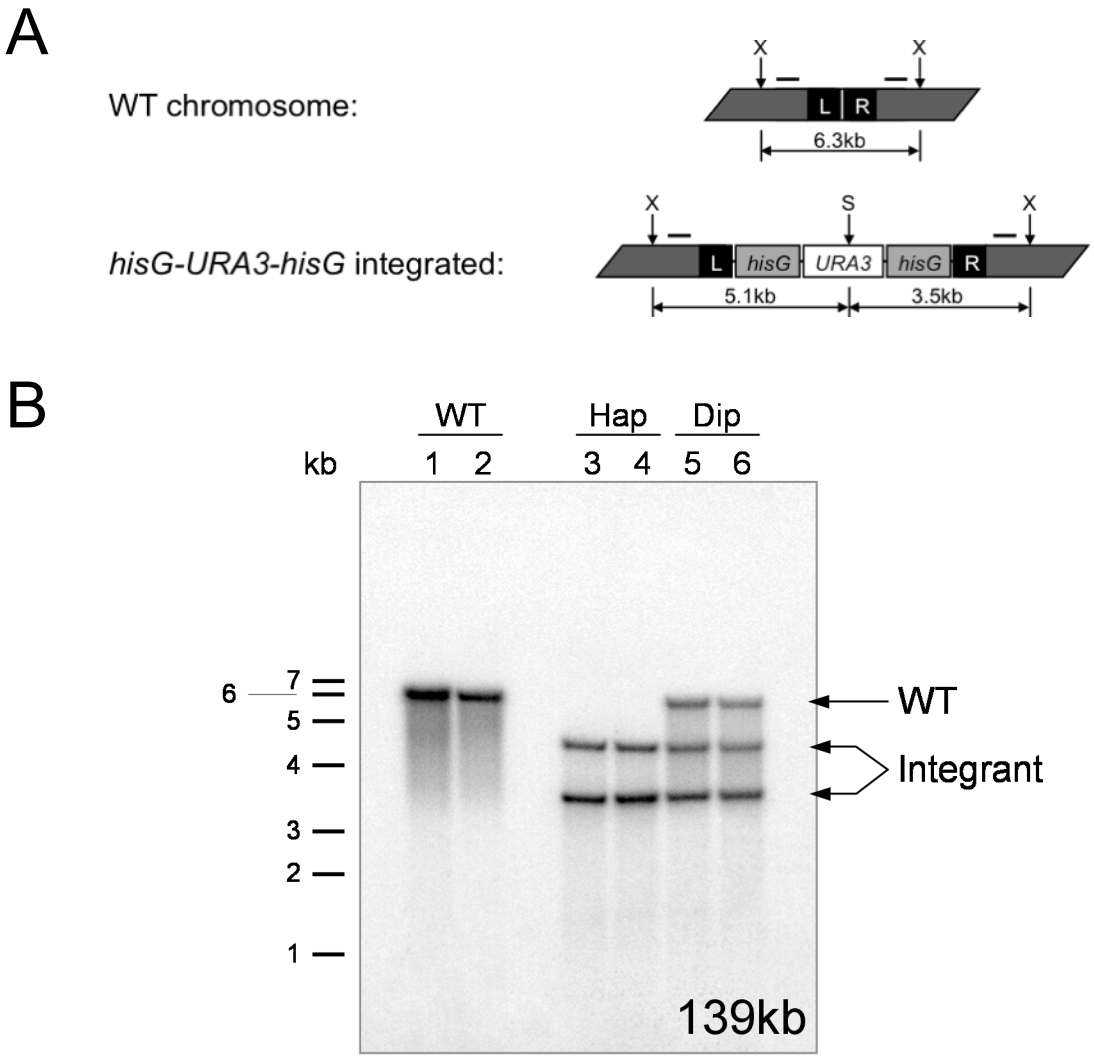

Figure 3.5. Integration of *hisG-URA3-hisG* at the 139kb locus.

(A) Schematic presentation of DNA structures resolved using probes upstream and downstream (dashed lines) of the integration site. The upper cartoon shows the genomic DNA before insertion of the construct, whilst the lower one shows an integrated *hisG-URA3-hisG* construct. "L" and "R" are the ~500bp sequences that flank the insertion point. Dashed lines indicate the position of 0.5kb probes used for the analysis. Vertical arrows mark relevant RE sites: S, *Stu*I; X, *Xho*I. Drawings are not to scale.

(B) Southern blot analysis. Both the upstream and the downstream probes are used in the same blot to generate the image above. 1-2, WT haploid and diploid strains, respectively, lacking the *hisG-URA3-hisG* construct; 3-4, haploid strains containing an integrated construct; 5-6, diploid strains heterozygous for the construct, derived from a cross of the haploid strains (lanes 3 and 4) with a WT strain. Known sizes of DNA markers (in kb) are shown on the left hand side and are approximate only.

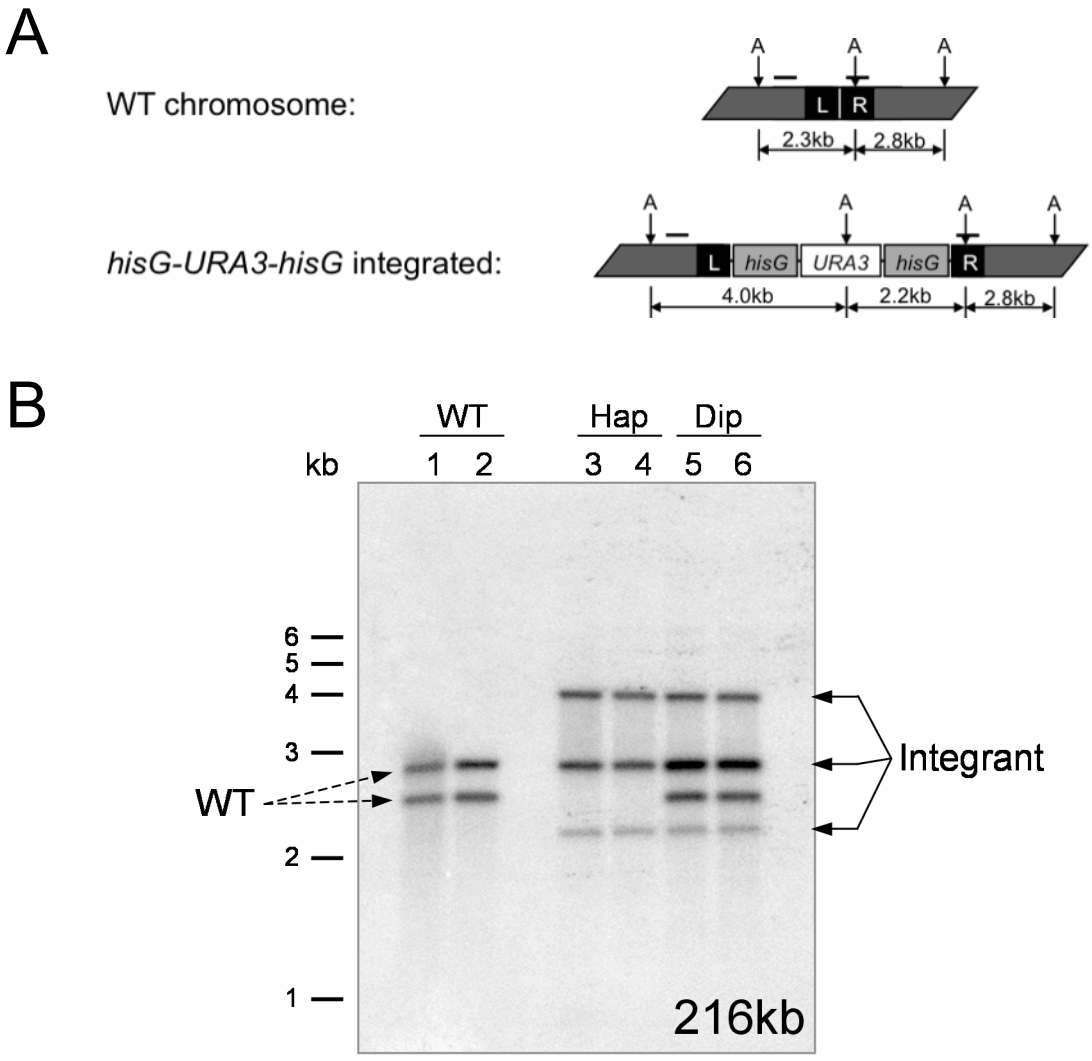

Figure 3.6. Integration of *hisG-URA3-hisG* at the 216kb locus.

(A) Schematic presentation of DNA structures resolved using probes upstream and downstream (dashed lines) of the integration site. The upper cartoon shows the genomic DNA before insertion of the construct, whilst the lower one shows an integrated *hisG-URA3-hisG* construct. "L" and "R" are the ~500bp sequences that flank the insertion point. Dashed lines indicate the position of 0.5kb probes used for the analysis. Vertical arrows mark relevant RE sites: A, *Apa*I. Drawings are not to scale.

(B) Southern blot analysis. Both the upstream and the downstream probes are used in the same blot to generate the image above. 1-2, WT haploid and diploid strains, respectively, lacking the *hisG-URA3-hisG* construct; 3-4, haploid strains containing an integrated construct; 5-6, diploid strains heterozygous for the construct, derived from a cross of the haploid strains (lanes 3 and 4) with a WT strain. Known sizes of DNA markers (in kb) are shown on the left hand side and are approximate only.

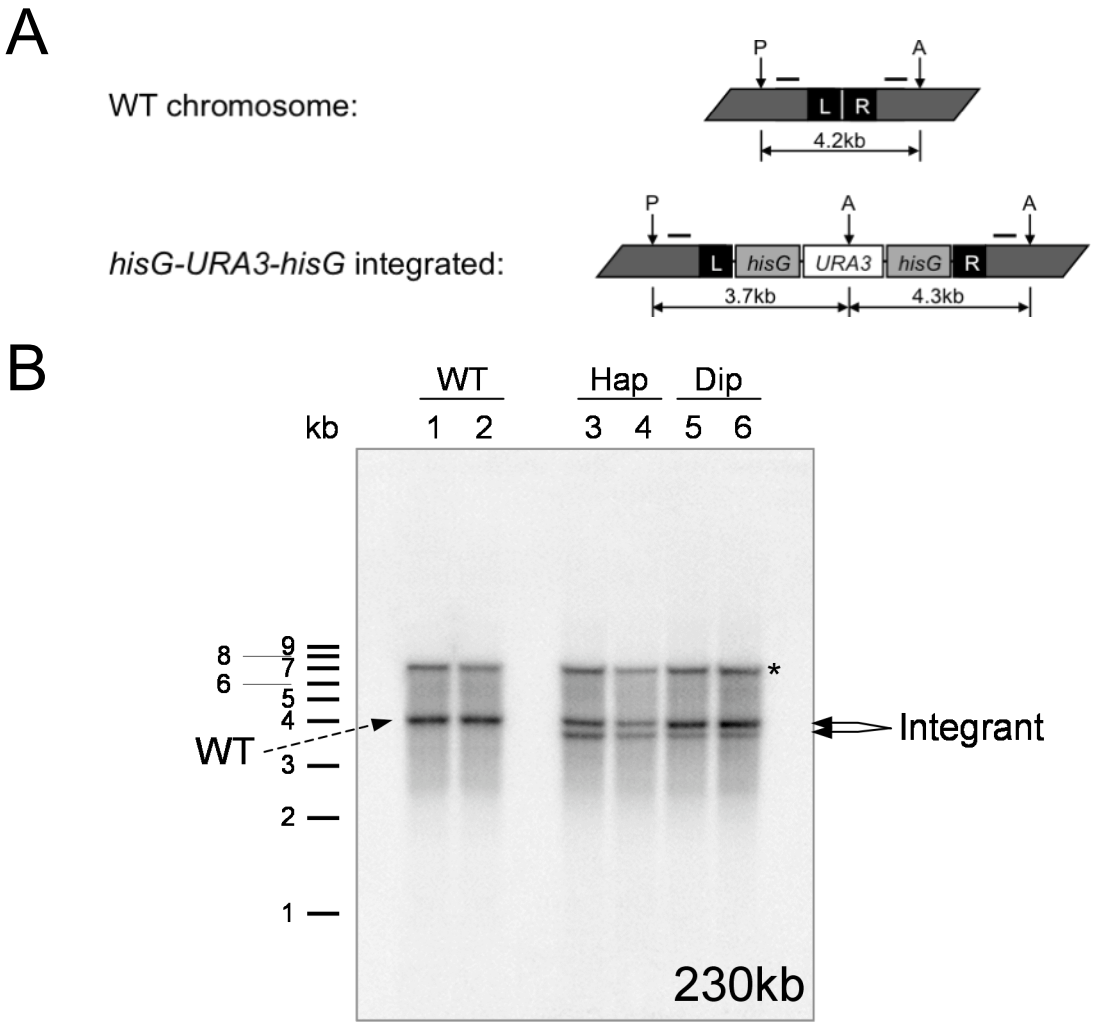

Figure 3.7. Integration of *hisG-URA3-hisG* at the 230kb locus.

(A) Schematic presentation of DNA structures resolved using probes upstream and downstream (dashed lines) of the integration site. The upper cartoon shows the genomic DNA before insertion of the construct, whilst the lower one shows an integrated *hisG-URA3-hisG* construct. "L" and "R" are the ~500bp sequences that flank the insertion point. Dashed lines indicate the position of 0.5kb probes used for the analysis. Vertical arrows mark relevant RE sites: A, *Apa*I; P, *Pme*I. Drawings are not to scale.

(B) Southern blot analysis. Both the upstream and the downstream probes are used in the same blot to generate the image above. 1-2, WT haploid and diploid strains, respectively, lacking the *hisG-URA3-hisG* construct; 3-4, haploid strains containing an integrated construct; 5-6, diploid strains heterozygous for the construct, derived from a cross of the haploid strains (lanes 3 and 4) with a WT strain. Known sizes of DNA markers (in kb) are shown on the left hand side and are approximate only. *; non-specific band.

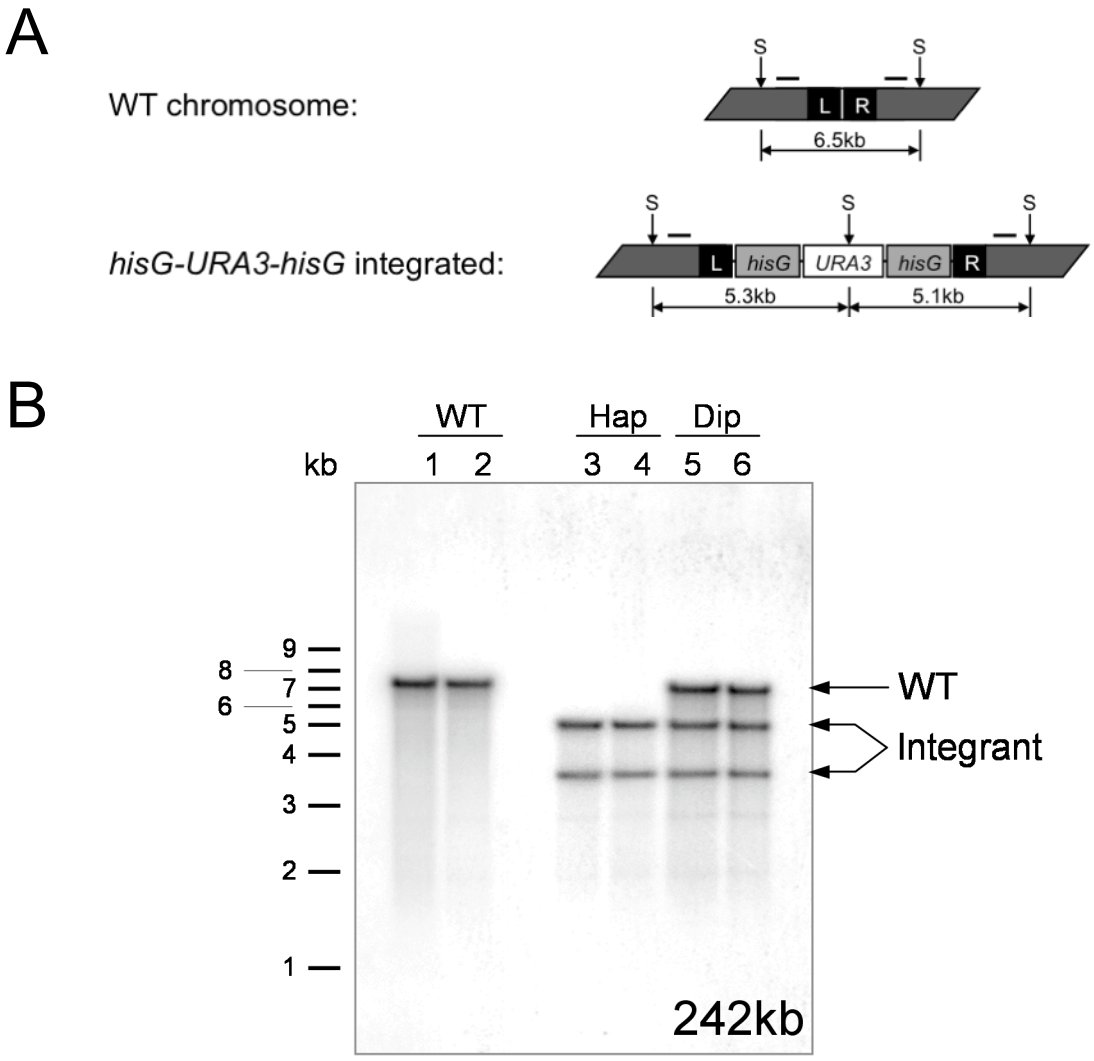

Figure 3.8. Integration of *hisG-URA3-hisG* at the 242kb locus.

(A) Schematic presentation of DNA structures resolved using probes upstream and downstream (dashed lines) of the integration site. The upper cartoon shows the genomic DNA before insertion of the construct, whilst the lower one shows an integrated *hisG-URA3-hisG* construct. "L" and "R" are the ~500bp sequences that flank the insertion point. Dashed lines indicate the position of 0.5kb probes used for the analysis. Vertical arrows mark relevant RE sites: S, *Stu*I. Drawings are not to scale.

(B) Southern blot analysis. Both the upstream and the downstream probes are used in the same blot to generate the image above. 1-2, WT haploid and diploid strains, respectively, lacking the *hisG-URA3-hisG* construct; 3-4, haploid strains containing an integrated construct; 5-6, diploid strains heterozygous for the construct, derived from a cross of the haploid strains (lanes 3 and 4) with a WT strain. Known sizes of DNA markers (in kb) are shown on the left hand side and are approximate only.

encompassed the 5' end of *URA3*, the entire left-hand side *hisG* repeat and the 500bp L sequence. Also, as every transformant analysed had the same banding pattern it was unlikely that this was due to an incorrect insertion of the construct. It was therefore likely that, as the S228C strain data had been used to design the transformation cassettes at each locus, certain differences (such as polymorphisms, small DNA changes within non-coding regions, and so on) would exist between that background and the SK1 strains used in this thesis. Thus the 242kb strains were assumed to be correct, and could be used for analysis of mutation rates (next chapter).

All *URA3* haploid strains were crossed with a WT haploid strain lacking the *hisG-URA3-hisG* construct, producing the expected banding pattern seen in columns 5 and 6 of Figures 3.4–3.8. These diploid strains were then sporulated, dissected, and *URA3* prototroph spores selected for to regenerate haploid cells containing the reporter construct. These haploid strains were used for assessing the rates of *URA3* inactivation (following chapters) rather than the original transformants. This additional step was performed because the transformation process can inadvertently produce secondary site mutations that could potentially affect the mutation rates within the *hisG-URA3-hisG*-containing strains. All strains were then re-checked by Southern blot analysis to ensure the construct had remained correctly integrated at each location. All of the *hisG-URA3-hisG* constructs remained stably integrated at their specific loci (data not shown).

Two independent transformants were used for each locus. A summary of all strains used for studying the rates of *URA3* inactivation is listed in Table 3.1 (page 95).

3.3 Effects of the *hisG-URA3-hisG* construct on strain fitness

3.3.1 Strain fitness in haploids

Before measuring the rate of *URA3* inactivation in these strains, the fitness of each was tested to ensure that no obvious effects occurred as a result of introducing the *hisG-URA3-hisG* construct into the five different loci in ChrIII. Spot-tests were a simple but effective way to test this. Log phase cultures of each strain were subjected

to serial dilutions and spotted onto agar plates. As a control, WT and *mec1-ts* strains, neither of which had an integrated construct, were used. The latter strain was sensitive to both HU and temperatures above 34˚C. With the exception of the two 216kb (replication termination) strains, all of the *URA3* strains grew similar to the WT (Figure 3.9). All of the strains grew on minimal media plates lacking uracil, showing that the *URA3* gene in the construct was functional. As expected, only the WT strain lacking a copy of *URA3* grew on 5-FOA media (the *mec1-ts* strain contained a functional copy of *URA3* not within the *hisG-URA3-hisG* construct and therefore also died in the presence of 5-FOA). A small number of isolated colonies were seen on the 5-FOA agar plate that originated from the construct-containing strains. It is therefore likely that some events leading to *URA3* inactivation had already occurred during the growth of these cells before being spotted onto 5-FOA media. None of the *URA3* strains were sensitive to 10mM HU.

3.3.2 The hisG-URA3-hisG construct inserted into the BUD23 ORF at the 216kb locus

Both of the 216kb strains had a slow growth phenotype at all four temperatures tested. Growth was less compromised at 30˚C than at the other temperatures, yet the strains still did not grow as well as either the WT or other construct-containing strains. This result was reproducible.

Although the construct had originally been designed to insert into intergenic regions there was still a possibility that the transformation process could have disrupted gene function in some way. Therefore, the genes upstream (*IMG1)* or downstream (*BUD23*) of the 216kb insert site were examined.

IMG1 encodes for a mitochondrial large subunit ribosomal protein. Deletion of this gene is viable, although Img1p is essential for maintenance of the mitochondrial genome since its deletion leads to the appearance of 100% of cytoplasmic petites (Coppée *et al*., 1996). *img1* cells are therefore not able to grow on medium using glycerol as the sole carbon source. Each strain had already been tested to see if they could grow under this specific condition in order to prevent the use of petite cells in

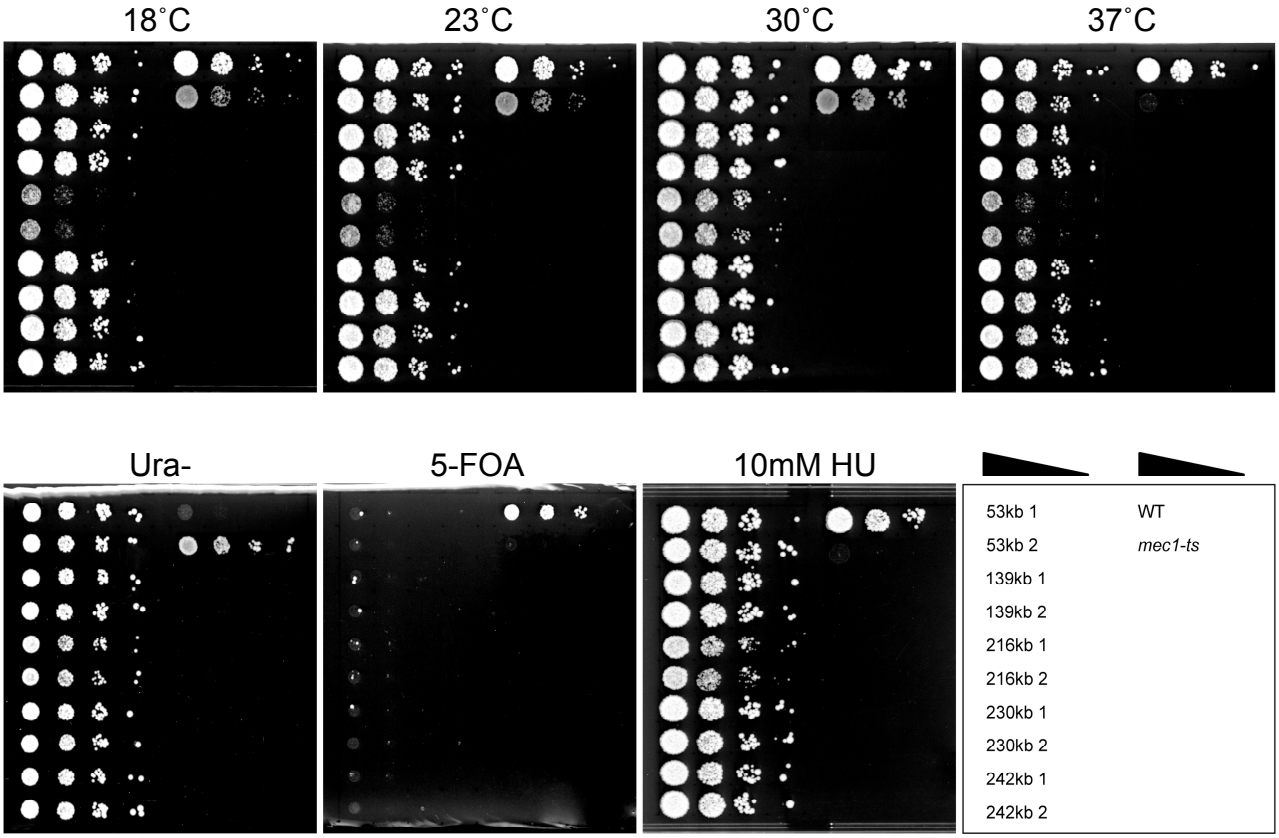

Figure 3.9. Effects of temperature on growth of haploid strains carrying a *hisG-URA3-hisG* construct at different loci on ChrIII.

Ten-fold serial dilutions of exponentially growing cells were spotted onto specified agar plates and grown at the indicated temperatures for 3-5 days. The uracil dropout (Ura-), 5-FOA and 10mM HU plates were incubated at 30˚C. The box in the lower right indicates the strains spotted onto the plates: WT and *mec1-ts* in this instance refer to strains lacking a *hisG-URA3-hisG* construct. *mec1-ts* is a control strain sensitive to both 10mM HU and temperatures above 34˚C.

this study (also see Figure 3.10). Insertion of the *hisG-URA3-hisG* construct had therefore not disrupted *IMG1* gene function.

BUD23 encodes an *S*-adenosylmethionine-dependent methyltransferase. Deletion of this gene is viable but leads to a reduced fitness at 30˚C in rich medium, but not when glycerol is used as the carbon source (Niewmierzycka and Clarke, 1999). The deletion strain is also sensitive to 0.5M $CaCl_2$ (Rieger *et al*., 1997). All of the strains used in Figure 3.9 were therefore spotted onto a rich media agar plate and one supplemented with 0.5M $CaCl_2$, and then incubated at 30˚C. It was found that the defects conferred by insertion of *hisG-URA3-hisG* into 216kb was not as dramatic as those reported for *bud23Δ* strains (Figure 3.10; Niewmierzycka and Clarke, 1999; Rieger *et al*., 1997).

Further examination revealed that the *hisG-URA3-hisG* reporter construct had inserted between the 96^{th} and 97^{th} nucleotides in the 3' end of the *BUD23* gene. Given that Bud23p is a multi-domain protein and that disruption of specific domains leads to differential sensitivities to rich medium and/or $CaCl_2$ (Niewmierzycka and Clarke, 1999, Rieger *et al*., 1997), it is possible that the modest sensitivities observed for the two 216kb strains was due to the dispensability of the disrupted region for its functions.

The two 216kb haploid strains were crossed with the WT strain (RCY2459) and then sporulated. Twenty tetrads derived from these diploids were dissected and analysed. In all cases, a 2:2 segregation of *URA3*:*ura3* cells was observed. *URA3* cells co-segregated with the slow growth phenotype as tested by growth on non-selective media and media lacking uracil. Integration of the *hisG-URA3-hisG* construct into *BUD23* was therefore the only factor that created the slow growth phenotype of the 216kb strains.

Based on these considerations, it was concluded that the *hisG-URA3-hisG* construct inserted into the 3' end of *BUD23*, which caused haploid transformants to grow slowly at all temperatures. Growth was least affected when cells were grown in rich media at 30˚C.

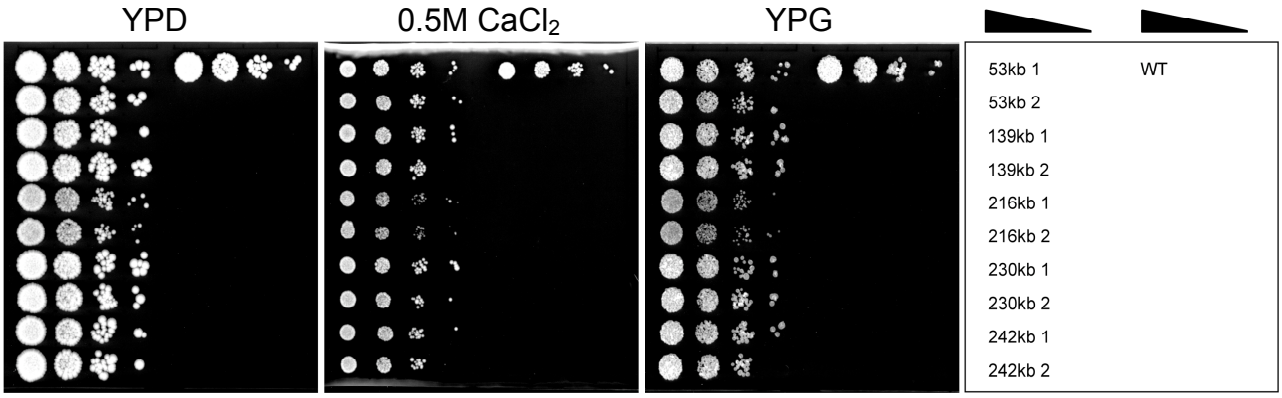

Figure 3.10. Effects of $CaCl_2$ and YPG on growth of haploid strains carrying a *hisG-URA3-hisG* construct at different loci on ChrIII.

Ten-fold serial dilutions of exponentially growing cells were spotted onto indicated agar plates and grown at 30˚C for 3-5 days. The box on the right indicates the strains spotted onto the plates: WT in this instance refers to a parental strain lacking an inserted *hisG-URA3-hisG* construct.

3.3.3 Strain fitness in diploids

The fitness of diploid strains was then tested. Figure 3.11 shows that most (see below) of the diploid strains grew similarly to the WT strain at 18˚C, 23˚C, 30˚C and 37˚C. All of the construct-containing strains grew on media lacking uracil, but not on 5-FOA plates. None of the strains were sensitive to 10mM HU. The slow growth phenotype of the 216kb strains was abolished in diploid cells. The WT copy of *BUD23* therefore complemented the *bud23* gene disrupted by the insertion of the *hisG-URA3-hisG* construct.

Upon further examination, the *hisG-URA3-hisG* cassette intended for an intergenic region around 53kb was found to have gone into the downstream gene, *GID7*. The insertion occurred 114bp from the 3' end. Although the insertion would most likely have disrupted Gid7p function in the degradation of fructose-1,6-bisphosphate, as the 53kb haploid strains grew comparable to the WT strain lacking a construct, it was concluded that the disruption did not lead to a compromise in fitness of the transformants.

All of the locations on ChrIII were looked at to verify no other genes had been disrupted by insertion of the construct. The *hisG-URA3-hisG* constructs had all inserted correctly into intergenic DNA at the 139kb, 230kb and 242kb loci.

3.4 Summary

All strains required for studying the recombination rate at each of the five chosen locations in ChrIII were created successfully and confirmed by Southern blot analysis. The 216kb haploid strains showed a slow growth phenotype at all temperatures in rich media, though this was less so at 30˚C and was abolished entirely in diploid cells. This phenotype was due to insertion of the *hisG-URA3-hisG* construct into the terminal 3' coding region of *BUD23*. In the 53kb strains, the construct had inserted into *GID7* with no obvious effects on fitness of the strains. The *URA3* gene was functional in all transformants for each of the five different locations in ChrIII.

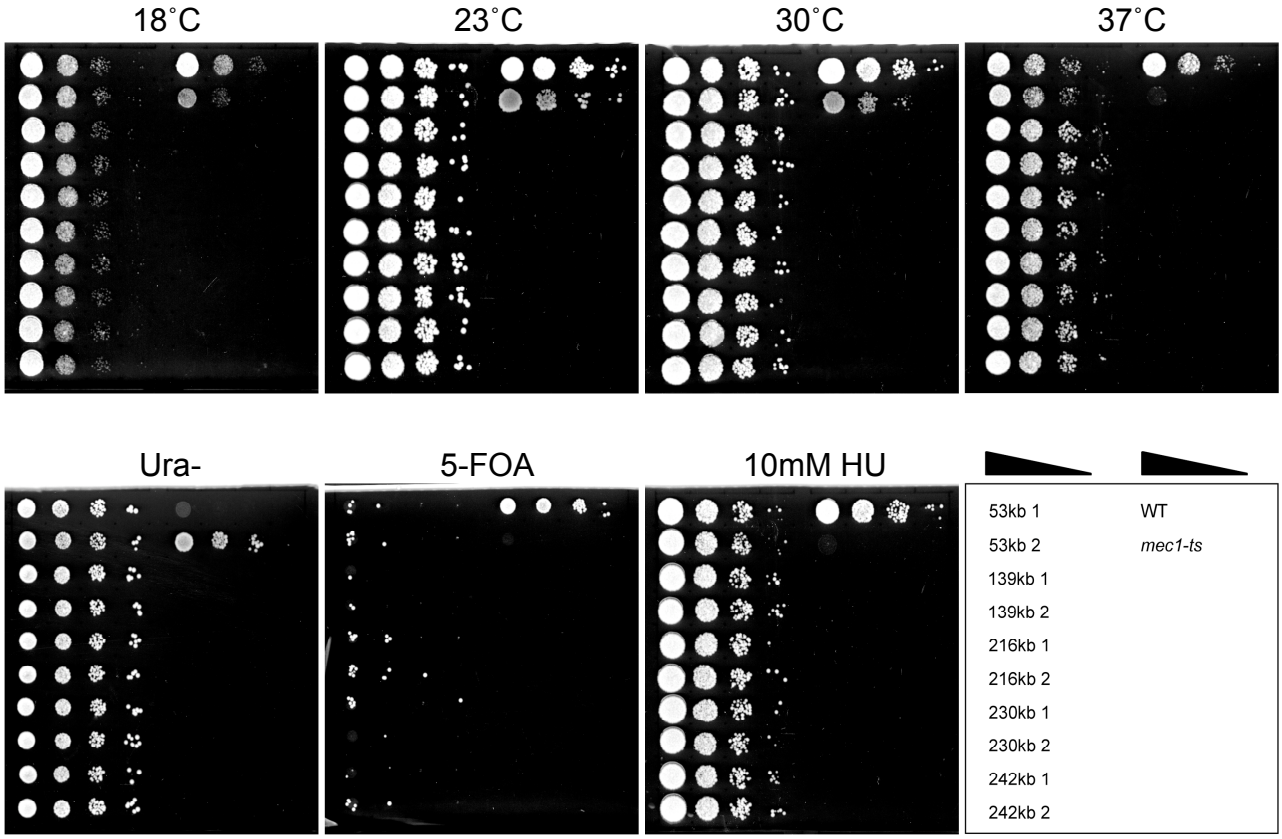

Figure 3.11. Effects of temperature on growth of diploid strains carrying a *hisG-URA3-hisG* construct at different loci on ChrIII.

Ten-fold serial dilutions of exponentially growing cells were spotted onto specified agar plates and grown at the indicated temperatures for 3-5 days. The uracil dropout (Ura-), 5-FOA and 10mM HU plates were incubated at 30˚C. The box in the lower right indicates the strains spotted onto the plates: WT and *mec1-ts* in this instance refer to strains lacking a *hisG-URA3-hisG* construct, whilst all other strains are heterozygous for the construct. *mec1-ts* is a control strain sensitive to both 10mM HU and temperatures above 34˚C.

Table 3.1. Summary table of all strains used for fluctuation analysis.

For each strain, all haploid and diploid cells are generated from the same parental WT haploid. For instance, 498, 499, 495…491 were all generated from the 463 haploid. "WT" in this instance means a cell with the *hisG-URA3-hisG* construct inserted at the specified location. Diploid cells are heterozygous for the construct, but homozygous for the indicated mutant/null allele. *mec1-40* and *top2-1* are both temperature-sensitive alleles.

[a] "1" and "2" refer to two independently-derived transformants. [b] Corresponds to JDCY (James D Cauwood Yeast) designation number.

Strain		Haploid						Diploid					
		WT	*sml1Δ*	*mec1Δ sml1Δ*	*mec1-40*	*top2-1*	*rrm3Δ*	WT	*sml1Δ*	*mec1Δ sml1Δ*	*mec1-40*	*top2-1*	*rrm3Δ*
53kb	1[a]	463[b]	498	499	495	482	480	477	503	500	501	489	491
	2[a]	465	479	478	484	483	481	469	487	486	488	490	482
139kb	1	228	333	335	328	388	297	179	365	368	369	401	407
	2	230	344	341	493	390	303	181	367	374	502	409	429
216kb	1	239	355	353	362	378	306	199	398	396	393	404	406
	2	243	357	359	360	380	307	203	397	395	392	417	408
230kb	1	232	338	337	305	384	300	185	366	375	309	403	316
	2	517	329	331	351	385	345	524	364	427	391	402	400
242kb	1	521	350	348	326	415	298	526	376	394	370	416	315
	2	237	293	291	399	382	346	237	312	311	444	410	411

Chapter 4.

Rates of *URA3* inactivation in optimal growth conditions

4.1. Introduction

4.1.1 Estimating the rate of mutation; the method of the median

Mutations can arise spontaneously in a population of cycling cells even in the absence of any selective pressure. Two different isogenic populations can produce a dramatically different number of mutants after a set number of cell divisions even if the mutation rates are identical. The reason for this is due to the different time at which a mutation event can occur during a clonal expansion. A mutation event that occurs early in a culture gives rise to many mutants after a defined number of cell divisions. Conversely, a mutation that occurs late in the number of cell cycles produces relatively few mutants. A number of parallel cultures will therefore each produce a different number of mutants depending on when the mutations occurred (Figure 4.1).

In this thesis the mutation rate is the rate of *URA3* inactivation in the *hisG-URA3-hisG* cassette, inserted at the five different loci within ChrIII. The "method of the median" was chosen as the means to estimate this mutation rate (Lea and Coulson, 1949). A number of parallel cultures set up from single colonies are used that each produce a number of mutants. As the timing of the mutagenic event(s) within these cultures is not identical, the number of mutants within each culture can vary significantly, and hence is the reason why this is also called "fluctuation analysis." The method of the median compensates for this degree of variation in number of mutants between cultures. Note that fluctuation analysis relies on a small number of fundamental but important assumptions: (i) each mutant plated grows on the selective media, (ii) the growth rate of mutant cells in a given culture does not differ from that of non-mutant cells, and (iii) mutations occur spontaneously in the absence of any selective agent.

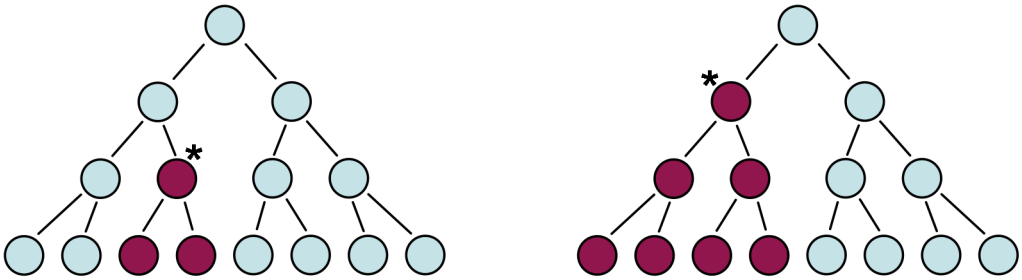

Figure 4.1. The timing of a mutagenic event affects the final mutant fraction of a clonally expanded population of cells.

A mutagenic event (*) that occurs late in a clonal population of proliferating cells produces fewer mutants than in one where a mutation is fixed early. A number of parallel cultures will therefore each produce a different number of mutants even if the mutation rate is the same in each.

4.1.2 Experimental system for fluctuation analysis

The mutation rate in the strains used throughout this thesis is a measure of the rate of *URA3* inactivation within the *hisG-URA3-hisG* construct. *URA3* encodes orotidine-5'phosphate decarboxylase, an enzyme that is required for the biosynthesis of uracil. Yeast with an active *URA3* gene converts the drug 5-FOA to the toxic pyrimidine analogue, 5-fluorouracil (Boeke *et al*., 1984). This is incorporated into DNA (and RNA), stopping DNA synthesis, which results in cell cycle arrest and eventual cell death. Yeast strains lacking a functional copy of *URA3* grow in the presence of 5-FOA, as long as the media is supplemented with uracil. Counting the number of cells able to grow on 5-FOA media and comparing this to the total number of cells in the culture therefore gives a measure of the number of *ura3* mutants within a given culture. This information is then used to determine an estimate of the mutation rate using the method of the median (Lea and Coulson, 1949).

In order to compare the mutation rates obtained on different days from various strains, it was necessary to establish standard conditions for fluctuation analysis. First, the number of parallel cultures used was as high as experimentally feasible and for this, 15 parallel cultures were used. This number has been used numerous times in earlier studies (such as Craven *et al*., 2002 and Sia *et al*., 1997). Secondly, the growth conditions of each culture should be kept as similar as possible. Strict incubation times were therefore devised, and, whenever possible, strains were grown using the same batch of media. Third, as the mutation rate is only an estimate, 95% confidence limits (CLs) were used as described by Weirdl *et al*. (1996; also see Materials & Methods). The latter served two purposes: the degree of variation between the 15 cultures could be assessed, and it would give a more objective viewpoint of the mutation rate. A larger degree of variation would indicate a less reliable estimate of the mutation rate, whilst a lower degree of variation would indicate a more reliable estimate; see Figure 4.2.

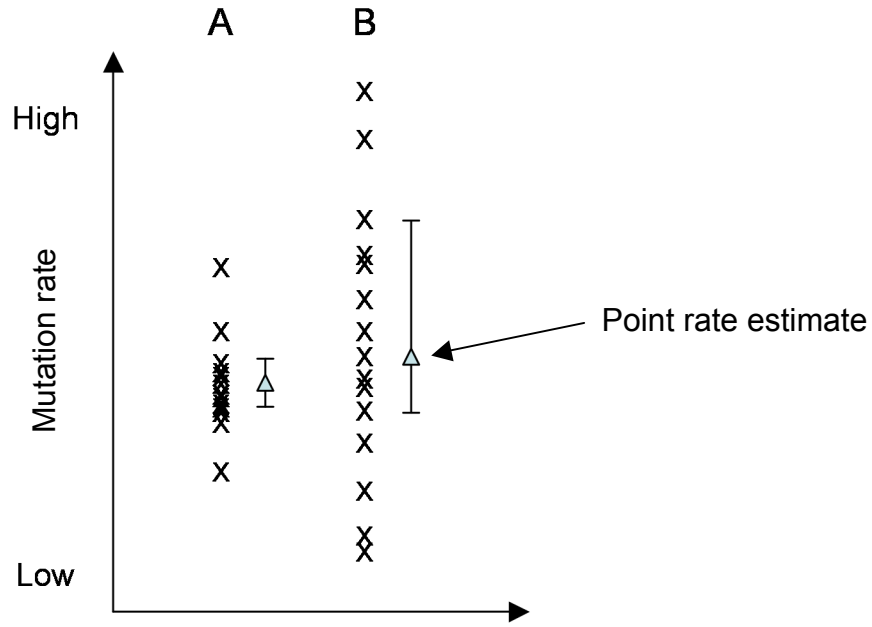

Figure 4.2. "Point estimates" and 95% CLs in fluctuation analysis.

The importance of using 95% confidence limits in conjunction with point estimates for mutation rates. In both column A and B, the mutation rate of each individual culture is plotted according to its value from high to low. Throughout this thesis, 15 parallel cultures are used; the 8th value is therefore used as the point estimate for the mutation rate (shaded triangle). The actual mutation rate is certain, to 95%, to be between the 4th and 12th values (Table A-25a; Dixon and Massey, 1969). In column A, the mutation rates are all tightly grouped, and are represented by the line drawing alongside. In column B the mutation rates are more widely spaced, and hence the 95% confidence intervals are much broader. The result shown for experiment A therefore gives a more reliable estimate of the mutation rate.

4.1.3 Inactivation of URA3

There is more than one way in which *URA3* can be inactivated. Recombination between the *hisG* repeats leaves one *hisG* copy within the DNA (see Section 1.5.1 of the Introduction). *URA3* can also be inactivated by small insertions or deletions, as well as non-recombinogenic events including point mutations, frame-shift errors, etc. Because of this, the rate of *URA3* inactivation was not quoted as a "recombination rate" and instead was referred to simply as a "mutation rate."

4.2 Results

4.2.1 Rates of URA3 inactivation in haploid strains

The mutation rate was first tested in haploid strains containing the *hisG-URA3-hisG* construct in the absence of any physiological stress. Spot tests of haploid strains described in Chapter 3 show that growth of all strains – including the 216kb (replication termination) strains – was best in non-selective media (YPD) at 30˚C compared to 18˚C, 23˚C or 37˚C (Figure 3.9, page 93). Mutation rates were therefore estimated using these conditions, and are used as a base measurement to which other growth conditions and/or genetic backgrounds will be compared to in the following chapters.

Preliminary experiments were conducted to determine the optimal growth conditions for strains grown in YPD media at 30˚C. *URA3* strains were patched directly onto YPG plates from -80˚C glycerol stocks to prevent the growth of petite cells. Cells were then streaked onto YPD agar plates for single colonies before being inoculated into 5mL YPD liquid media. Serial dilutions of the parallel cultures were then made and plated onto both selective (5-FOA) and non-selective (YPD) plates to determine the number of mutants and the total cell count. These numbers were then used to estimate the rate of *URA3* inactivation using the method of the median (Lea and Coulson, 1949). Exact incubation times utilised throughout these studies are shown in Figure 4.3.

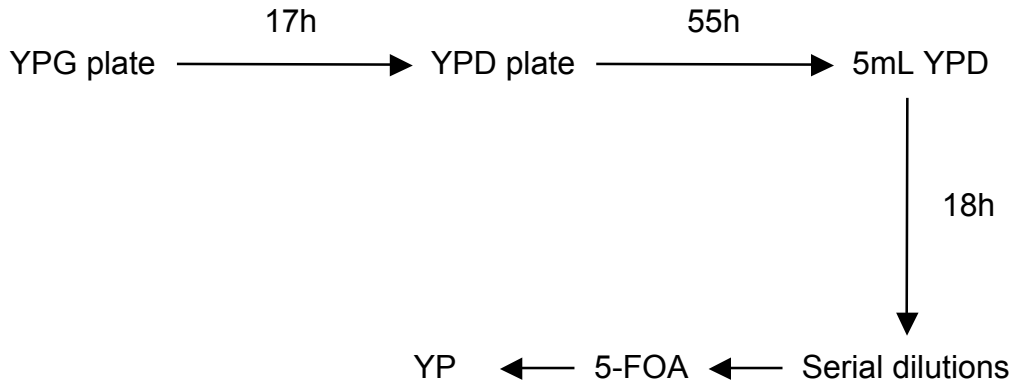

Figure 4.3. Clonal expansion protocol utilised for fluctuation analysis.

Cells were patched onto YPG directly from -80˚C glycerol stocks. After 17h, cells were streaked for single colonies on non-selective media; colonies had reached a suitable size (~2-3mm in diameter) after 55h. Single colonies were then used to inoculate 15 different flasks containing 5mL liquid YPD. Serial dilutions of these cultures were made after 18h incubation; dilutions plated onto YPD media were direct dilutions from those plated on 5-FOA plates. Unless indicated otherwise, strains were incubated at 30˚C throughout the entire process.

For these fluctuation analyses 15 parallel cultures were set up from single colonies and subjected to the growth protocol outlined above. Two independent transformants were used for each locus, and are hereafter named "1" and "2". It was ensured these strains were non-petite, and correct integration of the *hisG-URA3-hisG* construct was confirmed by Southern blot analyses (previous chapter). Due to the degree of variation that can occur between strains and individual cultures, the mutation rates were given to one decimal place only.

Figure 4.4 shows the rate of *URA3* inactivation in haploid strains grown in optimal conditions at 30°C. The point estimate is the mutation rate derived from the median value of the 15 cultures, and is represented by a black diamond for each individual strain. Capped lines represent 95% CLs. The specific values for each locus are shown in Figure 4.4A (second column). A statistical test previously employed by Weirdl *et al*. (1996) was chosen to ensure no statistical difference existed between the mutation rates of strains 1 and 2 for each locus. Essentially, the 15 individual mutation rates for strains 1 and 2 were pooled into one list. These values were ranked in order from highest to lowest, and Chi square (χ^2) analyses performed. If no statistical difference existed between the two sets of mutation rates, the top half of this list would contain equal numbers (7.5) from each strain. Deviations from this ratio would result in a χ^2 value that equated to a specific probability. Chi square values of 3.84 and above *(*corresponding to probability values of less than 0.05) were judged significant. No statistical difference in the rate of *URA3* inactivation was observed between the two strains at each locus.

The average mutation rates were then calculated for all five loci (Figure 4.4C and last column of 4.4A). These varied from 1.8 – 2.1 x 10^{-5} events/cell/generation.

To assess the variation amongst the five different loci within these haploid strains, the mutation rates were normalised against the lowest rate, in this case, 1.8 x 10^{-5} for the 230kb (origin) locus. The fold-difference values between the mutation rates of all five locations varied from only 1.0- to 1.1-fold (Figures 4.5A and 4.5B). The dashed line represents the normalised value obtained when the 230kb rate was divided by itself and is for reference only. Chi square analyses were once again used to see if

A

Strain		Mutation Rate (95% CL)[a]	Fold-difference between 1&2	Average Mut Rate
53kb	1	2.1×10^{-5} (1.6-2.4)	1.1	2.1×10^{-5}
	2	2.0×10^{-5} (1.9-2.2)		
139kb	1	1.8×10^{-5} (1.7-2.1)	1.1	1.9×10^{-5}
	2	2.0×10^{-5} (1.7-2.0)		
216kb	1	2.2×10^{-5} (1.8-3.2)	1.2	2.0×10^{-5}
	2	1.8×10^{-5} (1.6-2.5)		
230kb	1	1.4×10^{-5} (1.2-1.8)	1.6	1.8×10^{-5}
	2	2.2×10^{-5} (1.4-2.8)		
242kb	1	2.1×10^{-5} (1.9-2.8)	1.2	1.9×10^{-5}
	2	1.7×10^{-5} (1.4-2.1)		

Location	Chromosomal Features
53kb	RSZ, Termination
139kb	RSZ, Termination, Ty2
216kb	Termination
230kb	Origin
242kb	None

B

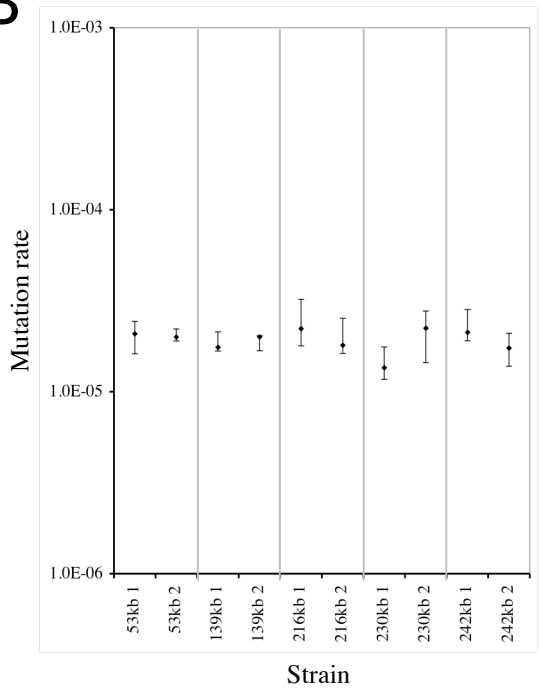

C

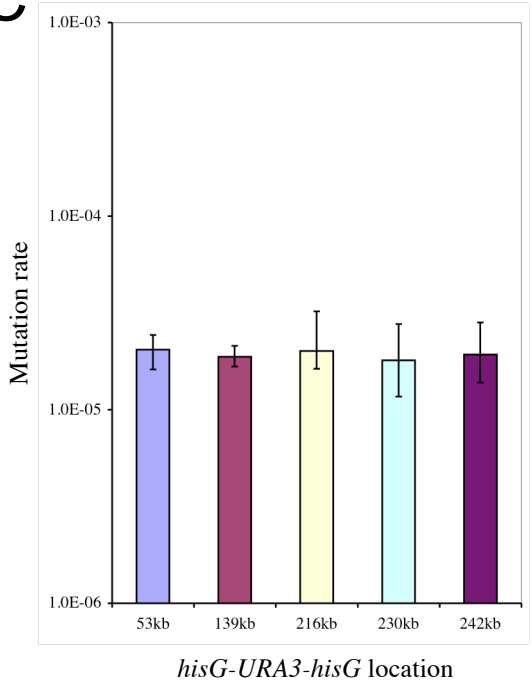

Figure 4.4. Rates of *URA3* inactivation in WT haploid strains grown in optimal conditions (YPD at 30˚C).

(A) For each locus, two independent rate measurements were done. The fraction of 5-FOA-resistant cells was measured in 15 independent cultures for each rate measurement. These fractions were converted to rates using the method of the median (Lea and Coulson, 1949). [a] 95% confidence limits (CL) were calculated as described previously (Wierdl *et al*., 1996). Chromosomal features at each locus are denoted on the right hand side.

(B) Individual rates are plotted. Capped lines indicate 95% CLs.

(C) The average mutation rate of the two strains is plotted. The smallest and largest CL value of the two strains was used for each location. Mutation rate is given as number of events/cell/generation.

A

Location Mutation rate[a]	Normalised mutation rate
53kb 2.1 x 10^{-5}	1.1
139kb 1.9 x 10^{-5}	1.1
216kb 2.0 x 10^{-5}	1.1
230kb 1.8 x 10^{-5}	1.0
242kb 1.9 x 10^{-5}	1.1

B

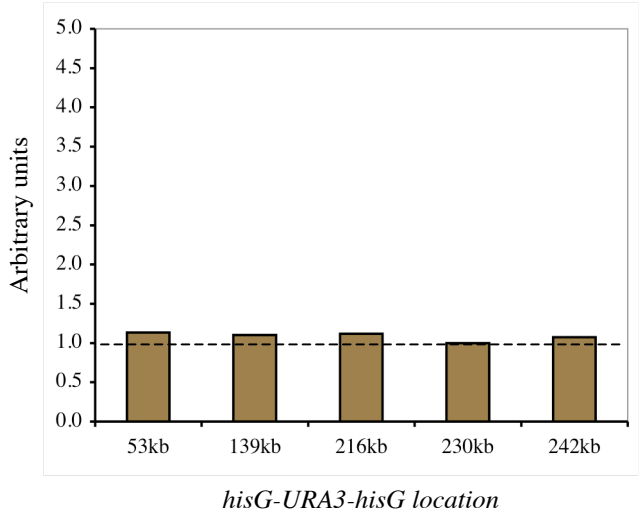

C

Location Mutation rate[a]	53kb 2.1 x 10^{-5}	139kb 1.9 x 10^{-5}	216kb 2.0 x 10^{-5}	230kb 1.8 x 10^{-5}	242kb 1.9 x 10^{-5}
53kb 2.1 x 10^{-5}		0.53 NSS	0.00 NSS	1.20 NSS	0.13 NSS
139kb 1.9 x 10^{-5}			0.13 NSS	0.53 NSS	0.53 NSS
216kb 2.0 x 10^{-5}				0.53 NSS	0.00 NSS
230kb 1.8 x 10^{-5}					1.20 NSS
242kb 1.9 x 10^{-5}					

Figure 4.5. Analysis of rates of *URA3* inactivation in WT haploid strains grown in optimal conditions (YPD at 30˚C).

(A) The average mutation rate at each locus was normalised against the lowest average rate.

(B) Normalised fold-differences from (A) are plotted.

(C) Chi-square analysis: pair-wise comparison of the mutation rates at each location. Shown in each panel are the Chi square (χ^2; upper) and probability (*P*; lower) values for each pair-wise combination. *P* values of less than 0.05 were deemed significant. NSS: not statistically significant. [a] Mutation rate is given as number of events/cell/generation.

these small fold-differences in mutation rate were statistically significant. To do this, the mutation rates for all 30 cultures of the 216kb locus (15 each from strains 1 and 2) were added to a list containing the 30 rates from one of the other four loci. These rates were ranked and χ^2 analyses performed as described above, with the exception that the expected outcome if there were no statistical difference in mutation rate between two loci was now 15/30 cultures in the top half of the list, rather than 7.5/15 as before in the earlier analyses. This method was used since it had already been shown that for each locus the mutation rates of the 1 and 2 strains did not statistically differ from each other, and hence the 30 rates from all the cultures could be pooled together. The results of this analysis are shown in Figure 4.5B. As expected from the low fold-differences in mutation rates between the loci and the 230kb rate, none of the mutation rates of the five different loci were statistically different from each other.

Figure 4.4B shows that the point rate estimates were very similar for all strains tested using the specific growth conditions in this chapter. The 95% CLs also overlapped for many of the strains. To assess if any statistical difference existed between any pair of the mutation rates, the above analysis was extended so that the mutation rate at each locus was compared in turn with the mutation rate of another. The results of this "pair-wise analysis" is shown in Figure 4.5C. As expected from the similar mutation rates and 95% CLs, no significant difference in the rates of *URA3* inactivation was found between any of the loci. The mutation rates in haploid strains grown in optimal conditions at 30˚C were therefore the same regardless of the location of the *hisG-URA3-hisG* construct within ChrIII.

4.2.2 Location of the hisG-URA3-hisG construct modulated the final cell counts of haploid strains

The spot tests in Figure 3.9 (page 93) show that the 216kb strains grew less than the other strains at all temperatures. This difference was less noticeable at 30˚C and hence was the reason why this temperature was used. The final cell counts of 15 parallel cultures following clonal expansion described in Figure 4.3 were compared (Table 4.1). No statistical difference existed between the 1 and 2 strains for any of

Table 4.1. Growth analysis of haploid strains used for fluctuation analysis in optimal growth conditions.

Strain		Cell count[a]	Average cell count[b]	Normalised[c]
53kb	1	126.3 ± 14.9	124.7 ± 14.8	1.6
	2	123.1 ± 15.1		
139kb	1	77.5 ± 14.2	103.1 ± 33.7	1.3
	2	128.7 ± 27.2		
216kb	1	90.3 ± 11.5	89.6 ± 14.2	1.1
	2	88.8 ± 16.8		
230kb	1	177.1 ± 21.9	185.5 ± 22.9	2.3
	2	193.9 ± 21.4		
242kb	1	81.7 ± 13.2	80.3 ± 12.1	1.0
	2	79.0 ± 11.2		

[a] Cell counts are made from serial dilutions of the 15 cultures used per strain, and plated onto non-selective media. No significant difference exists between the 1 and 2 strains, as determined by Student's t-test. [b] All cell counts from strains 1 and 2 were pooled and the average cell count taken from all 30 cultures, with the standard deviation given as ± values. [c] The average cell count of each locus was normalised to the lowest value, in this case, the value for the 242kb locus. By definition, this value is always "1.0."

Location	Chromosomal Features
53kb	RSZ, Termination
139kb	RSZ, Termination, Ty2
216kb	Termination
230kb	Origin
242kb	None

the five loci, as determined by Student's t-test analysis (*P* values of 0.05 were taken to be significant). All 30 cultures were then pooled (15 from strains 1 and 2) to produce an average cell count for each location. These values were then normalised to the lowest average cell count, in this case, the value for the 242kb (no chromosomal features) location. Given that 242kb strains grew well on spot tests (Figure 3.9), the latter observation is somewhat unexpected. Both loci within RSZs (53kb and 139kb) had very similar cell counts, whilst the origin (230kb) had the highest.

The location of the *hisG-URA3-hisG* construct therefore modulated the cell count of strains grown in optimal conditions. It is worth noting here, though, that the mutation rate derived from fluctuation analysis is independent of time and therefore also independent of the number of cell cycles in any culture. The difference in cell count between the strains therefore had no consequence on their respective mutation rates, regardless of their different growth rates.

4.2.3 Rates of URA3 inactivation in diploid strains

The mutation rates were next tested in diploid strains. To create the diploid strains, the haploids used in the earlier sections were crossed with a WT strain that didn't have an integrated *hisG-URA3-hisG* reporter construct. *URA3* diploids were selected by replica plating onto appropriate selection plates, and by morphology. As shown in the previous chapter, correct integration of the construct was confirmed in these diploid strains for each of the five loci.

All of the diploids were derived from their respective haploid strains. For example, the diploid 53kb strain 1 was derived from a cross of haploid 53kb strain 1 with the WT strain; the same applied for strain 2, and so on. (Table 3.1, page 98). All diploid strains were heterozygous for the *hisG-URA3-hisG* construct. Homozygous diploids were not chosen for this analysis, as the likelihood of inactivating two *URA3* alleles within the same cell would be very low. Hence, even if one allele of *URA3* were inactivated the cell would die in the presence of 5-FOA due to one functional copy of *URA3* still being present. If this were the case, the observed mutation rate would

be much lower than the actual mutation rate and thus would not be a reliable method to use.

Figure 3.11 (page 97) shows spot tests of diploid strains grown on various media at four different temperatures. Optimal growth occurred in non-selective (YPD) media at 30˚C for all strains: the slow growth phenotype of the 216kb strains was abolished. This temperature was therefore used for these strains and, as the haploid growth conditions were the same, the effect of ploidy could be directly compared for each of the five loci.

Figure 4.6 shows the result of fluctuation analyses for all diploid strains grown in optimal conditions. The point estimate is the mutation rate derived from the median value of 15 cultures, and is represented by black squares for each individual strain. Capped lines represent 95% CLs. The specific values for each strain are shown in Figure 4.6A (second column). Little variation existed between the mutation rates for strains 1 and 2 for each locus: the fold-difference between them varied from only 1.0- to 1.2-fold. Chi-square analysis found that no statistical difference existed between the mutation rates of strains 1 and 2 for any of the five loci. The mutation rates of the two independently derived strains were therefore consistent at each location.

The average rates of *URA3* inactivation were then calculated for each locus, as shown in Figures 4.6A (last column) and 4.6C. These varied from 1.1 x 10^{-5} events/cell/generation to as much as 3.3 x 10^{-5}. Of immediate interest is that, unlike the haploid strains grown under the same conditions, the mutation rates of these diploid strains differed. To assess the observed differences in mutation rate, the average mutation rates were normalised against the lowest rate. In this case, the lowest rate was for the 216kb (replication termination) locus. In haploid strains the lowest mutation rate was for 230kb (replication origin), though there was no significant difference in mutation rate between locations in that instance. Figure 4.7A shows that the fold-differences of these normalised values ranged from 1.3- to 2.9-fold. The highest differences from the 216kb rate were from the 230kb (origin) and 242kb (no features) loci, with 2.7- and 2.9-fold differences, respectively. The

A

Strain		Mutation Rate (95% CL)[a]	Fold-difference between 1&2	Average Mut Rate
53kb	1	1.9×10^{-5} (1.5-2.1)	1.0	1.9×10^{-5}
	2	1.9×10^{-5} (1.8-2.5)		
139kb	1	1.4×10^{-5} (1.1-1.5)	1.0	1.4×10^{-5}
	2	1.4×10^{-5} (1.2-1.7)		
216kb	1	1.1×10^{-5} (1.0-1.7)	1.0	1.1×10^{-5}
	2	1.1×10^{-5} (1.1-1.2)		
230kb	1	3.2×10^{-5} (3.1-4.5)	1.2	3.0×10^{-5}
	2	2.7×10^{-5} (2.3-3.5)		
242kb	1	3.5×10^{-5} (2.9-4.1)	1.2	3.3×10^{-5}
	2	3.0×10^{-5} (2.8-4.0)		

Location	Chromosomal Features
53kb	RSZ, Termination
139kb	RSZ, Termination, Ty2
216kb	Termination
230kb	Origin
242kb	None

B

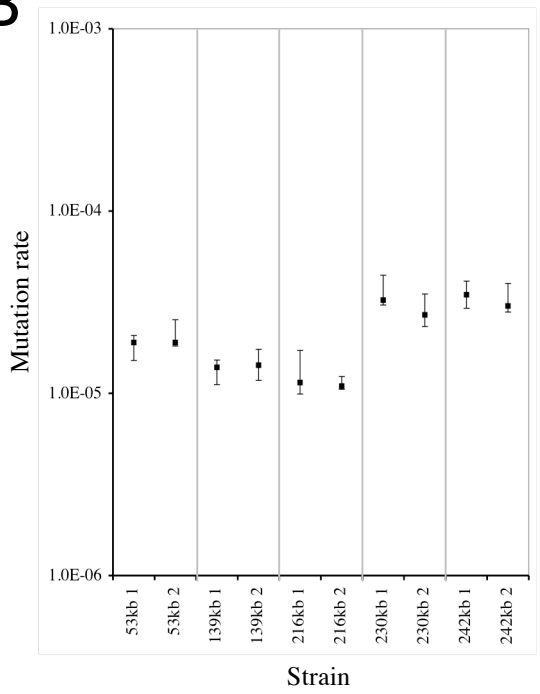

C

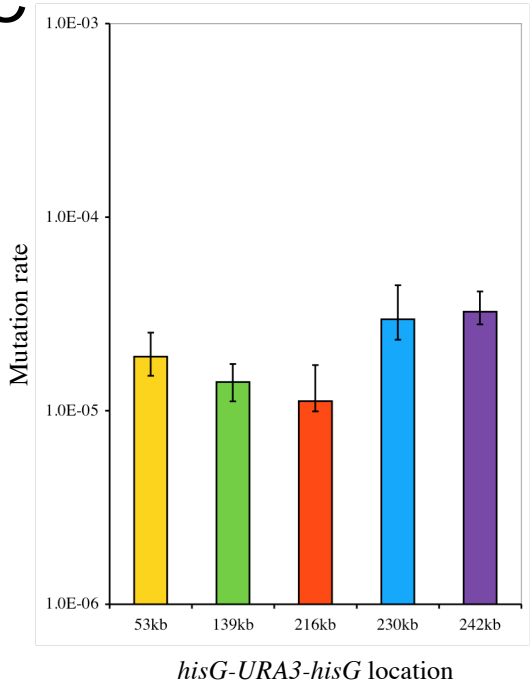

Figure 4.6. Rates of *URA3* inactivation in WT diploid strains grown in optimal conditions (YPD at 30˚C).

(A) All strains are heterozygous for the *hisG-URA3-hisG* reporter construct. For each locus, two independent rate measurements were done. The fraction of 5-FOA-resistant cells was measured in 15 independent cultures for each rate measurement. These fractions were converted to rates using the method of the median (Lea and Coulson, 1949). [a]95% confidence limits (CL) were calculated as described previously (Wierdl *et al*., 1996). Chromosomal features at each locus are shown are denoted on the right hand side.

(B) Individual rates are plotted. Capped lines indicate 95% CLs.

(C) The average mutation rate of the two strains is plotted. The smallest and largest CL value of the two strains was used for each location. Mutation rate is given as number of events/cell/generation.

A

Location Mutation rate[a]	Normalised mutation rate
53kb 1.9 x 10^{-5}	1.7
139kb 1.4 x 10^{-5}	1.3
216kb 1.1 x 10^{-5}	1.0
230kb 3.0 x 10^{-5}	2.7
242kb 3.3 x 10^{-5}	2.9

B

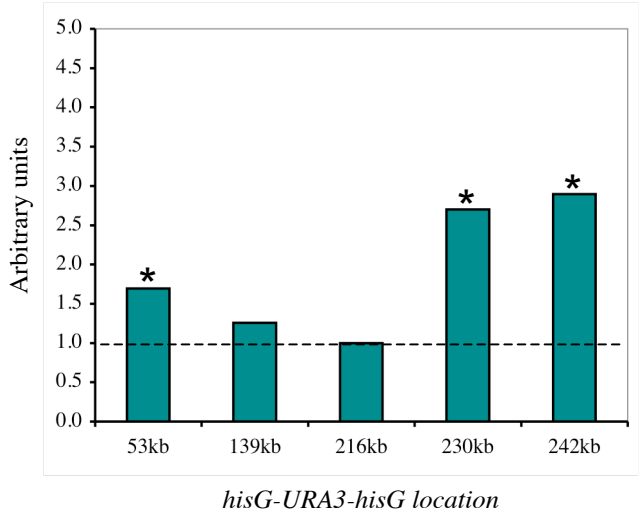

C

Location Mutation rate[a]	53kb 1.9 x 10^{-5}	139kb 1.4 x 10^{-5}	216kb 1.1 x 10^{-5}	230kb 3.0 x 10^{-5}	242kb 3.3 x 10^{-5}
53kb 1.9 x 10^{-5}		10.80 *P*~0.001	8.53 *P*<0.01	10.80 *P*~0.001	10.80 *P*~0.001
139kb 1.4 x 10^{-5}			3.33 NSS	16.13 *P*<0.001	19.20 *P*<0.001
216kb 1.1 x 10^{-5}				26.13 *P*<0.001	26.13 *P*<0.001
230kb 3.0 x 10^{-5}					0.13 NSS
242kb 3.3 x 10^{-5}					

Figure 4.7. Analysis of rates of *URA3* inactivation in WT diploid strains grown in optimal conditions (YPD at 30˚C).

(A) The average mutation rate at each locus was normalised against the lowest average rate.

(B) Normalised fold-differences from (A) are plotted. "*" denotes a significant statistical difference.

(C) Chi-square analysis: pair-wise comparison of the mutation rates at each location. Shown in each panel are the Chi square (χ^2; upper) and probability (*P*; lower) values for each pair-wise combination. *P* values of less than 0.05 were deemed significant. NSS: not statistically significant. [a] Mutation rate is given as number of events/cell/generation.

two loci within RSZs, 53kb and 139kb, had differences of 1.7- and 1.3-fold, respectively. Chi square analyses were performed as described above to see if these differences in mutation rate were statistically significant. It was found that the rates of *URA3* inactivation at the 139kb and 216kb loci were statistically indistinguishable. The mutation rates at the 53kb, 230kb and 242kb loci were all statistically higher than the 216kb locus, however, as shown by the starred (*) symbol above the relevant bars in Figure 4.7B. This was a different result than was seen for the haploid strains, where none of the mutation rates differed statistically from each other.

The pair-wise analysis used earlier was then performed on the diploid mutation rates. The mutation rates were found to be statistically different between all loci, with two exceptions. The mutation rates of the 139kb and 216kb loci were statistically the same, as were the 230kb and 242kb loci. This result therefore contrasted with that seen for the haploid strains.

In summary, the mutation rates of the two loci within RSZs (53kb and 139kb) were both lower than the 230kb (origin) or 242kb (no features) loci. The mutation rate of the 216kb locus was significantly lower than all other loci except 139kb. The mutation rates of the 230kb and 242kb loci were not significantly different from each other, but were higher than the other three loci. In conclusion, the rate of *URA3* inactivation varied depending on the location of the *hisG-URA3-hisG* construct in ChrIII when diploid strains were grown under non-selective conditions at 30°C.

4.2.4 Effects of ploidy on the rate of URA3 *inactivation in optimal growth conditions*

As a final comparison the mutation rates were compared between diploids and haploids grown in the same conditions. As all of the diploid strains were derived from the haploid strains, the affect of ploidy could be observed for each locus in ChrIII.

Figure 4.8A shows the individual mutation rates of diploid (black-filled squares) and haploid (grey-filled diamonds) grown in optimal conditions. The point rate estimates

and 95% CLs were very similar for only the 53kb locus. To calculate a fold-difference between the diploid and haploid mutation rates for each locus, the rate for diploid strain 1 was divided by the rate for haploid strain 1: the same was done for strain 2 and the average of these values was used to plot an average fold-increase in mutation rate for each locus (Figure 4.8B). A mixture of results was seen. The mutation rates at the 53kb locus were very similar between haploids and diploids, with only a 0.9-fold difference. For the 139kb and 216kb loci a decrease was seen in the diploid strains (0.8- and 0.6-fold, respectively), whilst an increase was observed for both the 230kb and 242kb loci (2.4- and 1.7-fold, respectively). Chi square analyses were once again used to determine if the observed fold-differences were significant. Of these values, only the 0.9-fold "difference" for the 53kb locus was statistically indistinguishable. For all other loci the mutation rates statistically differed between diploids and haploids.

In summary, ploidy affected the mutation rates of four out of five loci. The only exception was the mutation rates of the 53kb locus (RSZ, termination). Specifically, for the 139kb (RSZ, termination, Ty2) and 216kb (termination) loci, a lower mutation rate was seen in the diploids, whilst for 230kb (active origin) and 242kb (no features) loci a higher mutation rate was seen in the diploid strains.

4.3 Discussion

The mutation rates were first analysed in haploid strains grown in optimal conditions at 30˚C. This temperature was chosen because the slow growth phenotype of the 216kb (replication termination) strains was less pronounced at this temperature than at 18˚C, 23˚C or 37˚C. Two independently derived strains were used for each locus to assess the mutation rate. Results showed that there were consistent mutation rates between strains 1 and 2 for each of the five locations: the difference at most being within 1.1-fold of each other. The method of fluctuation analysis using the experimental conditions in this chapter produced consistent results that were therefore reliable.

A

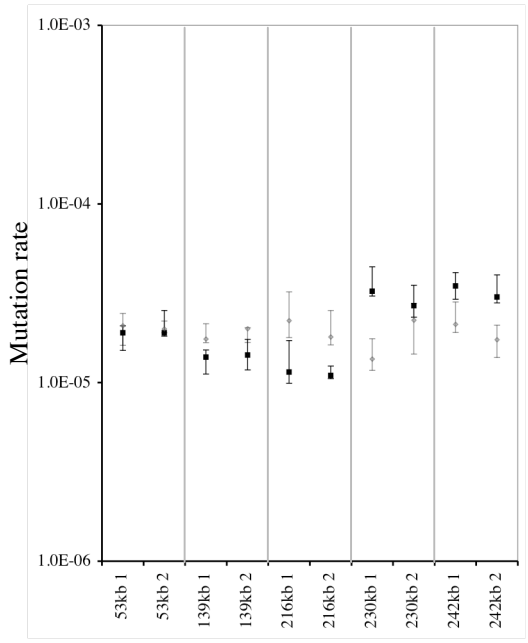

B

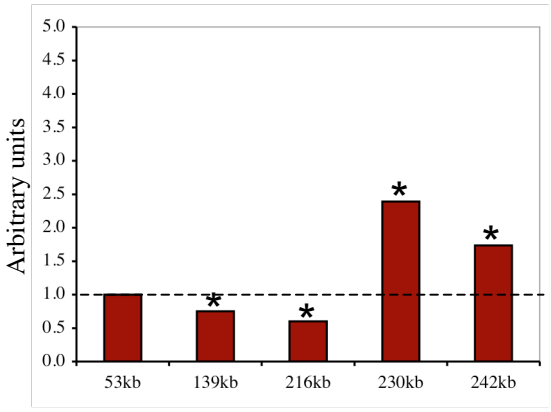

C

Construct location	Average mutation rate		Fold-difference[a] Diploid/ Haploid	Chi square and *P* values[b]
	Diploid	Haploid		
53kb	1.9×10^{-5}	2.1×10^{-5}	1.0	0.13, NSS
139kb	1.4×10^{-5}	1.9×10^{-5}	0.8	10.80, $P \sim 0.001$
216kb	1.1×10^{-5}	2.0×10^{-5}	0.6	8.53, $P < 0.01$
230kb	3.0×10^{-5}	1.8×10^{-5}	2.4	13.33, $P < 0.001$
242kb	3.3×10^{-5}	1.9×10^{-5}	1.7	13.33, $P < 0.001$

Figure 4.8. Effects of ploidy on the rates of *URA3* inactivation in WT strains grown in optimal conditions (YPD at 30˚C).

(A) Individual mutation rates of WT haploid (grey diamonds) and diploid (black squares) strains.

(B) Graph showing the fold-difference in mutation rates of diploid over haploid WT strains for each locus. "*" denotes a significant statistical difference. Values are taken from (C).

(C) [a] Where possible, for each location the mutation rate of strain 1 (diploid) was divided by the mutation rate of strain 1 (haploid). The same was done for strain 2. The fold-difference was then averaged over these two values for each locus. [b] Significant differences were calculated by χ^2 analyses, as described in the text. χ^2 values are given first, *P* values second. *P* values of less than 0.05 were deemed significant. NSS: not statistically significant.

The rate of *URA3* inactivation at all five loci varied from 1.8- to 2.0 x 10^{-5} events/cell/generation in haploids. These rates were statistically the same when compared by χ^2 analyses. Therefore, the mutation rate did not differ depending on the location of the construct in ChrIII in haploid cells when grown in optimal conditions.

Zhang *et al*. (2006) used a *leu2-URA3-leu2* construct to study direct repeat recombination in different mutant backgrounds. WT strains had a recombination rate of 1.1 ± 0.4 x 10^{-5} events/cell/generation when grown in non-selective conditions. The ± value in this case was the standard deviation between three independent fluctuation tests, using five parallel cultures for each. There were several differences between Zhang's and the experimental methods used in this thesis: a much lower number of parallel cultures were used for each fluctuation analysis, strains were derived from S228C, 95% CLs were not quoted, and different incubation times were used. Also, the construct was only inserted into one location of ChrV, so it is not known if the rate of recombination differed in a location-specific manner. Another study used a similar construct (*gal10-URA3-gal10*) inserted within ChrII and found rates of *URA3* inactivation to be 2.0 x 10^{-5} events/cell/generation (Thomas and Rothstein, 1989). Despite there being experimental differences compared to those used in this study, it was interesting that the mutation rates of the strains used in this thesis were similar to the recombination rates seen in these earlier studies. Levels of gross chromosomal rearrangements (GCRs), for instance, had recombination rates typically in the 10^{-7}-10^{-10} ranges (Chen and Kolodner, 1999; Kanellis *et al*., 2007), which are obviously more than 100-fold less than those mutation rates observed here.

The mutation rates in diploid strains were also studied, using the same growth conditions as the haploids. For each locus the mutation rates of the two strains derived from independent transformants did not differ statistically. The highest mutation rates were for the 230kb (origin) and 242kb (no features) locations (3.0 and 3.2 x 10^{-5} events/cell/generation, respectively), which were significantly higher than the mutation rates of the other three loci. The 216kb (termination) location had a mutation rate of 1.1 x 10^{-5} events/cell/generation, which was significantly lower than those at the other loci. Finally, the two loci within RSZs had similar mutation rates,

but the rate at the 53kb locus was statistically higher than the 139kb rate (1.9 and 1.4 x 10^{-5} events/cell/generation, respectively). The mutation rate in diploid strains grown in optimal conditions therefore varied, depending on the location of the *hisG-URA3-hisG* construct in ChrIII.

Although the mutation rate varied, statistically, in diploid strains grown in YPD, the highest difference between the five different locations was only 3-fold. In meiosis, the rate at which a sequence recombines is profoundly affected by its genomic location (Gerton *et al*., 2000). In a study conducted by Lichten *et al*. (1987), for example, the frequency of allelic meiotic recombination between heteroallelic *leu2* sequences at five different genomic locations varied almost 40-fold. This was not observed in mitotic cell cycles using the *hisG-URA3-hisG* construct and specific growth conditions in this chapter. Lichten and Haber (1989) subsequently also reported weak position effects of recombination in mitotic cells, although the experimental conditions utilised differed from those used here.

Finally, the diploid mutation rates were compared to their respective haploid rates for each locus. The rates of *URA3* inactivation in diploids were statistically different from their respective haploids for all loci except at the 53kb locus. In diploids, the mutation rate was lower than in haploids for both the 139kb and 216kb loci, but higher for both 230kb and 242kb. The rate of *URA3* inactivation was therefore affected by ploidy.

The rates of *URA3* inactivation measured in optimal growth conditions discussed in this chapter serve as a reference mutation rate, to which other growth conditions and/or mutant backgrounds will be compared to in the following chapters.

Chapter 5.

Temperature and hydroxyurea

5.1 Introduction

The previous chapter tested the rates of *URA3* inactivation in haploid and diploid strains, grown under optimal conditions in terms of temperature, nutrient availability, and the lack of exogenous stress. The rate of *URA3* inactivation was now tested in these same strains under two conditions that incurred different types of physiological stress: a general inhibitor of DNA replication, and temperature.

5.1.1 Hydroxyurea

As discussed in the Introduction, HU is a general inhibitor of DNA replication. Many previous studies have used HU concentrations in the 100-300mM range, which leads to robust activation of DNA checkpoints and prolonged replication fork stalling. For instance, using 200mM HU results in replication fork stalling after forks have progressed approximately 5-8kb from active origins (Lengronne *et al*., 2001). Although cells adapt after a certain amount of time, this could be disadvantageous if used for the strains in this thesis, as the nearest active origins are more than 12kb away for four out of the five *hisG-URA3-hisG* insertion locations (see Figure 3.1, page 77), and thus replication forks would not even reach the constructs at these loci in high concentrations of HU before fork stalling in the preliminary round of DNA replication. Instead, a low dose of HU (10mM) was used to test the mutation rates in haploid and diploid strains. In WT strains S-phase progression proceeds slower at this dose than in the absence of HU. But the extent of slowing down is notably attenuated when compared to that in the presence of 100-200mM HU, which elicits robust S-phase checkpoint responses (Bagley and Cha, unpublished). Importantly, *mec1Δ sml1Δ* cells exposed to 10mM HU acquire chromosome breaks at RSZs during G_2/M (Hashash *et al*., submitted), while the same cells exposed to 100mM

HU die due to irreversible fork collapse during S-phase (Hashash *et al*., submitted; Lopes *et al*., 2001). Although it has not been directly tested, the fact that 10mM HU induces breaks specifically at RSZs in *mec1Δ sml1Δ* cells indicates that forks have stalled at these loci in the mutant, and suggests that the same might also be true for WT cells. It is unknown, however, if forks stall in non-RSZ regions at this concentration.

5.1.2 Temperature

As mentioned in the Introduction, various studies have reported the potential mutagenic effects of temperature. In this study, the effects of temperature in the context of locations in the genome and ploidy were systematically addressed.

5.2 Results

5.2.1 Effects of 10mM on rates of URA3 inactivation

5.2.1.1 Rates of URA3 inactivation in haploid strains grown in media supplemented with 10mM HU

Haploid strains were grown at 30˚C in media supplemented with 10mM HU. All strains containing the *hisG-URA3-hisG* construct grew similarly to a parental WT strain when spotted onto rich media supplemented with 10mM HU at 30˚C (Figure 3.9, page 93). Figure 5.1B shows the result of HU-treated strains (black triangles) subjected to fluctuation analyses, along with the result for the same strains grown in optimal conditions (grey diamonds; previous chapter). The specific mutation rates for each HU-treated strain are shown in Figure 5.1A. The difference in mutation rates between the two independently derived strains varied from only 1.0- to 1.3-fold for all five loci (third column, 5.1A), which were not statistically significant (χ^2 analysis).

The 95% CL values were larger under the 10mM HU condition than for those produced from optimal growth conditions (Chapter 4). When haploid strains were grown in YPD at 30˚C, for instance, the largest difference between the smallest and largest CL value was less than 0.5 x 10^{-5} events/cell/generation for the majority of

A

Strain		Mutation Rate (95% CL)[a]	Fold-difference between 1&2	Average Mut Rate
53kb	1	5.7×10^{-5} (4.5-10.3)	1.0	5.6×10^{-5}
	2	5.5×10^{-5} (5.1-8.5)		
139kb	1	5.4×10^{-5} (3.7-5.7)	1.0	5.3×10^{-5}
	2	5.2×10^{-5} (4.1-6.5)		
216kb	1	6.7×10^{-5} (5.7-9.7)	1.1	6.5×10^{-5}
	2	6.3×10^{-5} (5.9-7.2)		
230kb	1	3.5×10^{-5} (2.8-4.5)	1.3	4.1×10^{-5}
	2	4.7×10^{-5} (3.5-5.3)		
242kb	1	5.8×10^{-5} (4.5-6.7)	1.3	6.6×10^{-5}
	2	7.3×10^{-5} (6.3-19.6)		

Location	Chromosomal Features
53kb	RSZ, Termination
139kb	RSZ, Termination, Ty2
216kb	Termination
230kb	Origin
242kb	None

B

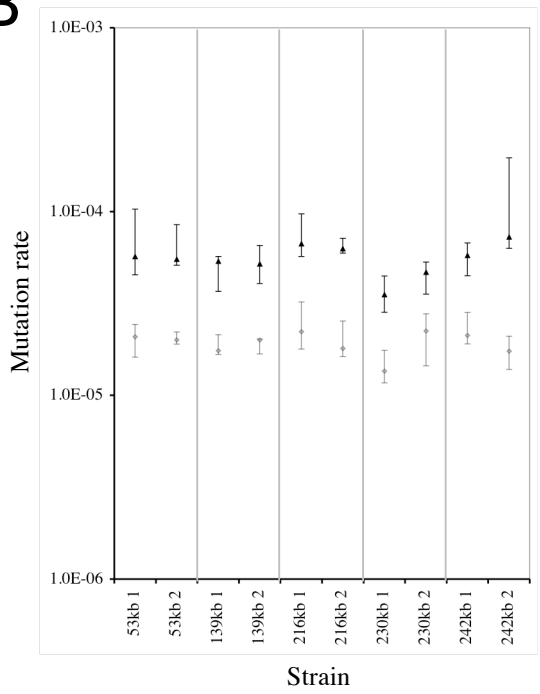

C

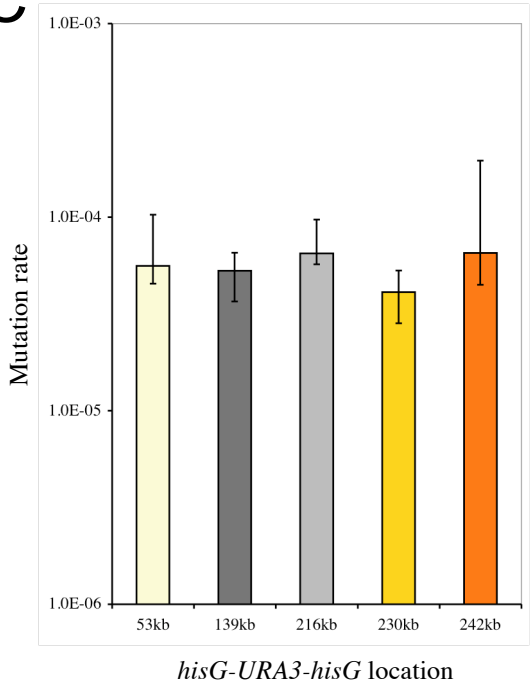

Figure 5.1. Rates of *URA3* inactivation in WT haploid strains grown in media supplemented with 10mM HU, at 30˚C.

(A) For each locus, two independent rate measurements were done. The fraction of 5-FOA-resistant cells was measured in 15 independent cultures for each rate measurement. These fractions were converted to rates using the method of the median (Lea and Coulson, 1949). [a] 95% confidence limits (CL) were calculated as described previously (Wierdl *et al*., 1996). Chromosomal features at each locus are denoted on the right hand side.

(B) Individual mutation rates of WT, HU (black triangles) and WT, optimal conditions (grey diamonds) are plotted. Capped lines indicate 95% CLs.

(C) The average of the two strains is plotted. The smallest and largest CL value of the two strains was used for each locus. Mutation rate is given as number of events/cell/generation.

the strains. When these same strains were grown in the presence of 10mM HU, however, this difference increased typically to over 2.0 x 10^{-5} and above (for instance the 95% CLs of *URA3* inactivation at the 139kb locus were 3.7 to 5.7 x 10^{-5} and 4.1 to 6.5 x 10^{-5} events/cell/generation, respectively, for strains 1 and 2).

The average rates of *URA3* inactivation were then calculated for each locus, as shown in Figures 5.1A (last column) and 5.1C. These varied from 4.1 x 10^{-5} to 6.6 x 10^{-5} events/cell/generation. To assess the potential differences in mutation rates between the five loci, each rate was normalised against the lowest value: in this case, the 230kb locus (origin). The 216kb (termination) and 242kb (no features) had the highest fold-differences from 230kb, both being 1.6-fold higher. The mutation rates of the 53kb (RSZ, termination) and 139kb (RSZ, termination, Ty2) loci were 1.4- and 1.3-fold higher than the 230kb rate, respectively (Figures 5.2A and 5.2B). Using χ^2 analyses, it was found that the fold-increases over the 230kb mutation rate for the 53kb, 216kb and 242kb loci were all statistically significant. The rates of *URA3* inactivation were statistically indistinguishable for the 139kb and 230kb loci.

The pair-wise analysis described in Section 4.2.1 (page 103) was used to compare the mutation rates between all five loci for haploid strains grown in the presence of 10mM HU. The mutation rates of the 53kb, 216kb and 242kb loci were not statistically different from each other. The mutation rates were statistically the same for the 53kb and 139kb loci, which were lower than the mutation rate for the 242kb locus ($P<0.01$). The only other statistically significant differences found were those already known from Figure 5.2B. These statistical analyses are summarised in Figure 5.2C.

In summary, for haploid strains grown in the presence of 10mM HU, the rates of *URA3* inactivation were the same for the 53kb, 216kb and 230kb loci, which were all statistically higher than the rate for the lowest (230kb; origin). The mutation rate of the 139kb locus was similar to the 53kb locus, but was significantly lower than the mutation rate of the 242kb strains. Exposure to 10mM HU therefore had small but significantly different effects on the mutation rate in haploid strains, depending on the location of the *hisG-URA3-hisG* construct in ChrIII.

A

Location Mutation rate[a]	Normalised mutation rate
53kb 5.6 x 10^{-5}	1.4
139kb 5.3 x 10^{-5}	1.3
216kb 6.5 x 10^{-5}	1.6
230kb 4.1 x 10^{-5}	1.0
242kb 6.6 x 10^{-5}	1.6

B

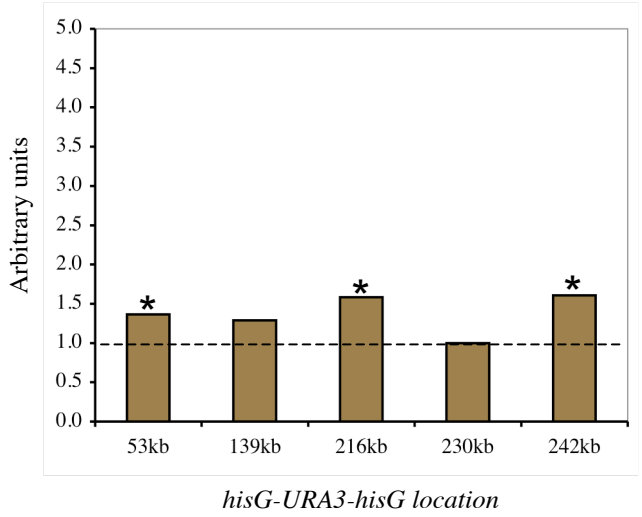

C

Location Mutation rate[a]	53kb 5.6 x 10^{-5}	139kb 5.3 x 10^{-5}	216kb 6.5 x 10^{-5}	230kb 4.1 x 10^{-5}	242kb 6.6 x 10^{-5}
53kb 5.6 x 10^{-5}		2.13 NSS	0.13 NSS	8.53 *P*<0.01	0.53 NSS
139kb 5.3 x 10^{-5}			3.33 NSS	3.33 NSS	10.80 *P*~0.001
216kb 6.5 x 10^{-5}				13.33 *P*<0.001	0.13 NSS
230kb 4.1 x 10^{-5}					10.80 *P*~0.001
242kb 6.6 x 10^{-5}					

Figure 5.2. Analysis of rates of *URA3* inactivation in WT haploid strains grown in media supplemented with 10mM HU, at 30˚C.

(A) The average mutation rate at each locus was normalised against the lowest average rate.

(B) Normalised fold-differences from (A) are plotted. "*" denotes a significant statistical difference.

(C) Chi-square analysis: pair-wise comparison of the mutation rates at each location. Shown in each panel are the Chi square (χ^2; upper) and probability (*P*; lower) values for each pair-wise combination. *P* values of less than 0.05 were deemed significant. NSS: not statistically significant. [a] Mutation rate is given as number of events/cell/generation.

Strains grown in optimal conditions are herein referred to as being grown in "YPD" for simplicity. Because both the incubation times and temperature for 10mM HU-treated strains were exactly the same as those as the same strains grown in YPD at 30°C (previous chapter's results), the affect of HU on the mutation rate could be observed for each specific locus. Note that this is different from the earlier analyses.Before, the mutation rates were compared between the five locations of the construct, under one particular growth condition. Now the mutation rates of a certain locus exposed to 10mM HU was compared to the rate measured in YPD for that same locus. For instance, the mutation rates were compared between the 53kb strains grown in 10mM HU and when grown in YPD.

The average mutation rates for haploid strains grown both in 10mM HU and YPD is shown in Figure 5.3A for all five loci. Figure 5.1B shows that the point estimates of the mutation rates (the rates derived from the median number of mutants from all 15 cultures per strain) were higher for all strains grown in media supplemented with 10mM HU compared to those grown in YPD. Also, no overlap was seen between any of the 95% CLs. To assess the potential differences in mutation rates for each locus in a quantitative manner, the mutation rate of strain 1 obtained in the presence of 10mM HU was divided by the mutation rate of the same strain obtained in the absence of drug (YPD). The same was done for strain 2 and these two values then averaged to produce an average fold-difference between strains grown in 10mM HU and those grown in YPD. Depending on the construct location within ChrIII, the mutation rate was 2.3- to 3.4-fold higher when strains were grown in HU (Figure 5.3B). Both loci within RSZs (53kb and 139kb) had very similar fold increases (2.8- and 2.9-fold), as did the 216kb (replication termination) and 242kb locations (no features; 3.3- and 3.4-fold, respectively). The 230kb locus had the lowest increase due to HU of 2.4-fold.

Chi square analyses revealed that the mutation rates were significantly higher for all five loci when grown in 10mM HU compared to the mutation rates in YPD ($P<0.001$ for all five). The 230kb (origin) locus had the lowest mutation rate out of all five loci when grown both in YPD and when exposed to 10mM HU. Unlike the result for

A

Construct location	Average mutation rate		Fold-difference[a] 10mM HU / 30˚C	Chi square and *P* values[b]
	10mM HU	30˚C		
53kb	5.6×10^{-5}	2.1×10^{-5}	2.8	12.30, $P<0.001$
139kb	5.3×10^{-5}	1.9×10^{-5}	2.9	19.20, $P<0.001$
216kb	6.5×10^{-5}	2.0×10^{-5}	3.3	19.20, $P<0.001$
230kb	4.1×10^{-5}	1.8×10^{-5}	2.4	19.20, $P<0.001$
242kb	6.6×10^{-5}	1.9×10^{-5}	3.5	26.13, $P<0.001$

B

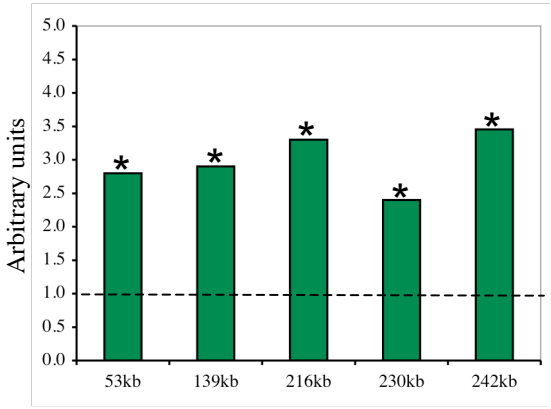

Figure 5.3. Effects of 10mM HU on the rates of *URA3* inactivation compared to those of optimal growth conditions in WT haploid strains, at 30˚C.

(A) For each location the mutation rate of strain 1 (10mM HU) was divided by the mutation rate of strain 1 (YPD). The same was done for strain 2. The fold-difference was then averaged over these two values for each locus. [b] Significant differences were calculated by χ^2 analyses, as described in the text. χ^2 values are given first, *P* values second. *P* values of less than 0.05 were deemed significant.

(B) Graph showing the fold-difference in mutation rates of WT haploid strains grown in 10mM HU over those grown in YPD for each locus. "*" denotes a significant statistical difference. Values are taken from (A).

10mM HU, however, the 230kb mutation rate was not significantly different from the mutation rates of the other loci when grown in YPD.

In conclusion, the mutation rate in haploid strains exposed to 10mM HU were ~3-fold higher than those grown in YPD at 30˚C, irrespective of the location of the construct.

5.2.1.2 Rates of URA3 inactivation in diploid strains grown in 10mM HU

Diploid *URA3* strains were grown in media supplemented with 10mM HU. All strains containing the *hisG-URA3-hisG* construct grew similarly to a congenic parental WT strain when spotted onto rich media supplemented with 10mM HU at 30˚C (Figure 3.11, page 97). Figure 5.4B shows the result for HU-treated strains (black-filled circles), along with the result for strains grown in YPD (grey squares). Specific values are given in Figure 5.4A. The fold-difference between the mutation rates of the two independently derived strains varied from only 1.1- to 1.2-fold for each locus. None of these differences were statistically significant (χ^2 analysis). There was a greater difference between the highest and lowest 95% CL values for all of these strains compared to their respective CL values when grown in YPD, as was also seen with the haploid strains.

The average mutation rates were then plotted. The lowest rate of *URA3* inactivation was 5.6 x 10^{-5} events/cell/generation for 139kb (RSZ, replication termination, Ty2), whilst the highest was 9.6 x 10^{-5} for 242kb (no features; Figure 5.4C). The average mutation rates for all five loci were normalised against the 139kb rate: these values ranged from 1.1- to 1.7-fold (Figure 5.5A). Chi square analyses were performed to assess the potential variation between these mutation rates. Of these values, the 1.6-, 1.5- and 1.7-fold increases for the 53kb, 230kb and 242kb loci, respectively, were significantly higher than the 139kb rate.

Pair-wise analysis was used to compare the mutation rates between each locus. The mutation rates of the 53kb, 230kb and 242kb loci were statistically indistinguishable from each other, which were all significantly higher than the rates of both the 139kb

A

Strain		Mutation Rate (95% CL)[a]	Fold-difference between 1&2	Average Mut Rate
53kb	1	8.6×10^{-5} (7.4-9.6)	1.1	8.9×10^{-5}
	2	9.2×10^{-5} (7.9-12.1)		
139kb	1	5.1×10^{-5} (4.6-6.4)	1.2	5.6×10^{-5}
	2	6.1×10^{-5} (4.9-8.5)		
216kb	1	5.5×10^{-5} (5.0-6.5)	1.2	6.2×10^{-5}
	2	6.8×10^{-5} (5.3-7.9)		
230kb	1	8.3×10^{-5} (7.2-9.9)	1.1	8.6×10^{-5}
	2	8.9×10^{-5} (7.6-9.2)		
242kb	1	10.2×10^{-5} (8.4-11.6)	1.1	9.6×10^{-5}
	2	9.0×10^{-5} (7.7-9.5)		

Location	Chromosomal Features
53kb	RSZ, Termination
139kb	RSZ, Termination, Ty2
216kb	Termination
230kb	Origin
242kb	None

B

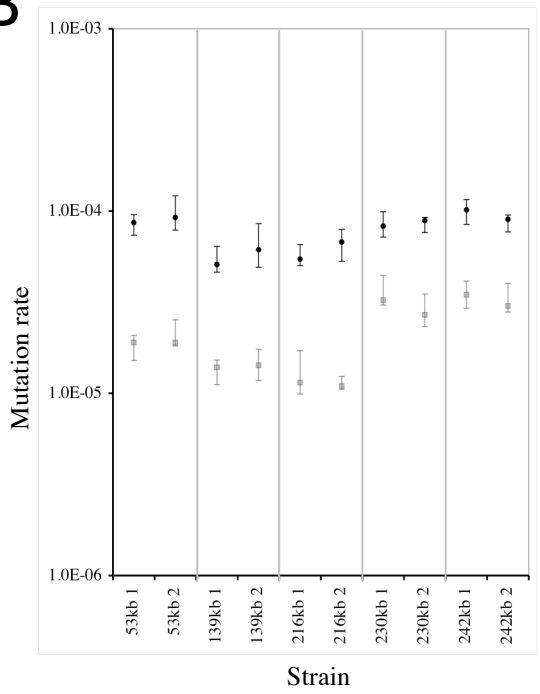

C

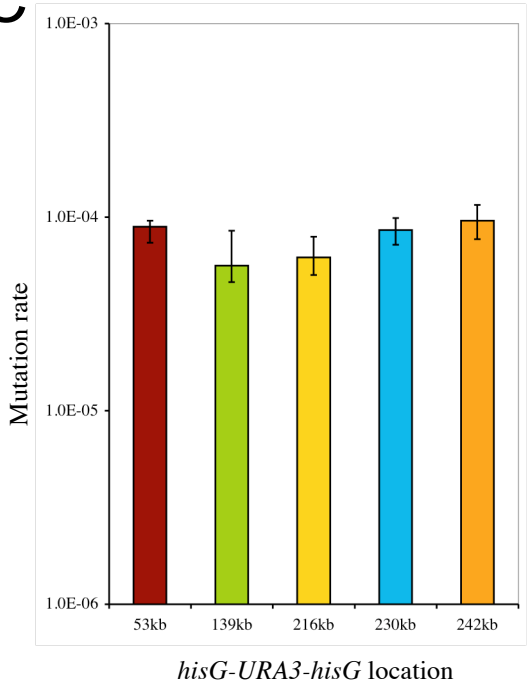

Figure 5.4. Rates of *URA3* inactivation in WT diploid strains grown in media supplemented with 10mM HU, at 30˚C.

(A) All strains are heterozygous for the *hisG-URA3-hisG* reporter construct. For each locus, two independent rate measurements were done. The fraction of 5-FOA-resistant cells was measured in 15 independent cultures for each rate measurement. These fractions were converted to rates using the method of the median (Lea and Coulson, 1949). [a] 95% confidence limits (CL) were calculated as described previously (Wierdl *et al*., 1996). Chromosomal features at each locus are denoted on the right hand side.

(B) Individual mutation rates of WT, HU (black circles) and WT, YPD (grey squares) are plotted. Capped lines indicate 95% CLs.

(C) The average of the two strains is plotted. The smallest and largest CL value of the two strains was used for each locus. Mutation rate is given as number of events/cell/generation.

A

Location Mutation rate[a]	Normalised mutation rate
53kb 8.9 x 10^{-5}	1.6
139kb 5.6 x 10^{-5}	1.0
216kb 6.2 x 10^{-5}	1.1
230kb 8.6 x 10^{-5}	1.5
242kb 9.6 x 10^{-5}	1.7

B

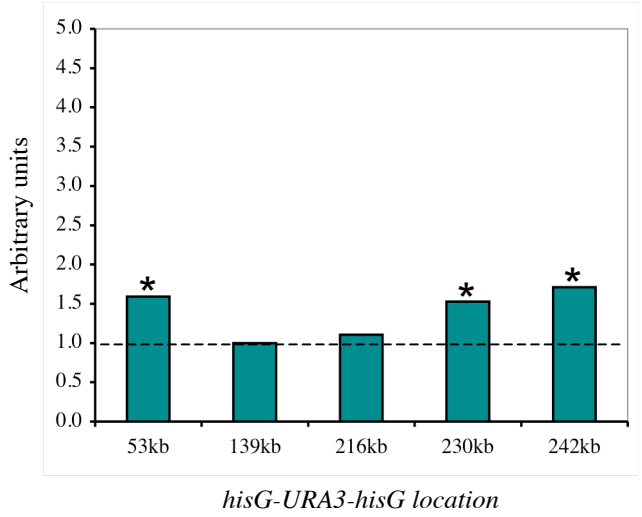

C

Location Mutation rate[a]	53kb 8.9 x 10^{-5}	139kb 5.6 x 10^{-5}	216kb 6.2 x 10^{-5}	230kb 8.6 x 10^{-5}	242kb 9.6 x 10^{-5}
53kb 8.9 x 10^{-5}		10.80 *P*~0.001	10.80 *P*~0.001	1.67 NSS	1.20 NSS
139kb 5.6 x 10^{-5}			0.13 NSS	5.40 *P*<0.05	16.13 *P*<0.001
216kb 6.2 x 10^{-5}				8.07 *P*<0.01	13.33 *P*<0.001
230kb 8.6 x 10^{-5}					1.67 NSS
242kb 9.6 x 10^{-5}					

Figure 5.5. Analysis of rates of *URA3* inactivation in WT diploid strains grown in media supplemented with 10mM HU, at 30˚C.

(A) The average mutation rate at each locus was normalised against the lowest average rate.

(B) Normalised fold-differences from (A) are plotted. "*" denotes a significant statistical difference.

(C) Chi-square analysis: pair-wise comparison of the mutation rates at each location. Shown in each panel are the Chi square (χ^2; upper) and probability (*P*; lower) values for each pair-wise combination. *P* values of less than 0.05 were deemed significant. NSS: not statistically significant. [a] Mutation rate is given as number of events/cell/generation.

and 216kb loci. The mutation rates of the 139kb and 216kb loci were statistically the same (Figure 5.5C). In summary, incubating diploid strains in 10mM HU had differential effects on the mutation rate, depending on the construct location in ChrIII.

The rate of *URA3* inactivation in diploid cells grown in 10mM HU was next compared against their respective mutation rates when grown in YPD at 30˚C for each of the five loci. Figure 5.4B shows that, like the haploid strains, the point estimate of the mutation rate was higher for every strain grown in HU than when grown in YPD, and none of the 95% CLs overlapped. Once again, an average fold-increase was calculated using the individual mutation rates for strains 1 and 2 under HU and YPD conditions, as detailed earlier in Section 5.2.2. The mutation rate increased 2.9- to 5.5-fold when diploid strains were grown in HU. The 53kb, 139kb and 216kb loci had very similar increases of 4.0- to 5.5-fold. The 230kb locus (origin) had the lowest increase in mutation rate of 2.9-fold, which was similar to the 3.0-fold increase observed for the 242kb (no features) locus. As expected, all of these fold-increases were statistically significant (Figures 5.6A, last column, and 5.6B).

In summary, exposure to 10mM HU in diploid strains increased the mutation rate over YPD rates for every locus examined in ChrIII. The extent of the increase for each locus was not uniform, however, as was seen in the haploid strains grown in the same conditions.

5.2.1.3 Effects of ploidy on the rate of URA3 inactivation in media supplemented with 10mM HU

As the diploid and haploid strains were grown using the same conditions, the mutation rates were compared to see if 10mM HU had differential effects on the mutation rate in a ploidy-specific manner. Figure 5.7A shows the individual point rate estimates of diploid (black-filled circles) and haploid (grey-filled triangles) strains grown in media supplemented with 10mM HU. There was a large degree of overlap between the 95% CL values for many of the strains, and the point rate

A

Construct location	Average mutation rate		Fold-difference[a] 10mM HU / 30˚C	Chi square and *P* values[b]
	10mM HU	30˚C		
53kb	8.9×10^{-5}	1.9×10^{-5}	4.7	30.00, $P<0.001$
139kb	5.6×10^{-5}	1.4×10^{-5}	4.0	26.13, $P<0.001$
216kb	6.2×10^{-5}	1.1×10^{-5}	5.5	26.13, $P<0.001$
230kb	8.6×10^{-5}	3.0×10^{-5}	3.0	8.07, $P<0.01$
242kb	9.6×10^{-5}	3.3×10^{-5}	3.0	30.00, $P<0.001$

B

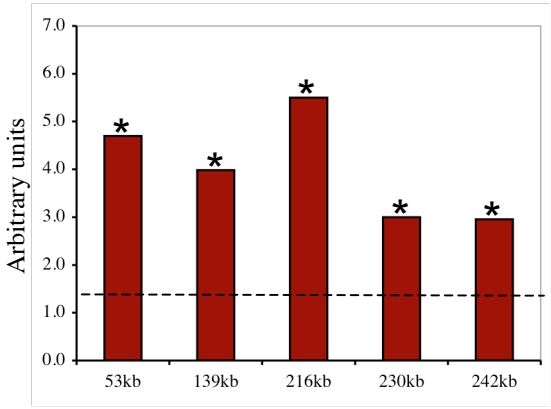

Figure 5.6. Effects of 10mM HU on the rates of *URA3* inactivation compared to those of optimal growth conditions in WT diploid strains, at 30˚C.

(A) [a] For each location the mutation rate of strain 1 (10mM HU) was divided by the mutation rate of strain 1 (YPD). The same was done for strain 2. The fold-difference was then averaged over these two values for each locus. [b] Significant differences were calculated by χ^2 analyses, as described in the text. χ^2 values are given first, *P* values second. *P* values of less than 0.05 were deemed significant.

(B) Graph showing the fold-difference in mutation rates of WT haploid strains grown in 10mM HU over those grown in YPD for each locus. "*" denotes a significant statistical difference. Values are taken from (A).

A

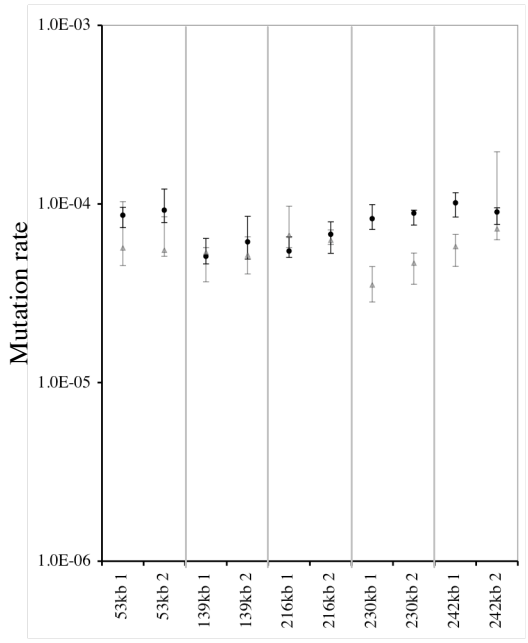

B

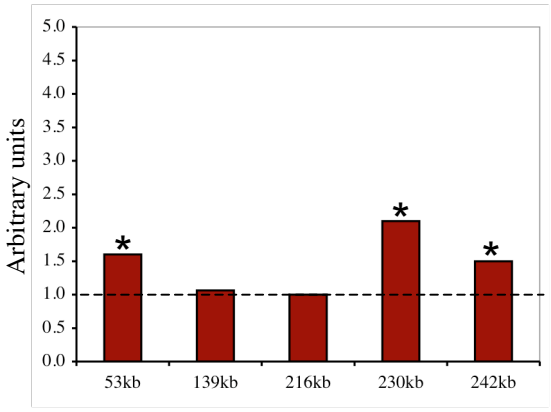

C

Construct location	Average mutation rate		Fold-difference[a] Diploid / Haploid	Chi square and *P* values[b]
	Diploid (HU)	Haploid (HU)		
53kb	8.9×10^{-5}	5.6×10^{-5}	1.6	4.80, $P<0.05$
139kb	5.6×10^{-5}	5.3×10^{-5}	1.1	1.20, NSS
216kb	6.2×10^{-5}	6.5×10^{-5}	1.0	0.13, NSS
230kb	8.6×10^{-5}	4.1×10^{-5}	2.1	11.27, $P<0.001$
242kb	9.6×10^{-5}	6.6×10^{-5}	1.5	6.53, $P<0.01$

Figure 5.7. Effects of ploidy on the rates of *URA3* inactivation in WT strains grown in media supplemented with 10mM HU, at 30˚C.

(A) Individual mutation rates of WT haploid (grey triangles) and diploid (black circles) strains grown in media supplemented with 10mM HU.

(B) Graph showing the fold-difference in mutation rates of diploid over haploid WT strains for each locus. "*" denotes a significant statistical difference. Values are taken from (C).

(C) For each location the mutation rate of strain 1 (diploid) was divided by the mutation rate of strain 1 (haploid). The same was done for strain 2. The fold-difference was then averaged over these two values for each locus. [b] Significant differences were calculated by χ^2 analyses, as described in the text. χ^2 values are given first, *P* values second. *P* values of less than 0.05 were deemed significant. NSS: not statistically significant.

estimates between the two types of cell were similar for both the 139kb and 216kb loci. The average fold-differences are plotted in Figure 5.7B. The mutation rates of diploid strains were divided by their respective haploid mutation rates at each locus: these varied from 1.0- to 2.1-fold. Of these values, the fold-increases for the 53kb (RSZ, termination), 230kb (origin) and 242kb (no features) loci were statistically significant, but not for the 139kb or 216kb loci (χ^2 analysis).

In summary, the rates of *URA3* inactivation at the 139kb and 216kb loci were statistically the same in haploid and diploid strains grown in 10mM HU. The mutation rates of the 53kb, 230kb and 242kb loci were significantly higher in the diploid strains than in the respective haploid strains.

5.2.2 Effects of temperature on rates of URA3 inactivation in diploid strains

The effects of temperature on the rate of *URA3* inactivation were tested in diploid strains. Figure 3.11 (page 97) shows that the growth of most strains was comparable to a parental WT strain at all four temperatures tested in non-selective (YPD) media. Growth at 18˚C was very slow for all strains and therefore was unsuitable to use with the specific incubation times established in the previous chapter. The mutation rates were therefore tested at 23˚C and 37˚C in diploid strains: one lower and one higher than the "optimal growth conditions" used in Chapter 4.

5.2.2.1 Rates of URA3 inactivation at 23˚C

Figure 5.8B shows the result for diploid strains grown in YPD at 23˚C (blue diamonds) and 37˚C (red crosses). Mutation rates of the same strains grown in YPD at 30˚C are also shown for comparison (green squares). Specific values for both temperatures are given in Figure 5.8A.

The mutation rates were first compared in strains grown at 23˚C. No statistical difference was found in the mutation rates for the two independently derived strains at the 53kb, 139kb or 216kb loci (χ^2 analysis). These calculations could not be

A

Strain		23°C Mutation Rate (95% CL)	23°C Fold-difference between 1&2[a]	23°C Average Mut Rate[b]	37°C Mutation Rate (95% CL)	37°C Fold-difference between 1&2[a]	37°C Average Mut Rate[b]
53kb	1	1.6 x 10^{-5} (1.3-1.9)	1.0	1. 6 x 10^{-5}	ND	-	-
	2	1.6 x 10^{-5} (1.4-2.0)			ND		
139kb	1	1.6 x 10^{-5} (1.4-2.0)	1.1	1.6 x 10^{-5}	3.7 x 10^{-5} (2.6-4.6)	1.0	3.7 x 10^{-5}
	2	1.5 x 10^{-5} (1.2-1.9)			3.7 x 10^{-5} (2.6-4.7)		
216kb	1	1.0 x 10^{-5} (0.9-1.4)	1.3	1.2 x 10^{-5}	5.9 x 10^{-5} (5.2-7.7)	1.2	6.4 x 10^{-5}
	2	1.3 x 10^{-5} (1.2-1.8)			6.9 x 10^{-5} (5.7-10.9)		
230kb	1	1.8 x 10^{-5} (1.4-2.0)	-	1.8 x 10^{-5}	6.2 x 10^{-5} (4.4-7.1)	-	6.2 x 10^{-5}
	2	ND			ND		
242kb	1	ND	-	1.8 x 10^{-5}	ND	-	6.9 x 10^{-5}
	2	1.8 x 10^{-5} (1.5-2.2)			6.9 x 10^{-5} (5.6-8.0)		

B

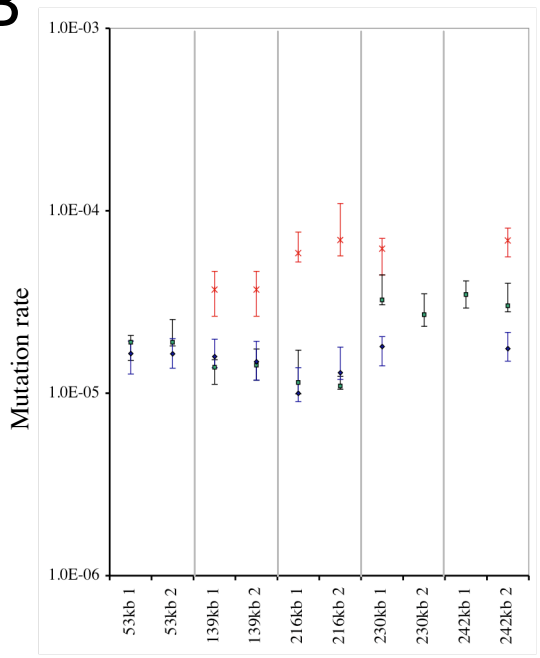

C

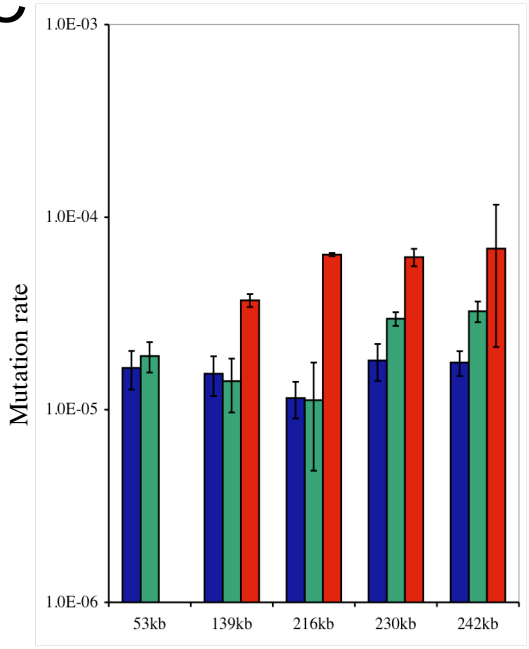

Figure 5.8. Rates of *URA3* inactivation in WT diploid strains grown in non-selective media at 23˚C, 30˚C and 37˚C.

(A) All strains are heterozygous for the *hisG-URA3-hisG* reporter construct. With the exception of the 230kb and 242kb loci, two independent rate measurements were done for each locus. The fraction of 5-FOA-resistant cells was measured in 15 independent cultures for each rate measurement. These fractions were converted to rates using the method of the median (Lea and Coulson, 1949). [a,b] Fold-differences and average mutation rates could not be calculated for the 230kb and 242kb loci. ND: not determined. Mutation rate is given as number of events/cell/generation.

(B) Individual mutation rates of WT, 23˚C (blue diamonds), 30˚C (green squares), and 37˚C (red crosses) are plotted. Capped lines indicate 95% CLs.

(C) Where possible, the average of the two strains is plotted for 23˚C (blue bars), 30˚C (green bars) and 37˚C (red bars). The smallest and largest CL value of the two strains was used for each locus.

applied for 230kb or 242kb, as fluctuation analyses were not performed for one of the two strains in both cases. The mutation rate data set for 23˚C (and 37˚C) is therefore not as complete as the other sets. Nevertheless, given the high reproducibility between strains 1 and 2 in all cases examined in this study, analysis of the data was continued.

The mutation rates were averaged for each locus (except for 230kb and 242kb). These were 1.6 x 10^{-5} events/cell/generation for 53kb and 139kb, 1.2 x 10^{-5} for 216kb, and 1.8 x 10^{-5} for both 230kb and 242kb (Figure 5.8A). The average mutation rate for each locus was then compared separately to the other four. For the 230kb and 242kb loci, the analysis based on 30 measurements per locus could not be used as they each only had results for 1 strain (15 cultures). This analysis was therefore adapted by separately comparing the parallel cultures from strains 1 and 2 of the 53kb, 139kb and 216kb loci to the 230kb or 242kb locations. As the mutation rates of the 1 and 2 strains were very similar for 53kb, 139kb and 216kb, the same statistical result was always achieved regardless if strain 1 or strain 2 was used. Figure 5.9A shows that when the mutation rates were normalised against the lowest one (216kb in this instance), the fold-difference varied from only 1.0- to 1.5-fold. Chi-square analyses revealed that no significant difference in mutation rate existed between any of the five loci. The mutation rate was therefore the same irrespective of location in diploid strains when grown in YPD media at 23˚C.

The rates of *URA3* inactivation for strains grown at 23˚C were then compared to their respective rates when grown at 30˚C. For example, the mutation rate of the 53kb strains grown at 23˚C was compared to their respective rates when at 30˚C. The 53kb, 139kb and 216kb loci had very similar mutation rates at both temperatures. This was not the case for the 230kb and 242kb loci, however, where the mutation rate was lower when strains were grown at 23˚C. This was confirmed by χ^2 analyses: no statistical difference was found between the mutation rates at 23˚C and 30˚C for 53kb, 139kb or 216kb, but the mutation rates were significantly lower at 23˚C compared to 30˚C for both 230kb and 242kb (P<0.01; Figure 5.10). The mutation rates for strains grown at 23˚C were therefore unchanged respective to the rates ar 30˚C for the 53kb, 139kb and 216kb loci, but was approximately halved (0.6-fold)

A

Location Mutation rate[a]	Normalised mutation rate
53kb 1.6 x 10^{-5}	1.3
139kb 1.6 x 10^{-5}	1.3
216kb 1.2 x 10^{-5}	1.0
230kb 1.8 x 10^{-5}	1.5
242kb 1.8 x 10^{-5}	1.5

B

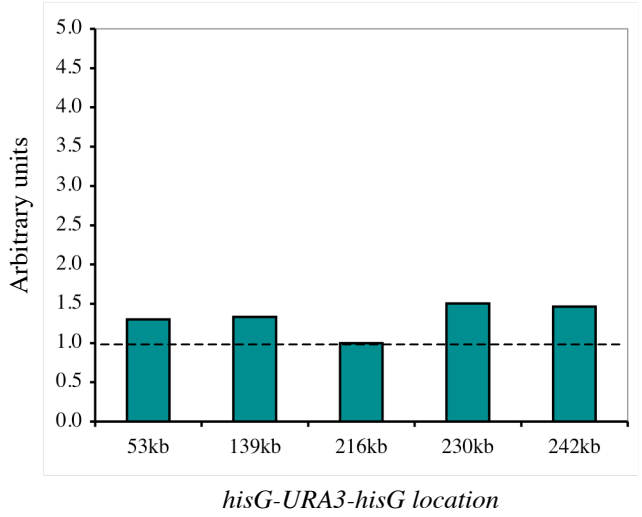

C

Location Mutation rate[a]	53kb 1.6 x 10^{-5}	139kb 1.6 x 10^{-5}	216kb 1.2 x 10^{-5}	230kb 1.8 x 10^{-5}	242kb 1.8 x 10^{-5}
53kb 1.6 x 10^{-5}		0.07 NSS	0.60 NSS	0.07 NSS	0.07 NSS
139kb 1.6 x 10^{-5}			1.67 NSS	1.67 NSS	1.67 NSS
216kb 1.2 x 10^{-5}				3.27 NSS	3.27 NSS
230kb 1.8 x 10^{-5}					0.07 NSS
242kb 1.8 x 10^{-5}					

Figure 5.9. Analysis of rates of *URA3* inactivation in WT diploid strains grown in non-selective media at 23˚C.

(A) The average mutation rate at each locus was normalised against the lowest average rate. [a] Mutation rate is given as number of events/cell/generation.

(B) Normalised fold-differences from (A) are plotted.

(C) Chi-square analysis: pair-wise comparison of the mutation rates at each location. Shown in each panel are the Chi square (χ^2; upper) and probability (*P*; lower) values for each pair-wise combination. *P* values of less than 0.05 were deemed significant. NSS: not statistically significant. [a] Mutation rate is given as number of events/cell/generation.

A

Construct location	Average mutation rate		Fold-difference[a] 23°C / 30° C	Chi square and *P* values[b]
	23°C	30°C		
53kb	1.6×10^{-5}	1.9×10^{-5}	0.9	0.60, NSS
139kb	1.6×10^{-5}	1.4×10^{-5}	1.1	0.60, NSS
216kb	1.2×10^{-5}	1.1×10^{-5}	1.1	1.67, NSS
230kb	1.8×10^{-5}	3.0×10^{-5}	0.6	8.07, $P<0.01$
242kb	1.8×10^{-5}	3.3×10^{-5}	0.6	8.07, $P<0.01$

B

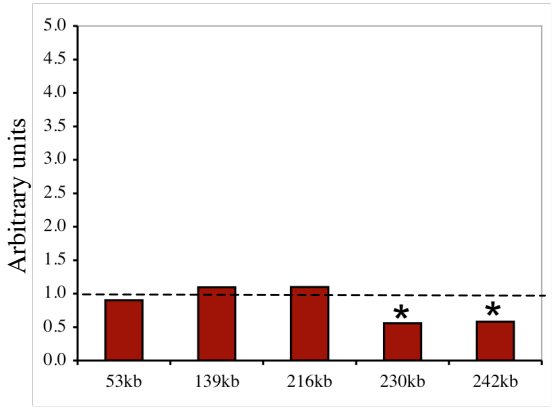

Figure 5.10. Comparison of the rates of *URA3* inactivation in WT diploid strains, grown in non-selective media at 23˚C and 30˚C.

(A) [a] For each location the mutation rate of strain 1 (23˚C) was divided by the mutation rate of strain 1 (30˚C). The same was done for strain 2. The fold-difference was then averaged over these two values for each locus. [b] Significant differences were calculated by χ^2 analyses, as described in the text. χ^2 values are given first, *P* values second. *P* values of less than 0.05 were deemed significant. NSS: not statistically significant.

(B) Graph showing the fold-difference in mutation rates of WT diploid strains grown at 23˚C over those grown at 30˚C, in YPD, for each locus. "*" denotes a significant statistical difference. Values are taken from (A).

for 230kb and 242kb at the lower temperature. Note that the first three loci corresponded to known replication terminations sites in the chromosome.

5.2.2.2 Rates of URA3 inactivation at 37˚C

The rates of *URA3* inactivation were next tested in non-selective media at 37˚C in WT diploid strains. Single colonies did not grow to a sufficient size at this temperature for the 53kb strains, since they produced very low colony counts on the resulting media plates after fluctuation analysis. The initial spot test (Figure 3.11, page 97) did not reveal obvious growth defect conferred by the insertion of tester constructs at the 53kb locus when grown at 37˚C. However, when the strains were streaked for single colonies and incubated at 37˚C, the sizes of individual colonies of 53kb strains were reproducibly small. An alternative was to incubate these strains for longer on YPD plates to increase the colony cell number, but this would have meant that the growth times were different to those used for the other strains. The 53kb strains were therefore not used for fluctuation analysis at 37˚C.

The rates of *URA3* inactivation were tested at the other four loci at 37˚C. The results are shown in Figure 5.8A (red crosses). No statistical difference in mutation rate was found between strains 1 and 2 for the 139kb or 216kb loci (χ^2 analyses).

The average mutation rates were then calculated and normalised against the lowest rate: in this case, 3.7 x 10^{-5} events/cell/generation at the 139kb locus (RSZ, termination, Ty2). The 216kb, 230kb and 242kb loci had similar mutation rates of 6.4, 6.2 and 6.9 x 10^{-5} mutation events/cell/generation, respectively, which were 1.7-1.9-fold higher than the rate at 139kb. Chi square analyses were performed to see if any significant difference existed between these mutation rates. As expected from these results, the mutation rates at the 216kb, 230kb and 242kb did not statistically differ from each other, but were all significantly higher than the rate seen for the 139kb strains (P<0.01; Figure 5.11). In terms of construct location, therefore, growing diploid strains at 37˚C produced similar mutation rates at the 216kb, 230kb and 242kb loci, which were almost twice the rate observed for the 139kb locus.

A

Location Mutation rate[a]	Normalised mutation rate
53kb N/D	-
139kb 3.7 x 10^{-5}	1.0
216kb 6.4 x 10^{-5}	1.7
230kb 6.2 x 10^{-5}	1.7
242kb 6.9 x 10^{-5}	1.9

B

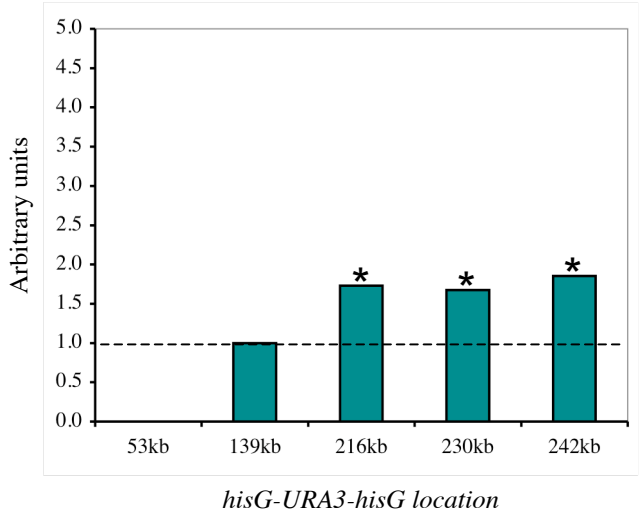

C

Location Mutation rate[a]	53kb N/D	139kb 3.7 x 10^{-5}	216kb 6.4 x 10^{-5}	230kb 6.2 x 10^{-5}	242kb 6.9 x 10^{-5}
53kb N/D					
139kb 3.7 x 10^{-5}			5.40 *P*<0.05	5.40 *P*<0.05	5.40 *P*<0.05
216kb 6.4 x 10^{-5}				0.07 NSS	0.07 NSS
230kb 6.2 x 10^{-5}					0.07 NSS
242kb 6.9 x 10^{-5}					

Figure 5.11. Analysis of rates of *URA3* inactivation in WT diploid strains grown in non-selective media at 37˚C.

(A) The average mutation rate at each locus was normalised against the lowest average rate. [a] Mutation rate is given as number of events/cell/generation.

(B) Normalised fold-differences from (A) are plotted. "*" denotes a significant statistical difference.

(C) Chi-square analysis: pair-wise comparison of the mutation rates at each location. Shown in each panel are the Chi square (χ^2; upper) and probability (*P*; lower) values for each pair-wise combination. *P* values of less than 0.05 were deemed significant. NSS: not statistically significant.

The mutation rates for 37˚C growth conditions were then compared to the rates for YPD (Figure 5.12). The rate of *URA3* inactivation at the 216kb (termination) locus was almost 6-fold higher at 37˚C than at 30˚C, whilst the rates at the other loci were only 1.9-2.7-fold higher. All of the rates for 37˚C were statistically higher than the respective rates seen for 30˚C (χ^2 analyses; $P<0.01$). When the 139kb, 230kb and 242kb strains were grown at 37˚C, the mutation rate increased uniformly when compared to their respective rates when grown at 30˚C. For the 216kb strains, however, the higher temperature had a much greater effect on the mutation rate.

5.3 Discussion

5.3.1 Mutagenic effects of 10mM HU

HU is a known inhibitor of DNA replication. The effects of a low drug dosage on the rate of *URA3* inactivation were compared between each of the five locations in ChrIII. In haploid strains, the 230kb (origin) locus had the lowest mutation rate, whilst the other loci had significantly higher rates that were indistinguishable from each other. The result for diploids treated with 10mM HU contrasted with the result seen for haploids: the 139kb (RSZ, termination, Ty2) and 216kb (termination) locations had the lowest mutation rates, whilst the 53kb, 230kb and 242kb loci had the highest. The mutation rates therefore varied in a ploidy-dependent manner when strains were exposed to 10mM HU.

The rate of *URA3* inactivation was then compared between the 10mM HU and YPD growth conditions for each location in ChrIII. In haploids, HU increased the mutation rate uniformly ~3-fold over those established in YPD conditions, irrespective of the construct location. In diploids, HU led to the largest fold-increase for the 53kb and 216kb loci, and the lowest fold-increase for the 230kb and 242kb loci. The fold-increase in mutation rate of the 10mM HU over YPD conditions therefore also varied, in a ploidy-dependent manner.

In diploids the 53kb (RSZ, termination), 139kb (RSZ, termination, Ty2) and 216kb (termination) loci had the highest fold-increases in mutation rate due to HU over YPD conditions. Due to these loci being within DNA replication termination sites,

A

Construct location	Average mutation rate		Fold-difference[a] 23°C / 30° C	Chi square and *P* values[b]
	37°C	30°C		
53kb	-	1.9×10^{-5}	-	-
139kb	3.7×10^{-5}	1.4×10^{-5}	2.7	5.40, $P<0.05$
216kb	5.4×10^{-5}	1.1×10^{-5}	5.7	11.27, $P<0.001$
230kb	6.2×10^{-5}	3.0×10^{-5}	1.9	5.40, $P<0.05$
242kb	6.9×10^{-5}	3.3×10^{-5}	2.3	8.07, $P<0.01$

B

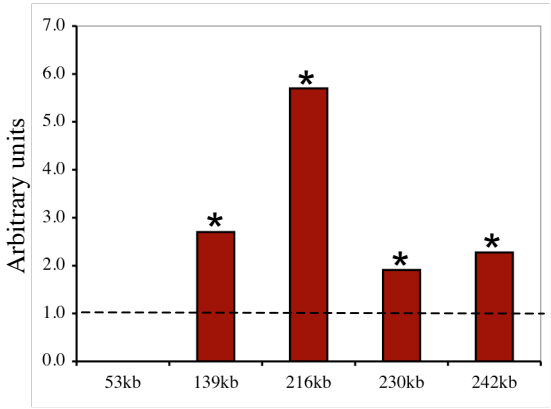

Figure 5.12. Comparison of the rates of *URA3* inactivation in WT diploid strains, grown in non-selective media at 37˚C and 30˚C.

(A) [a] For each location the mutation rate of strain 1 (37˚C) was divided by the mutation rate of strain 1 (30˚C). The same was done for strain 2. The fold-difference was then averaged over these two values for each locus. [b] Significant differences were calculated by χ^2 analyses, as described in the text. χ^2 values are given first, *P* values second. *P* values of less than 0.05 were deemed significant.

(B) Graph showing the fold-difference in mutation rates of WT diploid strains grown at 37˚C over those grown at 30˚C, in YPD, for each locus. "*" denotes a significant statistical difference. Values are taken from (A).

replication through these regions may be slower than through the 230kb (origin) or 242kb (no chromosomal features) loci. Because the first three regions are intrinsically difficult to replicate, and because HU slows the rate of fork progression even more, perhaps the low concentration of HU used impeded replication for these regions to an even greater degree than for the 230kb or 242kb loci. This would increase the possibility of fork stalling within replication termination sites, potentially resulting in increased genetic instability such as recombination, which could lead to an increase in *URA3* inactivation. What was striking, however, is that this location-dependent increase in mutation rate due to HU was only observed in diploid strains.

Previous reports have studied the effects of HU on recombination rates using a system different to that used in this thesis. Recombination is often measured between two alleles at just one locus within a chromosome when grown in high concentrations of HU, for instance, whereas the system used here measured the rate of *URA3* inactivation at five different locations of ChrIII in low doses of HU. This study has revealed that the location of the *hisG-URA3-hisG* reporter construct within yeast ChrIII affected the recombination rate when haploids and diploids were treated even with a low dose of HU. An earlier study also reported much higher rates of mutation (~38-fold) than those observed in this chapter (Barbera and Petes, 2006). In that study, however, a different strain background, growth conditions and higher concentrations of HU (100mM) were used, so direct comparisons with this study cannot be made. Work presented in this chapter has also shown that, when the mutation rates of strains grown in 10mM HU were compared to those of strains grown in non-selective conditions, the mutation rates increased uniformly in haploids regardless of the construct location, but differentially in diploids.

5.3.2 Mutagenic effects of high temperature

The effect of temperature on the rate of *URA3* inactivation was studied in diploid strains at three different temperatures, 23˚C, 30˚C and 37˚C. In terms of location (*cis* factors) the mutation rate was statistically the same for all strains when grown at 23˚C, irrespective of the location of the reporter construct within ChrIII. When these

rates at 23˚C were compared to their respective rates at 30˚C, the mutation rate of the construct at 230kb (origin) and 242kb (no features) increased when the temperature was increased from 23˚C to 30˚C, but not for constructs within replication termination regions (53kb, 139kb and 216kb).

The incubation temperature was then increased to 37˚C. The mutation rates were statistically indistinguishable between the 216kb, 230kb and 242kb loci, which were statistically higher than the rate seen for the 139kb locus at this temperature. When these were compared to the respective 30˚C rates, however, the 139kb, 230kb and 242kb loci had a uniform fold-increase of ~2-3-fold, whilst the 216kb location had a ~6-fold increase. When the mutation rates were compared between strains grown at 23˚C and those grown at 37˚C, all four loci showed an increase in mutation rate, with the fold increase ranging between 2.4- (139kb locus) and 5.6-fold (216kb locus).

In agreement with the results of earlier studies (such as Evans and Parry, 1975), increasing the temperature diploid strains were incubated at caused an increase in the mutation rate. It has been shown here that the effects were not uniform, however, with respect to the location of the construct within ChrIII, and when compared to the mutation rates of the respective strains grown at 30˚C. At elevated temperatures, certain proteins are destabilised and their function reduced but, as temperature can have so many different effects on cellular metabolism, it cannot accurately be predicted what exactly happened at the biochemical level. As all of the strains used in this study were isogenic, the effects of temperature (and HU) were the same in every cell, and the only difference between them was the location the construct inserted at in ChrIII, therefore, the differences seen in mutation rate were only due to the location of the *hisG-URA3-hisG* construct.

The rate of *URA3* inactivation was therefore significantly increased at 37˚C for all loci tested, but the extent of the fold-increases was not uniform. Strong position effects have also been observed in meiosis, where “hot” and “cold” spots of recombination exist (Gerton *et al*., 2000). It has been shown here, however, that the mutation rate can vary in a location-dependent manner, even within one chromosome, in mitotic cell cycles at different temperatures.

Chapter 6.

MEC1

6.1 Introduction

One important gene in the regulation of genome stability in mammalian cells is ATM (Shiloh, 1997). The cellular phenotypes in human cells lacking ATM include sensitivity to DNA damaging agents, increased end-to-end chromosome fusions associated with shortened telomeres (Pandita *et al*., 1995) and elevated levels of mitotic recombination (Meyn, 1993). Mutations in the structurally related gene ATR are associated with embryonic lethality and chromosomal fragmentation (Brown and Baltimore, 2003). ATM and ATR are proteins required for checkpoint responses to DNA damaging agents, such as the phosphorylation of a number of proteins that lead to cell cycle arrest in response to DNA damage (Shiloh, 2001). It is likely that the elevated levels of genome instability observed in strains with ATM or ATR mutations reflect both inefficient repair of spontaneous DNA damage and defects in telomere metabolism.

The *S. cerevisiae* genes *MEC1* and *TEL1* are related to the mammalian genes ATR (Kato and Ogawa, 1994; Weinert *et al*., 1994) and ATM (Greenwell *et al*., 1995; Morrow *et al*., 1995), respectively. Strains with single mutations in *MEC1*, but not *TEL1*, are sensitive to DNA damaging agents and fail to arrest the cell cycle in response to DNA damage or inhibition of DNA synthesis (Weinert *et al*., 1994). Tel1p appears to have a role in the repair of DNA damage that is functionally redundant with that of Mec1p because *mec1 tel1* double mutant strains are more sensitive to DNA damaging agents than are *mec1* strains (Morrow *et al*., 1995; Sanchez *et al*., 1996) and an extra copy of *TEL1* partially suppresses the DNA damage sensitivity of *mec1* strains (Morrow *et al*., 1995).

The effect *mec1* has on meiotic recombination has been well documented (Kato and Ogawa, 1994; Lydall *et al*., 1996; Grushcow *et al*., 1999). *MEC1* acts to promote normal meiotic recombination; *mec1* mutants exhibit aberrant synapsis formation, elevated levels of ectopic recombination and a dramatic loss in spore viability (Grushcow *et al*., 1999), and also appear to undergo meiosis I before all recombination events are complete (Lydall *et al*., 1996). The effects of eliminating Mec1p on mitotic recombination have also been assessed, where inactivation of Mec1p has been linked to an increase in rates of recombination (Myung *et al*., 2001; Craven *et al*., 2002). However, the effects of *mec1* mutation rates on regions for the genome associated with specific loci has not been assessed. The rates of *URA3* inactivation in strains carrying the *hisG-URA3-hisG* reporter construct were therefore assessed in both a *mec1Δ* and *mec1-40* background. The *mec1-40* allele was one of two isolated alleles used to identify RSZs in ChrIII (Cha and Kleckner, 2002; also see Introduction). Of particular interest were the mutation rates at the two loci within RSZ, 53kb and 139kb, given the preferred chromosome breakage at these loci following thermal inactivation of Mec1p in *mec1-40* strains.

6.2 Results

6.2.1 Strain construction.

mec1 null mutants require an inactive copy of *SML1* (Suppressor of Mec1 Lethality) for viability. Sml1p is an inhibitor of ribonucleotide reductase and regulates dNTP production. It binds Rnr1 protein of the ribonucleotide reductase protein complex, inhibiting ribonucleotide reductase activity when DNA synthesis is not required (Zhao *et al*., 1998; Chabes *et al*., 1999). After DNA damage or at S-phase, Mec1p and its effector kinase, Rad53p, phosphorylates Sml1p, leading to its degradation and removal of inhibitory action on Rnr1p (Zhao *et al*., 2001).

It is inappropriate to compare the mutation rates of *mec1Δ sml1Δ* strains to WT strains grown at the same temperature (Chapter 4) to specifically assess the effects of *mec1Δ* on the mutation rate, since this would not take into consideration any effects that the *SML1* deletion may have. The mutation rates of *mec1Δ sml1Δ* strains should

therefore be compared to *sml1Δ* strains for this purpose. This was tested first in haploid strains.

To produce the strains required for this chapter the WT haploids (used in the previous two chapters) were crossed with a *mec1Δ sml1Δ* strain (RCY309), then sporulated and dissected. *URA3* prototroph spores were selected for that had either the *sml1Δ* marker, or both an *sml1Δ* and *mec1Δ* marker. These haploids were then crossed with either an *sml1Δ* strain or *mec1Δ sml1Δ* strain to produce the appropriate homozygous diploids that were heterozygous for the *hisG-URA3-hisG* construct. The strains used in this chapter are listed in Table 3.1, page 98.

Spot tests of *sml1Δ* strains grown on non-selective media at 18˚C, 23˚C, 30˚C and 37˚C are shown in Figure 6.1. WT and *sml1Δ* strains lacking an inserted *hisG-URA3-hisG* construct are also shown for comparison (right hand side). Growth of all strains, including the 216kb ones, was optimal at 30˚C. This temperature was therefore chosen for *sml1Δ* strains. Any *trans* effects that *sml1Δ* had on the mutation rate could also be observed since the WT strains were also grown at 30˚C (Chapter 4).

Before the mutation rates were tested in the *sml1Δ* strains at 30˚C it was ensured that growth was also optimal for the *mec1Δ sml1Δ* strains at this temperature. Spot tests showing growth of these strains at 18˚C, 23˚C, 30˚C and 37˚C are shown in Figure 6.2, with a *mec1Δ sml1Δ* strain lacking the reporter construct also shown for comparison. Once again, the only suboptimal growth was for the 216kb strains, which were least-affected at 30˚C out of all four temperatures tested. Both *sml1Δ* and *mec1Δ sml1Δ* strains were therefore incubated at this temperature.

To check that the damage sensitivity of *mec1* null strains was not altered, *mec1Δ sml1Δ* strains were also spotted onto 10mM HU agar plates at the same time as non-selective (YPD) plates (Figure 6.2, lower panel). As expected, none of the *mec1Δ sml1Δ* strains grew in the presence of HU and growth of the WT strain was unaffected.

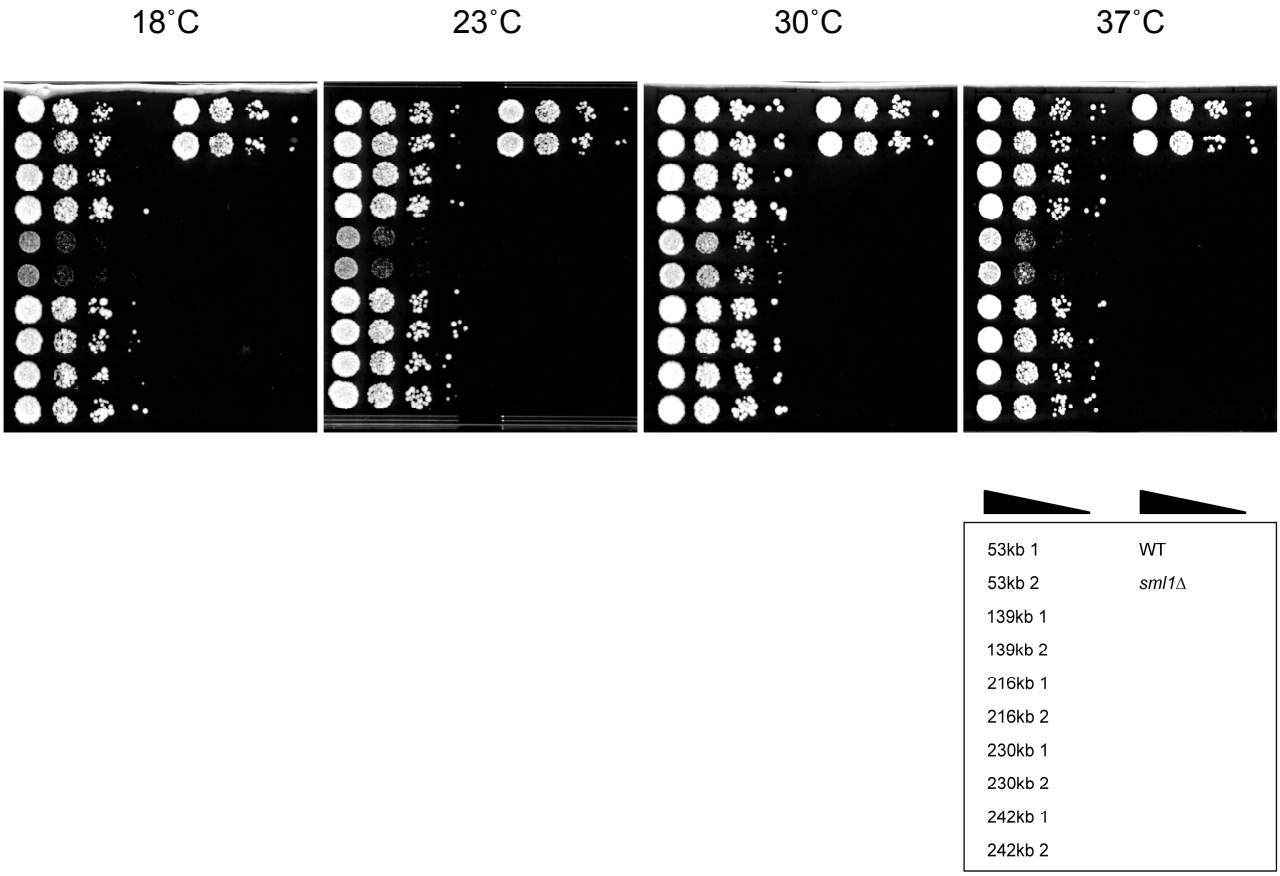

Figure 6.1. Effects of temperature on growth of *sm11Δ* haploid strains carrying a *hisG-URA3-hisG* construct at different loci on ChrIII.

Ten-fold serial dilutions of exponentially growing cells were spotted onto YPD plates and grown at the indicated temperatures for 3-5 days. The box in the lower right indicates the strains spotted onto the plates: WT and *sm11Δ* in this instance refer to strains lacking a *hisG-URA3-hisG* construct.

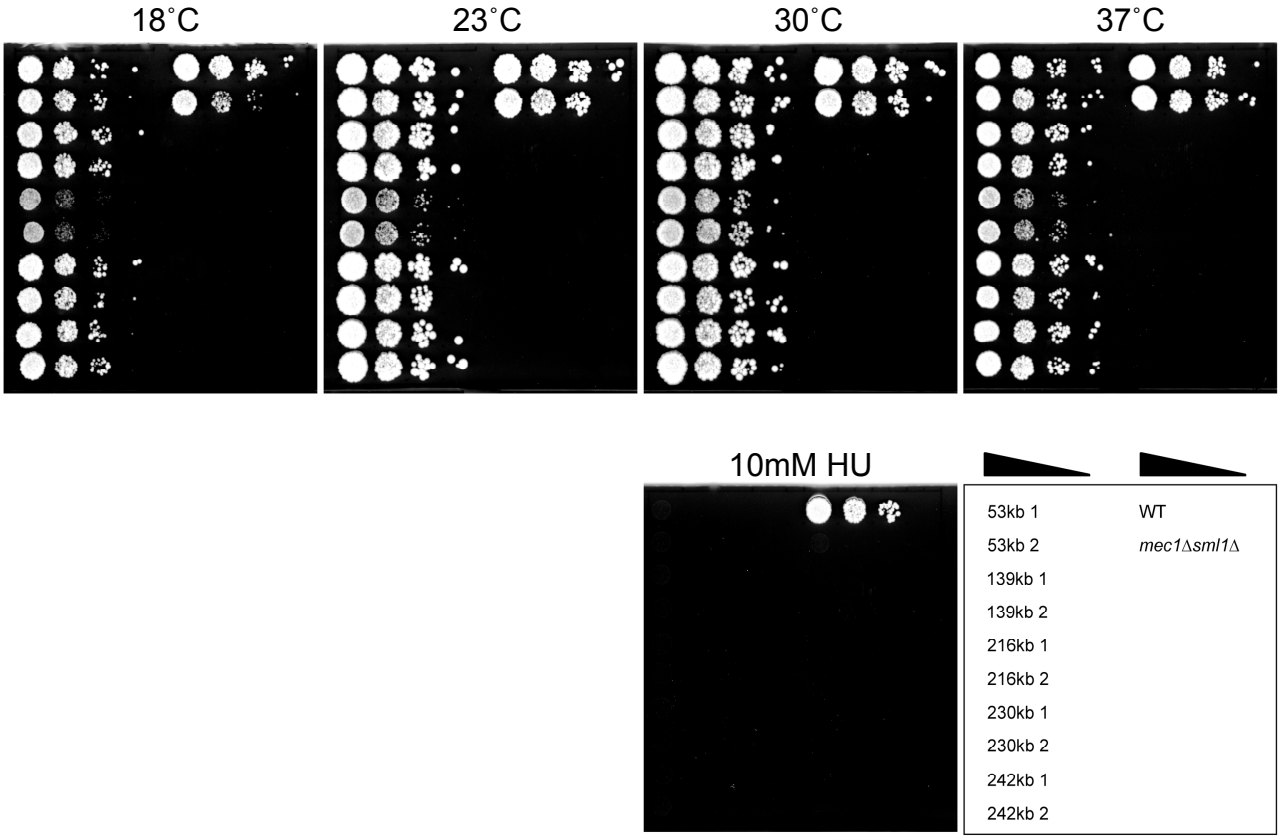

Figure 6.2. Effects of temperature on growth of *mec1Δ sml1Δ* haploid strains carrying a *hisG-URA3-hisG* construct at different loci on ChrIII.

Ten-fold serial dilutions of exponentially growing cells were spotted onto YPD plates (top row) or media supplemented with 10mM HU (bottom row) and grown at the indicated temperatures for 3-5 days. The box in the lower right indicates the strains spotted onto the plates: WT and *mec1*Δ *sm11*Δ in this instance refer to strains lacking a *hisG-URA3-hisG* construct.

6.2.2 Rates of URA3 inactivation in sml1Δ haploid strains

The results for individual *sml1Δ* haploid strains grown at 30˚C are shown in Figure 6.3B (black diamonds) alongside the mutation rates of their respective WT strains (grey triangles). Specific values are given in Figure 6.3A. As in the previous chapter, only one strain was used for the 230kb and 242kb loci. For the remaining loci, no significant difference existed in the mutation rates between the two independently derived strains (χ^2 analyses).

The rates of *URA3* inactivation in haploid *sml1Δ* strains were averaged for the 53kb, 139kb and 216kb locations. The mutation rates among the five loci ranged from 1.7 x 10^{-5} events/cell/generation at the 242kb locus (no features), to 2.4 x 10^{-5} for the 216kb locus (termination; Figures 6.3A and 6.3C). To assess the variation amongst these mutation rates, the rates at each locus were normalised against the lowest one. These values ranged from 1.1- to 1.4-fold, which were not statistically significant (χ^2 analysis, Figures 6.4A and 6.4B). This analysis was extended so that the mutation rates at each locus were separately compared to the other four loci. No statistical difference existed between any of the mutation rates (χ^2 analyses, Figure 6.4C). There was therefore no *cis* effect on the rate of *URA3* inactivation in haploid strains in the absence of Sml1p.

To observe any *trans* effects deletion of *SML1* had on the rate of *URA3* inactivation in haploid strains, the rates of the *sml1Δ* strains were compared to the mutation rates of their respective WT strains grown in non-selective media at 30˚C. Figure 6.3A shows that the point rate estimates were very similar in *sml1Δ* strains compared to their respective WT strains, and the 95% CLs overlapped. As expected, no statistical difference was found between the rates of the two genotypes at any of the five loci (Figure 6.5).

In summary, the mutation rates of *sml1Δ* haploid strains were indistinguishable from the rates of their respective WT strains grown using the same conditions.

A

Strain		Mutation Rate (95% CL)[a]	Fold-difference between 1&2	Average Mut Rate[b]
53kb	1	2.1×10^{-5} (1.8-3.9)	1.2	2.0×10^{-5}
	2	1.8×10^{-5} (1.4-2.1)		
139kb	1	1.6×10^{-5} (1.3-2.5)	1.2	1.8×10^{-5}
	2	1.9×10^{-5} (1.6-2.5)		
216kb	1	2.3×10^{-5} (1.7-2.9)	1.1	2.4×10^{-5}
	2	2.5×10^{-5} (2.2-2.9)		
230kb	1	2.1×10^{-5} (1.6-2.5)	-	2.1×10^{-5}
	2	ND		
242kb	1	ND	-	1.7×10^{-5}
	2	1.7×10^{-5} (1.5-2.2)		

Location	Chromosomal Features
53kb	RSZ, Termination
139kb	RSZ, Termination, Ty2
216kb	Termination
230kb	Origin
242kb	None

B

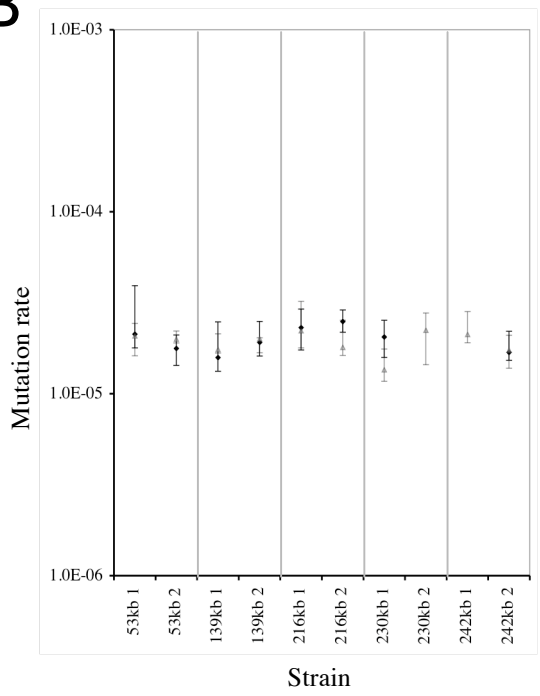

C

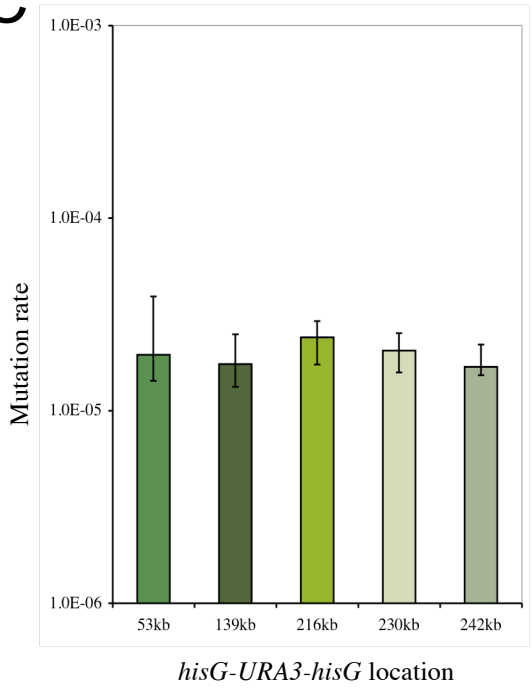

Figure 6.3. Rates of *URA3* inactivation in *sml1Δ* haploid strains.

(A) For each locus, except 230kb and 242kb, two independent rate measurements were done. The fraction of 5-FOA-resistant cells was measured in 15 independent cultures for each rate measurement. These fractions were converted to rates using the method of the median (Lea and Coulson, 1949). [a] 95% confidence limits (CL) were calculated as described previously (Wierdl *et al*., 1996). Chromosomal features at each locus are denoted on the right hand side. ND: not determined.

(B) Individual mutation rates are plotted for *sml1Δ* (black diamonds) and WT (grey triangles) haploid strains. Capped lines indicate 95% CLs.

(C) The average mutation rate of the two strains is plotted, where possible. The smallest and largest CL value of the two strains was used for each location. Mutation rate is given as number of events/cell/generation.

A

Location Mutation rate[a]	Normalised mutation rate
53kb 2.0 x 10^{-5}	1.2
139kb 1.8 x 10^{-5}	1.1
216kb 2.4 x 10^{-5}	1.4
230kb 2.1 x 10^{-5}	1.2
242kb 1.7 x 10^{-5}	1.0

B

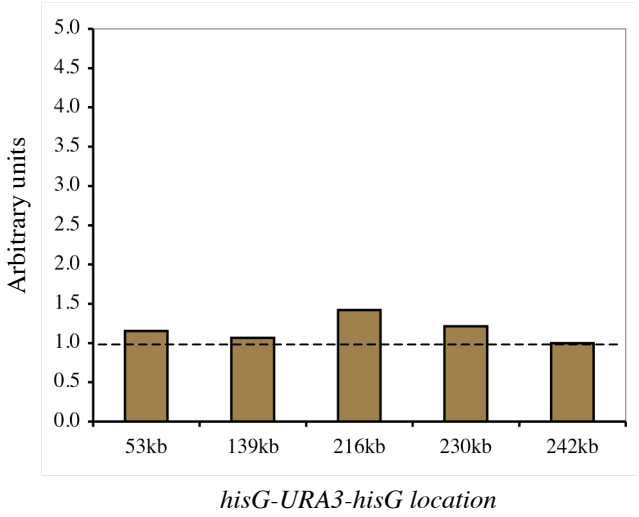

C

Location Mutation rate[a]	53kb 2.0 x 10^{-5}	139kb 1.8 x 10^{-5}	216kb 2.4 x 10^{-5}	230kb 2.1 x 10^{-5}	242kb 1.7 x 10^{-5}
53kb 2.0 x 10^{-5}		0.13 NSS	3.33 NSS	0.60 NSS	0.60 NSS
139kb 1.8 x 10^{-5}			1.20 NSS	0.60 NSS	1.67 NSS
216kb 2.4 x 10^{-5}				0.07 NSS	3.27 NSS
230kb 2.1 x 10^{-5}					0.67 NSS
242kb 1.7 x 10^{-5}					

Figure 6.4. Analysis of rates of *URA3* inactivation in *sml1Δ* haploid strains.

(A) The average mutation rate at each locus was normalised against the lowest average rate.

(B) Normalised fold-differences from (A) are plotted.

(C) Chi-square analysis: pair-wise comparison of the mutation rates at each location. Shown in each panel are the Chi square (χ^2; upper) and probability (*P*; lower) values for each pair-wise combination. *P* values of less than 0.05 were deemed significant. NSS: not statistically significant. [a] Mutation rate is given as number of events/cell/generation.

A

Construct location	Average mutation rate		Fold-difference[a] *sml1Δ*/ WT	Chi square and *P* values[b]
	sml1Δ	WT		
53kb	2.0×10^{-5}	2.0×10^{-5}	1.0	0.53, NSS
139kb	1.8×10^{-5}	1.9×10^{-5}	0.9	0.13, NSS
216kb	2.4×10^{-5}	2.0×10^{-5}	1.2	0.53, NSS
230kb	2.1×10^{-5}	1.8×10^{-5}	1.2	1.67, NSS
242kb	1.7×10^{-5}	1.9×10^{-5}	1.0	0.07, NSS

B

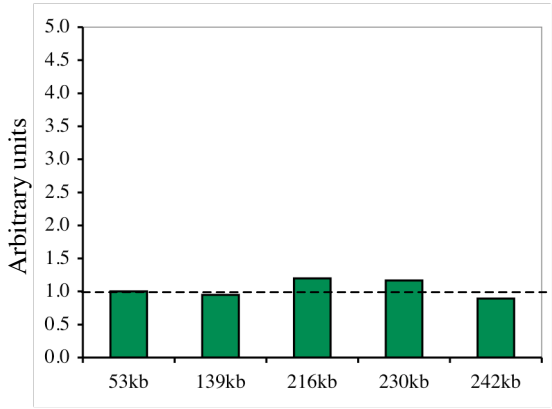

Figure 6.5. Effects of *sml1Δ* on the rates of *URA3* inactivation compared to those in WT haploid strains grown in the same conditions (YPD at 30˚C).

(A) [a] Where possible, for each location the mutation rate of strain 1 (*sml1Δ*) was divided by the mutation rate of strain 1 (WT). The same was done for strain 2. The fold-difference was then averaged over these two values for each locus. [b] Significant differences were calculated by χ^2 analyses, as described in the text. χ^2 values are given first, *P* values second. *P* values of less than 0.05 were deemed significant. NSS: not statistically significant.

(B) Graph showing the fold-difference in mutation rates of *sml1Δ* over WT haploid strains for each locus. Values are taken from (A).

6.2.3 Rates of URA3 inactivation in mec1Δ sml1Δ haploid strains

The rates of *URA3* inactivation were measured in *mec1Δ sml1Δ* haploid strains. Results of fluctuation analyses are shown in Figure 6.6B for *mec1Δ sml1Δ* strains (light blue squares) alongside the rates of their respective *sml1Δ* strains (grey diamonds). Once again, only one strain was used for the 230kb and 242kb loci. For the remaining loci, no significant difference existed in the mutation rates between the two independently derived strains (χ^2 analyses).

The average mutation rate was calculated, where possible. The mutation rates among the five loci ranged from 0.7 x 10^{-5} events/cell/generation at 216kb (termination), to 2.3 x 10^{-5} for 53kb (RSZ, termination; Figure 6.6C). The average mutation rates were then normalised against the lowest value – in this case, the value for 216kb – as shown in Figures 6.7A and 6.7B. The rates of *URA3* inactivation at the 216kb and 230kb loci were very similar (1.1-fold difference), the rate at 139kb was 1.7-fold higher than that at 216kb, 242kb was 2.0-fold higher than the rate at 216kb and 53kb had the highest fold-difference over 216kb of over 3-fold. The only differences that were significant were between the rates at the 53kb and 216kb loci, and between the rates at the 139kb and 216kb loci (χ^2 analyses). Due to the large difference between the upper and lower 95% CL at the 242kb locus, however, the mutation rate at this locus was not statistically different from the mutation rate at 216kb, despite the point rate estimate being 2.0-fold higher.

The mutation rate at each locus was then separately compared against the other loci using pair-wise analysis. This analysis found that the only statistical differences in the mutation rates were between the 53kb and 216kb loci, and between 139kb and 216kb loci (Figure 6.7B). In both cases the rate at the 216kb locus was significantly lower than the rates at the 53kb and 139kb loci. All of the other location mutation rates were statistically indistinguishable from each other (Figure 6.7C).

The effects of *mec1Δ sml1Δ* on the mutation rate in haploid strains could now be compared to the rates in their respective *sml1Δ* strains. Figure 6.8B shows that the point rate estimates and 95% CLs for the 53kb, 139kb and 242kb loci were very

A

Strain		Mutation Rate (95% CL)[a]	Fold-difference between 1&2	Average Mut Rate[b]
53kb	1	2.4×10^{-5} (1.3-3.9)	1.1	2.3×10^{-5}
	2	2.2×10^{-5} (1.9-3.2)		
139kb	1	1.4×10^{-5} (1.2-2.6)	1.4	1.2×10^{-5}
	2	1.0×10^{-5} (0.5-1.8)		
216kb	1	0.5×10^{-5} (0.3-1.1)	1.8	0.7×10^{-5}
	2	0.9×10^{-5} (0.8-1.6)		
230kb	1	0.8×10^{-5} (0.5-1.2	-	0.8×10^{-5}
	2	ND		
242kb	1	ND	-	1.4×10^{-5}
	2	1.4×10^{-5} (1.0-2.1)		

Location	Chromosomal Features
53kb	RSZ, Termination
139kb	RSZ, Termination, Ty2
216kb	Termination
230kb	Origin
242kb	None

B

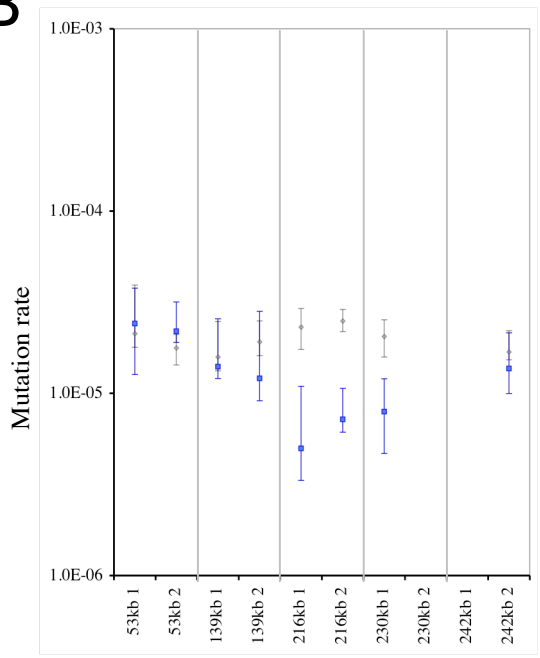

C

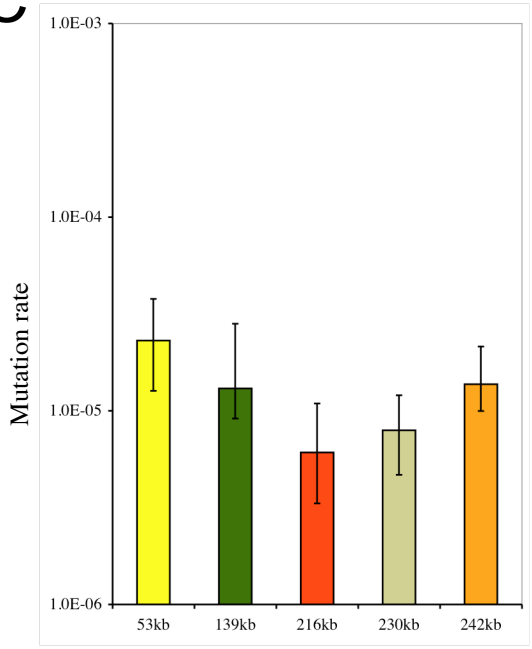

Figure 6.6. Rates of *URA3* inactivation in *mec1Δ sml1Δ* haploid strains.

(A) For each locus, except 230kb and 242kb, two independent rate measurements were done. The fraction of 5-FOA-resistant cells was measured in 15 independent cultures for each rate measurement. These fractions were converted to rates using the method of the median (Lea and Coulson, 1949). [a] 95% confidence limits (CL) were calculated as described previously (Wierdl *et al*., 1996). [b] Average mutation rates could not be calculated for the 230kb or 242kb loci. Chromosomal features at each locus are denoted on the right hand side. ND: not determined.

(B) Individual rates are plotted for *mec1Δ sml1Δ* (blue squares) and WT (grey diamonds) haploid strains. Capped lines indicate 95% CLs.

(C) The average mutation rate of the two strains is plotted, where possible. The smallest and largest CL value of the two strains was used for each location. Mutation rate is given as number of events/cell/generation.

A

Location Mutation rate[a]	Normalised mutation rate
53kb 2.3 x 10^{-5}	3.3
139kb 1.2 x 10^{-5}	1.7
216kb 0.7 x 10^{-5}	1.0
230kb 0.8 x 10^{-5}	1.1
242kb 1.4 x 10^{-5}	2.0

B

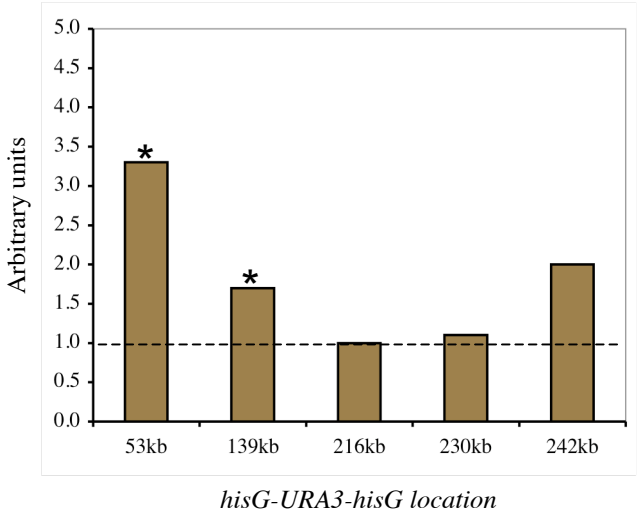

C

Location Mutation rate[a]	53kb 2.3 x 10^{-5}	139kb 1.2 x 10^{-5}	216kb 0.7 x 10^{-5}	230kb 0.8 x 10^{-5}	242kb 1.4 x 10^{-5}
53kb 2.3 x 10^{-5}		1.20 NSS	10.80 *P*<0.01	3.27 NSS	0.07 NSS
139kb 1.2 x 10^{-5}			4.80 *P*<0.05	3.27 NSS	0.07 NSS
216kb 0.7 x 10^{-5}				0.60 NSS	0.60 NSS
230kb 0.8 x 10^{-5}					1.67 NSS
242kb 1.4 x 10^{-5}					

Figure 6.7. Analysis of rates of *URA3* inactivation in *mec1Δ sml1Δ* haploid strains.

(A) The average mutation rate at each locus was normalised against the lowest average rate.

(B) Normalised fold-differences from (A) are plotted. "*" denotes a significant statistical difference.

(C) Chi-square analysis: pair-wise comparison of the mutation rates at each location. Shown in each panel are the Chi square (χ^2; upper) and probability (*P*; lower) values for each pair-wise combination. *P* values of less than 0.05 were deemed significant. NSS: not statistically significant. [a] Mutation rate is given as number of events/cell/generation.

A

Construct location	Average mutation rate		Fold-difference[a]	Chi square and
	mec1Δ sml1Δ	*sml1Δ*	*mec1Δ sml1Δ/ sml1Δ*	*P* values[b]
53kb	2.3×10^{-5}	2.0×10^{-5}	1.2	0.13, NSS
139kb	1.2×10^{-5}	1.8×10^{-5}	0.8	2.13, NSS
216kb	0.7×10^{-5}	2.4×10^{-5}	0.3	16.13, $P<0.001$
230kb	0.8×10^{-5}	2.1×10^{-5}	0.4	8.07, $P<0.01$
242kb	1.4×10^{-5}	1.7×10^{-5}	0.8	0.60, NSS

B

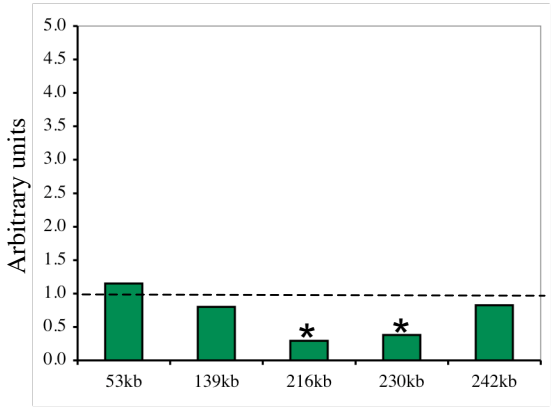

Figure 6.8. Effects of *mec1Δ sml1Δ* on the rates of *URA3* inactivation compared to those in *sml1Δ* haploid strains grown in the same conditions (YPD at 30˚C).

(A) [a] Where possible, for each location the mutation rate of strain 1 (*mec1Δ sml1Δ*) was divided by the mutation rate of strain 1 (*sml1Δ*). The same was done for strain 2. The fold-difference was then averaged over these two values for each locus. [b] Significant differences were calculated by χ^2 analyses, as described in the text. χ^2 values are given first, *P* values second. *P* values of less than 0.05 were deemed significant. NSS: not statistically significant.

(B) Graph showing the fold-difference in mutation rates of *mec1Δ sml1Δ* over *sml1Δ* haploid strains for each locus. "*" denotes a significant statistical difference. Values are taken from (A).

A

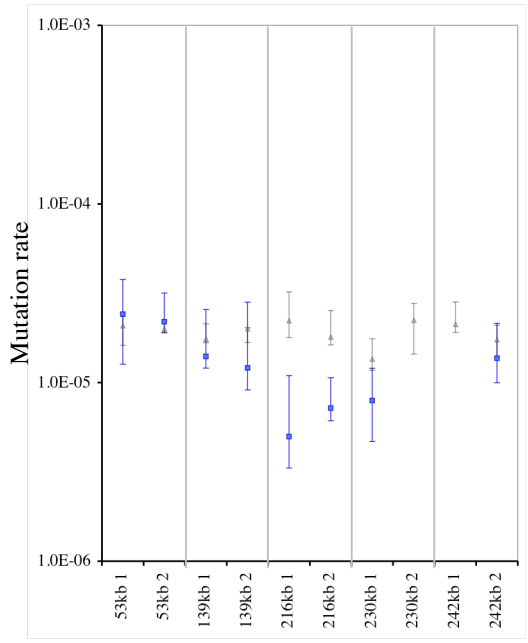

B

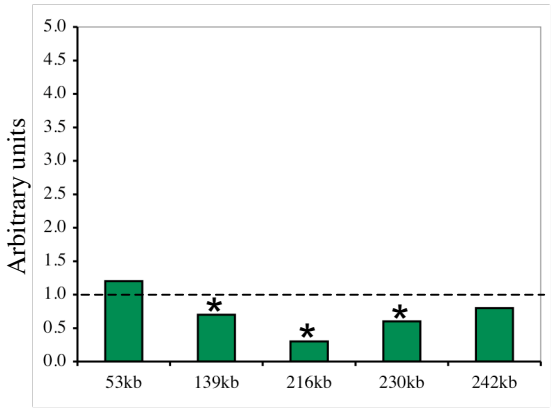

C

Construct location	Average mutation rate		Fold-difference[a]	Chi square and
	mec1Δ sml1Δ	WT	*mec1Δ sml1Δ*/ WT	*P* values[b]
53kb	2.3 x 10^{-5}	2.0 x 10^{-5}	1.2	1.20, NSS
139kb	1.3 x 10^{-5}	1.9 x 10^{-5}	0.7	4.80, $P<0.05$
216kb	0.6 x 10^{-5}	2.0 x 10^{-5}	0.3	16.13, $P<0.001$
230kb	0.8 x 10^{-5}	1.8 x 10^{-5}	0.6	5.40, $P<0.05$
242kb	1.4 x 10^{-5}	1.9 x 10^{-5}	0.8	0.60, NSS

Figure 6.9. Effects of *mec1Δ sml1Δ* on the rates of *URA3* inactivation compared to those in WT haploid strains grown in the same conditions (YPD at 30˚C).

(A) Individual mutation rates of *mec1Δ sml1Δ* (blue squares) and WT (grey triangles) haploid strains.

(B) Graph showing the fold-difference in mutation rates of *mec1Δ sml1Δ* over WT haploid strains for each locus. "*" denotes a significant statistical difference. Values are taken from (C).

(C) [a] Where possible, for each location the mutation rate of strain 1 (*mec1Δ sml1Δ*) was divided by the mutation rate of strain 1 (WT). The same was done for strain 2. The fold-difference was then averaged over these two values for each locus. [b] Significant differences were calculated by χ^2 analyses, as described in the text. χ^2 values are given first, *P* values second. *P* values of less than 0.05 were deemed significant. NSS: not statistically significant.

similar for the *mec1Δ sml1Δ* and *sml1Δ* strains. It was confirmed by χ^2 analyses that no significant difference existed in the mutation rates between the two genotypes at these loci. For 216kb and 230kb, however, the mutation rates were significantly lower in the *mec1Δ sml1Δ* strains than in the *sml1Δ* strains ($P<0.001$ and $P<0.01$, respectively). These findings are summarised in Figure 6.8.

Out of interest, the rates of *URA3* inactivation in haploid *mec1Δ sml1Δ* strains were compared to the mutation rates of their respective WT strains (Figure 6.9). The mutation rates of the 139kb, 216kb and 230kb loci in *mec1Δ sml1Δ* strains all decreased compared to their WT rates ($P<0.05$, <0.001 and <0.05, respectively), but no difference was found in the rates for the 53kb and 242kb loci between the two genotypes. This result was very similar to the comparison seen between the mutation rates of the *mec1Δ sml1Δ* and *sml1Δ* strains, as the rates of *sml1Δ* and WT strains were statistically indistinguishable. One exception was that the rate at the 139kb locus in the *mec1Δ sml1Δ* background was significantly lower than the rate of the WT, but was not significantly lower than the rate in the *sml1Δ* background.

6.2.4 Rates of URA3 inactivation in sml1Δ diploid strains

Spot tests of *sml1Δ* diploid strains grown at various temperatures on non-selective media are shown in Figure 6.10. An *sml1Δ* strain lacking an inserted *hisG-URA3-hisG* construct is also shown for comparison (second row, right hand side). Growth of all strains was optimal at 30˚C, and was therefore chosen for the incubation temperature for these strains. Since WT strains were also grown at 30˚C (Chapter 3), any effects that *sml1Δ* had on the mutation rate could also be compared to the WT.

Before the mutation rates of the diploid *sml1Δ* strains were tested at 30˚C it was also ensured that growth was optimal for the *mec1Δ sml1Δ* strains at this temperature. Spot tests showing growth of these strains at 18˚C, 23˚C, 30˚C and 37˚C are shown in Figure 6.11, with a *mec1Δ sml1Δ* strain lacking the reporter construct also shown in the second row (right hand side). Of the four temperatures tested, optimal growth for all strains was at 30˚C. Both *sml1Δ* and *mec1Δ sml1Δ* strains were therefore grown at this temperature.

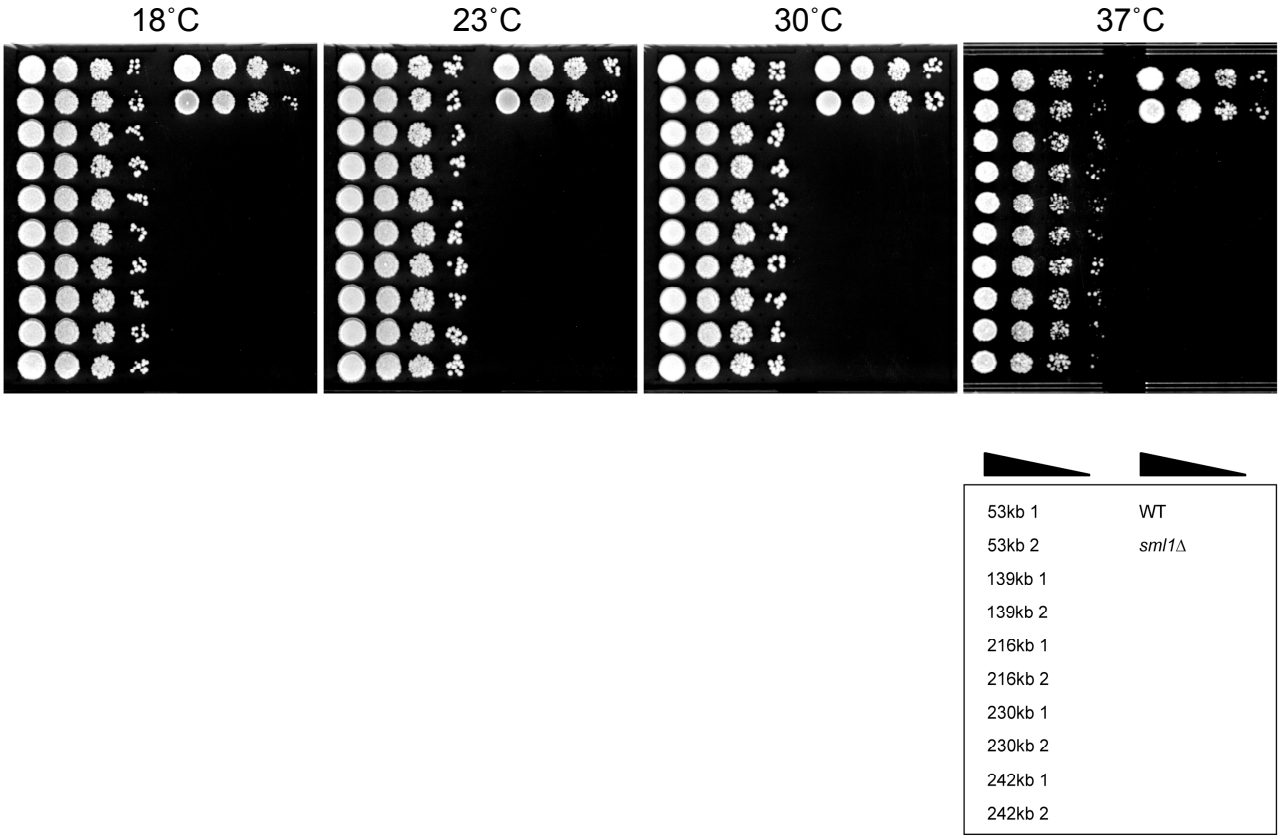

Figure 6.10. Effects of temperature on growth of *sml1Δ* diploid strains carrying a *hisG-URA3-hisG* construct at different loci on ChrIII.

Ten-fold serial dilutions of exponentially growing cells were spotted onto YPD plates and grown at the indicated temperatures for 3-5 days. The box in the lower right indicates the strains spotted onto the plates: WT and *sml1Δ* in this instance refer to strains lacking a *hisG-URA3-hisG* construct.

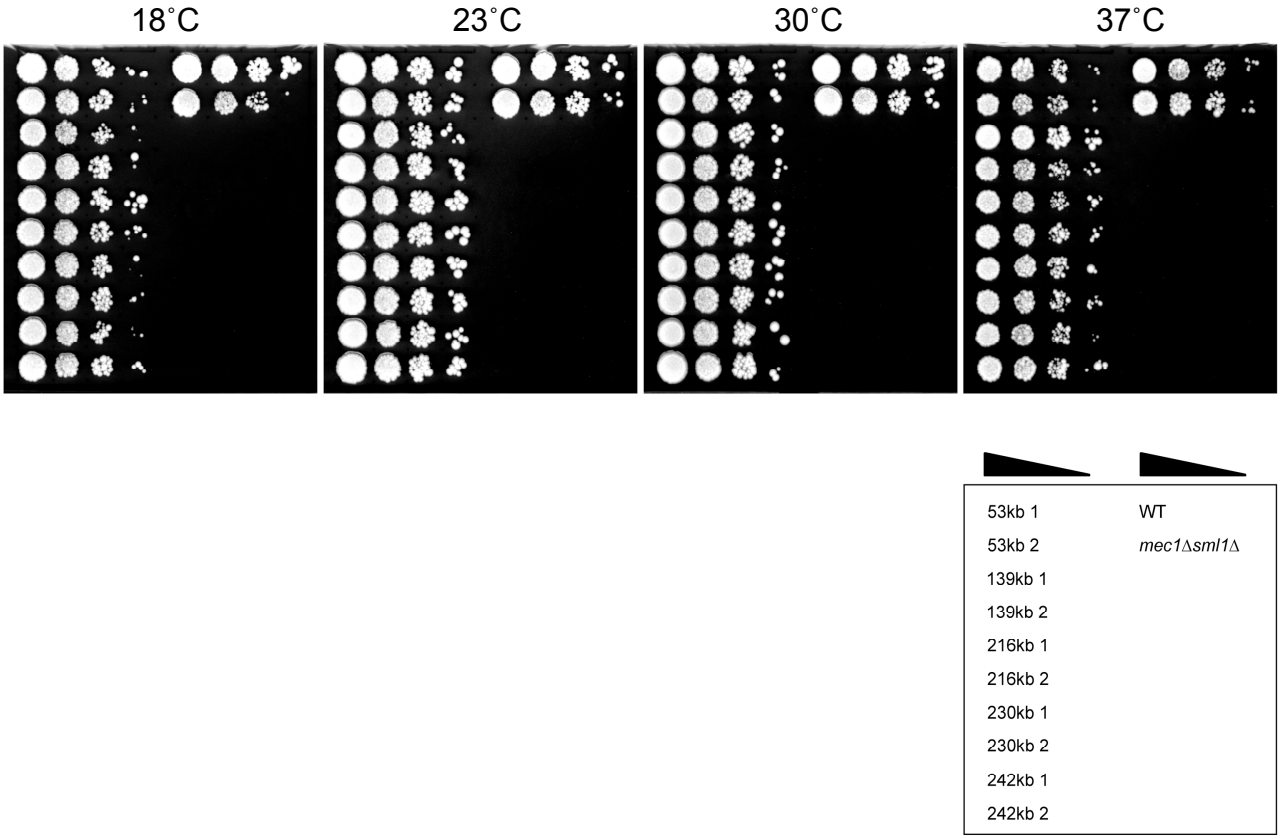

Figure 6.11. Effects of temperature on growth of *mec1Δ sml1Δ* diploid strains carrying a *hisG-URA3-hisG* construct at different loci on ChrIII.

Ten-fold serial dilutions of exponentially growing cells were spotted onto YPD plates and grown at the indicated temperatures for 3-5 days. The box in the lower right indicates the strains spotted onto the plates: WT and *mec1Δ sml1* in this instance refer to strains lacking a *hisG-URA3-hisG* construct.

The mutation rates of diploid *sml1Δ* strains were tested first. Figure 6.12 shows the result of fluctuation analyses for these strains. The mutation rate at each locus varied from 1.6 x 10^{-5} events/cell/generation at 139kb (RSZ, termination, Ty2), to 2.8 x 10^{-5} at 53kb (RSZ, termination). To assess the potential variation in these mutation rates, the mutation rates at each locus were normalised against the lowest value (139kb). These values varied from 1.1- to 1.3-fold for the 216kb, 230kb and 242kb loci, but the rate at the 53kb locus was 1.8-fold higher than the rate at the 139kb locus. Chi square analyses found that, of these values, only the 1.8 fold-differences between the mutation rates at the 53kb and 139kb loci were statistically significant (Figure 6.13). Further analysis found that the rates of *URA3* inactivation at the 139kb, 216kb, 230kb and 242kb were statistically indistinguishable. The mutation rate at the 53kb locus, however, was significantly higher than the rates at the other four loci (Figure 6.13C). There was therefore one *cis* effect seen in diploid *sml1Δ* strains.

The *sml1Δ* diploid mutation rates were then compared to their respective WT mutation rates to see if any *trans*-specific effects existed (Figure 6.14). Absence of Sml1p significantly increased the mutation rate for the 53kb (RSZ, termination) and 216kb (termination) loci. For the 139kb locus (RSZ, termination, Ty2) the mutation rates were indistinguishable between the two different conditions. In the two locations devoid of termination sites, 230kb (origin) and 242kb (no discernable features), elimination of Sml1p led to lower mutation rates ($P<0.001$ and $P<0.05$, respectively). In summary, the rates of *URA3* inactivation were modulated to a different extent at each locus in *sml1Δ* diploid strains compared to the rates of their respective WT diploid strains.

6.2.5 Rates of URA3 inactivation in mec1Δ sml1Δ diploid strains

The mutation rates were then tested in *mec1Δ sml1Δ* diploid strains. The result of fluctuation analyses for these strains are shown in Figure 6.15B (black-filled circles) alongside the rates of their respective *sml1Δ* strains (grey crosses). Once again, little variation existed in the mutation rates between the two independent transformants for the three loci tested, and no statistical difference was found (χ^2 analyses).

A

Strain		Mutation Rate (95% CL)[a]	Fold-difference between 1&2	Average Mut Rate[b]
53kb	1	2.9×10^{-5} (2.4-5.5)	1.1	2.8×10^{-5}
	2	2.6×10^{-5} (2.1-2.9)		
139kb	1	1.7×10^{-5} (1.3-2.2)	1.1	1.6×10^{-5}
	2	1.5×10^{-5} (1.2-1.7)		
216kb	1	1.7×10^{-5} (1.5-2.1)	1.0	1.7×10^{-5}
	2	1.7×10^{-5} (1.4-2.1)		
230kb	1	2.0×10^{-5} (1.5-2.3)	-	2.0×10^{-5}
	2	ND		
242kb	1	ND	-	1.9×10^{-5}
	2	1.9×10^{-5} (1.5-2.3)		

Location	Chromosomal Features
53kb	RSZ, Termination
139kb	RSZ, Termination, Ty2
216kb	Termination
230kb	Origin
242kb	None

B

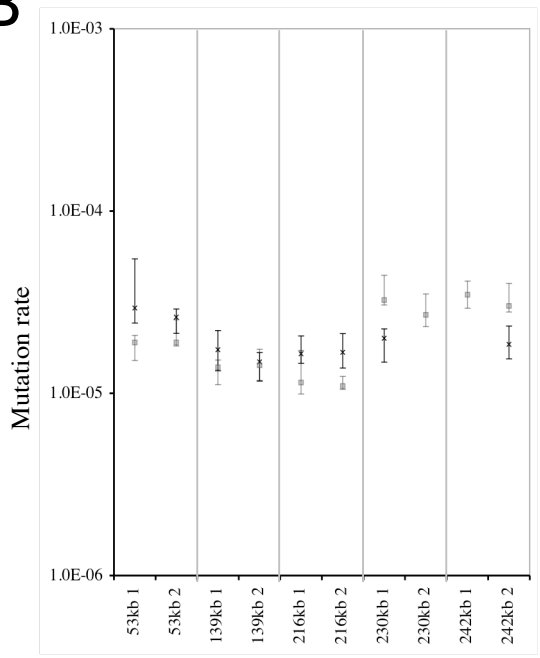

C

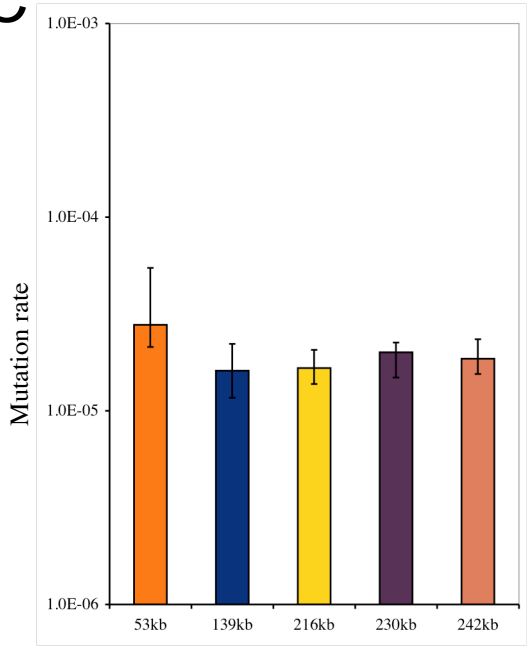

Figure 6.12. Rates of *URA3* inactivation in *sml1Δ* diploid strains.

(A) All strains were homozygous for *sml1Δ* and heterozygous for the *hisG-URA3-hisG* reporter construct. For each locus, except 230kb and 242kb, two independent rate measurements were done. The fraction of 5-FOA-resistant cells was measured in 15 independent cultures for each rate measurement. These fractions were converted to rates using the method of the median (Lea and Coulson, 1949). [a] 95% confidence limits (CL) were calculated as described previously (Wierdl *et al*., 1996). [b] Average mutation rates could not be calculated for the 230kb or 242kb loci. Chromosomal features at each locus are denoted on the right hand side. ND: not determined.

(B) Individual rates are plotted for *sml1Δ* (black crosses) and WT (grey squares) diploid strains. Capped lines indicate 95% CLs.

(C) The average mutation rate of the two strains is plotted, where possible. The smallest and largest CL value of the two strains was used for each location. Mutation rate is given as number of events/cell/generation.

A

Location Mutation rate[a]	Normalised mutation rate
53kb 2.8 x 10^{-5}	1.8
139kb 1.6 x 10^{-5}	1.0
216kb 1.7 x 10^{-5}	1.1
230kb 2.0 x 10^{-5}	1.3
242kb 1.9 x 10^{-5}	1.2

B

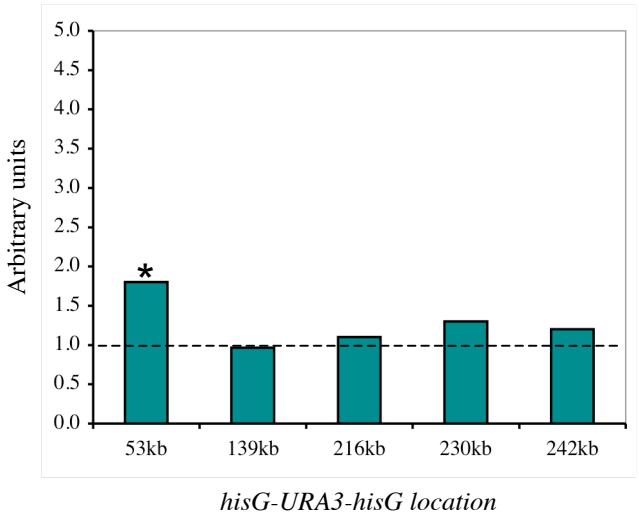

C

Location Mutation rate[a]	53kb 2.8 x 10^{-5}	139kb 1.6 x 10^{-5}	216kb 1.7 x 10^{-5}	230kb 2.0 x 10^{-5}	242kb 1.9 x 10^{-5}
53kb 2.8 x 10^{-5}		13.33 *P*<0.001	10.80 *P*~0.001	5.40 *P*<0.05	8.07 *P*<0.01
139kb 1.6 x 10^{-5}			0.00 NSS	0.07 NSS	0.60 NSS
216kb 1.7 x 10^{-5}				0.07 NSS	0.07 NSS
230kb 2.0 x 10^{-5}					0.07 NSS
242kb 1.9 x 10^{-5}					

Figure 6.13. Analysis of rates of *URA3* inactivation in *sml1Δ* diploid strains.

(A) The average mutation rate at each locus was normalised against the lowest average rate.

(B) Normalised fold-differences from (A) are plotted. "*" denotes a significant statistical difference.

(C) Chi-square analysis: pair-wise comparison of the mutation rates at each location. Shown in each panel are the Chi square (χ^2; upper) and probability (*P*; lower) values for each pair-wise combination. *P* values of less than 0.05 were deemed significant. NSS: not statistically significant.

A

Construct location	Average mutation rate		Fold-difference[a] *sml1Δ* / WT	Chi square and *P* values[b]
	sml1Δ	WT		
53kb	2.8×10^{-5}	1.9×10^{-5}	1.5	8.53, $P<0.01$
139kb	1.6×10^{-5}	1.4×10^{-5}	1.1	0.53, NSS
216kb	1.7×10^{-5}	1.1×10^{-5}	1.5	10.80, $P<0.01$
230kb	2.0×10^{-5}	3.0×10^{-5}	0.6	11.27, $P<0.001$
242kb	1.9×10^{-5}	3.2×10^{-5}	0.6	5.40, $P<0.05$

B

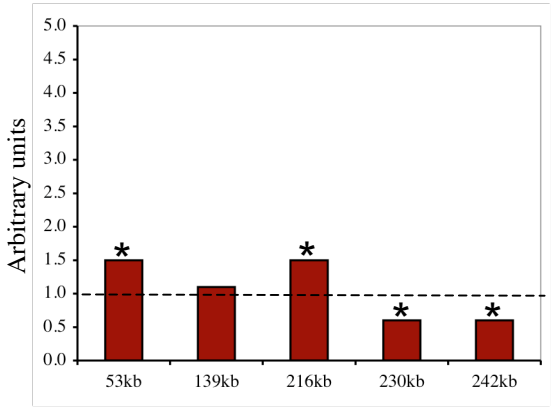

Figure 6.14. Effects of *sml1Δ* on the rates of *URA3* inactivation compared to those in WT diploid strains grown in the same conditions (YPD at 30˚C).

(A) [a] Where possible, for each location the mutation rate of strain 1 (*sml1Δ*) was divided by the mutation rate of strain 1 (WT). The same was done for strain 2. The fold-difference was then averaged over these two values for each locus. [b] Significant differences were calculated by χ^2 analyses, as described in the text. χ^2 values are given first, *P* values second. *P* values of less than 0.05 were deemed significant. NSS: not statistically significant.

(B) Graph showing the fold-difference in mutation rates of *sml1Δ* over WT diploid strains for each locus. "*" denotes a significant statistical difference. Values are taken from (A).

A

Strain		Mutation Rate (95% CL)[a]	Fold-difference between 1&2	Average Mut Rate[b]
53kb	1	7.6×10^{-5} (4.6-10.6)	1.1	7.3×10^{-5}
	2	7.0×10^{-5} (5.8-10.2)		
139kb	1	2.8×10^{-5} (2.2-4.0)	1.2	3.1×10^{-5}
	2	3.3×10^{-5} (2.7-4.7)		
216kb	1	4.0×10^{-5} (2.9-5.1)	1.1	3.9×10^{-5}
	2	3.8×10^{-5} (2.9-5.7)		
230kb	1	5.1×10^{-5} (3.3-7.1)	-	5.1×10^{-5}
	2	ND		
242kb	1	ND	-	6.0×10^{-5}
	2	6.0×10^{-5} (4.8-9.2)		

Location	Chromosomal Features
53kb	RSZ, Termination
139kb	RSZ, Termination, Ty2
216kb	Termination
230kb	Origin
242kb	None

B

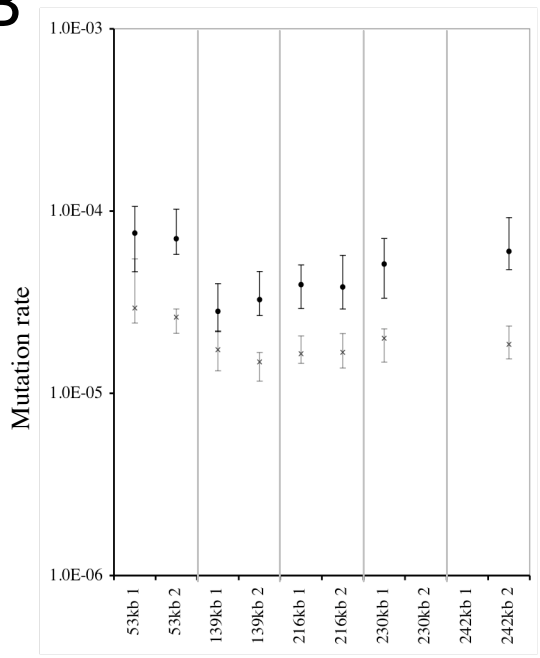

C

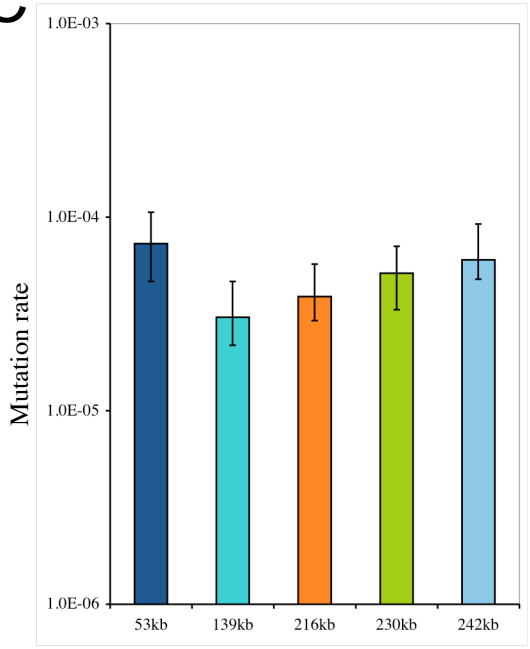

Figure 6.15. Rates of *URA3* inactivation in *mec1Δ sml1Δ* diploid strains.

(A) All strains were homozygous for *mec1Δ sml1Δ* and heterozygous for the *hisG-URA3-hisG* reporter construct. For each locus, except 230kb and 242kb, two independent rate measurements were done. The fraction of 5-FOA-resistant cells was measured in 15 independent cultures for each rate measurement. These fractions were converted to rates using the method of the median (Lea and Coulson, 1949). [a] 95% confidence limits (CL) were calculated as described previously (Wierdl *et al.*, 1996). [b] Where possible, the average mutation rates were calculated. Relevant chromosomal features at each locus are denoted on the right hand side. ND: not determined.

(B) Individual rates are plotted for *mec1Δ sml1Δ* (black-filled circles) and *sml1Δ* (grey crosses) diploid strains. Capped lines indicate 95% CLs.

(C) The average mutation rate of the two strains is plotted, where possible. The smallest and largest CL value of the two strains was used for each location. Mutation rate is given as number of events/cell/generation.

The mutation rate for each location ranged from 3.1 x 10^{-5} events/cell/generation for 139kb (RSZ, termination, Ty2) to 7.3 x 10^{-5} for 53kb (RSZ, termination), as shown in Figure 6.15C. The mutation rate at each locus was then normalised against the lowest value (139kb) to assess the potential variation. These values ranged from 1.3- to 2.4-fold. Of these values, the respective 2.4- and 1.9-fold increases for the 53kb and 242kb loci were significantly higher than the mutation rate at the 139kb locus. The mutation rates at the 216kb and 230kb loci were statistically indistinguishable from the rate at the 139kb locus.

The mutation rates at each locus were then separately compared against the rates at the other loci. The result of this pair-wise analysis is shown in Figure 6.16C. The mutation rate of the 53kb location was significantly higher than the 139kb and 216kb rates ($P<0.01$ and $P<0.05$, respectively). The mutation rate at the 242kb (no features) locus was higher than the rates at both the 139kb ($P<0.05$) and 216kb ($P\sim0.05$) loci. All other mutation rates were statistically indistinguishable from each other. This was surprising since the point rate estimates were not very similar to each other (the lowest was 3.1 x 10^{-5} events/cell/generation, and the highest, 7.3 x 10^{-5}). The 95% CLs for the *mec1Δ sml1Δ* were much greater than those in the previous results chapters, however, so just looking at the point rate estimates without taking these into account is misleading. There were therefore differential effects on the mutation rate in *mec1Δ sml1Δ* diploid strains for each of the five loci in ChrIII.

The affects of *mec1Δ sml1Δ* on the mutation rate in diploid strains could now be compared to the mutation rates in their respective *sml1Δ* strains. Figure 6.15B shows that, unlike in haploids, the point rate estimates and 95% CLs did not have any large degree of overlap for any of the five locations between the two genotypes. All of the five locations had a uniform increase in mutation rate of ~2.5-fold in the *mec1Δ sml1Δ* strains compared to the rates of their respective *sml1Δ* strains. It was confirmed by χ^2 analyses that these fold-increases were significant (Figure 6.17). The rate of *URA3* inactivation therefore increased uniformly for all loci in diploid *mec1Δ sml1Δ* strains compared to the rates in *sml1Δ* strains.

The mutation rates in *mec1Δ sml1Δ* diploid strains rates were also compared to the

A

Location Mutation rate[a]	Normalised mutation rate
53kb 7.3 x 10^{-5}	2.4
139kb 3.1 x 10^{-5}	1.0
216kb 3.9 x 10^{-5}	1.3
230kb 5.1 x 10^{-5}	1.6
242kb 6.0 x 10^{-5}	1.9

B

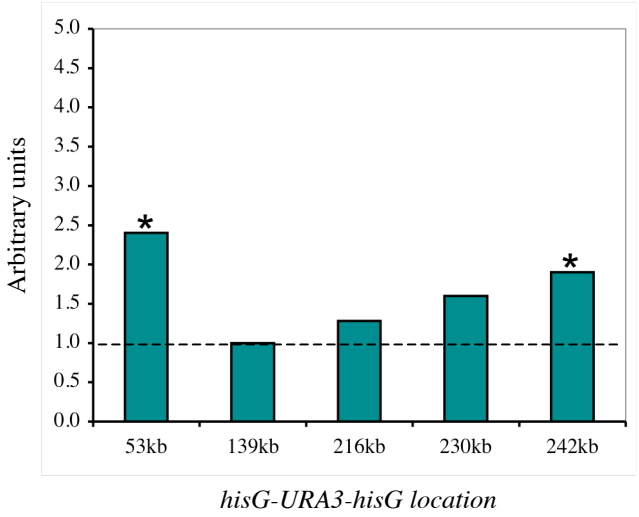

C

Location Mutation rate[a]	53kb 7.3 x 10^{-5}	139kb 3.1 x 10^{-5}	216kb 3.9 x 10^{-5}	230kb 5.1 x 10^{-5}	242kb 6.0 x 10^{-5}
53kb 7.3 x 10^{-5}		8.07 P<0.01	5.40 P<0.05	1.67 NSS	0.60 NSS
139kb 3.1 x 10^{-5}			0.60 NSS	1.67 NSS	5.40 P<0.05
216kb 3.9 x 10^{-5}				0.60 NSS	3.27 P~0.05
230kb 5.1 x 10^{-5}					1.67 NSS
242kb 6.0 x 10^{-5}					

Figure 6.16. Analysis of rates of *URA3* inactivation in *mec1Δ sml1Δ* diploid strains.

(A) The average mutation rate at each locus was normalised against the lowest average rate.

(B) Normalised fold-differences from (A) are plotted. "*" denotes a significant statistical difference.

(C) Chi-square analysis: pair-wise comparison of the mutation rates at each location. Shown in each panel are the Chi square (χ^2; upper) and probability (P; lower) values for each pair-wise combination. P values of less than 0.05 were deemed significant. NSS: not statistically significant.

A

Construct location	Average mutation rate		Fold-difference[a]	Chi square and
	mec1Δ sml1Δ	*sml1Δ*	*mec1Δ sml1Δ / sml1Δ*	*P* values[b]
53kb	7.3×10^{-5}	2.8×10^{-5}	2.6	8.07, $P<0.01$
139kb	3.1×10^{-5}	1.6×10^{-5}	1.9	8.07, $P<0.01$
216kb	3.9×10^{-5}	1.7×10^{-5}	2.3	8.07, $P<0.01$
230kb	5.1×10^{-5}	2.0×10^{-5}	2.6	11.27, $P<0.001$
242kb	6.0×10^{-5}	1.9×10^{-5}	3.2	11.27, $P<0.001$

B

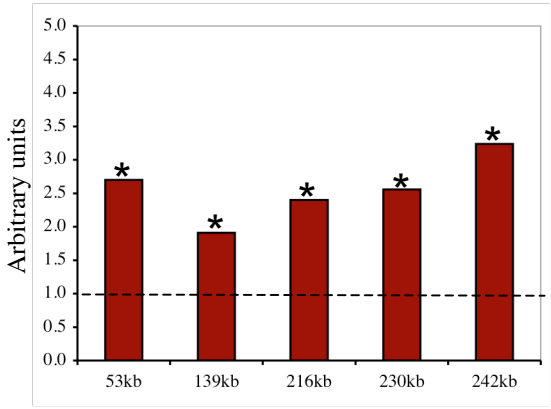

Figure 6.17. Effects of *mec1Δ sml1Δ* on the rates of *URA3* inactivation compared to those in *sml1Δ* diploid strains grown in the same conditions (YPD at 30˚C).

(A) [a] Where possible, for each location the mutation rate of strain 1 (*mec1Δ sml1Δ*) was divided by the mutation rate of strain 1 (*sml1Δ*). The same was done for strain 2. The fold-difference was then averaged over these two values for each locus. [b] Significant differences were calculated by χ^2 analyses, as described in the text. χ^2 values are given first, *P* values second. χ^2 values of 3.84 were deemed significant ($P<0.05$).

(B) Graph showing the fold-difference in mutation rates of *mec1Δ sml1Δ* over *sml1Δ* diploid strains for each locus. "*" denotes a significant statistical difference. Values are taken from (A).

rates of their respective WT strains. Figure 6.18 shows that the mutation rates in diploid *mec1Δ sml1Δ* strains were significantly higher than the rates in their WT strains for all five loci. For the 139kb, 230kb and 242kb loci these fold-differences were 2.2-, 1.6- and 2.0-fold, respectively. For the 53kb and 216kb loci the fold-differences were higher, being 3.9- and 3.5-fold, respectively.

6.2.6 Effects of ploidy on rates of URA3 inactivation in sml1Δ and mec1Δ sml1Δ strains

The mutation rates of diploid *sml1Δ* strains were compared against the rates of their respective haploid *sml1Δ* strains. These are shown in Figure 6.19A; diploids are represented by black crosses and haploids by grey-filled diamonds. The point rate estimates were similar and some overlap existed in the 95% CLs between the two situations. The fold-differences were then calculated between the mutation rates of the diploid and haploid strains. These ranged from 0.7- to 1.5-fold, as shown in Figures 6.19B and 6.19C. Of these values, only the 1.5-fold value for the 53kb locus was found to be significant (χ^2 analysis).

The same comparison was made between the rates of *URA3* inactivation in diploid and haploid *mec1Δ sml1Δ* strains. Figure 6.20A shows individual mutation rates for diploid (black-filled circles) and haploid (blue-filled squares) *mec1Δ sml1Δ* strains. Unlike the rates seen for the *sml1Δ* strains, the point rate estimates of the diploid strains were all higher than the haploids, and no overlap existed in the 95% CL values for four out of the five loci (there was a small amount of overlap for the 139kb strains only). The average fold-differences between diploids and haploids was calculated as before, and plotted in Figure 6.20B (see Figure 6.20C for specific values). These fold-differences varied from 2.4- to 6.6-fold, and it was found by χ^2 analyses that all of these values were significant ($P<0.01$, and lower). The rates of *URA3* inactivation in *mec1Δ sml1Δ* diploids were therefore significantly higher than the rates in their respective *mec1Δ sml1Δ* haploid strains.

A

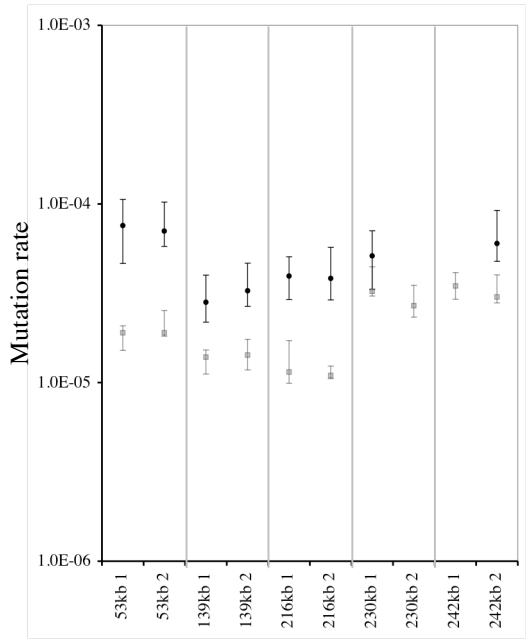

B

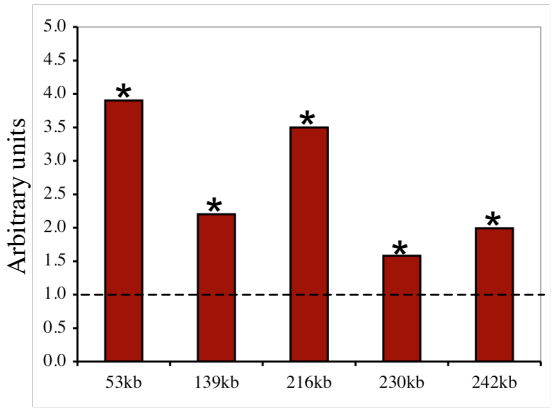

C

Construct location	Average mutation rate		Fold-difference[a]	Chi square and
	mec1Δ sml1Δ	WT	*mec1Δ sml1Δ* / WT	*P* values[b]
53kb	7.3×10^{-5}	1.9×10^{-5}	3.9	11.27, $P<0.001$
139kb	3.1×10^{-5}	1.4×10^{-5}	2.2	11.27, $P<0.001$
216kb	3.9×10^{-5}	1.1×10^{-5}	3.5	15.00, $P<0.001$
230kb	5.1×10^{-5}	3.0×10^{-5}	1.6	5.27, $P<0.01$
242kb	6.0×10^{-5}	3.2×10^{-5}	2.0	8.07, $P<0.01$

Figure 6.18. Effects of *mec1Δ sml1Δ* on the rates of *URA3* inactivation compared to those in WT diploid strains grown in the same conditions (YPD at 30˚C).

(A) Individual mutation rates of *mec1Δ sml1Δ* (black circles) and WT (grey squares) diploid strains.

(B) Graph showing the fold-difference in mutation rates of *mec1Δ sml1Δ* over haploid WT strains for each locus. "*" denotes a significant statistical difference. Values are taken from (C).

(C) [a] Where possible, for each location the mutation rate of strain 1 (*mec1Δ sml1Δ*) was divided by the mutation rate of strain 1 (WT). The same was done for strain 2. The fold-difference was then averaged over these two values for each locus. [b] Significant differences were calculated by χ^2 analyses, as described in the text. χ^2 values are given first, *P* values second. *P* values of less than 0.05 were deemed significant.

A

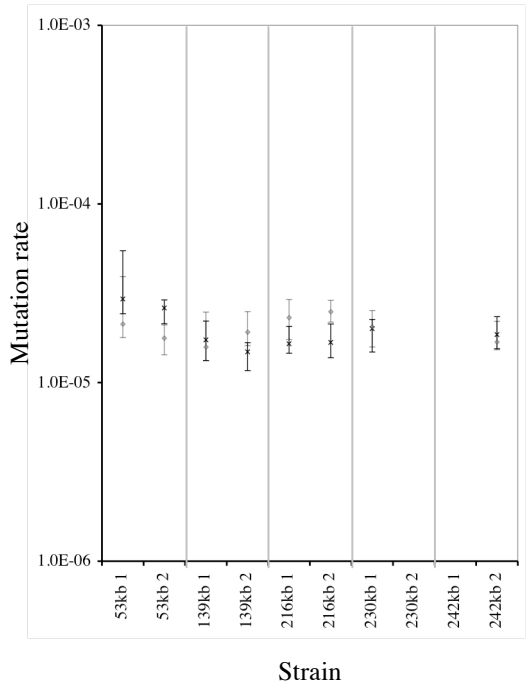

B

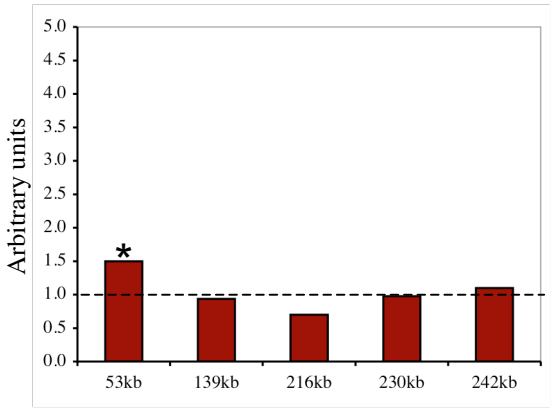

C

Construct location	Average mutation rate		Fold-difference[a] Diploid / Haploid	Chi square and *P* values[b]
	Diploid	Haploid		
53kb	2.8×10^{-5}	2.0×10^{-5}	1.5	6.53, *P*~0.01
139kb	1.6×10^{-5}	1.8×10^{-5}	0.9	0.53, NSS
216kb	1.7×10^{-5}	2.4×10^{-5}	0.7	3.33, NSS
230kb	2.0×10^{-5}	2.1×10^{-5}	1.0	0.07, NSS
242kb	1.9×10^{-5}	1.7×10^{-5}	1.1	3.27, NSS

Figure 6.19. Effects of ploidy on the rates of *URA3* inactivation in *sml1Δ* strains grown in YPD at 30˚C.

(A) Individual mutation rates of *sml1Δ* haploid (grey diamonds) and diploid (black crosses) strains.

(B) Graph showing the fold-difference in mutation rates of diploid over haploid *sml1Δ* strains for each locus. "*" denotes a significant statistical difference. Values are taken from (C).

(C) [a] Where possible, for each location the mutation rate of strain 1 (diploid) was divided by the mutation rate of strain 1 (haploid). The same was done for strain 2. The fold-difference was then averaged over these two values for each locus. [b] Significant differences were calculated by χ^2 analyses, as described in the text. χ^2 values are given first, *P* values second. *P* values of less than 0.05 were deemed significant. NSS: not statistically significant.

A

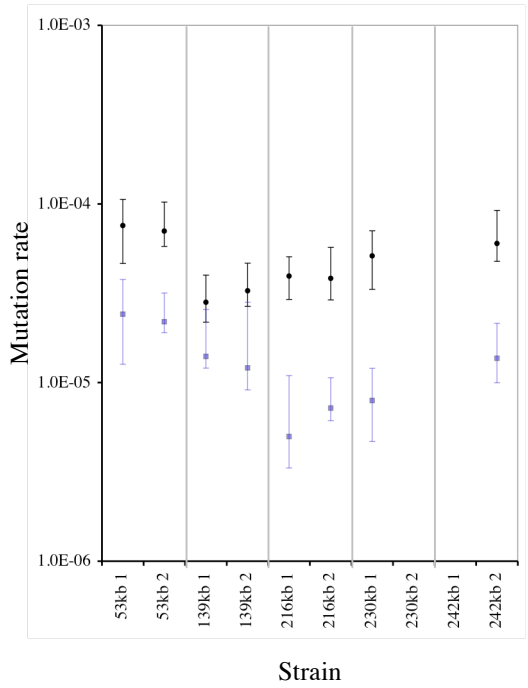

B

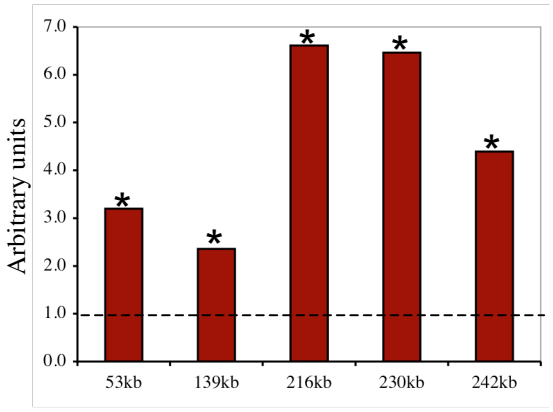

C

Construct location	Average mutation rate		Fold-difference[a] Diploid / Haploid	Chi square and *P* values[b]
	Diploid	Haploid		
53kb	7.3×10^{-5}	2.3×10^{-5}	3.2	11.27, $P<0.001$
139kb	3.1×10^{-5}	1.2×10^{-5}	2.4	11.27, $P<0.001$
216kb	3.9×10^{-5}	0.7×10^{-5}	6.6	11.27, $P<0.001$
230kb	5.1×10^{-5}	0.8×10^{-5}	6.5	11.27, $P<0.001$
242kb	6.0×10^{-5}	1.4×10^{-5}	4.4	8.07, $P<0.01$

Figure 6.20. Effects of ploidy on the rates of *URA3* inactivation in *mec1Δ sml1Δ* strains grown in YPD at 30˚C.

(A) Individual mutation rates of *mec1Δ sml1Δ* haploid (blue squares) and diploid (black circles) strains.

(B) Graph showing the fold-difference in mutation rates of diploid over haploid *mec1Δ sml1Δ* strains for each locus. "*" denotes a significant statistical difference. Values are taken from (C).

(C) [a] Where possible, for each location the mutation rate of strain 1 (diploid) was divided by the mutation rate of strain 1 (haploid). The same was done for strain 2. The fold-difference was then averaged over these two values for each locus. [b] Significant differences were calculated by χ^2 analyses, as described in the text. χ^2 values are given first, *P* values second. *P* values of less than 0.05 were deemed significant.

6.2.7 Haploid mec1-40 strains

6.2.7.1 Preparation for analysis of mec1-40 haploid strains; kinetics of commitment to inviability at 37˚C

mec1-40 is one of two *MEC1* temperature sensitive mutant alleles used to identify RSZs in ChrIII (Cha and Kleckner, 2002). Both mutations confer known *mec1* null phenotypes at the non-permissive temperature, which include cell inviability and absence of DNA damage checkpoint responses. I wanted to investigate if the rates of *URA3* inactivation differed using this allele compared to those seen in the absence of Mec1p, and if so, whether it specifically affected the mutation rates at regions within RSZs.

To create appropriate *mec1-40* haploid strains, WT haploid strains containing the *hisG-URA3-hisG* construct were crossed with a *mec1-40* strain and the resulting diploids were sporulated. *URA3* prototroph spore clones that co-segregated with the appropriate mutant allele markers were selected. Crossing these haploids with the original *mec1-40* haploid strain made homozygous diploid strains.

Spot tests of haploid *mec1-40* strains containing the *hisG-URA3-hisG* reporter construct grown on YPD at various temperatures are shown in Figure 6.21. WT and *mec1-40* strains lacking the construct are shown as a comparison (first and second row, respectively, right hand side). With the exception of the 216kb strains, all of the *URA3* strains grew similarly to the *mec1-40* strain lacking a reporter construct at all four temperatures tested. At 37˚C nearly all *mec1-40* cells died, as expected (Cha and Kleckner, 2002). The *hisG-URA3-hisG* construct did not therefore affect the growth of *mec1-40* strains compared to a congenic *mec1-40* strain lacking a reporter construct.

In Cha and Kleckner's original paper (2002), DNA breaks occurred in RSZs at non-permissive temperatures when the *mec1-4* and *mec1-40* alleles were used. Breaks did not occur at the permissive temperature. As the *mec1-40* strains containing the *hisG-URA3-hisG* reporter construct were temperature-sensitive, the standard fluctuation analysis growth conditions used in earlier chapters could not be used. Growing these

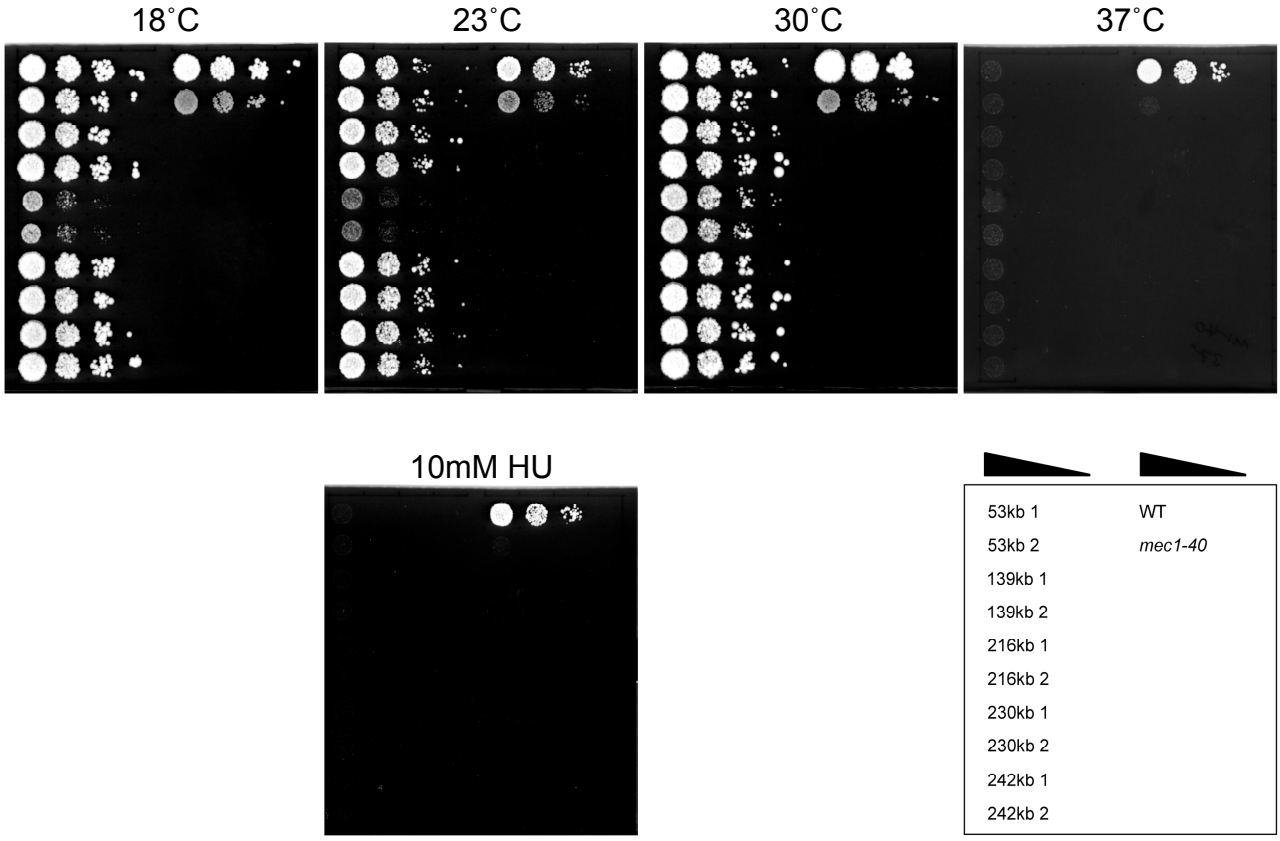

Figure 6.21. Effects of temperature on growth of *mec1-40* haploid strains carrying a *hisG-URA3-hisG* construct at different loci on ChrIII.

Ten-fold serial dilutions of exponentially growing cells were spotted onto YPD plates (top row) or media supplemented with 10mM HU (bottom row) and grown at the indicated temperatures for 3-5 days. The box in the lower right indicates the strains spotted onto the plates: WT and *mec1-40* in this instance refer to strains lacking a *hisG-URA3-hisG* construct.

strains at 30˚C and recording the mutation rate would therefore not be a valid representation of the mutation rate in the absence of Mec1p function, as partially functional protein would still be present. A situation was therefore required where, ideally, *URA3* strains were incubated at 37˚C to inactivate the protein for as long a time as possible without losing viability. Otherwise certain fractions of either 5-FOA-resistant or non-resistant cells could be lost due to cell death resulting from Mec1p inactivation, and thus the observed mutation rate may not accurately reflect the actual mutation rate.

Therefore, before the rates of *URA3* loss could be measured in *mec1-40* strains, the viability of a *mec1-40* strain was tested when exposed to the non-permissive temperature. For this purpose, a *mec1-40* strain lacking a *hisG-URA3-hisG* construct was utilised. In order to do this the *mec1-40* strain was first incubated at 23˚C on solid media. A colony was then used to inoculate 5mL of non-selective (YPD) media. After 1.5h incubation at 23˚C the culture was shifted to 37˚C and aliquots taken at various time points. The aliquots were plated onto YPD agar plates and incubated at 23˚C to observe the cell survival. This is summarised in Figure 6.22A.

The result for the haploid *mec1-40* strain (lacking the *hisG-URA3-hisG* construct) grown at 37˚C is shown in Figure 6.22B. Cell viability of this strain increased to a maximum of ~175% the original cell count over the first two hours, remained at this cell count for the next two hours, then started to decrease after the 4.5h time point. It was decided that the ideal conditions to incubate *mec1-40* strains at 37˚C would be for as long as possible without inducing cell death. For this purpose, *mec1-40* haploid strains were grown at 37˚C for 4h. Specific incubation times are detailed in Figure 6.23.

6.2.7.2 Rates of URA3 inactivation in WT haploid strains, using mec1-40 growth conditions

The *mec1-40* haploid strains containing an integrated *hisG-URA3-hisG* cassette could not be compared to the haploid WT strains incubated at 30˚C since the conditions for fluctuation analysis were now different. The mutation rates of haploid

A

B

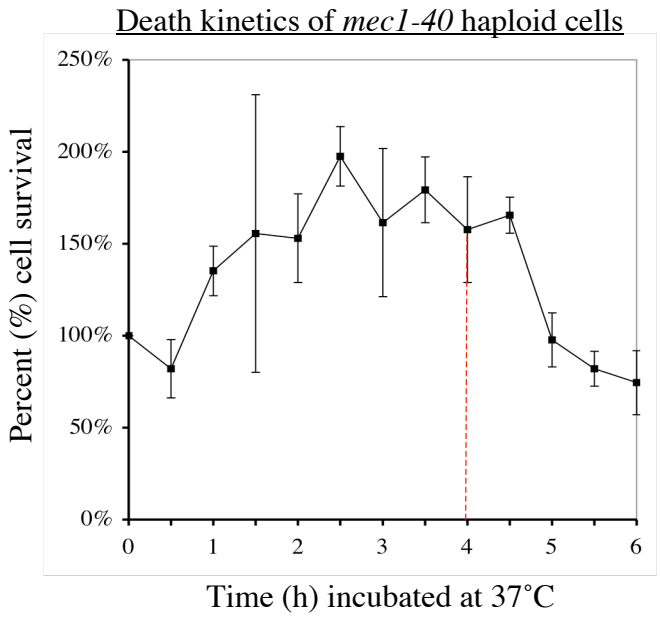

Figure 6.22. Testing haploid *mec1-40* strains for fluctuation analysis incubation times: kinetics of commitment to inviability.

(A) Flow chart detailing incubation times used to test a *mec1-40* haploid for death kinetics. Cells were patched onto YPG directly from -80˚C glycerol stocks. After 17h at 23˚C, cells were streaked for single colonies on non-selective (YPD) media; colonies had reached a suitable size after 55h incubation at 23˚C. Single colonies were then used to inoculate three different flasks containing 5mL liquid YPD, which were incubated at 23˚C. After 1.5h (t=0) the flasks were shifted to the non-permissive temperature (37˚C) and aliquots taken every 30 minutes. These were plated onto non-selective (YPD) agar plates and incubated at the permissive temperature (23˚C) to allow cells to recover. After 3-4 days colonies were counted and compared to the t=0 count to determine the percentage cell death at each time point.

(B) Result of death kinetics analysis used in (A). Error bars indicate the standard deviation between three independent cultures.

WT strains used in the previous two chapters were therefore assessed using the haploid *mec1-40* incubation times specified in Figure 6.23. The results of the WT strains grown using these conditions are shown in Figure 6.24B (black diamonds), with mutation rates of the same strains grown at 30˚C (grey triangles) shown as a comparison. Specific values are given in Figure 6.24A. The 216kb strains were not tested due to their slow growth phenotype. For the 53kb and 139kb loci, for which data was available, no difference in mutation rate was observed between the two independently derived strains (χ^2 analysis). In Figure 6.24C the mutation rates, where applicable, were averaged for each location. These ranged from 2.3 x 10^{-5} events/cell/generation for 230kb (origin) to 3.0 x 10^{-5} for 139kb (RSZ, termination, Ty2).

To assess the variation in mutation rate amongst the different loci, the average rates were normalised against the lowest rate, in this case, the rate at the 230kb locus. These values ranged from 1.2- to 1.3-fold, as shown in Figure 6.25A. None of these values statistically differed from each other (χ^2 analyses). This analysis was extended so that all mutation rates were compared by pair-wise analysis (Figure 6.25C). As expected by the similar point rate estimates and degree of overlap between the 95% CLs, all of the mutation rates were statistically indistinguishable from each other.

The mutation rates of the WT strains grown under *mec1-40* conditions were then compared to the mutation rates of their respective WT strains grown at 30˚C for each location. Figure 6.24B shows that the point rate estimates were higher for the WT (*mec1-40*) strains than the WT (30˚C) ones, though there was a small degree of overlap between the 95% CL values. For each location there was an approximate 1.5-fold increase in the mutation rates of the WT (*mec1-40* conditions) over the rates of the WT (30˚C) strains. However, χ^2 analyses revealed that none of these fold-differences were statistically significant, as shown in Figure 6.26.

In summary, the mutation rates of WT haploid strains grown using the *mec1-40* conditions were statistically the same regardless of the *hisG-URA3-hisG* location within ChrIII. There was therefore no *cis* effect on the mutation rates between the

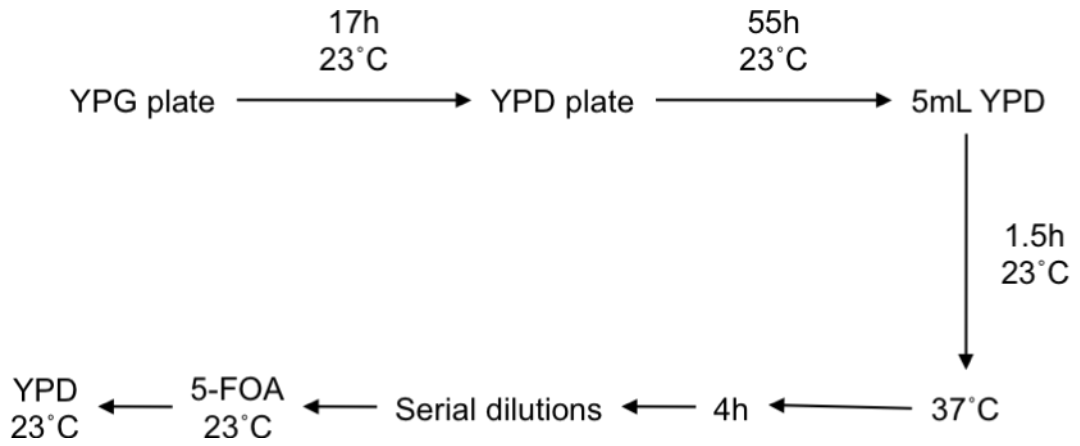

Figure 6.23. Incubation times used for fluctuation analysis of haploid *mec1-40* strains.

Based on the results of Figure 6.22B (page 175), haploid *mec1-40* strains containing the *hisG-URA3-hisG* construct were incubated for these specific durations for fluctuation analysis.

A

Strain		Mutation Rate (95% CL)[a]	Fold-difference between 1&2	Average Mut Rate[b]
53kb	1	2.8×10^{-5} (2.0-3.9)	1.0	2.8×10^{-5}
	2	2.8×10^{-5} (1.9-3.4)		
139kb	1	3.4×10^{-5} (1.8-6.2)	1.3	3.0×10^{-5}
	2	2.6×10^{-5} (1.6-3.9)		
216kb	1	ND	-	-
	2	ND		
230kb	1	2.3×10^{-5} (2.0-3.0)	-	2.3×10^{-5}
	2	ND		
242kb	1	ND	-	2.8×10^{-5}
	2	2.8×10^{-5} (1.9-3.6)		

Location	Chromosomal Features
53kb	RSZ, Termination
139kb	RSZ, Termination, Ty2
216kb	Termination
230kb	Origin
242kb	None

B

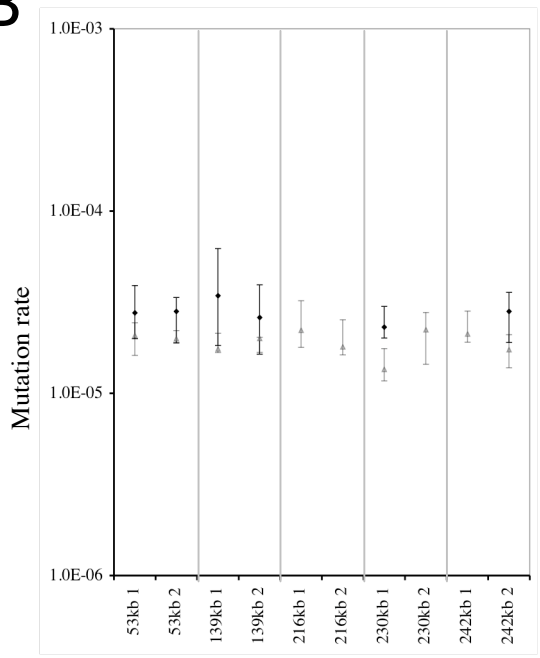

C

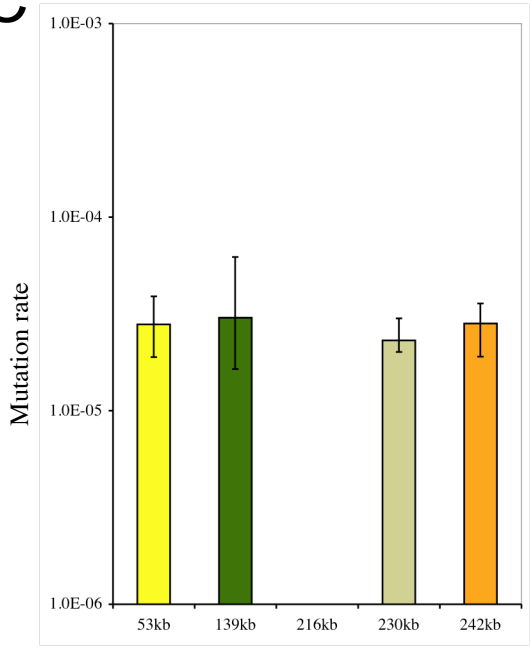

Figure 6.24. Rates of *URA3* inactivation in WT haploid strains grown using *mec1-40* conditions.

(A) Two independent rate measurements were done for the 53kb and 139kb loci. The fraction of 5-FOA-resistant cells was measured in 15 independent cultures for each rate measurement. These frequencies were converted to rates using the method of the median (Lea and Coulson, 1949). [a] 95% confidence limits (CL) were calculated as described previously (Wierdl *et al*., 1996). [b] Where possible, the average mutation rates were calculated. Relevant chromosomal features at each locus are denoted on the right hand side. ND: not determined.

(B) Individual rates are plotted for WT [*mec1-40*] (black diamonds) and WT [30°C] (grey triangles) haploid strains. Capped lines indicate 95% CLs.

(C) The average mutation rate of the two strains is plotted, where possible. The smallest and largest CL value of the two strains was used for each location. Mutation rate is given as number of events/cell/generation.

A

Location Mutation rate[a]	Normalised mutation rate
53kb 2.1 x 10^{-5}	1.1
139kb 1.9 x 10^{-5}	1.1
216kb 2.0 x 10^{-5}	1.1
230kb 1.8 x 10^{-5}	1.0
242kb 1.9 x 10^{-5}	1.1

B

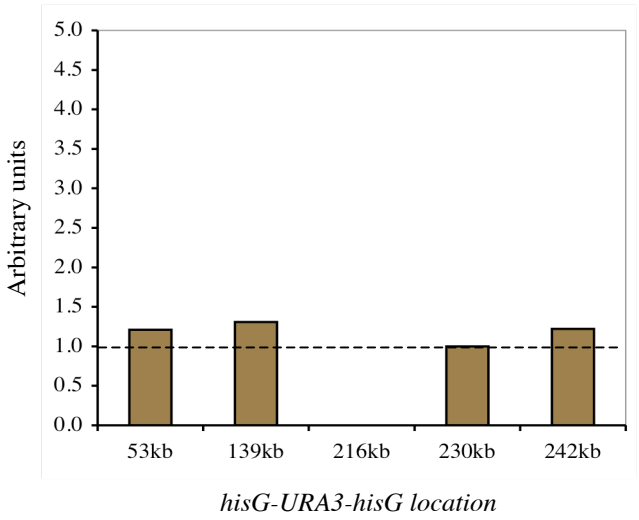

C

Location Mutation rate[a]	53kb 2.8 x 10^{-5}	139kb 3.0 x 10^{-5}	216kb NSS	230kb 2.3 x 10^{-5}	242kb 2.8 x 10^{-5}
53kb 2.8 x 10^{-5}		0.13 NSS		0.60 NSS	0.07 NSS
139kb 3.0 x 10^{-5}				0.60 NSS	0.07 NSS
216kb NSS					
230kb 2.3 x 10^{-5}					0.07 NSS
242kb 2.8 x 10^{-5}					

Figure 6.25. Analysis of rates of *URA3* inactivation in WT haploid strains grown using *mec1-40* conditions.

(A) The average mutation rate at each locus was normalised against the lowest average rate. [a] Mutation rate is given as number of events/cell/generation.

(B) Normalised fold-differences from (A) are plotted.

(C) Chi-square analysis: pair-wise comparison of the mutation rates at each location. Shown in each panel are the Chi square (χ^2; upper) and probability (*P*; lower) values for each pair-wise combination. *P* values of less than 0.05 were deemed significant. NSS: not statistically significant. [a] Mutation rate is given as number of events/cell/generation.

A

Construct location	Average mutation rate		Fold-difference[a] WT (*mec1-40*) / WT (30˚C)	Chi square and *P* values[b]
	WT (*mec1-40*)	WT (30˚C)		
53kb	2.8×10^{-5}	2.0×10^{-5}	1.4	0.13, NSS
139kb	3.0×10^{-5}	1.9×10^{-5}	1.6	1.20, NSS
216kb	-	-	-	-
230kb	2.3×10^{-5}	1.8×10^{-5}	1.6	1.67, NSS
242kb	2.8×10^{-5}	1.9×10^{-5}	1.6	0.60, NSS

B

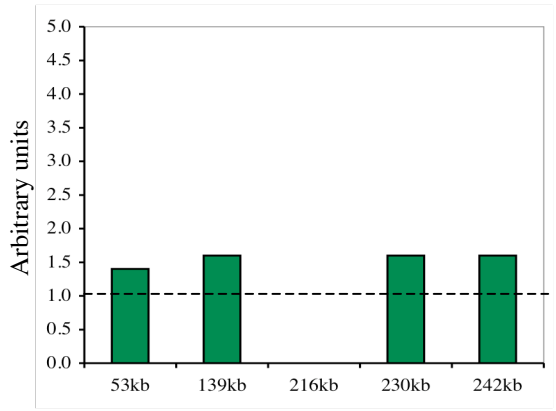

Figure 6.26. Effects of *mec1-40* growth conditions on the rates of *URA3* inactivation compared to optimal conditions (YPD at 30˚C), in WT haploid strains.

(A) [a] Where possible, for each location the mutation rate of strain 1 (WT [*mec1-40*]) was divided by the mutation rate of strain 1 (WT [30˚C]). The same was done for strain 2. The fold-difference was then averaged over these two values for each locus. [b] Significant differences were calculated by χ^2 analyses, as described in the text. χ^2 values are given first, *P* values second. *P* values of less than 0.05 were deemed significant. NSS: not statistically significant.

(B) Graph showing the fold-difference in mutation rates of WT haploid strains grown using *mec1-40* conditions over optimal conditions (YPD at 30˚C) for each locus. Values are taken from (A).

four different tested loci when strains were grown using the established *mec1-40* conditions. When the mutation rates of the WT strains grown using the *mec1-40* conditions were compared against their respective mutation rates when grown at 30˚C in YPD, they were also found to be statistically indistinguishable from each other. The difference in incubation time and temperature between those used here and those in Chapter 4 therefore had little effect on the mutation rate in WT haploid strains.

6.2.7.3 Rates of URA3 inactivation in mec1-40 haploid strains

The mutation rates of haploid *mec1-40* strains were tested at the four loci studied in the above section. Figure 6.27B shows the individual mutation rates of *mec1-40* (red squares) and WT (grey diamond) strains grown using the *mec1-40* conditions; specific values are given in Figure 6.27A. No difference in mutation rate existed between the two independently derived strains for the 53kb and 139kb loci (χ^2 analysis). These mutation rates were averaged, where applicable, for each locus, as shown in Figure 6.27C. Both loci within RSZs, 53kb and 139kb, had the highest mutation rates of 5.3 and 6.3 x 10^{-5} events/cell/generation, respectively, whilst the 230kb (origin) and 242kb (no features) had the lowest rates of 3.8 and 4.8 x 10^{-5} events/cell/generation, respectively. To assess the potential difference between these mutation rates, the rates were first normalised against the rate at the 230kb locus. These values ranged from 1.3 to 1.7-fold. Despite the largest fold-difference between the mutation rates of the largest (139kb) and smallest (230kb) loci, χ^2 analyses revealed that, statistically, none of these fold-differences were significant (Figure 6.28A and 6.28B). This pair-wise analysis was extended to assess if any of the mutation rates differed significantly from each other. Despite the differences seen in the point rate estimates (Figure 6.27B), all of the mutation rates were statistically indistinguishable from each other, as shown in Figure 6.28C. The transient thermal inactivation of Mec1p in *mec1-40-ts* strains therefore had no affect on the mutation rates of *URA3* inactivation for all loci tested.

The rates of *URA3* inactivation for each locus in the *mec1-40* strains were then compared against the mutation rates of their respective WT strains grown under the

A

Strain		Mutation Rate (95% CL)[a]	Fold-difference between 1&2	Average Mut Rate
53kb	1	6.0×10^{-5} (3.4-8.4)	1.3	5.3×10^{-5}
	2	4.6×10^{-5} (2.6-7.1)		
139kb	1	8.0×10^{-5} (6.5-10.4)	1.7	6.3×10^{-5}
	2	4.6×10^{-5} (3.6-9.3)		
216kb	1	-	-	-
	2	-		
230kb	1	3.8×10^{-5} (3.0-6.2)	-	3.8×10^{-5}
	2	ND		
242kb	1	ND	-	4.8×10^{-5}
	2	4.8×10^{-5} (3.1-6.2)		

Location	Chromosomal Features
53kb	RSZ, Termination
139kb	RSZ, Termination, Ty2
216kb	Termination
230kb	Origin
242kb	None

B

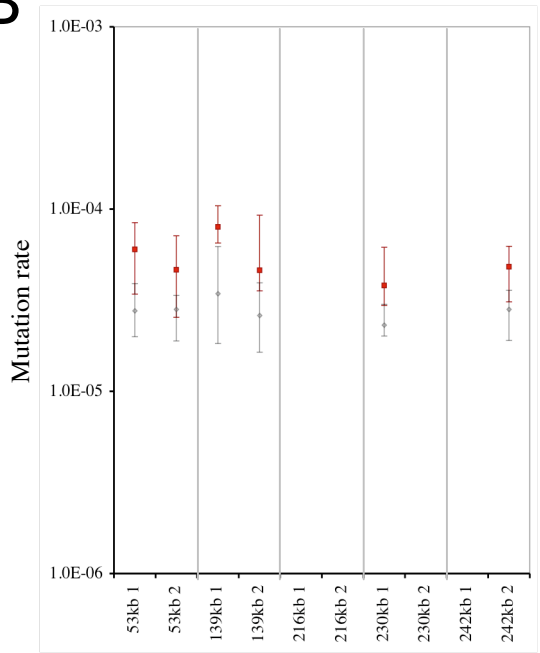

C

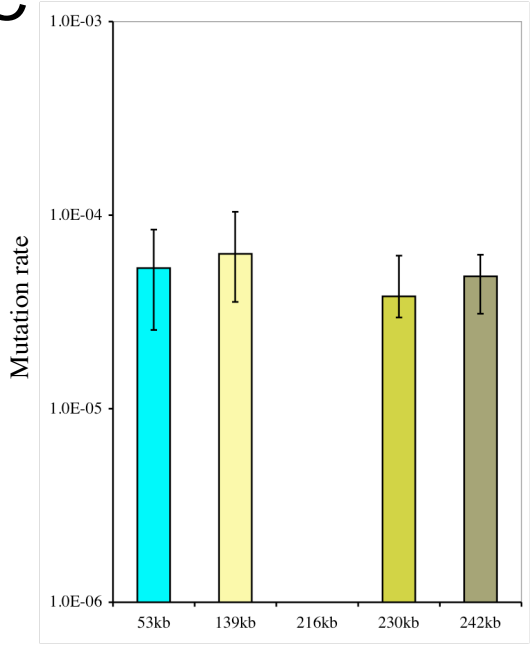

Figure 6.27. Rates of *URA3* inactivation in *mec1-40* haploid strains grown using *mec1-40* conditions.

(A) Two independent rate measurements were done for the 53kb and 139kb loci. The fraction of 5-FOA-resistant cells was measured in 15 independent cultures for each rate measurement. These frequencies were converted to rates using the method of the median (Lea and Coulson, 1949). [a] 95% confidence limits (CL) were calculated as described previously (Wierdl *et al*., 1996). [b] Where possible, the average mutation rates were calculated. Relevant chromosomal features at each locus are denoted on the right hand side. ND: not determined.

(B) Individual rates are plotted for *mec1-40* (red squares) and WT (grey diamonds) haploid strains. Capped lines indicate 95% CLs.

(C) The average mutation rate of the two strains is plotted, where possible. The smallest and largest CL value of the two strains was used for each location. Mutation rate is given as number of events/cell/generation.

A

Location Mutation rate[a]	Normalised mutation rate
53kb 5.3 x 10^{-5}	1.4
139kb 6.3 x 10^{-5}	1.7
216kb ND	-
230kb 3.8 x 10^{-5}	1.0
242kb 4.8 x 10^{-5}	1.3

B

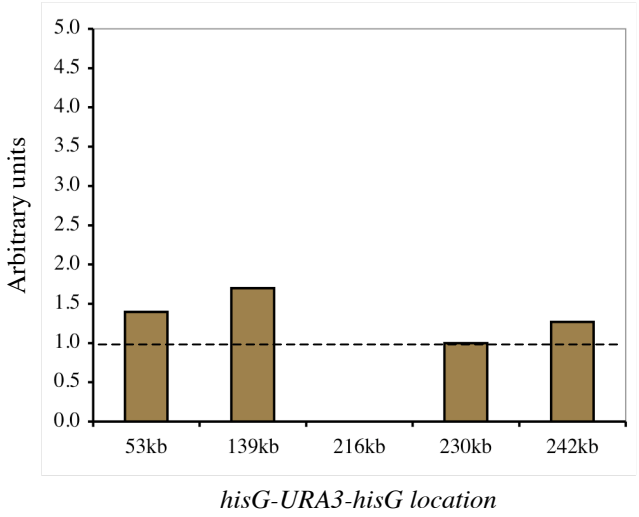

C

Location Mutation rate[a]	53kb 5.3 x 10^{-5}	139kb 6.3 x 10^{-5}	216kb ND	230kb 3.8 x 10^{-5}	242kb 4.8 x 10^{-5}
53kb 5.3 x 10^{-5}		1.20 NSS		0.60 NSS	0.07 NSS
139kb 6.3 x 10^{-5}				3.27 NSS	1.67 NSS
216kb ND					
230kb 3.8 x 10^{-5}					0.60 NSS
242kb 4.8 x 10^{-5}					

Figure 6.28. Analysis of rates of *URA3* inactivation in *mec1-40* haploid strains grown using *mec1-40* conditions.

(A) The average mutation rate at each locus was normalised against the lowest average rate.

(B) Normalised fold-differences from (A) are plotted.

(C) Chi-square analysis: pair-wise comparison of the mutation rates at each location. Shown in each panel are the Chi square (χ^2; upper) and probability (*P*; lower) values for each pair-wise combination. *P* values of less than 0.05 were deemed significant. NSS: not statistically significant. [a] Mutation rate is given as number of events/cell/generation.

same conditions. This comparison showed a ~2-fold-increase for both the 53kb and 139kb loci, whilst the 230kb and 242kb loci each had a 1.7-fold increase. Despite the fold-increases being similar for all four loci between the two genotypes, statistically only the two loci within RSZs, 53kb and 139kb, had significantly higher mutation rates in the *mec1-40* backgrounds compared to the rates in their respective WT strains grown under the same conditions. The mutation rates of the *mec1-40* and WT strains were statistically indistinguishable for the 230kb (origin) and 242kb (no features) loci (Figure 6.29).

In summary, in a haploid *mec1-40* background the mutation rates were significantly higher at the 53kb and 139kb loci compared to the rates of their respective WT strains grown using the same conditions. Both of these locations were in RSZs. At 230kb and 242kb the mutation rates were statistically indistinguishable between the two genotypes.

6.2.8 Diploid mec1-40 strains

6.2.8.1 Preparation for analysis of mec1-40 diploid strains; kinetics of commitment to inviability at 37˚C

Spot tests of diploid *mec1-40* strains containing the *hisG-URA3-hisG* reporter construct grown on YPD media plates at various temperatures are shown in Figure 6.30. Once again, a WT and *mec1-40* strain lacking the construct are shown for comparison. All of the *URA3 mec1-40* strains grew similarly to the *mec1-40* strain at all temperatures tested. At 37˚C most of the *mec1-40* cells died. The colonies that grew were most likely due to spontaneous mutations that partly suppressed the temperature sensitivity of the *mec1-40* allele. This result was slightly less dramatic than in haploid *mec1-40* strains, where nearly all cells died at the non-permissive temperature. This agreed with earlier work in the lab that showed *mec1-40* diploid strains do not die as quickly as *mec1-40* haploid strains.

The viability of a diploid *mec1-40* strain lacking the reporter construct was tested at 37˚C in the same manner used for the haploid *mec1-40* strain, with the exception that aliquots were taken every 2h rather than every 30min. The result is shown in Figure

A

Construct location	Average mutation rate		Fold-difference[a] *mec1-40* / WT (*mec1-40*)	Chi square and *P* values[b]
	mec1-40	WT (*mec1-40*)		
53kb	5.3×10^{-5}	2.8×10^{-5}	1.9	3.33, *P*~0.05
139kb	6.3×10^{-5}	3.0×10^{-5}	2.1	6.53, *P*~0.01
216kb	-	-	-	-
230kb	3.8×10^{-5}	2.3×10^{-5}	1.7	0.60, NSS
242kb	4.8×10^{-5}	2.8×10^{-5}	1.7	0.60, NSS

B

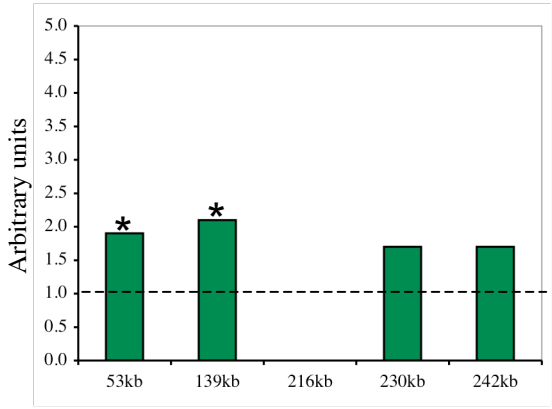

Figure 6.29. Effects of *mec1-40* on the rates of *URA3* inactivation compared to those in WT haploid strains grown in the same conditions.

(A) [a] Where possible, for each location the mutation rate of strain 1 (*mec1-40*) was divided by the mutation rate of strain 1 (WT). The same was done for strain 2. The fold-difference was then averaged over these two values for each locus. [b] Significant differences were calculated by χ^2 analyses, as described in the text. χ^2 values are given first, *P* values second. *P* values of less than 0.05 were deemed significant. NSS: not statistically significant.

(B) Graph showing the fold-difference in mutation rates of *mec1-40* over WT haploid strains for each locus. "*" denotes a significant statistical difference. Values are taken from (A).

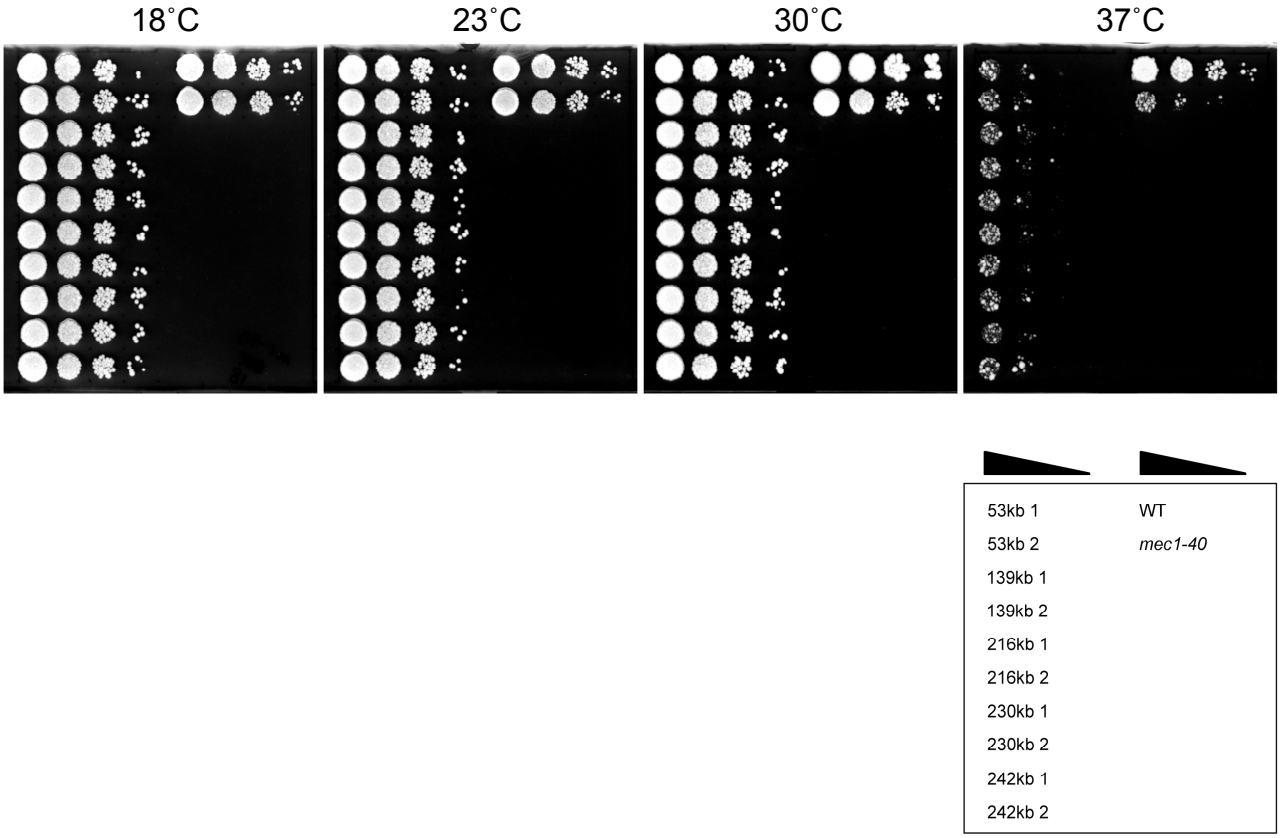

Figure 6.30. Effects of temperature on growth of *mec1-40* diploid strains carrying a *hisG-URA3-hisG* construct at different loci on ChrIII.

Ten-fold serial dilutions of exponentially growing cells were spotted onto YPD plates and grown at the indicated temperatures for 3-5 days. The box in the lower right indicates the strains spotted onto the plates: WT and *mec1-40* in this instance refer to strains lacking a *hisG-URA3-hisG* construct.

A

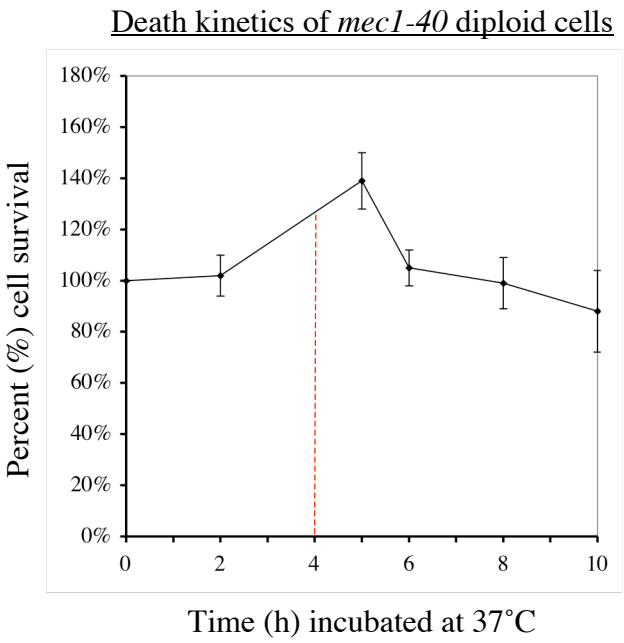

B

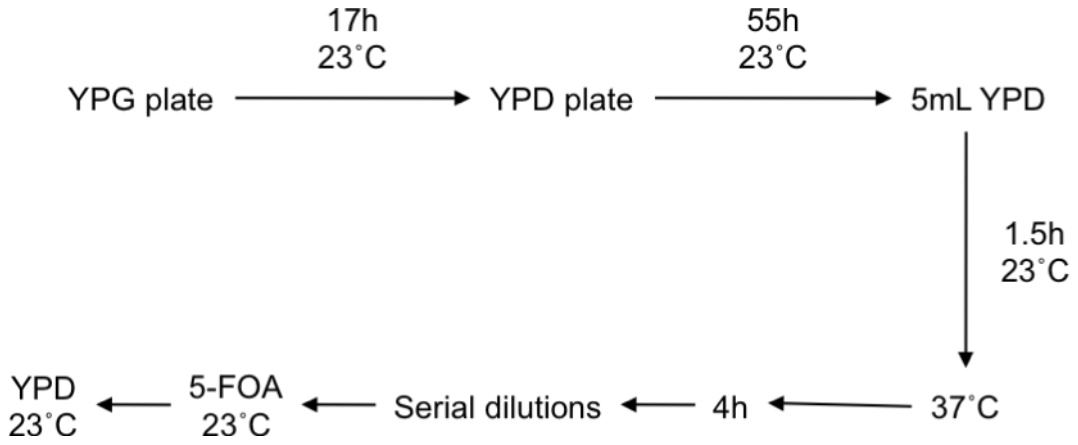

Figure 6.31. Testing diploid *mec1-40* strains for fluctuation analysis incubation times: kinetics of commitment to inviability.

(A) Death kinetic analysis of a diploid *mec1-40* strain. Incubation times are the same as those used in Figure 6.22A. Error bars indicate the standard deviation between three independent cultures.

(B) Based on the results of (A), diploid *mec1-40* strains containing the *hisG-URA3-hisG* construct were incubated for these specific durations for fluctuation analysis.

6.31A. The cell count increased for the initial 5h up to a maximum of ~140% of the original (t=0) time points. After 5h incubation cell viability began to decrease, and

continued to do so for the next five hours. The lowest cell viability was at t=10h, where the cell populations were ~85% of the original cell count at t=0.

It was reasoned that the ideal conditions to use for diploid *mec1-40* strains would be as long a time as possible at 37˚C whilst maintaining viability. Therefore, samples were taken following 4 hours' incubation at 37˚C, while the culture was still increasing in cell number.

6.2.8.2 Rates of URA3 inactivation in WT diploid strains, using mec1-40 growth conditions

The mutation rates were first tested in diploid WT strains using the *mec1-40* incubation times. Note that, unlike haploids, the 216kb strains could now be used for fluctuation analysis since the slow growth phenotype did not exist in diploids. Figure 6.32B shows the individual mutation rates of WT diploid strains grown using the *mec1-40* incubation times compared with the same strains grown at 30˚C. No statistical difference in mutation rate was found between the two independently derived strains for the 53kb, 139kb and 216kb loci (χ^2 analysis).

The mutation rates were then averaged for each location, where applicable. These ranged from 2.0 x 10^{-5} events/cell/generation for 216kb (replication termination) to 3.3 x 10^{-5}, for 242kb (no features), as shown in Figures 6.32A and 6.32C. Pair-wise analysis was performed to see if these mutation rates were statistically different from each other. As Figure 6.33 shows, the only statistical difference found was that 216kb had a significantly lower mutation rate than the other four locations (P<0.05). All of the other mutation rates were statistically indistinguishable from each other.

The mutation rates for each location were then compared against the respective rates of the same strains grown at 30˚C. Figure 6.34A shows that no statistical difference was found between the two conditions for every location except for 216kb (replication termination), which had a significantly higher mutation rate for the WT

A

Strain		Mutation Rate (95% CL)[a]	Fold-difference between 1&2	Average Mut Rate[b]
53kb	1	2.6×10^{-5} (1.9-3.3)	1.0	2.6×10^{-5}
	2	2.6×10^{-5} (2.2-3.2)		
139kb	1	3.1×10^{-5} (2.3-3.8)	1.1	3.0×10^{-5}
	2	2.8×10^{-5} (2.1-3.3)		
216kb	1	1.8×10^{-5} (1.5-2.0)	1.2	2.0×10^{-5}
	2	2.1×10^{-5} (1.7-2.6)		
230kb	1	2.6×10^{-5} (2.3-3.3)	-	2.6×10^{-5}
	2	ND		
242kb	1	ND	-	3.3×10^{-5}
	2	3.3×10^{-5} (2.4-4.2)		

Location	Chromosomal Features
53kb	RSZ, Termination
139kb	RSZ, Termination, Ty2
216kb	Termination
230kb	Origin
242kb	None

B

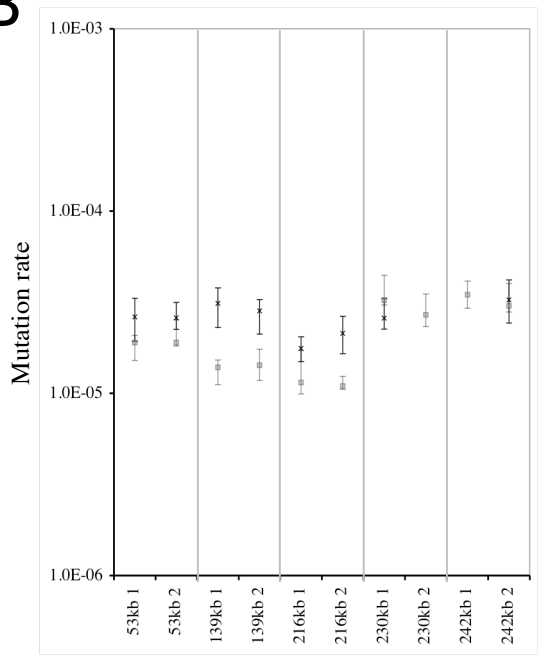

C

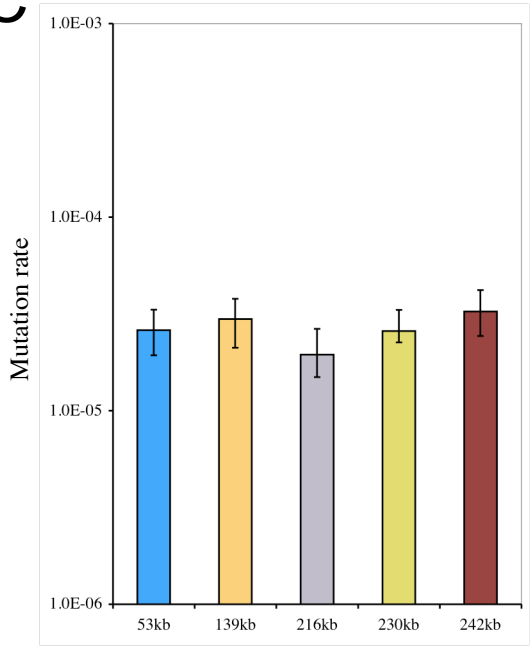

Figure 6.32. Rates of *URA3* inactivation in diploid WT strains grown using *mec1-40* conditions.

(A) Two independent rate measurements were done for the 53kb, 139kb and 216kb loci. The fraction of 5-FOA-resistant cells was measured in 15 independent cultures for each rate measurement. These frequencies were converted to rates using the method of the median (Lea and Coulson, 1949). [a] 95% confidence limits (CL) were calculated as described previously (Wierdl *et al*., 1996). [b] Where possible, the average mutation rates were calculated. Relevant chromosomal features at each locus are denoted on the right hand side. ND: not determined.

(B) Individual rates are plotted for WT [*mec1-40*] (black crosses) and WT [30˚C] (grey squares) diploid strains. Capped lines indicate 95% CLs.

(C) The average mutation rate of the two strains is plotted, where possible. The smallest and largest CL value of the two strains was used for each location. Mutation rate is given as number of events/cell/generation.

A

Location Mutation rate[a]	Normalised mutation rate
53kb 2.6 x 10^{-5}	1.3
139kb 3.0 x 10^{-5}	1.5
216kb 2.0 x 10^{-5}	1.0
230kb 2.6 x 10^{-5}	1.3
242kb 3.3 x 10^{-5}	1.6

B

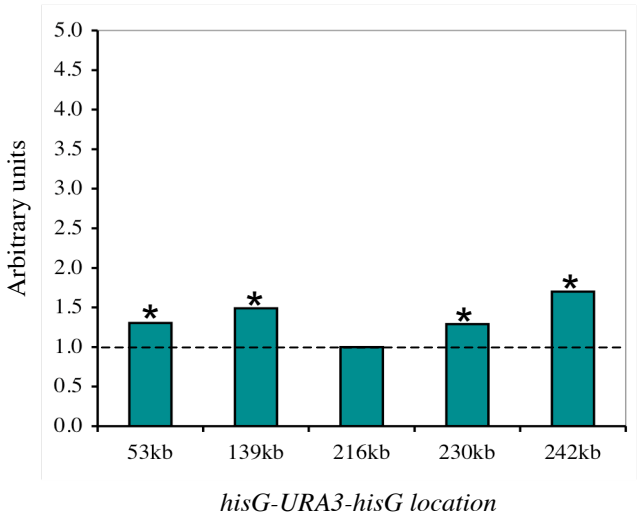

C

Location Mutation rate[a]	53kb 2.6 x 10^{-5}	139kb 3.0 x 10^{-5}	216kb 2.0 x 10^{-5}	230kb 2.6 x 10^{-5}	242kb 3.3 x 10^{-5}
53kb 2.6 x 10^{-5}		0.13 NSS	4.80 *P*<0.05	0.07 NSS	0.07 NSS
139kb 3.0 x 10^{-5}			3.33 *P*~0.05	0.60 NSS	0.60 NSS
216kb 2.0 x 10^{-5}				5.40 *P*<0.05	5.40 *P*<0.05
230kb 2.6 x 10^{-5}					0.07 NSS
242kb 3.3 x 10^{-5}					

Figure 6.33. Analysis of rates of *URA3* inactivation in WT diploid strains grown using *mec1-40* conditions.

(A) The average mutation rate at each locus was normalised against the lowest average rate. [a] Mutation rate is given as number of events/cell/generation.

(B) Normalised fold-differences from (A) are plotted. "*" denotes a significant statistical difference.

(C) Chi-square analysis: pair-wise comparison of the mutation rates at each location. Shown in each panel are the Chi square (χ^2; upper) and probability (*P*; lower) values for each pair-wise combination. *P* values of less than 0.05 were deemed significant. NSS: not statistically significant. [a] Mutation rate is given as number of events/cell/generation.

A

Construct location	Average mutation rate		Fold-difference[a] WT (*mec1-40*) / WT (30°C)	Chi square and *P* values[b]
	WT (*mec1-40*)	WT (30°C)		
53kb	2.6×10^{-5}	1.9×10^{-5}	1.4	0.13, NSS
139kb	3.0×10^{-5}	1.4×10^{-5}	2.1	3.33, NSS
216kb	2.0×10^{-5}	1.1×10^{-5}	1.7	4.80, $P<0.05$
230kb	2.6×10^{-5}	3.0×10^{-5}	0.8	3.27, NSS
242kb	3.3×10^{-5}	3.2×10^{-5}	1.1	0.07, NSS

B

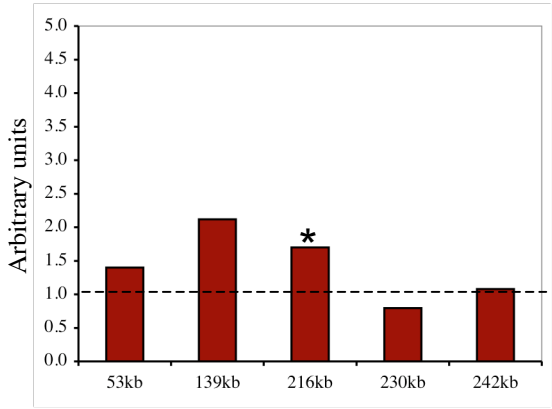

Figure 6.34. Effects of *mec1-40* growth conditions on the rates of *URA3* inactivation compared to optimal conditions (YPD at 30˚C), in WT diploid strains.

(A) [a] Where possible, for each location the mutation rate of strain 1 (WT [*mec1-40*]) was divided by the mutation rate of strain 1 (WT [30˚C]). The same was done for strain 2. The fold-difference was then averaged over these two values for each locus. [b] Significant differences were calculated by χ^2 analyses, as described in the text. χ^2 values are given first, *P* values second. *P* values of less than 0.05 were deemed significant. NSS: not statistically significant.

(B) Graph showing the fold-difference in mutation rates of WT diploid strains grown using *mec1-40* conditions over optimal conditions (YPD at 30˚C) for each locus. "*" denotes a significant statistical difference. Values are taken from (A).

strains grown using the *mec1-40* conditions. In conclusion, therefore, the mutation rate in diploid WT strains grown using the *mec1-40* incubation times was the same regardless of the *hisG-URA3-hisG* construct in ChrIII except at 216kb, which had a significantly lower rate than the other four locations. Some *cis* effect was therefore seen in the rates of *URA3* inactivation when WT strains were grown using the *mec1-40* incubation times. A temperature-specific effect on mutation rate was also observed in WT diploid strains grown at 30˚C and 37˚C. When the mutation rates for these strains were compared to those when the same strains were grown at 30˚C, all the rates were statistically indistinguishable for all locations with the exception of, once again, the 216kb locus, which had a significantly higher mutation rate under the *mec1-40* conditions.

6.2.8.3 Rates of URA3 inactivation in mec1-40 diploid strains

Figure 6.35 shows the mutation rates of diploid *mec1-40* (blue squares) and WT (grey crosses) strains grown using the *mec1-40* conditions. No difference was found in the mutation rates of the two independently derived strains for the 53kb, 139kb and 216kb loci (χ^2 analysis).

Where possible, the mutation rates were averaged for each location. The 242kb (no features) locus had the highest mutation rate of 9.4 x 10^{-5} events/cell/generation, whilst the remaining four loci all had similar mutation rates of ~5 x 10^{-5} events/cell/generation (Figures 6.35A and 6.35C). To assess the potential variation in these mutation rates, the mutation rates were normalised against the lowest value, at 216kb (replication termination). These values ranged from 1.0- to 2.0-fold. Of these values, only the 2-fold difference between the rates of the 242kb and 216kb loci was statistically significant (Figure 6.36). This pair-wise analysis was then extended so that the mutation rates at all loci were compared. With the exception of the statistical difference between the rates at the 216kb and 242kb loci, the mutation rates at all other loci were statistically indistinguishable from each other. There was therefore only one *cis* effect seen in *mec1-40* diploid strains grown using the conditions established in this chapter.

A

Strain		Mutation Rate (95% CL)[a]	Fold-difference between 1&2	Average Mut Rate[b]
53kb	1	5.1×10^{-5} (3.9-6.5)	1.0	5.1×10^{-5}
	2	5.0×10^{-5} (4.0-7.0)		
139kb	1	5.9×10^{-5} (2.4-8.9)	1.1	5.7×10^{-5}
	2	5.4×10^{-5} (3.9-7.2)		
216kb	1	5.0×10^{-5} (3.8-10.0)	1.1	4.7×10^{-5}
	2	4.4×10^{-5} (3.8-5.2)		
230kb	1	5.2×10^{-5} (4.1-7.7)	-	5.2×10^{-5}
	2	ND		
242kb	1	ND	-	9.4×10^{-5}
	2	9.4×10^{-5} (5.8-11.1)		

Location	Chromosomal Features
53kb	RSZ, Termination
139kb	RSZ, Termination, Ty2
216kb	Termination
230kb	Origin
242kb	None

B

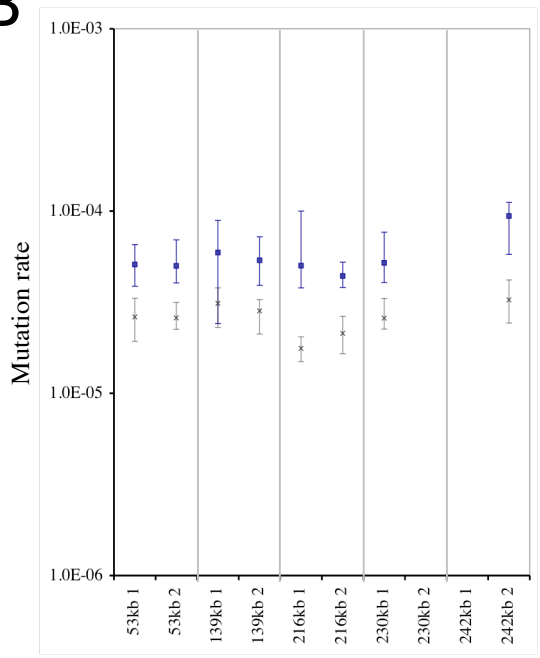

C

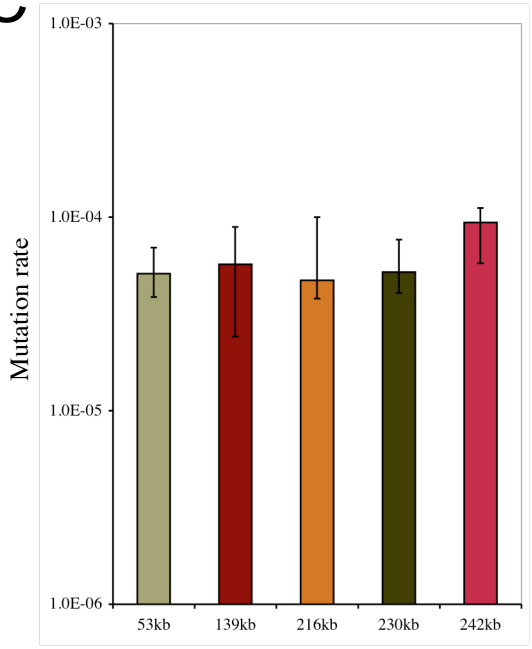

Figure 6.35. Rates of *URA3* inactivation in *mec1-40* diploid strains grown using *mec1-40* conditions.

(A) Two independent rate measurements were done for the 53kb, 139kb and 216kb loci. The fraction of 5-FOA-resistant cells was measured in 15 independent cultures for each rate measurement. These frequencies were converted to rates using the method of the median (Lea and Coulson, 1949). [a] 95% confidence limits (CL) were calculated as described previously (Wierdl *et al*., 1996). [b] Where possible, the average mutation rates were calculated. Relevant chromosomal features at each locus are denoted on the right hand side.

(B) Individual rates are plotted for *mec1-40* (blue squares) and WT (grey crosses) diploid strains. Capped lines indicate 95% CLs.

(C) The average mutation rate of the two strains is plotted, where possible. The smallest and largest CL value of the two strains was used for each location. Mutation rate is given as number of events/cell/generation.

A

Location Mutation rate[a]	Normalised mutation rate
53kb 5.1 x 10^{-5}	1.1
139kb 5.7 x 10^{-5}	1.2
216kb 4.7 x 10^{-5}	1.0
230kb 5.2 x 10^{-5}	1.1
242kb 9.4 x 10^{-5}	2.0

B

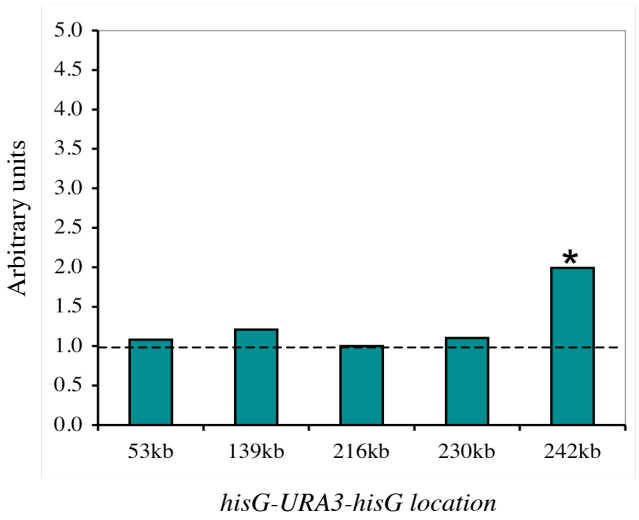

C

Location Mutation rate[a]	53kb 5.1 x 10^{-5}	139kb 5.7 x 10^{-5}	216kb 4.7 x 10^{-5}	230kb 5.2 x 10^{-5}	242kb 9.4 x 10^{-5}
53kb 5.1 x 10^{-5}		0.00 NSS	0.53 NSS	0.60 NSS	3.27 NSS
139kb 5.7 x 10^{-5}			0.53 NSS	0.60 NSS	1.67 NSS
216kb 4.7 x 10^{-5}				1.67 NSS	5.27 P<0.05
230kb 5.2 x 10^{-5}					1.67 NSS
242kb 9.4 x 10^{-5}					

Figure 6.36. Analysis of rates of *URA3* inactivation in *mec1-40* diploid strains grown using *mec1-40* conditions.

(A) The average mutation rate at each locus was normalised against the lowest average rate. [a] Mutation rate is given as number of events/cell/generation.

(B) Normalised fold-differences from (A) are plotted. "*" denotes a significant statistical difference.

(C) Chi-square analysis: pair-wise comparison of the mutation rates at each location. Shown in each panel are the Chi square (χ^2; upper) and probability (P; lower) values for each pair-wise combination. P values of less than 0.05 were deemed significant. NSS: not statistically significant. [a] Mutation rate is given as number of events/cell/generation.

Figure 6.35B shows that the mutation rates were higher in the *mec1-40* strains than in their respective WT strains grown under the same conditions for all five loci. The fold-difference between these two genotypes was calculated and χ^2 analyses performed to see if the observed increases in mutation rate in *mec1-40* strains were significant. These values ranged from 1.9- to 2.9-fold. Among these, the fold differences at the 53kb, 216kb and 242kb loci were found to be statistically significant (Figure 6.37). For the 139kb and 230kb locations, however, χ^2 values of 3.33 and 3.27, respectively, were found. These values corresponded to *P* values of 93.2% and 92.9%, respectively.

In summary, therefore, the 242kb (no features) location had a significantly higher mutation rate than the other four locations in a diploid *mec1-40* background. The mutation rates for these four loci did not differ statistically from each other. All loci had a significantly higher rate in the *mec1-40* strains than in their respective WT strains grown under the same conditions.

6.2.9 Effects of ploidy on rates of URA3 inactivation in mec1-40 strains

As a final comparison, the mutation rates of diploid and haploid *mec1-40* strains were compared. This was possible since the growth conditions were identical. Figure 6.38 shows individual mutation rates of diploid (black squares) and haploid (grey squares) *mec1-40* strains. Where possible, the rates of *URA3* inactivation in the 5strains for each locus. These values varied from 0.9- to 2.0-fold. It was found by χ^2 analyses that none of the mutation rates differed statistically, as might have been expected from the similar point rate estimates and overlapping 95% CLs (Figure 6.38A). The mutation rates in diploid and haploid *mec1-40* strains were therefore statistically the same for all loci tested.

6.3 Discussion

The effect of inactivating Mec1p, a key checkpoint protein, on the rates of *URA3* inactivation at different loci was assessed. Due to its essential nature, a second site

A

Construct location	Average mutation rate		Fold-difference[a] *mec1-40* / WT (*mec1-40*)	Chi square and *P* values[b]
	mec1-40	WT (*mec1-40*)		
53kb	5.1×10^{-5}	2.6×10^{-5}	1.9	8.53, $P<0.01$
139kb	5.7×10^{-5}	3.0×10^{-5}	1.9	3.33, NSS
216kb	4.7×10^{-5}	2.0×10^{-5}	2.5	19.20, $P<0.001$
230kb	5.2×10^{-5}	2.6×10^{-5}	2.0	3.27, NSS
242kb	9.4×10^{-5}	3.3×10^{-5}	2.9	5.40, $P<0.05$

B

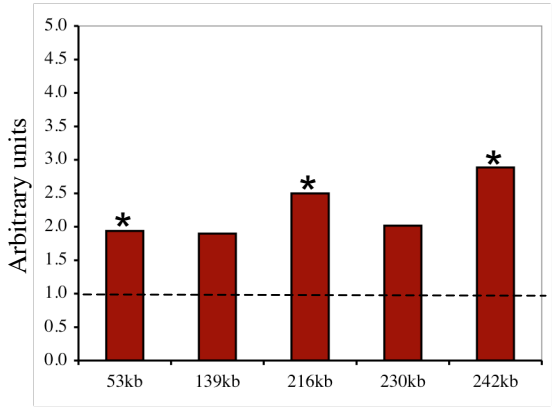

Figure 6.37. Effects of *mec1-40* on the rates of *URA3* inactivation compared to those in WT diploid strains grown in the same conditions.

(A) [a] Where possible, for each location the mutation rate of strain 1 (*mec1-40*) was divided by the mutation rate of strain 1 (WT). The same was done for strain 2. The fold-difference was then averaged over these two values for each locus. [b] Significant differences were calculated by χ^2 analyses, as described in the text. χ^2 values are given first, *P* values second. *P* values of less than 0.05 were deemed significant. NSS: not statistically significant.

(B) Graph showing the fold-difference in mutation rates of *mec1-40* over WT diploid strains for each locus. "*" denotes a significant statistical difference. Values are taken from (A).

A

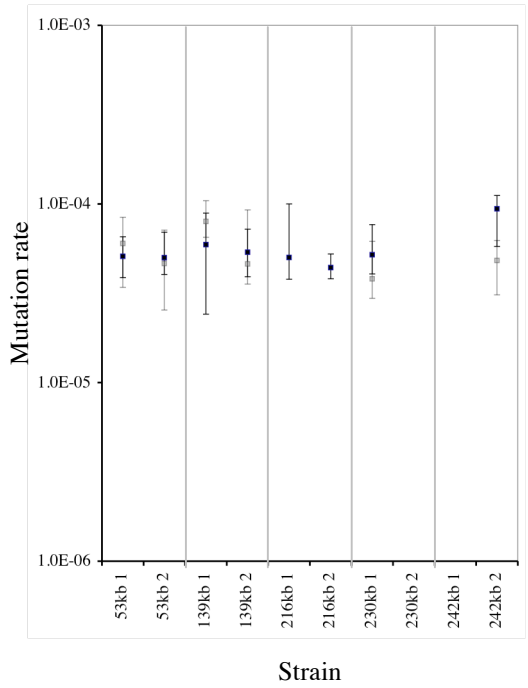

B

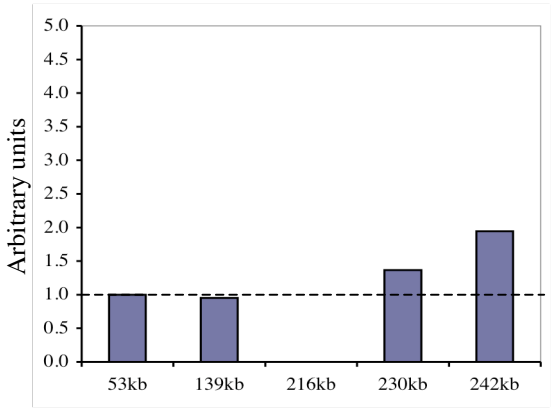

C

Construct location	Average mutation rate		Fold-difference[a] Diploid / Haploid	Chi square and *P* values[b]
	Diploid	Haploid		
53kb	5.1×10^{-5}	5.3×10^{-5}	1.0	0.00, NSS
139kb	5.7×10^{-5}	6.3×10^{-5}	0.9	0.53, NSS
216kb	4.7×10^{-5}	-	-	-
230kb	5.2×10^{-5}	3.8×10^{-5}	1.4	1.67, NSS
242kb	9.4×10^{-5}	4.8×10^{-5}	2.0	3.27, NSS

Figure 6.38. Effects of ploidy on the rates of *URA3* inactivation in *mec1-40* strains grown using *mec1-40* conditions.

(A) Individual mutation rates of *mec1-40* haploid (grey squares) and *mec1-40* diploid (dark blue squares) strains.

(B) Graph showing the fold-difference in mutation rates of diploid over haploid *mec1-40* strains for each locus. Values are taken from (C).

(C) [a] Where possible, for each location the mutation rate of strain 1 (diploid) was divided by the mutation rate of strain 1 (haploid). The same was done for strain 2. The fold-difference was then averaged over these two values for each locus. [b] Significant differences were calculated by χ^2 analyses, as described in the text. χ^2 values are given first, *P* values second. *P* values of less than 0.05 were deemed significant. NSS: not statistically significant.

suppressor, *sml1Δ*, kept *mec1*-null strains viable. Therefore, it was necessary to first assess the rates of *URA3* inactivation in *sml1Δ* strains. In haploid *sml1Δ* strains no *cis* effect was seen. When compared to the mutation rates of their respective WT strains grown in the same conditions, no mutagenic effects of *sml1Δ* was seen either. On the other hand, both *cis* and *trans* effects were observed in diploid *sml1Δ* strains. Specifically, the rate of *URA3* inactivation at the 53kb locus (RSZ, termination) was significantly higher than the rates at the other four loci. Also, compared to WT strains, the mutation rates were significantly higher for the 53kb and 216kb (termination) loci, yet lower for the 230kb (origin) and 242kb (no features) loci.

Previous studies have observed modest (less than 2-fold) increases in the mutation rate of *sml1Δ* strains when compared to control strains (Craven *et al*., 2002; Admire *et al*., 2006). Although small increases were observed in the haploid *sml1Δ* strains used in this study, they were not found to be significant. Of particular interest was that the mutation rates decreased in diploid *sml1Δ* strains for the 230kb and 242kb loci when compared to the mutation rates of their respective WT strains. This was unexpected since it is thought the absence of Sml1p leads to more error-prone DNA replication as a result of unregulated dNTP production, which, in turn, could lead to an increase in mutation rate. Indeed, an *sml1* mutation has been shown to increase instability involving base-pair changes (Chabes *et al*., 2003), and in another study it suppressed DNA fork stalling and breakage (Cha and Kleckner, 2002). It has been demonstrated here that, in diploid *sml1Δ* strains, the rate of *URA3* inactivation is modulated in both a *cis* and *trans* specific manner, and that this is location dependent. There was also a difference when the mutation rates of diploid and haploid *sml1Δ* strains were compared: the mutation rate at the 53kb locus was significantly higher in the diploid *sml1Δ* strain than in its respective haploid *sml1Δ* strain, but the rates at all other loci were statistically the same.

In haploid *mec1Δ sml1Δ* strains the two loci within RSZs, 53kb and 139kb, had mutation rates that were 3.3- and 1.7-fold higher, respectively, than that at the 216kb locus (termination). Nevertheless, due to the large degree of variation in the 95% CL values, it was not possible to establish statistical significance. Other studies using *MEC1* mutants (either null or temperature sensitive) have also shown a larger degree

of variation in mutation rates in these mutant backgrounds compared to those of other genes such as *rrm3Δ*, *sml1Δ*, etc (Craven *et al*., 2002; Myung and Kolodner, 2002; Admire *et al*., 2006), suggesting that inactivation of Mec1p may lead to clonal variations regarding mutation rates.

To assess the specific affects of *mec1Δ* in *URA3* inactivation, the mutation rates of the haploid *mec1Δ sml1Δ* strains were compared to those of the *sml1Δ* strains. Unexpectedly, the rates at the 216kb (termination) and 230kb (origin) loci decreased in the *mec1Δ sml1Δ* strains, yet the rates at the other three loci were indistinguishable between the two genotypes.

In diploid *mec1Δ sml1Δ* strains mutation rates varied 2.4-fold among the five loci. Once again, the large degree of overlap between the 95% CL values made statistical analysis difficult. When the mutation rates in *mec1Δ sml1Δ* strains were compared to those in *sml1Δ* strains, there was a uniform 2-3-fold increase in mutation rate at all five loci. The mutation rates of diploid *mec1Δ sml1Δ* strains were also found to be significantly higher than the haploids at all five loci. The extent of the increases, however, was not uniform, as the lowest fold-differences were found in the loci within RSZs (2.4-fold), and the highest at 216kb (6.6-fold).

Other reports have studied the rate of gross chromosomal rearrangements (GCR) in *mec1Δ sml1Δ* strains (Chen and Kolodner, 1999; Myung *et al*., 2001[b]). GCRs are events that lead to the simultaneous loss of two closely linked genes. Of note was that one of these studies also found ploidy-specific effects in *mec1Δ sml1Δ* strains, like those found here. Rates of mitotic recombination at the *CAN1* locus (ChrV), for instance, increased 10-fold in diploid *mec1Δ sml1Δ* strains but only 2-fold in haploid *mec1Δ sml1Δ* strains compared to WT controls (Craven *et al*., 2002). Another study found that the mutation rates were elevated ~200-fold in *mec1Δ sml1Δ* strains (Myung *et al*., 2001[b]), which are much higher than the 2-3-fold increases observed in this chapter.

Using the temperature-sensitive allele *mec1-40* allowed assessment of the rate of *URA3* inactivation in the absence of Mec1p function in an *SML1* background. When

the mutation rates of *mec1-40* haploid strains were tested, no *cis* effect was seen amongst the four loci tested. When compared to the mutation rates of their respective WT strains incubated under the same conditions, statistically significant increases were seen for the 53kb and 139kb loci, where the rate of the *mec1-40* strains were 2-fold higher than in the WT strains. Of note was that these two loci were in RSZs.

In diploid *mec1-40* strains a different situation was seen. When assessing the potential differences in mutation rate between the five loci, only the rate at the 242kb (no features) locus was significantly higher than the rates at the other loci. All the other mutation rates were statistically the same. When these mutation rates were compared to those of WT strains grown under the same conditions, a uniform 2-3-fold increase was seen for all five loci in the *mec1-40* strains.

As a final comparison, the mutation rates of the diploid and haploid *mec1-40* strains were compared. These were statistically indistinguishable. There were therefore no ploidy-specific affects on the mutation rates seen in *mec1-40* strains using the growth conditions established in this chapter.

In diploid strains, therefore, the rates of *URA3* inactivation increased uniformly in both *mec1Δ sml1Δ* and *mec1-40* strains compared to the relevant control strains. The loci within RSZ, 53kb and 139kb, were not affected more than the rates at the other loci, suggesting that chromosome breakage prone regions might not be recombination hotspots.

Summary

Effects of ploidy were observed again with diploids in the *mec1Δ sml1Δ*, and *mec1-40* backgrounds all exhibiting higher mutation rates than the corresponding haploids. The extent of mutagenic effects of Mec1p inactivation in both *mec1Δ* and *mec1-40-ts* strains were surprisingly modest. Furthermore, for locations 216kb and 230kb in *mec1Δ sml1Δ* haploids, the rates were actually smaller than those measured in *sml1Δ* strains. Currently the reasons for these observations remain unknown. Note that the current observations differ significantly from previous ones, where inactivation of

Mec1p had been linked repeatedly to greatly elevated mutation rates (Myung *et al*., 2001[b]; Craven *et al*., 2002). The difference could be due to the nature of constructs utilized, the location of the genome where the reporter constructs were introduced, and/or other differences in the experimental designs.

Chapter 7.

RRM3

7.1 Introduction

Rrm3p has been discussed in detail in the Introduction (Section 1.4.1.4). As DSBs do not form in an *rrm3Δ mec1-ts* strain background at the non-permissive temperature with partial restoration of cell viability (Nadia Hashash, unpublished results), the rates of *URA3* inactivation were assessed in *rrm3Δ* strains harboring the *hisG-URA3-hisG* reporter construct.

7.2 Results

7.2.1 Rates of URA3 inactivation in rrm3Δ haploid strains

To produce the strains required for this chapter, WT haploids were crossed with an *rrm3Δ* strain (NHY246), and then sporulated, dissected, and uracil prototroph spore clones selected for that co-segregated with the appropriate mutant gene marker. It was ensured that none of the resulting strains were petite and had mating-type '***a***', as per the original parental strains. These haploids were then re-crossed with NHY246 to produce the homozygous diploid strains.

Spot tests of *rrm3Δ* strains grown at 18, 23, 30 and 37˚C are shown in Figure 7.1. The parental WT and *rrm3Δ* strains lacking an inserted *hisG-URA3-hisG* construct are also shown for comparison (first and second rows, respectively, right hand side). Growth of all strains was optimal at 30˚C, including the 216kb strains, which grew very poorly at both 18˚C and 37˚C. *rrm3Δ* strains were therefore grown at 30˚C. This meant that the effect of *rrm3Δ* on mutation rate for each locus could be directly compared against the mutation rates of their respective WT strains grown in optimal conditions at 30˚C (Chapter 3).

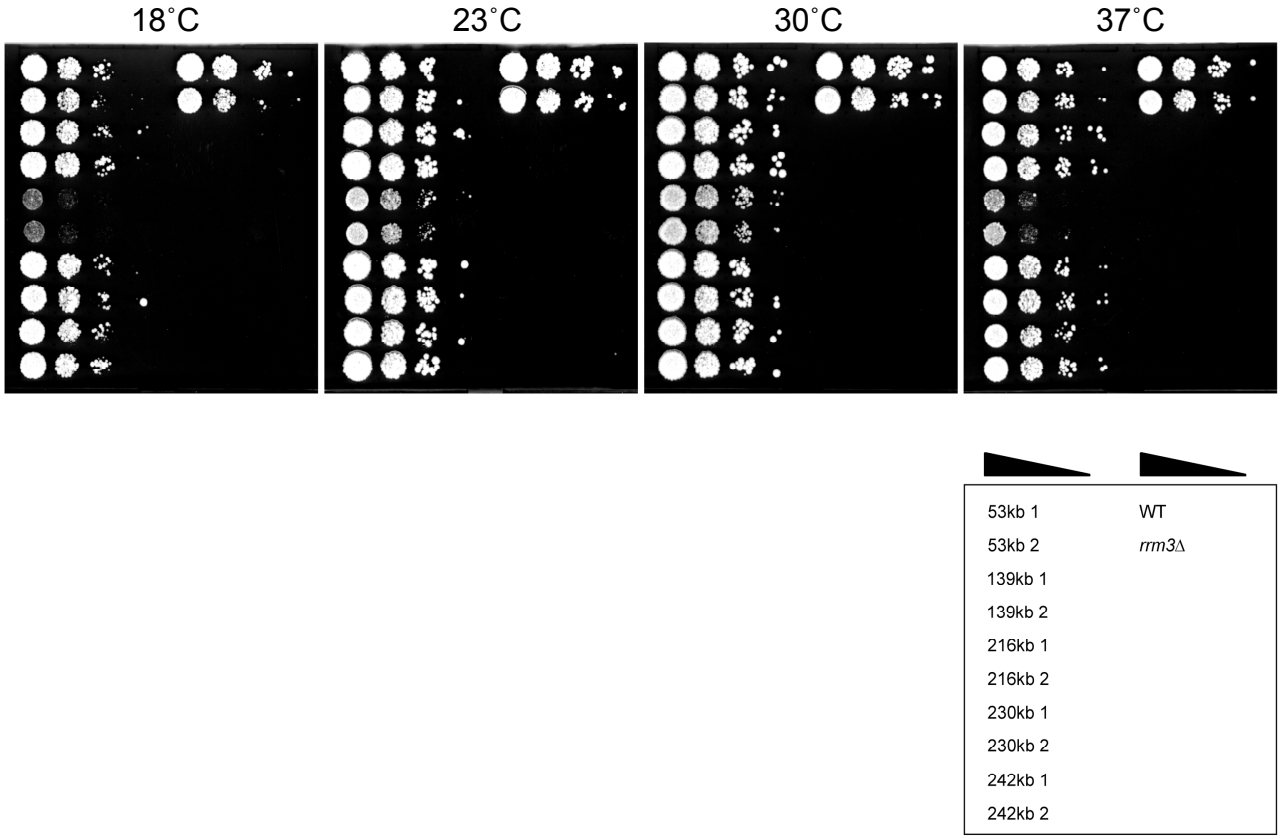

Figure 7.1. Effects of temperature on growth of *rrm3*Δ haploid strains carrying a *hisG-URA3-hisG* construct at different loci on ChrIII.

Ten-fold serial dilutions of exponentially growing cells were spotted onto YPD plates and grown at the indicated temperatures for 3-5 days. The box in the lower right indicates the strains spotted onto the plates: WT and *rrm3Δ* in this instance refer to strains lacking a *hisG-URA3-hisG* construct.

Rates of *URA3* inactivation for each haploid *rrm3Δ* strains harboring the reporter construct at specific loci are shown alongside their WT rates in Figure 7.2B. Specific values are listed in Figure 7.2A. No statistical difference in mutation rate was found between the two independently derived strains for any locus (χ^2 analysis). These mutation rates were averaged for each location, as shown in Figure 7.2C. These ranged from the lowest value of 1.1 x 10^{-5} events/cell/generation for 216kb (replication termination) to 2.1 x 10^{-5} for 53kb (RSZ, replication termination). To assess the variation among different locations, the mutation rates were normalised against the lowest rate observed at 216kb. These normalised values ranged from 1.0 – 1.9-fold (Figure 7.3A). Among these, only the 1.9-fold increase for the 53kb locus was statistically significant (Figures 7.3A and 7.3B). The rates for all five loci were then compared by pair-wise analysis, as shown in Figure 7.3C. This shows that the 53kb rate was significantly higher than the 139kb, 216kb and 242kb rates, but not for the 230kb rate (which had a χ^2 value of 3.27). All other mutation rates did not differ statistically from each other.

The rates of *URA3* inactivation for the five loci were compared between the *rrm3Δ* background and their respective WT rates grown under the same conditions at 30˚C. Figure 7.2B shows that the point rate estimates and 95% CLs were very similar for four of the five loci except 216kb, which had a lower mutation rate for the *rrm3Δ* strains than its WT strains. Figures 7.4A and 7.4B show that, with the exception of the 53kb locus, all loci showed small (0.6-0.8) fold-decreases in the *rrm3Δ* rates compared to the WT rates. Among them, only the 0.6-fold decrease at the 216kb locus was statistically significant.

In summary, the rate of *URA3* inactivation in haploid *rrm3Δ* cells harboring the reporter construct at different locations was statistically the same for all loci except 53kb, which was higher. There was therefore little or no *cis* affect on mutation rate in the absence of Rrm3p in haploid cells for four of the five loci. When these rates were compared to their respective WT rates they were statistically indistinguishable, with the exception of 216kb, which had a small but significantly lower mutation rate in the *rrm3Δ* strains.

A

Strain		Mutation Rate (95% CL)[a]	Fold-difference between 1&2	Average Mut Rate[b]
53kb	1	2.1×10^{-5} (1.8-2.9)	1.1	2.1×10^{-5}
	2	2.0×10^{-5} (1.6-2.4)		
139kb	1	1.4×10^{-5} (1.3-1.7)	1.2	1.6×10^{-5}
	2	1.7×10^{-5} (1.4-2.1)		
216kb	1	1.1×10^{-5} (0.9-1.6)	1.0	1.1×10^{-5}
	2	1.1×10^{-5} (0.9-1.6)		
230kb	1	1.5×10^{-5} (1.2-2.6)	-	1.5×10^{-5}
	2	ND		
242kb	1	ND	-	1.1×10^{-5}
	2	1.1×10^{-5} (0.9-1.5)		

Location	Chromosomal Features
53kb	RSZ, Termination
139kb	RSZ, Termination, Ty2
216kb	Termination
230kb	Origin
242kb	None

B

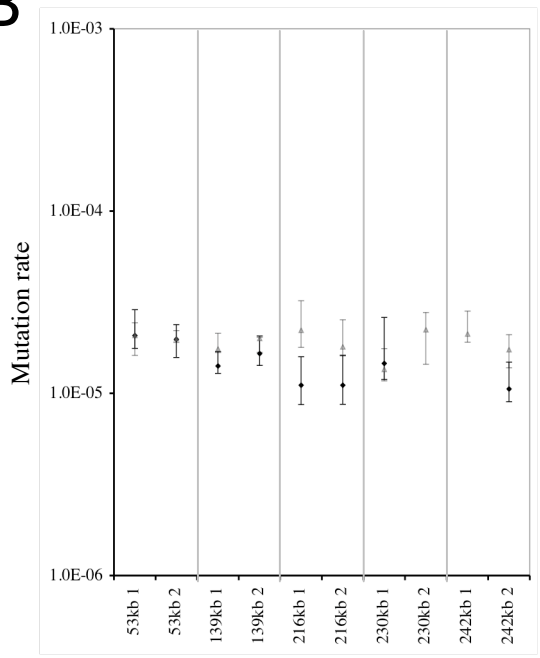

C

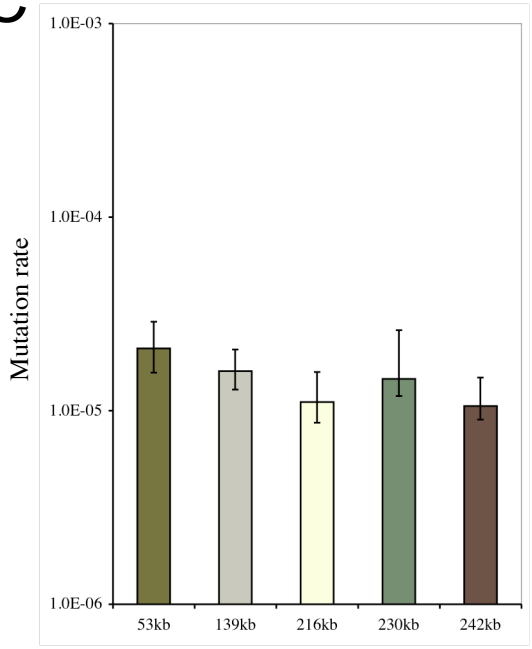

Figure 7.2. Rates of *URA3* inactivation in *rrm3Δ* haploid strains grown in YPD at 30˚C.

(A) Two independent rate measurements were done for the 53kb, 139kb and 216kb loci. The fraction of 5-FOA-resistant cells was measured in 15 independent cultures for each rate measurement. These frequencies were converted to rates using the method of the median (Lea and Coulson, 1949). [a] 95% confidence limits (CL) were calculated as described previously (Wierdl *et al*., 1996). [b] Where possible, the average mutation rates were calculated. Relevant chromosomal features at each locus are denoted on the right hand side. ND: not determined.

(B) Individual rates are plotted for *rrm3Δ* (black diamonds) and WT (grey triangles) haploid strains. Capped lines indicate 95% CLs.

(C) The average mutation rate of the two strains is plotted, where possible. The smallest and largest CL value of the two strains was used for each location. Mutation rate is given as number of events/cell/generation.

A

Location Mutation rate[a]	Normalised mutation rate
53kb 2.1 x 10^{-5}	1.9
139kb 1.6 x 10^{-5}	1.5
216kb 1.1 x 10^{-5}	1.0
230kb 1.5 x 10^{-5}	1.4
242kb 1.1 x 10^{-5}	1.0

B

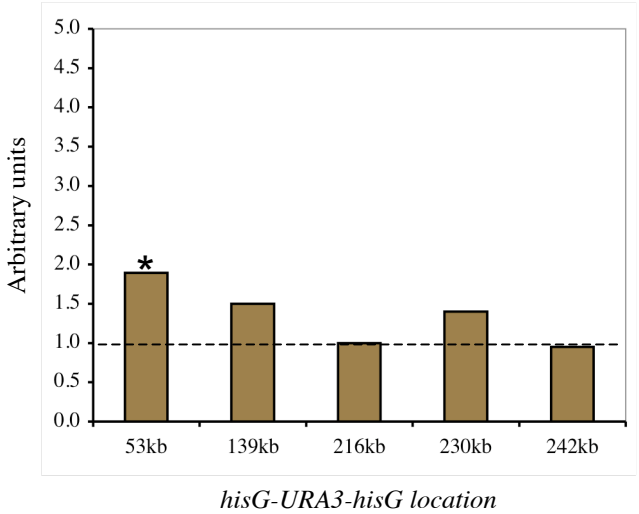

C

Location Mutation rate[a]	53kb 2.1 x 10^{-5}	139kb 1.6 x 10^{-5}	216kb 1.1 x 10^{-5}	230kb 1.5 x 10^{-5}	242kb 1.1 x 10^{-5}
53kb 2.1 x 10^{-5}		4.80 *P*<0.05	8.53 *P*<0.01	3.27 NSS	8.07 *P*<0.01
139kb 1.6 x 10^{-5}			2.13 NSS	0.60 NSS	3.27 NSS
216kb 1.1 x 10^{-5}				1.67 NSS	0.07 NSS
230kb 1.5 x 10^{-5}					1.67 NSS
242kb 1.1 x 10^{-5}					

Figure 7.3. Analysis of rates of *URA3* inactivation in *rrm3Δ* haploid strains grown in YPD at 30˚C.

(A) The average mutation rate at each locus was normalised against the lowest average rate.

(B) Normalised fold-differences from (A) are plotted. "*" denotes a significant statistical difference.

(C) Chi-square analysis: pair-wise comparison of the mutation rates at each location. Shown in each panel are the Chi square (χ^2; upper) and probability (*P*; lower) values for each pair-wise combination. *P* values of less than 0.05 were deemed significant. NSS: not statistically significant. [a] Mutation rate is given as number of events/cell/generation.

A

Construct location	Average mutation rate		Fold-difference[a] *rrm3Δ* / WT	Chi square and *P* values[b]
	rrm3Δ	WT		
53kb	2.1×10^{-5}	2.0×10^{-5}	1.0	0.00, NSS
139kb	1.6×10^{-5}	1.9×10^{-5}	0.8	2.13, NSS
216kb	1.1×10^{-5}	2.0×10^{-5}	0.6	10.80, *P*~0.001
230kb	1.5×10^{-5}	1.8×10^{-5}	0.8	0.07, NSS
242kb	1.1×10^{-5}	1.9×10^{-5}	0.6	1.67, NSS

B

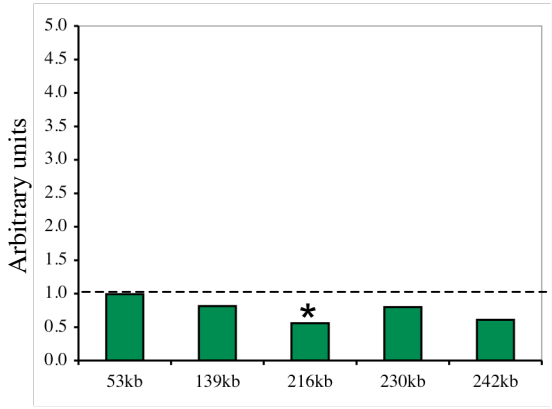

Figure 7.4. Effects of *rrm3Δ* on the rates of *URA3* inactivation compared to those in WT haploid strains grown in the same conditions (YPD at 30˚C).

(A) [a] Where possible, for each location the mutation rate of strain 1 (*rrm3Δ*) was divided by the mutation rate of strain 1 (WT). The same was done for strain 2. The fold-difference was then averaged over these two values for each locus. [b] Significant differences were calculated by χ^2 analyses, as described in the text. χ^2 values are given first, *P* values second. *P* values of less than 0.05 were deemed significant. NSS: not statistically significant.

(B) Graph showing the fold-difference in mutation rates of *rrm3Δ* over WT haploid strains for each locus. "*" denotes a significant statistical difference. Values are taken from (A).

7.2.2 Rates of URA3 inactivation in rrm3Δ diploid strains

Spot tests of diploid *rrm3Δ* strains are shown in Figure 7.5, with the parental WT and *rrm3Δ* strains lacking a *hisG-URA3-hisG* construct shown for comparison (top and bottom rows, respectively, right hand side). Growth of these strains was comparable to that of the WT strain at all temperatures, and the optimal temperature was once again at 30˚C. *rrm3Δ* diploid strains were therefore grown at 30˚C, enabling these mutation rates to be compared against both their respective WT diploid and the *rrm3Δ* haploid mutation rates.

The mutation rates of individual *rrm3Δ* diploid strains are shown in Figure 7.6. Figure 7.6A shows that little (1.0–1.1-fold) difference existed between the two independently derived strains for the three loci where the analysis was possible (confirmed by χ^2 analysis). The rates of *URA3* inactivation for the *rrm3Δ* strains (black diamonds) are shown alongside the mutation rates for the respective WT strains (grey crosses; Figure 7.6B). The average rate of *URA3* inactivation estimates for the 53kb, 216kb, 230kb and 242kb loci were very similar, ranging only from 5.3 x 10^{-5} events/cell/generation to 6.7 x 10^{-5}, as shown in Figures 7.6A and 7.6C. The 139kb locus, however, had a lower rate of 3.2 x 10^{-5} events/cell/generation. The mutation rates for all five loci were therefore normalised against the 139kb rate to assess the variation. Figure 7.7A shows that the fold-differences ranged from 1.7- to 2.1-fold. Among these, χ^2 analyses found that all four loci had a significantly higher mutation rate than the rate at the 139kb locus (Figures 7.7B and 7.7C). Pair-wise analysis was then performed to observe any difference between any of the locations. As expected by the similar rate of *URA3* inactivation estimates and overlapping 95% CL values shown in Figures 7.6B and 7.6C, the mutation rates at the 53kb, 216kb, 230kb and 242kb loci were all statistically indistinguishable from each other whilst all being significantly higher than the 139kb rate (Figure 7.7C).

The mutation rates of the *rrm3Δ* strains were then compared against the rates of their respective WT strains for each locus. The 139kb, 230kb and 242kb loci had an approximate 2-fold increase over their WT rates, whilst 53kb had a 3-fold increase and 216kb had the highest increase of almost 6-fold. Figures 7.8A and 7.8B show

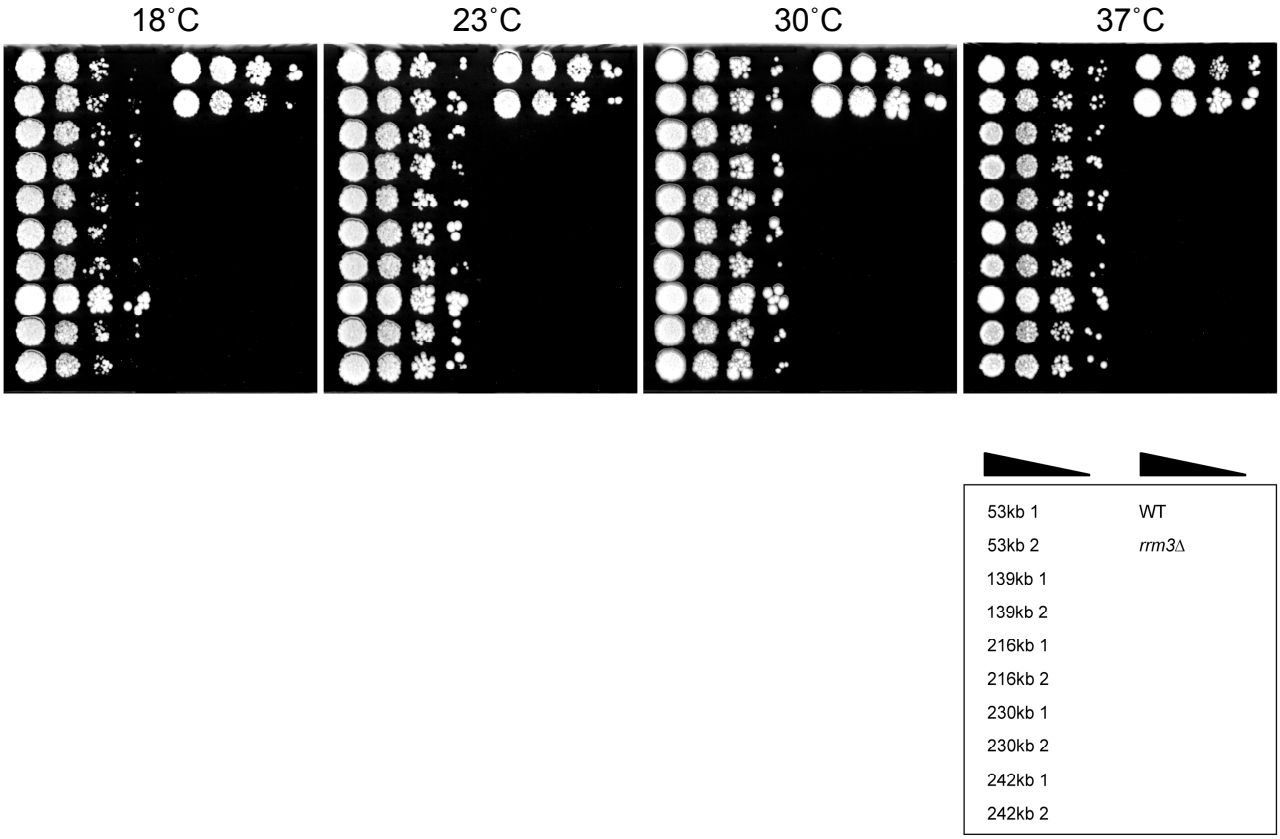

Figure 7.5. Effects of temperature on growth of *rrm3Δ* diploid strains carrying a *hisG-URA3-hisG* construct at different loci on ChrIII.

Ten-fold serial dilutions of exponentially growing cells were spotted onto YPD plates and grown at the indicated temperatures for 3-5 days. The box in the lower right indicates the strains spotted onto the plates: WT and *rrm3Δ* in this instance refer to strains lacking a *hisG-URA3-hisG* construct.

A

Strain		Mutation Rate (95% CL)[a]	Fold-difference between 1&2	Average Mut Rate[b]
53kb	1	5.2×10^{-5} (4.5-8.0)	1.0	5.3×10^{-5}
	2	5.3×10^{-5} (4.7-7.0)		
139kb	1	3.1×10^{-5} (2.3-4.1)	1.0	3.2×10^{-5}
	2	3.2×10^{-5} (2.7-4.3)		
216kb	1	6.8×10^{-5} (5.4-8.4)	1.1	6.5×10^{-5}
	2	6.2×10^{-5} (5.3-8.2)		
230kb	1	6.0×10^{-5} (5.3-7.9)	-	6.0×10^{-5}
	2	ND		
242kb	1	ND	-	6.7×10^{-5}
	2	6.7×10^{-5} (6.2-7.7)		

Location	Chromosomal Features
53kb	RSZ, Termination
139kb	RSZ, Termination, Ty2
216kb	Termination
230kb	Origin
242kb	None

B

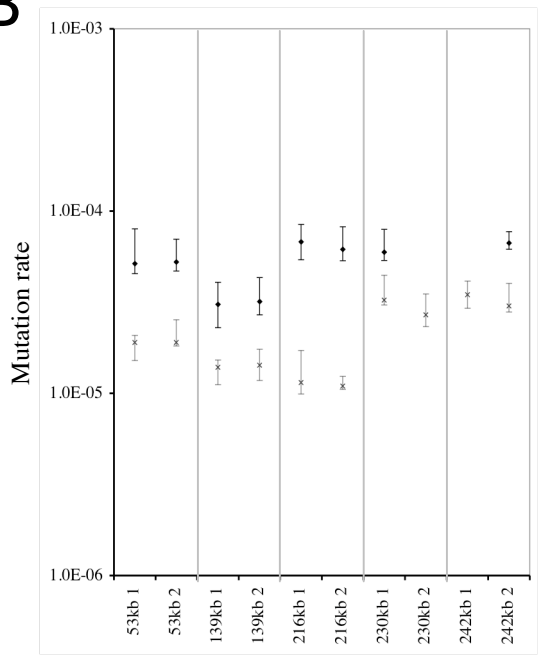

C

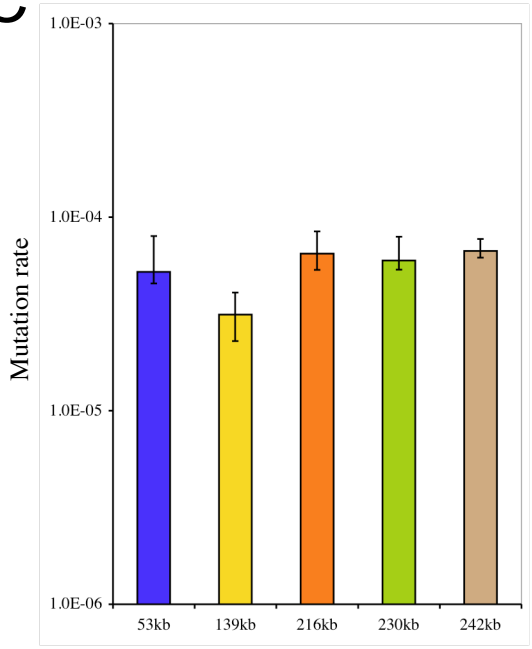

Figure 7.6. Rates of *URA3* inactivation in *rrm3Δ* diploid strains grown in YPD at 30˚C.

(A) All strains were homozygous for *rrm3*Δ and heterozygous for the *hisG-URA3-hisG* reporter construct. For each locus, except 230kb and 242kb, two independent rate measurements were done. The fraction of 5-FOA-resistant cells was measured in 15 independent cultures for each rate measurement. These frequencies were converted to rates using the method of the median (Lea and Coulson, 1949). [a] 95% confidence limits (CL) were calculated as described previously (Wierdl *et al*., 1996). [b] Where possible, the average mutation rates were calculated. Relevant chromosomal features at each locus are denoted on the right hand side. ND: not determined.

(B) Individual rates are plotted for *rrm3Δ* (black diamonds) and WT (grey crosses) diploid strains. Capped lines indicate 95% CLs.

(C) The average mutation rate of the two strains is plotted, where possible. The smallest and largest CL value of the two strains was used for each location. Mutation rate is given as number of events/cell/generation.

A

Location Mutation rate[a]	Normalised mutation rate
53kb 5.3 x 10^{-5}	1.7
139kb 3.2 x 10^{-5}	1.0
216kb 6.5 x 10^{-5}	2.0
230kb 6.0 x 10^{-5}	1.9
242kb 6.7 x 10^{-5}	2.1

B

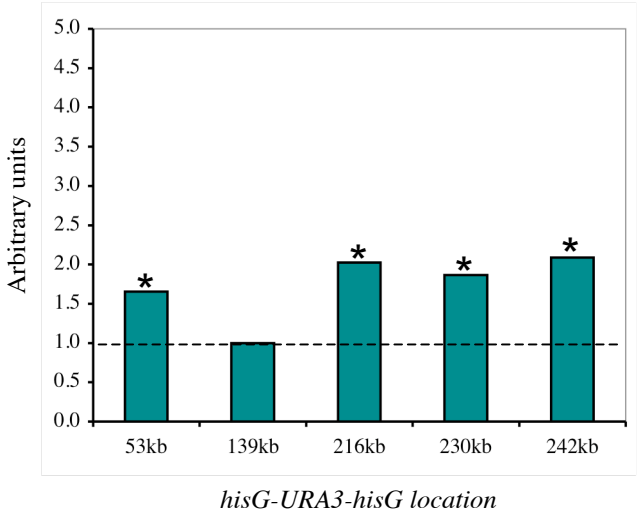

C

Location Mutation rate[a]	53kb 5.3 x 10^{-5}	139kb 3.2 x 10^{-5}	216kb 6.5 x 10^{-5}	230kb 6.0 x 10^{-5}	242kb 6.7 x 10^{-5}
53kb 5.3 x 10^{-5}		10.80 *P*~0.001	1.20 NSS	0.60 NSS	1.67 NSS
139kb 3.2 x 10^{-5}			19.20 *P*<0.001	5.40 *P*<0.05	11.27 *P*<0.001
216kb 6.5 x 10^{-5}				0.60 NSS	1.67 NSS
230kb 6.0 x 10^{-5}					1.67 NSS
242kb 6.7 x 10^{-5}					

Figure 7.7. Analysis of rates of *URA3* inactivation in *rrm3Δ* diploid strains grown in YPD at 30˚C.

(A) The average mutation rate at each locus was normalised against the lowest average rate. [a] Mutation rate is given as number of events/cell/generation.

(B) Normalised fold-differences from (A) are plotted. "*" denotes a significant statistical difference.

(C) Chi-square analysis: pair-wise comparison of the mutation rates at each location. Shown in each panel are the Chi square (χ^2; upper) and probability (*P*; lower) values for each pair-wise combination. *P* values of less than 0.05 were deemed significant. NSS: not statistically significant.

A

Construct location	Average mutation rate		Fold-difference[a] *rrm3Δ* / WT	Chi square and *P* values[b]
	rrm3Δ	WT		
53kb	5.3×10^{-5}	1.9×10^{-5}	2.8	26.13, $P<0.001$
139kb	3.2×10^{-5}	1.4×10^{-5}	2.2	16.13, $P<0.001$
216kb	6.5×10^{-5}	1.1×10^{-5}	5.8	26.13, $P<0.001$
230kb	6.0×10^{-5}	3.0×10^{-5}	1.8	5.40, $P<0.05$
242kb	6.7×10^{-5}	3.2×10^{-5}	2.2	15.00, $P<0.001$

B

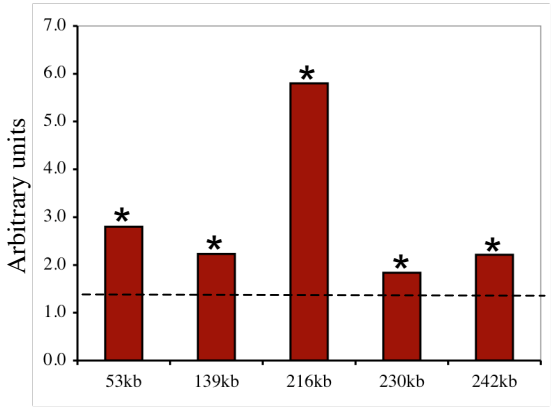

Figure 7.8. Effects of *rrm3Δ* on the rates of *URA3* inactivation compared to those of WT diploid strains, grown in YPD at 30˚C.

(A) [a] For each location the mutation rate of strain 1 (*rrm3Δ*) was divided by the mutation rate of strain 1 (WT). The same was done for strain 2. The fold-difference was then averaged over these two values for each locus. [b] Significant differences were calculated by χ^2 analyses, as described in the text. χ^2 values are given first, *P* values second. *P* values of less than 0.05 were deemed significant. NSS: not statistically significant.

(B) Graph showing the fold-difference in mutation rates of *rrm3Δ* over WT diploid strains for each locus. "*" denotes a significant statistical difference. Values are taken from (A).

that these fold-increases of the mutation rates in *rrm3Δ* strains over WT strains were significant for all five loci, as judged by χ^2 analysis.

In conclusion, the mutation rates of every locus were statistically indistinguishable from each other with the exception of 139kb, which was significantly lower. Despite the lower mutation rate for the 139kb locus, it was found that all of the rates for *rrm3Δ* strains increased significantly over the rates observed for their respective diploid WT strains.

7.2.3 Effects of ploidy on rates of URA3 inactivation in rrm3Δ strains

Finally, the mutation rates of the *rrm3Δ* haploid and *rrm3Δ* diploid strains were compared to assess the effects of ploidy. Figure 7.9A shows the results for individual diploid (black diamonds) and haploid (grey diamonds) *rrm3Δ* strains. At each locus the mutation rate estimates were increased in the diploid strains, and no overlap was present between the 95% CLs. The average fold-increase of diploid over haploid *rrm3Δ* mutation rates is shown in Figure 7.9B; specific values are shown in 7.9C. These values varied from 2.1- to 6.3-fold. The 216kb (replication termination) and 242kb (no features) loci both had a ~6-fold increase, the 230kb locus had a 4-fold increase whilst the two locations within RSZs had the least increases of 2.6- and 2.1-fold. All of these fold-increases were statistically significant, as judged by χ^2 analyses (P<0.001 for all five loci).

7.2.4 Growth analysis of haploid and diploid rrm3Δ strains

Earlier studies have shown that *rrm3* strains have a marked delay in replication of all chromosomes (Azvolinsky *et al*., 2006). The authors did not, however, examine whether such delay in genome duplication would be reflected in the growth rate. To address this issue, the final cell count of the *rrm3Δ* strains at the completion of the specified incubation period was compared to that of their respective WT strains grown under the same growth conditions (non-selective media at 30˚C). Table 7.1 shows the individual cell counts and average cell counts of haploid strains for each locus. Student's t-test was used to compare the cell counts of the WT and *rrm3Δ*

A

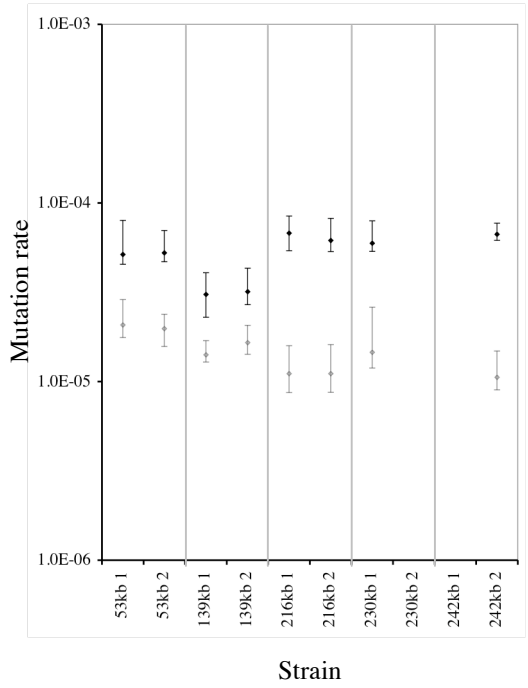

B

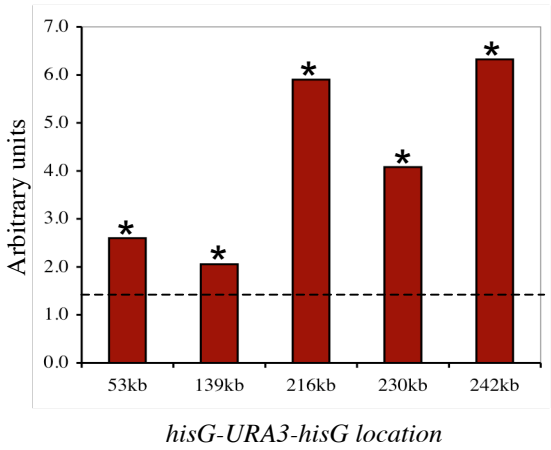

C

Construct location	Average mutation rate		Fold-difference[a] Diploid / Haploid	Chi square and *P* values[b]
	Diploid	Haploid		
53kb	5.3 x 10^{-5}	2.1 x 10^{-5}	2.6	22.53, $P<0.001$
139kb	3.2 x 10^{-5}	1.6 x 10^{-5}	2.1	13.33, $P<0.001$
216kb	6.5 x 10^{-5}	1.1 x 10^{-5}	5.9	26.13, $P<0.001$
230kb	6.0 x 10^{-5}	1.5 x 10^{-5}	4.1	11.27, $P<0.001$
242kb	6.7 x 10^{-5}	1.1 x 10^{-5}	6.3	15.00, $P<0.001$

Figure 7.9. Effects of ploidy on the rates of *URA3* inactivation in *rrm3Δ* strains grown in YPD at 30˚C.

(A) Individual mutation rates of WT haploid (grey diamonds) and diploid (black diamonds) strains.

(B) Graph showing the fold-difference in mutation rates of diploid over haploid *rrm3Δ* strains for each locus. "*" denotes a significant statistical difference. Values are taken from (C).

(C) [a] Where possible, for each location the mutation rate of strain 1 (diploid) was divided by the mutation rate of strain 1 (haploid). The same was done for strain 2. The fold-difference was then averaged over these two values for each locus. [b] Significant differences were calculated by χ^2 analyses, as described in the text. χ^2 values are given first, *P* values second. *P* values of less than 0.05 were deemed significant. NSS: not statistically significant.

cultures; a *P* value of 0.05 was judged significant. No difference in the cell counts were seen for the 53kb (RSZ, termination), 139kb (RSZ, termination, Ty2) and 230kb (origin) loci. Surprisingly, however, a higher cell count was seen in the *rrm3Δ* strains for the 216kb (termination) and 242kb (no features) loci.

The cell counts of the diploid *rrm3Δ* strains were also compared to their respective WT cell counts. A significantly lower cell count was seen for all five loci ($P<0.01$) in the *rrm3Δ* strains, as shown in Table 7.2.

The diploid *rrm3Δ* cell counts were also compared to their respective haploid *rrm3Δ* counts. The cell counts were significantly lower for the 53kb and 216kb loci in the diploid *rrm3Δ* strains. In contrast, the cell counts of the 139kb, 230kb and 242kb *rrm3Δ* loci were similar in both the diploid and haploid strains. The 139kb locus, for instance, had a haploid *rrm3Δ* cell count of 104.3 ± 13.5, and for the diploids, 101.2 ± 25.4. Student's t-test analysis was applied, and showed that no statistical difference existed between the haploid and diploid cell counts for the 139kb, 230kb and 242kb loci, but was significantly lower for the 53kb and 216kb loci ($P<0.001$; Table 7.2).

7.3 Discussion

The rates of *URA3* inactivation found in the haploid *rrm3Δ* strains ranged from 1.1 – 2.1 x 10^{-5} events/cell/generation. This is comparable to published recombination rates of 1.5 x 10^{-5} events/cell/generation found in a tRNA-rich 184-kb region on ChrVII by Ivessa and colleagues (2003). Whereas that study found a small but significant increase in interchromosomal recombination in *rrm3Δ* cells compared to WT controls (3.7-fold; $P<0.05$), the mutation rates found in this study were not significantly different from the WT rates tested earlier in the thesis (Chapter 4). The 216kb locus (termination) even had a small but significant decrease in the mutation rates of the *rrm3Δ* strains compared to their respective WT strains. As the nature of the mutation events have not yet been clarified, it cannot reliably be proposed that intrachromosomal recombination between the two *hisG* repeats in these strains, rather than interchromosomal recombination in Ivessa's, are the reason for the difference between the two sets of results.

Table 7.1. Growth analysis of WT and *rrm3*Δ strains, grown under non-selective conditions at 30˚C.

Strain		HAPLOIDS				
		WT		*rrm3Δ*		
		Cell count[a]	Av Cell count[b]	Cell count[a]	Av Cell count[b]	*P*[c]
53kb	1	126.3 ± 14.9	124.7 ± 14.8	126.5 ± 12.7	125.3 ± 11.7	0.87
	2	123.1 ± 15.1		124.1 ± 11.0		
139kb	1	77.5 ± 128.7	103.1 ± 33.7	103.5 ± 11.6	104.3 ± 13.5	0.86
	2	128.7 ± 27.2		105.1 ± 15.5		
216kb	1	90.3 ± 11.5	89.6 ± 14.2	131.5 ± 30.7	141.6 ± 29.2	<0.001
	2	88.8 ± 16.8		151.8 ± 24.5		
230kb	1	193.9 ± 21.4	140.9 ± 57.4	121.8 ± 14.0	124.8 ± 13.6	0.14
	2	87.9 ± 19.0		127.9 ± 12.9		
242kb	1	81.7 ± 13.2	80.3 ± 12.1	103.7 ± 12.9	102.3 ± 15.0	<0.001
	2	79.0 ± 11.2		100.9 ± 17.2		

Strain		DIPLOIDS				
		WT		*rrm3Δ*		
		Cell count[a]	Av Cell count[b]	Cell count[a]	Av Cell count[b]	*P*[c]
53kb	1	136.0 ± 11.8	144.3 ± 15.0	81.8 ± 10.4	80.7 ± 9.8	<0.001
	2	152.7 ± 13.3		79.6 ± 9.3		
139kb	1	193.3 ± 29.0	175.0 ± 35.0	95.1 ± 20.5	101.2 ± 25.4	<0.001
	2	156.7 ± 31.4		107.2 ± 28.9		
216kb	1	197.9 ± 30.9	199.9 ± 25.2	115.4 ± 15.3	107.5 ± 15.8	<0.001
	2	201.8 ± 18.8		99.5 ± 12.0		
230kb	1	140.2 ± 12.2	149.7 ± 18.3	97.5 ± 15.0	128.9 ± 35.2	<0.001
	2	159.3 ± 18.7		160.3 ± 15.2		
242kb	1	153.4 ± 19.4	158.6 ± 16.7	107.0 ± 17.4	106.9 ± 16.6	<0.001
	2	163.8 ± 11.9		106.9 ± 16.4		

[a] Cell counts are made from serial dilutions of the 15 cultures used per strain, and plated onto non-selective media.

[b] All cell counts from strains 1 and 2 were pooled and the average cell count taken from all 30 cultures, with the standard deviation given as ± values.

[c] *P* values represent the probability that the average cell count from the WT strains are the same as the cell count of the *rrm3Δ* strains, as determined by Student's t-test. When the *P* values differed between strains 1 and 2 for any condition (for instance, between strains 1 and 2 for the *rrm3Δ* 216kb haploids), the cell count of strain 1 (WT) was compared to the cell count of strain 1 (*rrm3Δ*) and a t-test performed independently from that of strain 2. In all cases, the same result was achieved as when the average cell count was used. *P* values of 0.05 were deemed significant.

Table 7.2. Cell count comparison of haploid and diploid *rrm3Δ* strains.

Strain		*rrm3Δ*				
		Haploid		Diploid		
		Cell count[a]	Av Cell count[b]	Cell count[a]	Av Cell count[b]	*P*[c]
53kb	1	126.5 ± 12.7	125.3 ± 11.7	81.8 ± 10.4	80.7 ± 9.8	<0.001
	2	124.1 ± 11.0		79.6 ± 9.3		
139kb	1	103.5 ± 11.6	104.3 ± 13.5	95.1 ± 20.5	101.2 ± 25.4	0.56
	2	105.1 ± 15.5		107.2 ± 28.9		
216kb	1	131.5 ± 30.7	141.6 ± 29.2	115.4 ± 15.3	107.5 ± 15.8	<0.001
	2	151.8 ± 24.5		99.5 ± 12.0		
230kb	1	121.8 ± 14.0	124.8 ± 13.6	97.5 ± 15.0	128.9 ± 35.2	0.56
	2	127.9 ± 12.9		160.3 ± 15.2		
242kb	1	103.7 ± 12.9	102.3 ± 15.0	107.0 ± 17.4	106.9 ± 16.6	0.27
	2	100.9 ± 17.2		106.9 ± 16.4		

[a] Cell counts were made from serial dilutions (5 x 10^6) of the 15 cultures used per strain, and plated onto non-selective media.

[b] All cell counts from strains 1 and 2 were pooled and the average cell count taken from all 30 cultures, with the standard deviation given as ± values.

[c] *P* values represent the probability that the average cell count from the WT strains are the same as the cell count of the *rrm3Δ* strains, as determined by Student's t-test. When the *P* values differed between strains 1 and 2 for any condition (for instance, between strains 1 and 2 for the *rrm3Δ* 216kb haploids), the cell count of strain 1 (WT) was compared to the cell count of strain 1 (*rrm3Δ*) and a t-test performed independently from that of strain 2. In all cases, the same result was achieved as when the average cell count was used. *P* values of 0.05 were deemed significant.

In summary, in haploid cells *rrm3Δ* had no effect on the mutation rate compared to the rate in WT cells. No *trans* effect was therefore seen in the *rrm3Δ* haploid strains. Of note, however, was that the rate of *URA3* inactivation at the 53kb locus was significantly higher than the rates at the other four loci; there was therefore a *cis* effect in these strains. In diploid strains an entirely different result was seen. The rates of *URA3* inactivation increased ~6-fold for the 216kb locus and ~2-3 fold for the other four loci in relation to the WT strains. These fold-increases were all statistically significant, having probability values of less than 0.05. Little *cis* effect was seen, however, as all loci had statistically the same mutation rate with the exception of the 139kb locus (RSZ, termination, Ty2), which was significantly lower. This was interesting since Ty1 elements are Rrm3p-dependent sites, and as such a greater mutation rate may have been predicted for the 139kb locus compared to the other four in the *rrm3Δ* strains. An earlier study reported, however, that retrotransposition is largely abolished in diploid strains (Errede *et al.*, 1980; Company and Errede, 1987).

Lack of Rrm3p therefore increased the mutation rate significantly at all five loci in diploid strains, but once again little or no *cis* effect was seen. This was a surprising result, since, with the exception of the 53kb (and possibly the 139kb) locus, none of the other loci are near known Rrm3p-dependent sites. Although it can be argued that a mutation "'hotspot" (in the form of the *hisG-URA3-hisG* construct) has been introduced at each locus (and therefore a higher mutation rate would be expected) since this was not found in haploid *rrm3Δ* strains, ploidy had a significant effect on the mutation rate. One reason for this could be chromosome inactivation. As Ivessa *et al*. (2003) found, however, the rate of chromosome loss in a haploid *rrm3Δ* strain containing two copies of ChrVII (Schulz and Zakian, 1994) is not significantly higher than in a corresponding WT strain. Possible reasons for the higher mutation rate seen in *rrm3Δ* diploid strains is discussed in more detail in Chapter 10.

Past studies have shown a marked delay in replication of all yeast chromosomes, even in regions where no known Rrm3p-dependent sites exist. The final cell counts of the haploid and diploid *rrm3Δ* strains following non-selective growth were therefore analysed to see whether such delay in genome duplication might be

reflected in the final cell count. Further work is needed to confirm the potential effects of *rrm3Δ*, ploidy, and location of a reporter construct insertion on growth rates, however. The correct analyses will require FACS of appropriate strains to directly assess the length of genome duplication and the accurate measurement of doubling-time based on multiple cell counts taken during log phase of the growth.

Chapter 8.

Topoisomerase II

8.1 Introduction

As mentioned in Introduction, the initial interest in Top2p was due to work in my lab finding that inactivation of Top2p suppressed DSB formation at RSZs in a *mec1-ts top2-ts* double mutant, raising the possibility that chromosome breakage at RSZs are catalysed by Top2p. Also, a study by Bermejo *et al*. (2007) found that Top2p localises to several locations within ChrIII, including at *ARS315*. As two of these localization signals coincided with the 53kb (RSZ, termination) and 230kb (origin) loci, the rate of *URA3* inactivation at these loci were of particular interest.

The effects of transiently inactivating Top2p were therefore assessed in strains containing the *hisG-URA3-hisG* construct.

8.2 Results

8.2.1 Haploid top2-1 strains

8.2.1.1 Preparation for analysis of top2-1 haploid strains; kinetics of commitment to inviability at 37˚C

Strains lacking a complete deletion of the *TOP2* gene could not be used to assess the rates of *URA3* inactivation since it is an essential gene. To circumvent this problem, a temperature-sensitive allele, *top2-1*, was chosen that replaced the endogenous *TOP2* allele. The *top2-1* mutation was originally identified by screening a collection of temperature sensitive lethal strains for temperature sensitive topoisomerase II activity (DiNardo *et al*., 1984). Yeast strains carrying the *top2-1* allele have normal topoisomerase II activity at 25˚C, greatly reduced enzyme activity at 30˚C, and have less than 10% of WT activity at 36˚C (Nitiss *et al*., 1993). *top2-1* strains were created by crossing WT haploids containing the *hisG-URA3-hisG* construct at

specific locations with JDCY248, a strain that has the endogenous *TOP2* allele replaced with *top2-1*. The resulting diploids were sporulated, dissected and *URA3* prototroph spores that co-segregated with a temperature-sensitive phenotype were selected. Crossing these haploid strains with JDCY248 once again and selecting temperature-sensitive *URA3* diploids made diploids homozygous for the *top2-1* allele, but heterozygous for the reporter construct. Strains were checked by replica plating onto suitable selection plates, and by cell morphology.

Spot tests of haploid *top2-1* strains containing the *hisG-URA3-hisG* reporter construct grown on YPD at various temperatures are shown in Figure 8.1. WT and *top2-1* strains lacking the construct are shown as a comparison (first and second row, respectively, right hand side). With the exception of the 216kb strains, all of the *URA3* strains grew similarly to the *top2-1* strain lacking a reporter construct at all four temperatures. At 37˚C all *top2-1* strains died, as expected. The 216kb strains were least affected at 30˚C yet grew very poorly at 18˚C and 23˚C. The lack of growth at these temperatures was not due to cell death, as cells grew after the plates were left at room temperature (approximately 26˚C) for 2-3 days (Figure 8.1). The *hisG-URA3-hisG* construct did not therefore affect the growth of *top2-1* strains compared to a congenic *top2-1* strain lacking a reporter construct.

As the *top2-1* strains containing a *hisG-URA3-hisG* construct strains were temperature-sensitive, the standard fluctuation analysis growth conditions used in earlier chapters could not be used. This is because the *top2-1* protein is degraded only at temperatures of 36˚C and above (Nitiss *et al*., 1993). Growing these strains at 30˚C and recording the mutation rate would therefore not be a valid representation of the mutation rate in the absence of Top2 function, as functional protein would still be present within a small proportion the cells (DiNardo *et al*., 1984). Another earlier study reported that *top2-1* strains are able to complete the first round of S-phase with similar kinetics to a control strain, grown at the non-permissive temperature (Bermejo *et al*., 2007). After the completion of the first cell cycle, however, *top2-1* strains accumulate chromosomal abnormalities (such as the formation of gaps and breaks within DNA) that are the result of errors caused in the first round of DNA replication in the absence of functional Top2p. As these errors would accumulate

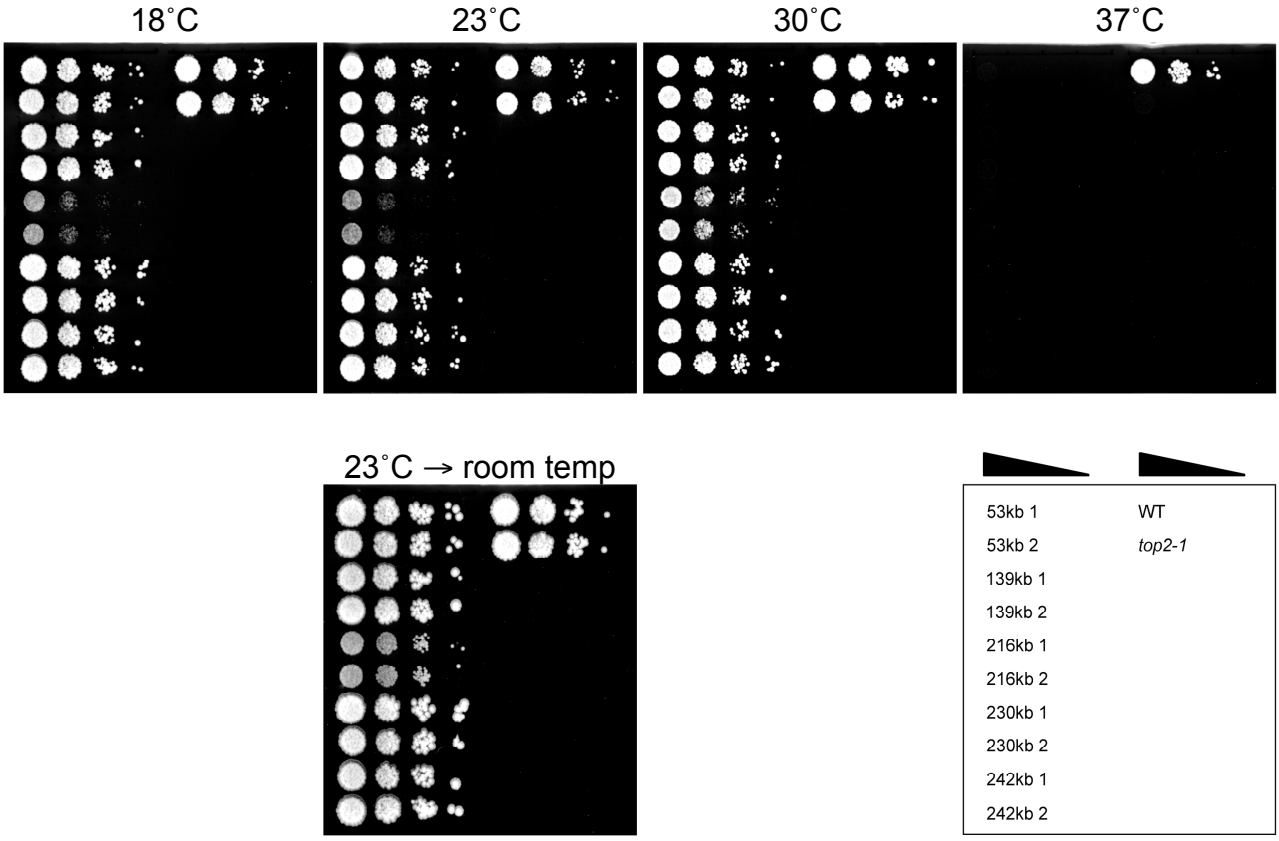

Figure 8.1. Effects of temperature on growth of *top2-1* haploid strains carrying a *hisG-URA3-hisG* construct at different loci on ChrIII.

Ten-fold serial dilutions of exponentially growing cells were spotted onto YPD plates and grown at the indicated temperatures for 3-5 days. The box in the lower right indicates the strains spotted onto the plates: WT and *top2-1* in this instance refer to strains lacking a *hisG-URA3-hisG* construct. Lack of growth at 18˚C and 23˚C for the 216kb strains was not due to cell death, as cells grew after these plates were left at room temperature (~26˚C) for a further 2-3 days (lower panel).

over time, resulting in cell death, a situation was therefore required where, ideally, strains were incubated at 37˚C to inactivate the protein for as long a time as possible without losing viability. Otherwise certain fractions of either 5-FOA-resistant or non-resistant cells could be lost due to cell death resulting from Top2p inactivation, and thus the observed mutation rate may not accurately reflect the actual mutation rate.

Therefore, before the rates of *URA3* loss could be measured in *top2-1* strains, the viability of a *top2-1* strain lacking a *hisG-URA3-hisG* construct was tested at the non-permissive temperature. In order to do this a *top2-1* haploid (JDCY248) was incubated using the same method as *mec1-40* strains tested for the kinetics of commitment to inviability (Chapter 6, and below in Figure 8.2). It was known both from previous work in the lab and Bermejo *et al.'s* (2007) work that *top2-1* strains lose viability very quickly at the non-permissive temperature. Aliquots were therefore taken every 30 minutes after cultures had been shifted to 37˚C. As before, the aliquots were plated onto YPD agar plates and incubated at 23˚C to observe the cell survival. This procedure was done in triplicate; the result for the haploid *top2-1* strain is shown in Figure 8.2B. Viability of this strain increased to a maximum of ~160% the original cell count, then rapidly decreased over the next 2.5h to 25%. As with the *mec1-40* strains used in Chapter 6, a condition for stressing *top2-1* strains as long as possible without inducing cell death was sought. For this purpose, *top2-1* haploid strains were grown at 37˚C for 90 minutes. Specific incubation times are detailed in Figure 8.3.

8.2.1.2 Rates of URA3 inactivation in WT haploid strains, using top2-1 growth conditions

Before the rate of *URA3* inactivation was tested in the *top2-1* strains, WT haploid strains containing the reporter construct (used in Chapter 4) were tested using the *top2-1* incubation times detailed in Figure 8.3. This would serve as a more appropriate control to ascertain the specific effects of *top2-1* on the mutation rate in haploids, since the growth conditions were now different from the WT strains grown either at 30˚C or using the *mec1-40* incubation times in Chapter 6. The results of the

A

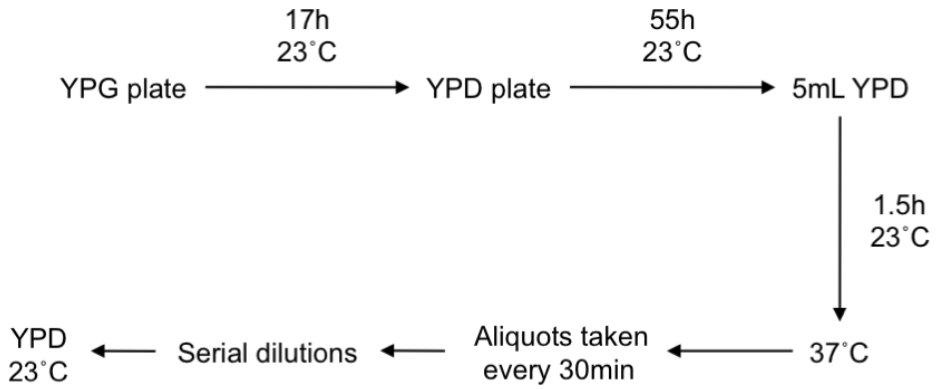

B

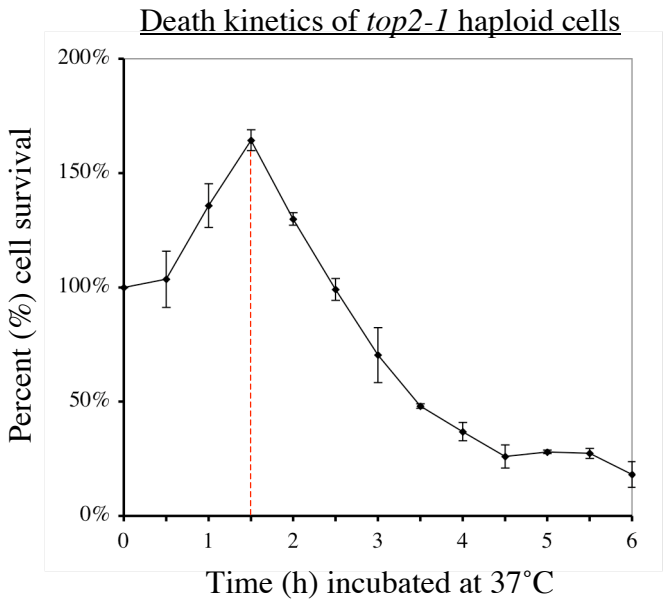

Figure 8.2. Testing haploid *top2-1* strains for fluctuation analysis incubation times: kinetics of commitment to inviability.

(A) Flow chart detailing incubation times used to test a *top2-1* haploid (JDCY248) for death kinetics. Cells were patched onto YPG directly from -80˚C glycerol stocks. After 17h at 23˚C, cells were streaked for single colonies on non-selective (YPD) media; colonies had reached a suitable size after 55h incubation at 23˚C. Single colonies were then used to inoculate three different flasks containing 5mL liquid YPD, which were incubated at 23˚C. After 1.5h (t=0) the flasks were shifted to the non-permissive temperature (37˚C) and aliquots taken every 30 minutes. These were plated onto non-selective (YPD) agar plates and incubated at the permissive temperature (23˚C) to allow cells to recover. After 3-4 days colonies were counted and compared to the t=0 count to determine the percentage cell death at each time point.

(B) Result of death kinetics analysis used in (A). Error bars indicate the standard deviation between three independent cultures.

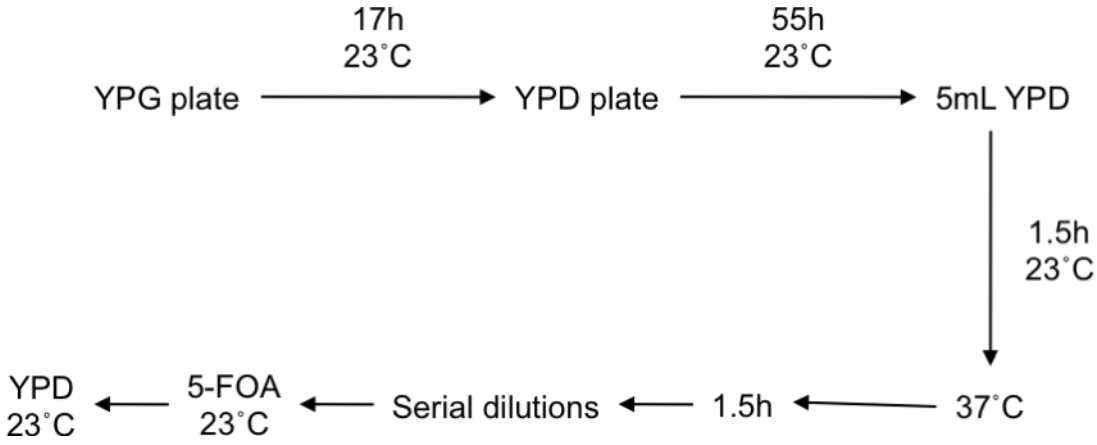

Figure 8.3. Incubation times used for fluctuation analysis of haploid *top2-1* strains.

Based on the results of the death kinetics in Figure 8.2, haploid *top2-1* strains containing the *hisG-URA3-hisG* construct were incubated at these specific times for fluctuation analysis.

WT strains grown using these conditions are shown in Figure 8.4B, with mutation rates of the same strains grown at 30˚C shown as a comparison. Specific values are given in Figure 8.4A. The 216kb strains were not tested due to their slow growth phenotype at 23˚C. For the 53kb and 139kb loci, for which data was available, no difference in mutation rate was observed between the two independently derived strains (χ^2 analysis). In Figure 8.4C the mutation rates, when applicable, were averaged for each location. The lowest value was 2.1 x 10^{-5} events/cell/generation cycle for 53kb (RSZ, termination), whilst the highest was 3.1 x 10^{-5} for 139kb (RSZ, termination, Ty2).

To assess the variation in mutation rate amongst the different loci, the average rates were normalised against the lowest rate, in this case, the rate at the 53kb locus. These values ranged only from 1.3- to 1.5-fold, as shown in Figure 8.5A. It was found by χ^2 analyses, however, that the rate of *URA3* inactivation at the 139kb locus was significantly higher than the rate at 53kb (Figure 8.5B). This analysis was extended; all mutation rates were compared by pair-wise analysis, as shown in Figure 8.5C. The only significant difference found by this analysis was between the mutation rates at the 53kb and 139kb loci; all other rates were statistically indistinguishable from each other. This was expected from the similar point rate estimates and overlapping 95% CL values shown in Figures 8.4A and 8.4B.

The mutation rates of the WT strains grown under *top2-1* conditions were then compared to the rates of the respective WT strains grown at 30˚C for each of the four locations. Figure 8.4B show that the point rate estimates were higher for the WT (*top2-1*) than the WT (30˚C) strains, consistent with the observed mutagenic effects of high temperature (Chapter 5). Note however, that there was a certain degree of overlap between the 95% CL values. The greatest fold-increase for the WT strains grown under these two conditions was only 1.6-fold, for 139kb, whilst the least was 1.1-fold for 53kb. Chi square analysis revealed that none of these fold-differences were statistically significant, as shown in Figures 8.6A and 8.6B.

In summary, the mutation rates of WT strains grown using the *top2-1* conditions were the same regardless of the *hisG-URA3-hisG* location within ChrIII, with the

A

Strain		Mutation Rate (95% CL)[a]	Fold-difference between 1&2	Average Mut Rate[b]
53kb	1	2.2×10^{-5} (1.8-3.1)	1.2	2.1×10^{-5}
	2	1.9×10^{-5} (1.7-2.5)		
139kb	1	2.8×10^{-5} (2.0-3.9)	1.2	3.1×10^{-5}
	2	3.4×10^{-5} (1.8-5.4)		
216kb	1	-	-	-
	2	-		
230kb	1	2.6×10^{-5} (1.9-3.1)	-	2.6×10^{-5}
	2	ND		
242kb	1	ND	-	2.9×10^{-5}
	2	2.9×10^{-5} (2.3-3.6)		

Location	Chromosomal Features
53kb	RSZ, Termination
139kb	RSZ, Termination, Ty2
216kb	Termination
230kb	Origin
242kb	None

B

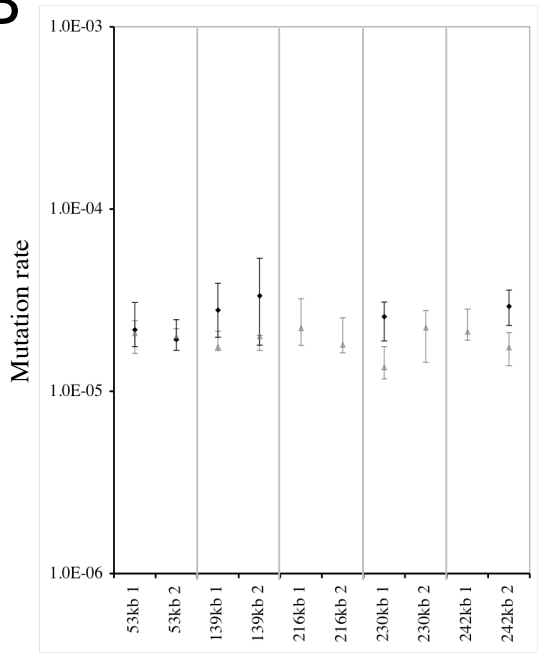

C

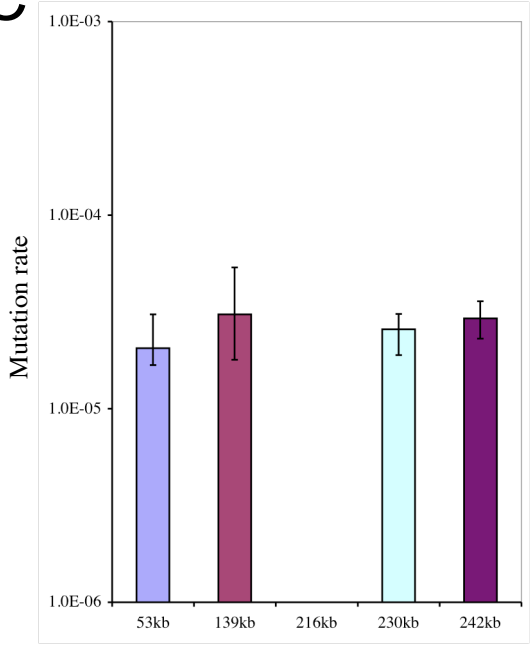

Figure 8.4. Rates of *URA3* inactivation in WT haploid strains grown using *top2-1* conditions.

(A) Two independent rate measurements were done for the 53kb and 139kb loci. The fraction of 5-FOA-resistant cells was measured in 15 independent cultures for each rate measurement. These frequencies were converted to rates using the method of the median (Lea and Coulson, 1949). [a] 95% confidence limits (CL) were calculated as described previously (Wierdl *et al*., 1996). [b] Where possible, the average mutation rates were calculated. Relevant chromosomal features at each locus are denoted on the right hand side. ND: not determined.

(B) Individual rates are plotted for WT [*top2-1*] (black diamonds) and WT [30˚C] (grey triangles) haploid strains. Capped lines indicate 95% CLs.

(C) The average mutation rate of the two strains is plotted, where possible. The smallest and largest CL value of the two strains was used for each location. Mutation rate is given as number of events/cell/generation.

A

Location Mutation rate[a]	Normalised mutation rate
53kb 2.1 x 10^{-5}	1.0
139kb 3.1 x 10^{-5}	1.5
216kb -	-
230kb 2.6 x 10^{-5}	1.3
242kb 2.9 x 10^{-5}	1.4

B

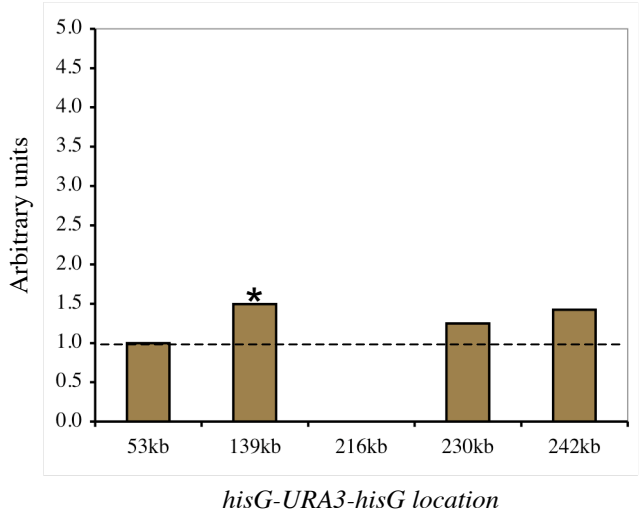

C

Location Mutation rate[a]	53kb 2.1 x 10^{-5}	139kb 3.1 x 10^{-5}	216kb NSS	230kb 2.6 x 10^{-5}	242kb 2.9 x 10^{-5}
53kb 2.1 x 10^{-5}		4.80 $P<0.05$		1.67 NSS	1.67 NSS
139kb 3.1 x 10^{-5}				0.07 NSS	0.60 NSS
216kb NSS					
230kb 2.6 x 10^{-5}					0.60 NSS
242kb 2.9 x 10^{-5}					

Figure 8.5. Analysis of rates of *URA3* inactivation in WT haploid strains grown using *top2-1* conditions.

(A) The average mutation rate at each locus was normalised against the lowest average rate.

(B) Normalised fold-differences from (A) are plotted. "*" denotes a significant statistical difference.

(C) Chi-square analysis: pair-wise comparison of the mutation rates at each location. Shown in each panel are the Chi square (χ^2; upper) and probability (*P*; lower) values for each pair-wise combination. *P* values of less than 0.05 were deemed significant. NSS: not statistically significant. [a] Mutation rate is given as number of events/cell/generation.

A

Construct location	Average mutation rate		Fold-difference[a] WT (*top2-1*) / WT (30°C)	Chi square and *P* values[b]
	WT (*top2-1*)	WT (30°C)		
53kb	2.1×10^{-5}	2.0×10^{-5}	1.1	0.60, NSS
139kb	3.1×10^{-5}	1.9×10^{-5}	1.6	0.13, NSS
216kb	-	2.0×10^{-5}	-	-
230kb	2.6×10^{-5}	1.8×10^{-5}	1.4	0.60, NSS
242kb	2.9×10^{-5}	1.9×10^{-5}	1.5	0.60, NSS

B

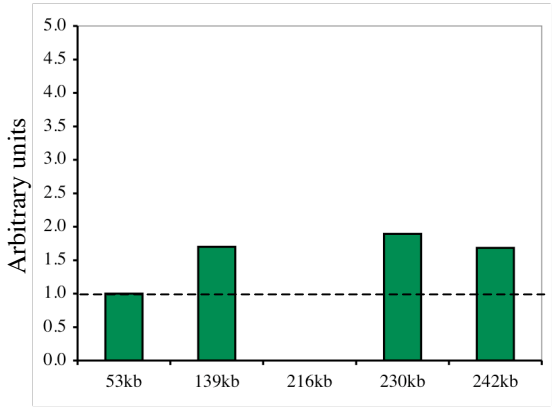

Figure 8.6. Effects of *top2-1* growth conditions on the rates of *URA3* inactivation compared to optimal conditions (YPD at 30˚C), in WT haploid strains.

(A) [a] Where possible, for each location the mutation rate of strain 1 (WT [*top2-1*]) was divided by the mutation rate of strain 1 (WT [30˚C]). The same was done for strain 2. The fold-difference was then averaged over these two values for each locus. [b] Significant differences were calculated by χ^2 analyses, as described in the text. χ^2 values are given first, *P* values second. *P* values of less than 0.05 were deemed significant. NSS: not statistically significant.

(B) Graph showing the fold-difference in mutation rates of WT haploid strains grown using *top2-1* conditions over optimal conditions (YPD at 30˚C) for each locus. Values are taken from (A).

exception being between the rates at the 53kb and 139kb loci. There was therefore one *cis* effect in mutation rates between the different loci when strains were grown using the established *top2-1* conditions. When the mutation rates of the four loci were compared to their respective rates when grown at a constant 30°C, they were also found to be statistically indistinguishable from each other. The difference in incubation temperatures between those used here and in Chapter 4 therefore had little effect on the mutation rate in haploid WT strains.

8.2.1.3 Rates of URA3 inactivation in top2-1 haploid strains

The mutation rates of haploid *top2-1* strains were tested at the four loci studied in the above section. Figure 8.7B shows the individual mutation rates of *top2-1* (black triangle) and WT (grey triangle) strains grown using the *top2-1* conditions; specific values are given in Figure 8.7A. No difference in mutation rate existed between the two independently derived transformants (χ^2 analysis). These mutation rates were averaged for each location, as shown in Figures 8.7A and 8.7C. The two loci within RSZs, 53kb and 139kb, had the highest mutation rates of 4.0- and 3.5 x 10^{-5} events/cell/generation, respectively, whilst 230kb and 242kb had slightly lower mutation rates of 2.2- and 3.0 x 10^{-5} events/cell/generation. The mutation rates were normalised against the lowest value (230kb), and varied from 1.3- to 1.8-fold (Figures 8.8A and 8.8B). It was found by χ^2 analysis that none of these fold-differences were statistically significant, and that, when all of the mutation rates were compared by pair-wise analysis, no statistical difference was found between the mutation rates at any of the four loci, as shown in Figure 8.8C. There was therefore no *cis* effect on the rate of *URA3* inactivation in haploid *top2-1* strains grown using the specific conditions established in this chapter.

The mutation rates of the haploid *top2-1* strains were compared against the rates of their respective WT strains grown under the same conditions. Figure 8.7A shows that the average mutation rates were very similar for the 139kb, 230kb and 242kb loci between the two genotypes. When the fold-differences were calculated for these three loci, they varied only from 0.9- to 1.2-fold and, unsurprisingly, the two mutation rates were not found to be statistically different from each other. For 53kb

A

Strain		Mutation Rate (95% CL)[a]	Fold-difference between 1&2	Average Mut Rate[b]
53kb	1	3.1×10^{-5} (2.4-4.0)	1.5	4.0×10^{-5}
	2	4.8×10^{-5} (3.3-6.0)		
139kb	1	3.8×10^{-5} (2.3-4.8)	1.2	3.5×10^{-5}
	2	3.2×10^{-5} (2.0-4.4)		
216kb	1	-	-	-
	2	-		
230kb	1	2.2×10^{-5} (2.0-4.7)	-	2.2×10^{-5}
	2	ND		
242kb	1	ND	-	3.0×10^{-5}
	2	3.0×10^{-5} (1.9-4.6)		

Location	Chromosomal Features
53kb	RSZ, Termination
139kb	RSZ, Termination, Ty2
216kb	Termination
230kb	Origin
242kb	None

B

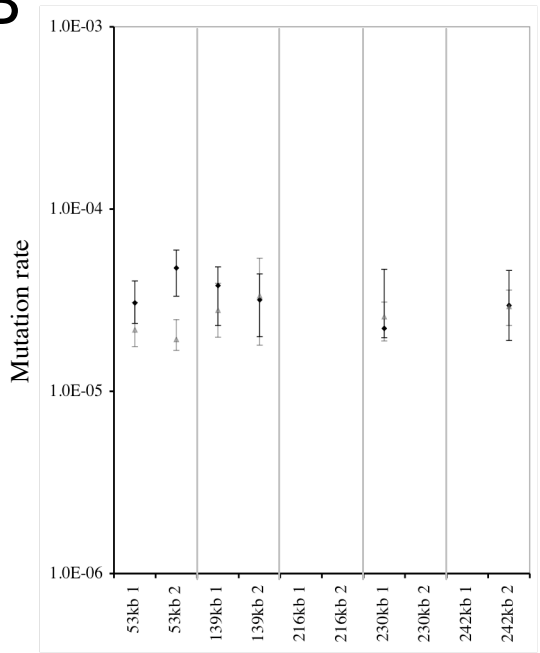

C

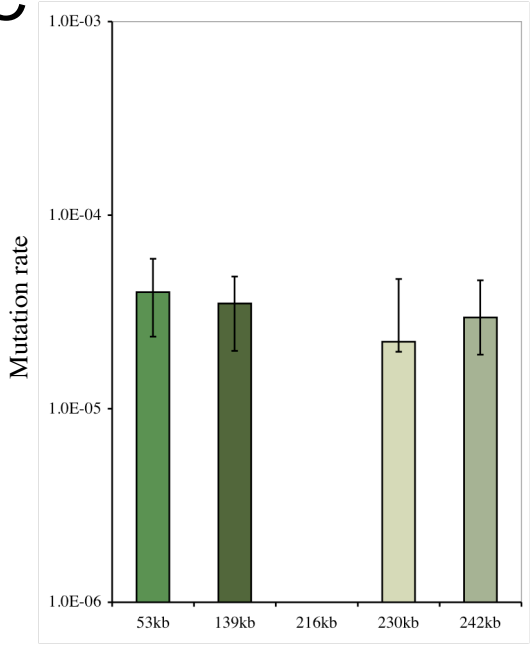

Figure 8.7. Rates of *URA3* inactivation in *top2-1* haploid strains grown using *top2-1* conditions.

(A) Two independent rate measurements were done for the 53kb and 139kb loci. The fraction of 5-FOA-resistant cells was measured in 15 independent cultures for each rate measurement. These frequencies were converted to rates using the method of the median (Lea and Coulson, 1949). [a] 95% confidence limits (CL) were calculated as described previously (Wierdl *et al*., 1996). [b] Where possible, the average mutation rates were calculated. Relevant chromosomal features at each locus are denoted on the right hand side. ND: mot determined.

(B) Individual rates are plotted for *top2-1* (black diamonds) and WT (grey triangles) haploid strains. Capped lines indicate 95% CLs.

(C) The average mutation rate of the two strains is plotted, where possible. The smallest and largest CL value of the two strains was used for each location. Mutation rate is given as number of events/cell/generation.

A

Location Mutation rate[a]	Normalised mutation rate
53kb 4.0 x 10^{-5}	1.8
139kb 3.5 x 10^{-5}	1.6
216kb ND	-
230kb 2.2 x 10^{-5}	1.0
242kb 3.0 x 10^{-5}	1.3

B

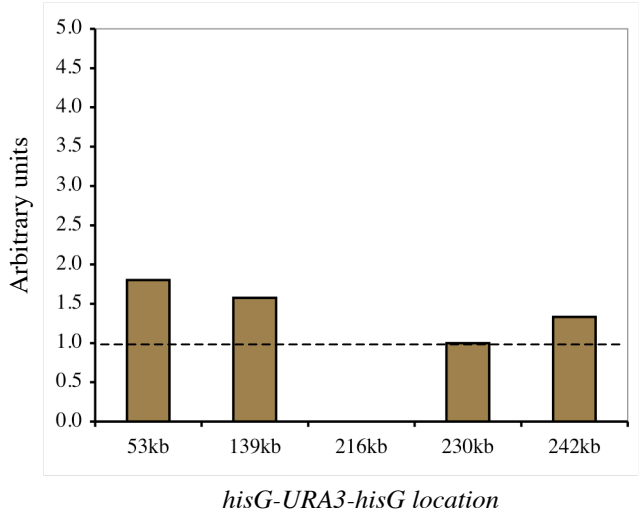

C

Location Mutation rate[a]	53kb 4.0 x 10^{-5}	139kb 3.5 x 10^{-5}	216kb ND	230kb 2.2 x 10^{-5}	242kb 3.0 x 10^{-5}
53kb 4.0 x 10^{-5}		0.13 NSS		1.67 NSS	1.67 NSS
139kb 3.5 x 10^{-5}				1.67 NSS	1.67 NSS
216kb ND					
230kb 2.2 x 10^{-5}					0.07 NSS
242kb 3.0 x 10^{-5}					

Figure 8.8. Analysis of rates of *URA3* inactivation in *top2-1* haploid strains grown using *top2-1* conditions.

(A) The average mutation rate at each locus was normalised against the lowest average rate.

(B) Normalised fold-differences from (A) are plotted.

(C) Chi-square analysis: pair-wise comparison of the mutation rates at each location. Shown in each panel are the Chi square (χ^2; upper) and probability (*P*; lower) values for each pair-wise combination. *P* values of less than 0.05 were deemed significant. NSS: not statistically significant. [a] Mutation rate is given as number of events/cell/generation.

(RSZ, replication termination), however, the *top2-1* mutation rate was 2.0-fold higher than the WT rate, which was statistically significant (P~0.01). These findings are shown in Figure 8.9.

In summary, the mutation rate in *top2-1* haploid cells did not vary depending on the location of the *hisG-URA3-hisG* cassette in ChrIII. There was therefore no *cis* effect in *top2-1* strains using these specific growth conditions. When these mutation rates were compared to the rates in WT strains grown using the same conditions, only the 53kb locus had a significantly higher rate. There was therefore only one specific *trans* effect in mutation rate between *top2-1* and WT strains grown using the same growth conditions, despite the lack of any *cis* effect observed between the mutation rates of the four loci tested.

8.2.2 Diploid top2-1 strains

8.2.2.1 Preparation for analysis of top2-1 diploid strains; kinetics of commitment to inviability at 37˚C

Spot tests of *top2-1* diploid strains grown in YPD at various temperatures are shown in Figure 8.10. These diploid strains were homozygous for the *top2*-1 allele, and heterozygous for the *hisG-URA3-hisG* construct. A WT and *top2-1* strain lacking a reporter construct are shown for comparison (first and second rows, respectively, right hand side). All *top2-1* strains grew less than the WT at all permissive temperatures tested. At 37˚C only the WT strain grew.

The viability of a diploid *top2-1* strain (JDCY446) lacking a *hisG-URA3-hisG* construct was tested at 37˚C in the same manner used for the haploid strains. The incubation times were exactly the same as used for the haploid *top2-1* strain in Figure 8.2; aliquots were taken every 30 minutes after the cultures had been transferred to 37˚C, and three parallel cultures were used. The result is shown in Figure 8.11. Cells grew to a maximum of ~140% the initial cell count after 60 minutes, but after this cell viability rapidly decreased and 95% of the original cell population was dead by 4h. Diploid *top2-1* strains were therefore incubated at 37˚C for one hour; specific incubation times are detailed in Figure 8.11B.

A

Construct location	Average mutation rate		Fold-difference[a]	Chi square and
	top2-1	WT (*top2-1*)	*top2-1* / WT (*top2-1*)	*P* values[b]
53kb	4.0×10^{-5}	2.1×10^{-5}	2.0	6.53, *P*~0.01
139kb	3.5×10^{-5}	3.1×10^{-5}	1.2	0.00, NSS
216kb	-	-	-	-
230kb	2.2×10^{-5}	2.6×10^{-5}	0.9	0.60, NSS
242kb	3.0×10^{-5}	2.9×10^{-5}	1.0	0.07, NSS

B

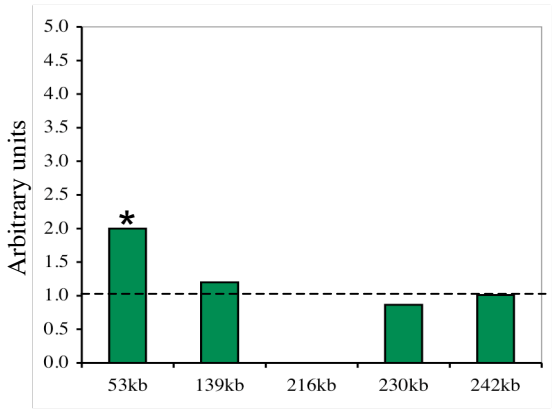

Figure 8.9. Effects of *top2-1* on the rates of *URA3* inactivation compared to those in WT haploid strains grown in the same conditions.

(A) [a] Where possible, for each location the mutation rate of strain 1 (*top2-1*) was divided by the mutation rate of strain 1 (WT). The same was done for strain 2. The fold-difference was then averaged over these two values for each locus. [b] Significant differences were calculated by χ^2 analyses, as described in the text. χ^2 values are given first, *P* values second. *P* values of less than 0.05 were deemed significant. NSS: not statistically significant.

(B) Graph showing the fold-difference in mutation rates of *top2-1* over WT haploid strains for each locus. "*" denotes a significant statistical difference. Values are taken from (A).

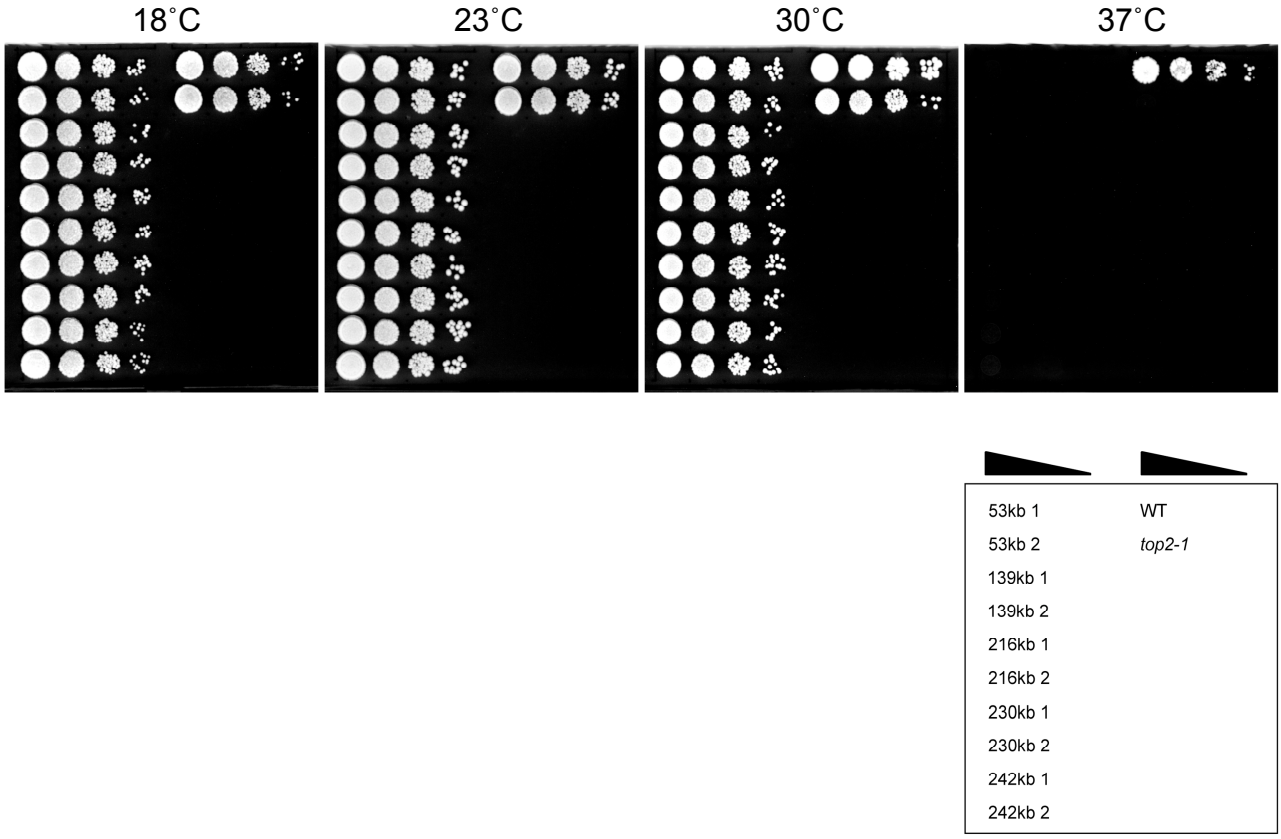

Figure 8.10. Effects of temperature on growth of *top2-1* diploid strains carrying a *hisG-URA3-hisG* construct at different loci on ChrIII.

Ten-fold serial dilutions of exponentially growing cells were spotted onto YPD plates and grown at the indicated temperatures for 3-5 days. The box in the lower right indicates the strains spotted onto the plates: WT and *top2-1* in this instance refer to strains lacking a *hisG-URA3-hisG* construct.

A

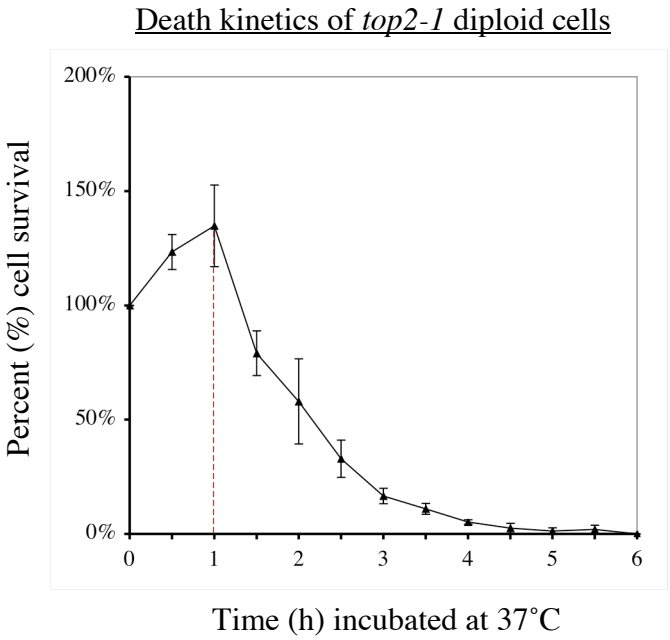

B

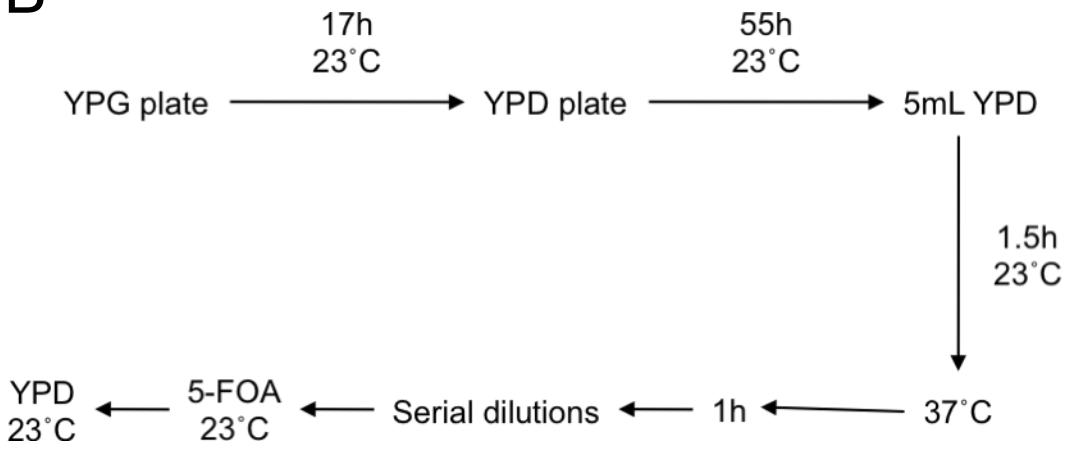

Figure 8.11. Testing diploid *top2-1* strains for fluctuation analysis incubation times: kinetics of commitment to inviability.

(A) Death kinetic analysis of a diploid *top2-1* strain (NHY311). Incubation times are the same as those used in Figure 8.2A. Error bars indicate the standard deviation between three independent cultures.

(B) Based on the results of the death kinetics in (A), diploid *top2-1* strains heterozygous for the *hisG-URA3-hisG* construct were incubated at these specific times for fluctuation analysis.

8.2.2.2 Rates of URA3 inactivation in WT diploid strains, using top2-1 growth conditions

Before the rates of *URA3* inactivation were tested in diploid *top2-1* strains, the mutation rates were first tested in WT strains using the *top2-1* growth conditions established in the previous section. The rates of individual strains (black-filled circles) are shown in Figure 8.12B, with rates for the same strains grown at 30˚C (grey crosses) shown for comparison. Specific values and 95% CLs are given in Figure 8.12A. No difference existed between the rates of strains 1 and 2 for the three loci where the analysis was possible, despite the observed 2-fold difference between the point rate estimates for the 139kb locus. These rates were averaged for each location, as shown in Figures 8.12A (last column) and 8.12C, and varied from 2.9 x 10^{-5} events/cell/generation for the 53kb locus (RSZ, termination) to only 3.5 x 10^{-5} for the 139kb locus (RSZ, termination, *Ty2*).

Figure 8.12C suggested that there was little or no difference in mutation rates for any of the five loci under these conditions. To assess this, the average mutation rates were normalised against the lowest value. The fold-increases over the 53kb rate varied from only 1.1- to 1.2-fold (Figure 8.13A). As expected, χ^2 analyses found no statistical difference between these mutation rates (Figure 8.13B). It was also found by pair-wise analysis that all of the mutation rates were statistically indistinguishable from each other (Figure 8.13C). The rate of *URA3* inactivation in WT diploid strains grown using the *top2-1* conditions did not therefore vary depending on the location of the construct in ChrIII.

The mutation rates of each location were then compared between the WT strains grown under the "*top2-1*" and those grown under the optimal ("30˚C" in YPD) conditions. Figure 8.12B shows that the mutation rates increased for the 53kb, 139kb and 216kb loci strains grown using the *top2-1* conditions, but not for the 230kb or 242kb loci. The fold-differences for the first three loci were 1.6, 2.6 and 2.8-fold, respectively, and 1.0 and 1.1-fold for the 230kb and 242kb loci. Chi square analysis found that the only significant differences between the two conditions were for the

A

Strain		Mutation Rate (95% CL)[a]	Fold-difference between 1&2	Average Mut Rate[b]
53kb	1	2.5×10^{-5} (1.6-3.5)	1.4	2.9×10^{-5}
	2	3.4×10^{-5} (2.3-5.1)		
139kb	1	4.7×10^{-5} (2.7-6.1)	2.0	3.5×10^{-5}
	2	2.4×10^{-5} (1.8-4.5)		
216kb	1	3.3×10^{-5} (2.3-5.2)	1.1	3.1×10^{-5}
	2	3.0×10^{-5} (2.1-3.7)		
230kb	1	3.3×10^{-5} (2.0-4.5)	-	3.3×10^{-5}
	2	ND		
242kb	1	ND	-	3.2×10^{-5}
	2	3.2×10^{-5} (2.6-7.8)		

Location	Chromosomal Features
53kb	RSZ, Termination
139kb	RSZ, Termination, Ty2
216kb	Termination
230kb	Origin
242kb	None

B

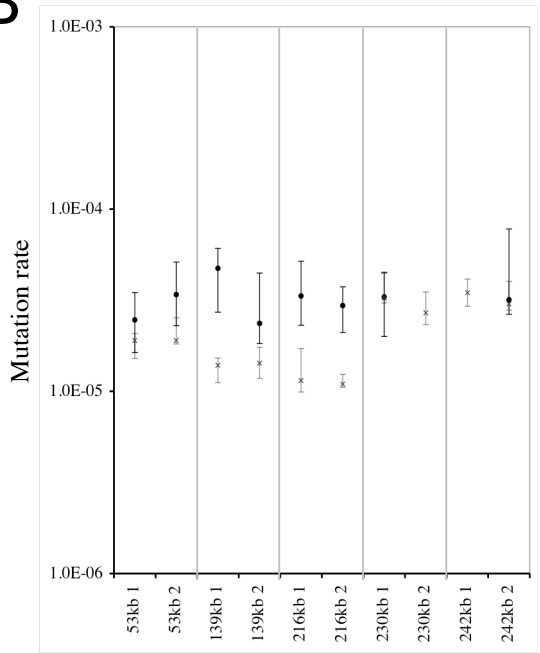

C

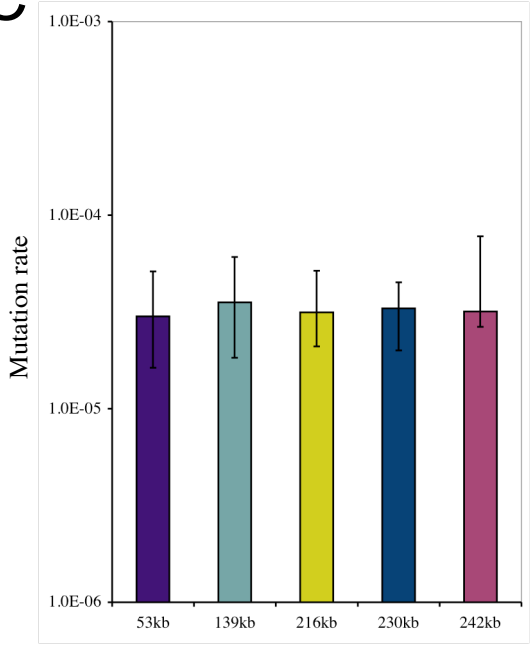

Figure 8.12. Rates of *URA3* inactivation in WT diploid strains grown using *top2-1* conditions.

(A) All strains were heterozygous for the *hisG-URA3-hisG* reporter construct. For each locus, except 230kb and 242kb, two independent rate measurements were done. The fraction of 5-FOA-resistant cells was measured in 15 independent cultures for each rate measurement. [a] 95% confidence limits (CL) were calculated as described previously (Wierdl *et al*., 1996). [b] Where possible, the average mutation rates were calculated. ND: not determined. Relevant chromosomal features at each locus are denoted on the right hand side.

(B) Individual rates are plotted for WT [*top2-1*] (black-filled circles) and WT [30°C] (grey crosses) diploid strains. Capped lines indicate 95% CLs.

(C) The average mutation rate of the two strains is plotted, where possible. The smallest and largest CL value of the two strains was used for each location. Mutation rate is given as number of events/cell/generation.

A

Location Mutation rate[a]	Normalised mutation rate
53kb 2.9 x 10^{-5}	1.0
139kb 3.5 x 10^{-5}	1.2
216kb 3.1 x 10^{-5}	1.1
230kb 3.3 x 10^{-5}	1.1
242kb 3.2 x 10^{-5}	1.1

B

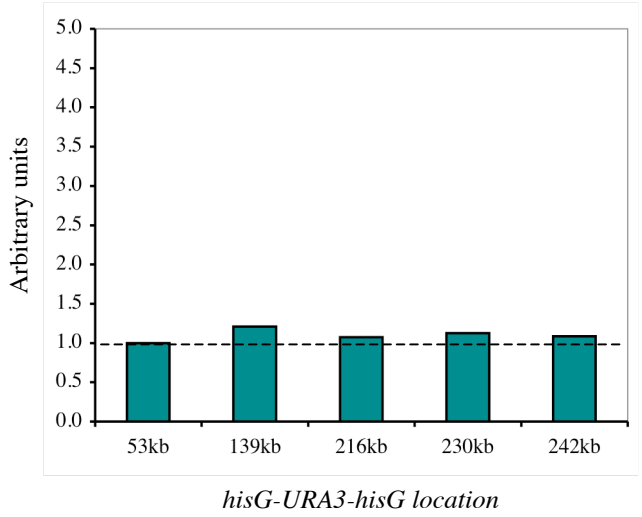

C

Location Mutation rate[a]	53kb 2.9 x 10^{-5}	139kb 3.5 x 10^{-5}	216kb 3.1 x 10^{-5}	230kb 3.3 x 10^{-5}	242kb 3.2 x 10^{-5}
53kb 2.9 x 10^{-5}		0.53 NSS	0.00 NSS	0.60 NSS	0.60 NSS
139kb 3.5 x 10^{-5}			1.20 NSS	1.67 NSS	1.67 NSS
216kb 3.1 x 10^{-5}				0.53 NSS	0.60 NSS
230kb 3.3 x 10^{-5}					0.53 NSS
242kb 3.2 x 10^{-5}					

Figure 8.13. Analysis of rates of *URA3* inactivation in WT diploid strains grown using *top2-1* conditions.

(A) The average mutation rate at each locus was normalised against the lowest average rate. [a] Mutation rate is given as number of events/cell/generation.

(B) Normalised fold-differences from (A) are plotted.

(C) Chi-square analysis: pair-wise comparison of the mutation rates at each location. Shown in each panel are the Chi square (χ^2; upper) and probability (*P*; lower) values for each pair-wise combination. *P* values of less than 0.05 were deemed significant. NSS: not statistically significant.

139kb (RSZ, termination, *Ty2*) and 216kb (termination) loci, as shown in Figures8.14A and 8.14B.

In summary, the mutation rates of diploid WT strains grown using the *top2-1* conditions were the same regardless of the construct location within ChrIII. Despite the lack of any *cis* effect being observed in these WT diploid strains using these specific growth conditions, however, when these rates were compared against the WT rates grown at constant 30˚C, the 139kb and 216kb rates were significantly higher whilst all other loci had statistically the same mutation rate. Location-specific effects on the rate of *URA3* inactivation in diploid strains were also found earlier in Chapter 5.

8.2.2.3 Rates of URA3 inactivation in top2-1 diploid strains

Next, the mutation rates were tested in the diploid *top2-1* strains. The rates of *URA3* inactivation for *top2-1* strains are shown in Figure 8.15B (black-filled circles) alongside their respective WT rates (grey circles) grown under the same conditions. Specific values are shown in Figure 8.15A. No statistical difference in mutation rate was found between the two independent transformants for any of the loci (χ^2 analysis). The mutation rates were averaged for each location, as shown in Figures 8.15A (last column) and 8.15C. These values ranged from 2.6 x 10^{-5} events/cell/generation for 230kb (origin), to 3.8 x 10^{-5} for 216kb (termination). The point rate estimates and 95% CL values were similar for all five loci, as was seen with the haploid *top2-1* strains.

To assess the variation in mutation rate between the different loci, the average mutation rates were normalised against the lowest mutation rate, 230kb. These values ranged from 1.1- to 1.4-fold: none of these fold-differences were found to be significant, as judged by χ^2 analyses (Figure 8.16). Pair-wise analysis was then performed to see if any of the mutation rates were statistically different from each other. Figure 8.16C shows that the mutation rates of all diploid *top2-1* strains were statistically the same (χ^2 analysis). There was therefore no *cis* effect on the rate of *URA3* inactivation in diploid *top2-1* strains grown using the specific conditions

A

Construct location	Average mutation rate		Fold-difference[a] WT (*top2-1*) / WT (30°C)	Chi square and *P* values[b]
	WT (*top2-1*)	WT (30°C)		
53kb	2.9×10^{-5}	1.9×10^{-5}	1.6	0.13, NSS
139kb	3.5×10^{-5}	1.4×10^{-5}	2.6	6.53, *P*~0.01
216kb	3.1×10^{-5}	1.1×10^{-5}	2.8	6.53, *P*~0.01
230kb	3.3×10^{-5}	3.0×10^{-5}	1.0	1.67, NSS
242kb	3.2×10^{-5}	3.2×10^{-5}	1.1	3.27, NSS

B

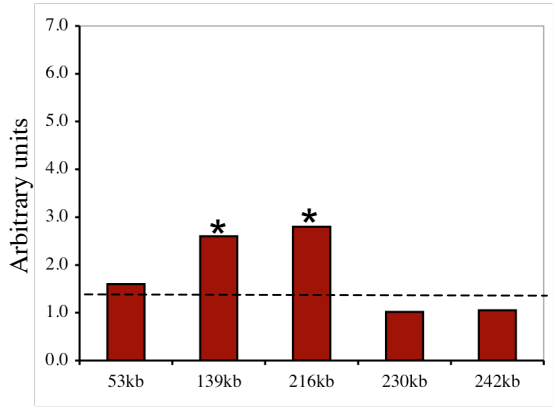

Figure 8.14. Effects of *top2-1* growth conditions on the rates of *URA3* inactivation compared to optimal growth conditions (YPD at 30˚C), in WT diploid strains.

(A) [a] Where possible, for each location the mutation rate of strain 1 (WT [*top2-1*]) was divided by the mutation rate of strain 1 (WT [30°C]). The same was done for strain 2. The fold-difference was then averaged over these two values for each locus. [b] Significant differences were calculated by χ^2 analyses, as described in the text. χ^2 values are given first, *P* values second. *P* values of less than 0.05 were deemed significant. NSS: not statistically significant.

(B) Graph showing the fold-difference in mutation rates of WT diploid strains grown using *top2-1* conditions over optimal growth conditions (YPD at 30°C) for each locus. "*" denotes a significant statistical difference. Values are taken from (A).

A

Strain		Mutation Rate (95% CL)[a]	Fold-difference between 1&2	Average Mut Rate[b]
53kb	1	2.8×10^{-5} (2.5-4.1)	1.0	2.9×10^{-5}
	2	2.9×10^{-5} (2.4-3.8)		
139kb	1	4.2×10^{-5} (2.3-6.8)	1.8	3.3×10^{-5}
	2	2.4×10^{-5} (1.5-3.6)		
216kb	1	3.1×10^{-5} (2.1-5.2)	1.4	3.8×10^{-5}
	2	4.4×10^{-5} (2.9-6.0)		
230kb	1	2.6×10^{-5} (1.9-4.8)	-	2.6×10^{-5}
	2	ND		
242kb	1	3.1×10^{-5} (1.9-4.4)	1.0	3.2×10^{-5}
	2	3.2×10^{-5} (2.6-4.4)		

Location	Chromosomal Features
53kb	RSZ, Termination
139kb	RSZ, Termination, Ty2
216kb	Termination
230kb	Origin
242kb	None

B

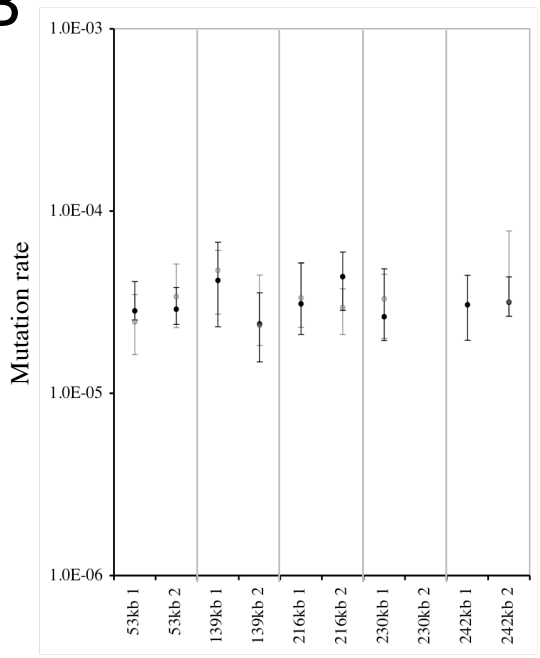

C

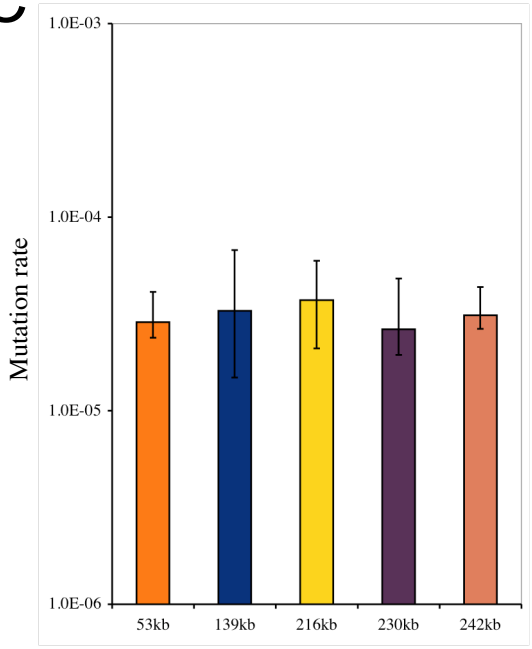

Figure 8.15. Rates of *URA3* inactivation in *top2-1* diploid strains grown using *top2-1* conditions.

(A) All strains were homozygous for *top2-1* and heterozygous for the *hisG-URA3-hisG* reporter construct. Except for 230kb, two independent rate measurements were done for each locus. The fraction of 5-FOA-resistant cells was measured in 15 independent cultures for each rate measurement. [a] 95% confidence limits (CL) were calculated as described previously (Wierdl *et al*., 1996). [b] Where possible, the average mutation rates were calculated. Relevant chromosomal features at each locus are denoted on the right hand side.

(B) Individual rates are plotted for *top2-1* (black-filled circles) and WT (grey-filled circles) diploid strains. Capped lines indicate 95% CLs.

(C) The average mutation rate of the two strains is plotted, where possible. The smallest and largest CL value of the two strains was used for each location. Mutation rate is given as number of events/cell/generation.

A

Location Mutation rate[a]	Normalised mutation rate
53kb 2.9 x 10^{-5}	1.1
139kb 3.3 x 10^{-5}	1.2
216kb 3.8 x 10^{-5}	1.4
230kb 2.6 x 10^{-5}	1.0
242kb 3.2 x 10^{-5}	1.2

B

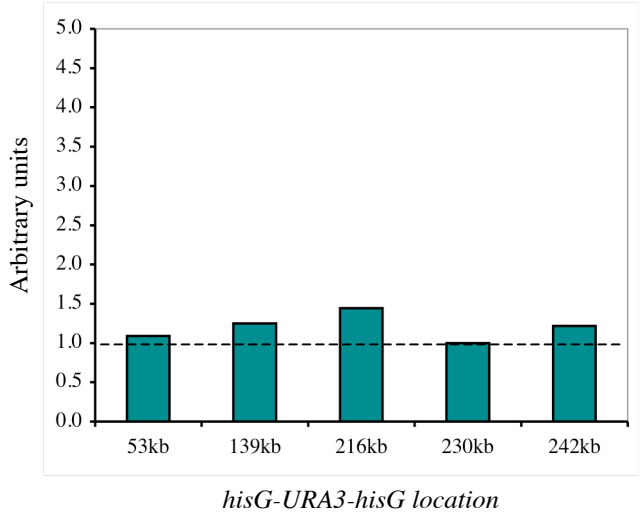

C

Location Mutation rate[a]	53kb 2.9 x 10^{-5}	139kb 3.3 x 10^{-5}	216kb 3.8 x 10^{-5}	230kb 2.6 x 10^{-5}	242kb 3.2 x 10^{-5}
53kb 2.9 x 10^{-5}		0.00 NSS	0.60 NSS	0.07 NSS	0.13 NSS
139kb 3.3 x 10^{-5}			1.67 NSS	0.60 NSS	0.00 NSS
216kb 3.8 x 10^{-5}				0.60 NSS	0.60 NSS
230kb 2.6 x 10^{-5}					0.07 NSS
242kb 3.2 x 10^{-5}					

Figure 8.16. Analysis of rates of *URA3* inactivation in *top2-1* diploid strains grown using *top2-1* conditions.

(A) The average mutation rate at each locus was normalised against the lowest average rate.

(B) Normalised fold-differences from (A) are plotted.

(C) Chi-square analysis: pair-wise comparison of the mutation rates at each location. Shown in each panel are the Chi square (χ^2; upper) and probability (*P*; lower) values for each pair-wise combination. *P* values of less than 0.05 were deemed significant. NSS: not statistically significant. [a] Mutation rate is given as number of events/cell/generation.

established in Section 8.3.1.

The mutation rates were compared between the *top2-1* strains and their respective WT strains grown using the same conditions. Figure 8.15B shows that the point rate estimates and 95% CL values for both of these genotypes were very similar for all strains tested. Figure 8.17 shows that the fold-differences varied from 0.8- to 1.5-fold, and, as expected, none of these values were statistically significant (χ^2 analysis).

In summary, therefore, the rates of *URA3* inactivation in diploid *top2-1* cells were statistically the same for all five loci using the specific growth conditions established earlier. When compared to the mutation rates of the respective WT strains grown using the same conditions, it was found that the mutation rates were also statistically indistinguishable. *top2-1* therefore had no *cis* or *trans* effect on the mutation rate in diploid strains using the growth conditions specific for this chapter.

8.2.3 Effects of ploidy on rates of URA3 inactivation in top2-1 strains

Finally, the rates of *URA3* inactivation in diploid and haploid *top2-1* strains were compared to assess any effect that ploidy had. It must be pointed out that, unlike in previous chapters, the growth conditions between these two situations were slightly different; haploid *top2-1* strains were incubated for 90 minutes at 37˚C whilst the diploid strains were incubated only for 60 minutes at 37˚C. It could be argued that, although the incubation times differed, both type of cells were incubated for as long as possible at the non-permissive temperature before losing cell viability, and therefore the two situations could be compared.

Figure 8.18A shows the individual mutation rates of diploid (black-filled circles) and haploid (grey triangles) *top2-1* strains. The mutation rate of strain 1 (diploid) was divided by the rate of strain 1 (haploid) to produce a fold-difference between the two mutation rates. The same was done for strain 2 and the average fold-difference between the rates of strains 1 and 2 used to plot the average fold-difference shown in Figures 8.18B and 8.18C (third column). These values ranged only from 0.8- to 1.2-

A

Construct location	Average mutation rate		Fold-difference[a]	Chi square and
	top2-1	WT (*top2-1*)	*top2-1* / WT (*top2-1*)	*P* values[b]
53kb	2.9 x 10^{-5}	2.9 x 10^{-5}	1.1	0.00, NSS
139kb	3.3 x 10^{-5}	3.5 x 10^{-5}	1.0	0.13, NSS
216kb	3.7 x 10^{-5}	3.1 x 10^{-5}	1.5	0.60, NSS
230kb	2.6 x 10^{-5}	3.3 x 10^{-5}	0.8	1.67, NSS
242kb	3.1 x 10^{-5}	3.2 x 10^{-5}	1.0	0.07, NSS

B

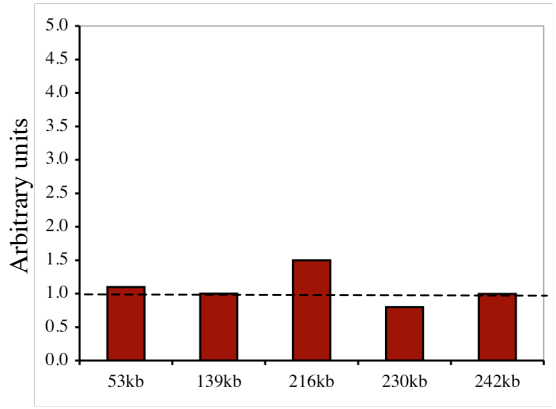

Figure 8.17. Effects of *top2-1* on the rates of *URA3* inactivation compared to those in WT diploid strains grown in the same conditions.

(A) [a] Where possible, for each location the mutation rate of strain 1 (*top2-1*) was divided by the mutation rate of strain 1 (WT). The same was done for strain 2. The fold-difference was then averaged over these two values for each locus. [b] Significant differences were calculated by χ^2 analyses, as described in the text. χ^2 values are given first, *P* values second. *P* values of less than 0.05 were deemed significant. NSS: not statistically significant.

(B) Graph showing the fold-difference in mutation rates of *top2-1* over WT diploid strains for each locus. Values are taken from (A).

A

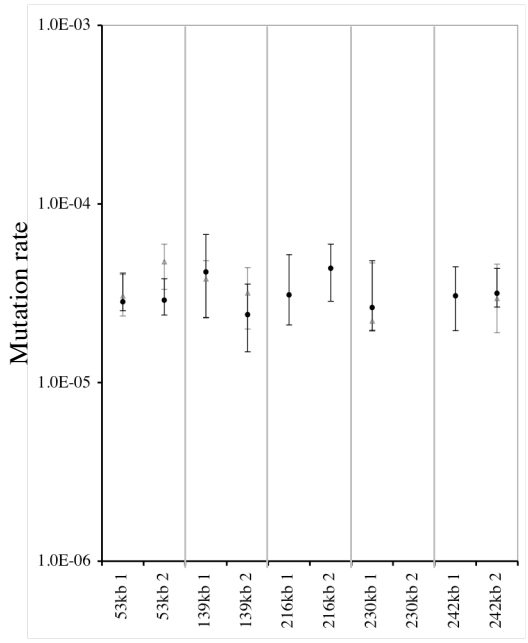

B

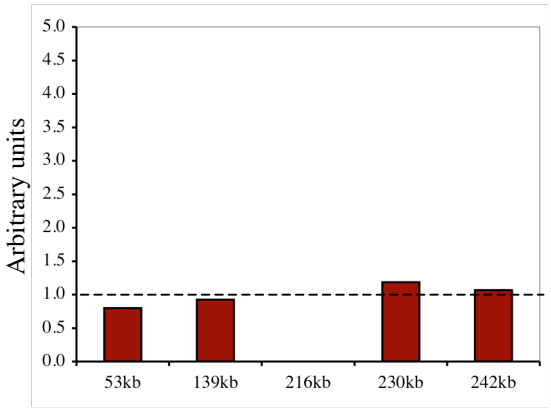

C

Construct location	Average mutation rate		Fold-difference[a] Diploid / Haploid	Chi square and *P* values[b]
	Diploid	Haploid		
53kb	2.9×10^{-5}	4.0×10^{-5}	0.8	0.53, NSS
139kb	3.3×10^{-5}	3.5×10^{-5}	0.9	0.00, NSS
216kb	3.8×10^{-5}	-	-	-
230kb	2.6×10^{-5}	2.2×10^{-5}	1.2	0.60, NSS
242kb	3.2×10^{-5}	3.0×10^{-5}	1.1	0.07, NSS

Figure 8.18. Effects of ploidy on the rates of *URA3* inactivation in *top2-1* strains grown using *top2-1* conditions.

(A) Individual mutation rates of *top2-1* haploid (grey triangles) and *top2-1* diploid (black-filled circles) strains.

(B) Graph showing the fold-difference in mutation rates of diploid over haploid *top2-1* strains for each locus. Values are taken from (C).

(C) [a] Where possible, for each location the mutation rate of strain 1 (diploid) was divided by the mutation rate of strain 1 (haploid). The same was done for strain 2. The fold-difference was then averaged over these two values for each locus. [b] Significant differences were calculated by χ^2 analyses, as described in the text. χ^2 values are given first, *P* values second. *P* values of less than 0.05 were deemed significant. NSS: not statistically significant.

fold (with the exception of the 216kb locus, which could not be compared as no haploid rates had been measured). Chi square analysis revealed that none of these values were statistically different. The mutation rate for *top2-1* strains was therefore statistically the same for diploid and haploid strains using the *top2-1*-specific growth conditions used in this chapter.

8.3 Discussion

Using the temperature-sensitive allele *top2-1* allowed the rate of *URA3* inactivation to be tested in strains containing the *hisG-URA3-hisG* reporter construct in the absence of Top2p function. When the mutation rates of *top2-1* haploid strains were tested, no *cis* effect was seen amongst the four loci tested. When compared to the mutation rates of their respective WT strains incubated under the same conditions, the only statistical difference seen was for the 53kb locus (RSZ, termination), where the rate of *top2-1* strains was 2-fold higher than in the WT strains.

In diploid strains a similar situation was seen. The mutation rates in both the WT and *top2-1* strains grown using the *top2-1*-specific incubation times, as in haploids, showed no *cis* effect. When the mutation rates of diploid WT (*top2-1* conditions) were compared to the rates of WT (constant 30°C) strains, the 139kb (RSZ, termination, Ty2) and 216kb (termination) loci had statistically higher mutation rates, possibly reflecting the mutagenic effects of high temperature. However, the rates at the other three loci were statistically the same, suggesting the presence of *cis*-specific effects associated with the effects of temperature on the mutation rate, as seen in Chapter 5.

In contrast to the modest mutagenic effects of Top2p inactivation observed here, previous studies have reported a 4- to 200- fold increase in mutation rates following Top2 inactivation (Sabourin *et al*., 2003; Christman *et al*., 1988). Note however, that the conditions utilised in the latter studies, including the mode of Top2p inactivation, the nature of the tester construct, the locations of tester construct insertion, and the duration of Top2 inactivation, were different than the conditions utilised in this study.

As a final comparison, the mutation rates were compared between *top2-1* haploid and diploid strains. No statistical difference was found. Therefore, regardless of ploidy, transient inactivation of Top2p had no effect, statistically, on the mutation rate of *top2-1* strains at any of the loci tested. One exception to this was the statistically higher 2-fold mutation rate seen for the haploid 53kb locus (RSZ, termination).

The modest effect of Top2 inactivation on mutation rate might not be surprising given the very short incubation times at the non-permissive temperature these strains were subjected to. In conclusion, transient inactivation of *top2-1* had little effect on the mutation rate in haploid or diploid strains.

Chapter 9.

Investigating the nature of URA3 inactivation

9.1 Introduction

In the results chapters so far the nature of acquiring 5-FOA-resistance was not assessed. Acquisition of 5-FOA-resistance in the strains used in this thesis was possible by a number of ways. In the original paper detailing how the *hisG-URA3-hisG* construct was created, for instance, more than 90% of all 5-FOA resistant colonies produced were shown to be the result of a "pop-out" event, leaving one copy of the two original *hisG* repeats in conjunction with excision of the *URA3* gene (Figure 1.1, page 39). The conditions used to create the 5-FOA resistant colonies in that particular case were different to those used in this thesis, however, and it cannot be assumed that the same result was achieved with the strains used here (Alani *et al*., 1987). The *URA3* gene may also have been inactivated through various means, such as frame-shift errors, small insertions and/ or deletions, ectopic recombination, etc, as discussed in Section 1.5.1 (page 38). This chapter therefore assesses the nature of genetic changes among 5-FOA-resistant colonies in both haploid and diploid strains. Since one of the major aims of this study was to examine the possible involvement of RSZs in genomic instability, the nature of genetic changes associated with the 53kb locus (RSZ, replication termination) were compared with those of the 242kb locus, the region of ChrIII with no discernable chromosomal features, for detailed analysis.

9.2 Results

After all 5-FOA-resistant colonies had been counted to estimate the mutation rate from fluctuation analysis, 20 independent haploid and diploid colonies were analysed from each strain grown under the various conditions and/or genotypes. One colony was taken at random from each of the 15 parallel cultures, with another

colony taken from the first 5 cultures (Figure 9.1). No bias was given towards any given colony shape or size. These 20 colonies were patched onto non-selective (YPD) agar plates and allowed to grow overnight at the appropriate non-selective temperature. This YPD plate was also replica-plated onto synthetic dropout media lacking uracil to confirm that none of the 5-FOA-resistant colonies were able to grow in the absence of uracil. Cells were then inoculated into 2mL YPD liquid media, grown overnight until saturation and genomic DNA harvested as detailed in the Materials & Methods. DNA was digested using the appropriate REs overnight, electrophoresed in agarose gels and Southern analysis performed. The 500bp probes used to confirm correct integration of the *hisG-URA3-hisG* construct into the chromosomal DNA (Chapter 3) were used for this analysis. These sequences were outside of both the *hisG-URA3-hisG* cassette and the 500bp genomic flanking sequences used to create the individual transformation cassettes (see Chapter 3 for more detail). All relevant RE sites used for these analyses are detailed in the accompanying figures and figure legends.

Of note is that loss of one *hisG* repeat and the *URA3* gene can be the result of SSA or by HRR. As it was not assessed in this chapter which particular repair mechanism resulted in the loss of these sequencies, however, "pop-out" is used to describe the end product only.

9.2.1 Southern blot analysis of 5-FOA-resistant haploids

Regardless of the growth condition or genotype, all haploid samples analysed contained DNA fragments that migrated as the intact *hisG-URA3-hisG* fragment did for both the 53kb and 242kb loci, as shown in Table 9.1. Given that the inactivation of *URA3* was confirmed by their inability to grow in the absence of uracil, the result shown in Table 9.1 suggests that the acquisition of 5-FOA-resistance in haploid strains was mediated by small changes in the *URA3* gene such as point mutations and/or small insertions/deletions, rather than the expected pop-out event. It is possible that pop-out events could have occurred at a very low frequency not detected by this analysis. If this were the case, as approximately 140 different

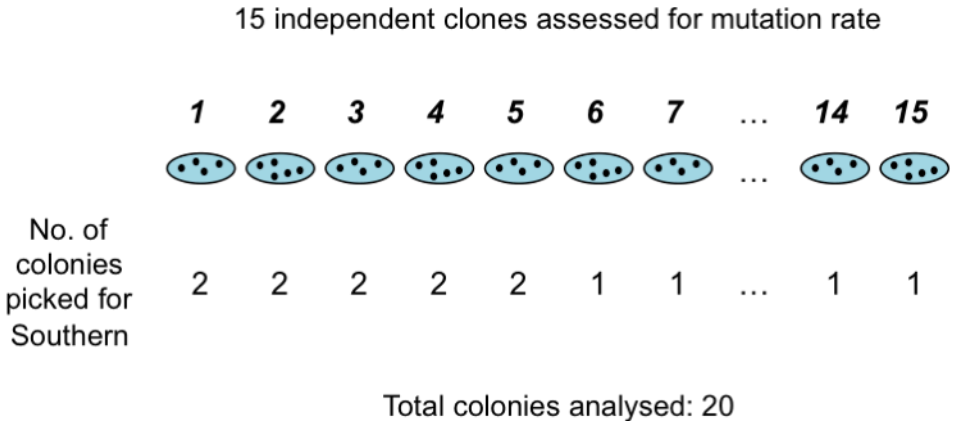

Figure 9.1. Sample selection for Southern blot analysis.

For the detailed Southern blot analysis of 5-FOA-resistant colonies, one colony was selected at random from each of the 15 parallel cultures. An additional colony was also taken from the first five cultures: 20 colonies in total were therefore analysed for each genotype/ growth condition.

5-FOA-resistant colonies were tested for each locus, the pop-out events would only occur at a frequency of <1% using the specific growth conditions.

9.2.2 Southern blot analysis of 5-FOA-resistant diploids

The same analysis was performed on the corresponding diploid genotypes and growth conditions. Additionally, strains grown at 23˚C and 37˚C were also analysed. As these diploid strains were heterozygous with respect to the *hisG-URA3-hisG* construct, the Southern protocol utilised detected both the unmodified WT fragment from the WT ChrIII and the fragment containing the *hisG-URA3-hisG* construct. This analysis revealed that a notable fraction of 5-FOA-resistant colonies had lost the entire *hisG-URA3-hisG* construct and flanking DNA sequences for both the 53kb and 242kb loci (Table 9.2), as only the WT fragments were detected. This could have been due to either a large recombination event that placed the construct in an ectopic location where the enzymes utilized for Southern analysis were not nearby, or by loss of the entire copy of ChrIII containing the construct. In the former case, recombination alone would not necessarily have inactivated the *URA3* gene without an additional loss of part/whole of the *URA3* gene necessary to confer the 5-FOA resistant/*ura3* phenotype. The lack of these type of changes within haploid strains is likely due to the fact that, being haploid, they cannot lose an entire chromosome and/or undergo gross chromosomal aberrations without consequently losing essential genes required for growth or survival.

Note that no pop-out events were detected in any of the colonies analysed for either the 53kb or 242kb loci for any of the diploid strains and/or conditions. A representative result from this analysis is shown in Figure 9.2 for the 242kb locus. These results will now be analysed in more detail.

9.2.2.1 Factors that regulate large genetic changes in diploid strains

From the results gathered for both loci, certain generalizations could be made under several different growth conditions and/ or mutant backgrounds. For simplicity, the 5-FOA-resistant colonies that arose from acquiring small insertions and/or deletions

Table 9.1 Summary of Southern blot analyses of 53kb and 242kb haploid 5-FOA-resistant colonies.

53kb

Genotype/ Growth Condition	*5-FOA-resistance*		
	Class I	*Class II*	*Class III*
WT (30˚C)	20/20 (100%)	-	-
WT (10mM HU)	20/20 (100%)	-	-
sml1Δ	20/20 (100%)	-	-
mec1Δsml1Δ	19/19 (100%)	-	-
mec1-40	19/19 (100%)	-	-
rrm3Δ	20/20 (100%)	-	-
top2-1	19/19 (100%)	-	-
TOTAL	137/137 (100%)	0/137 (<0.7%)	0/137 (<0.7%)

242kb

Genotype/ Growth Condition	*5-FOA-resistance*		
	Class I	*Class II*	*Class III*
WT (30˚C)	20/20 (100%)	-	-
WT (10mM HU)	20/20 (100%)	-	-
sml1Δ	20/20 (100%)	-	-
mec1Δsml1Δ	20/20 (100%)	-	-
mec1-40	20/20 (100%)	-	-
rrm3Δ	20/20 (100%)	-	-
top2-1	20/20 (100%)	-	-
TOTAL	140/140 (100%)	0/140 (<0.7%)	0/140 (<0.7%)

Class I mutants are the likely result of small changes in the *URA3* gene such as point mutations and/or small insertions/deletions that lead to its inactivation. Class II mutants are due to loss of the entire *hisG-URA3-hisG* construct (and flanking sequences) from its original integration point. Class III mutants are those that have acquired 5-FOA-resistance by pop-out events. 'WT' in this instance refers to strains having no other mutant phenotype than the integrated *hisG-URA3-hisG* construct at the specified locus.

Table 9.2. Summary of Southern blot analyses of 53kb and 242kb diploid 5-FOA-resistant colonies.

53kb

Genotype/ Growth Condition	*5-FOA-resistance*		
	Class I	*Class II*	*Class III*
WT (23˚C)	19/20 (95%)	1/20 (5%)	-
WT (30˚C)	16/20 (80%)	4/20 (20%)	-
WT (37˚C)	13/17 (76%)	4/17 (24%)	-
WT (10mM HU)	7/19 (37%)	12/19 (63%)	-
sml1Δ	16/20 (80%)	4/20 (20%)	-
mec1Δsml1Δ	8/20 (40%)	12/20 (60%)	-
mec1-40	18/20 (90%)	2/20 (10%)	-
rrm3Δ	7/20 (35%)	13/20 (65%)	-
top2-1	16/20 (80%)	4/20 (20%)	-
TOTAL	120/176 (68%)	56/176 (32%)	0/176 (<0.6%)

242kb

Genotype/ Growth Condition	*5-FOA-resistance*		
	Class I	*Class II*	*Class III*
WT (23˚C)	18/20 (90%)	2/20 (10%)	-
WT (30˚C)	17/20 (85%)	3/20 (15%)	-
WT (37˚C)	15/20 (75%)	5/20 (25%)	-
WT (10mM HU)	13/20 (65%)	7/20 (35%)	-
sml1Δ	0/20 (0%)	20/20 (100%)	-
mec1Δsml1Δ	9/20 (45%)	11/20 (55%)	-
mec1-40	17/20 (85%)	3/20 (15%)	-
rrm3Δ	2/20 (10%)	18/20 (90%)	-
top2-1	20/20 (100%)	0/20 (0%)	-
TOTAL	111/180 (62%)	69/180 (38%)	0/180 (<0.6%)

Class I mutants are the likely result of small changes in the *URA3* gene such as point mutations and/or small insertions/deletions that lead to its inactivation. Class II mutants are due to loss of the entire *hisG-URA3-hisG* construct (and flanking sequences) from its original integration point. Class III mutants are those that have acquired 5-FOA-resistance by pop-out events. 'WT' in this instance refers to strains having no other mutant phenotype than the integrated *hisG-URA3-hisG* construct at the specified locus.

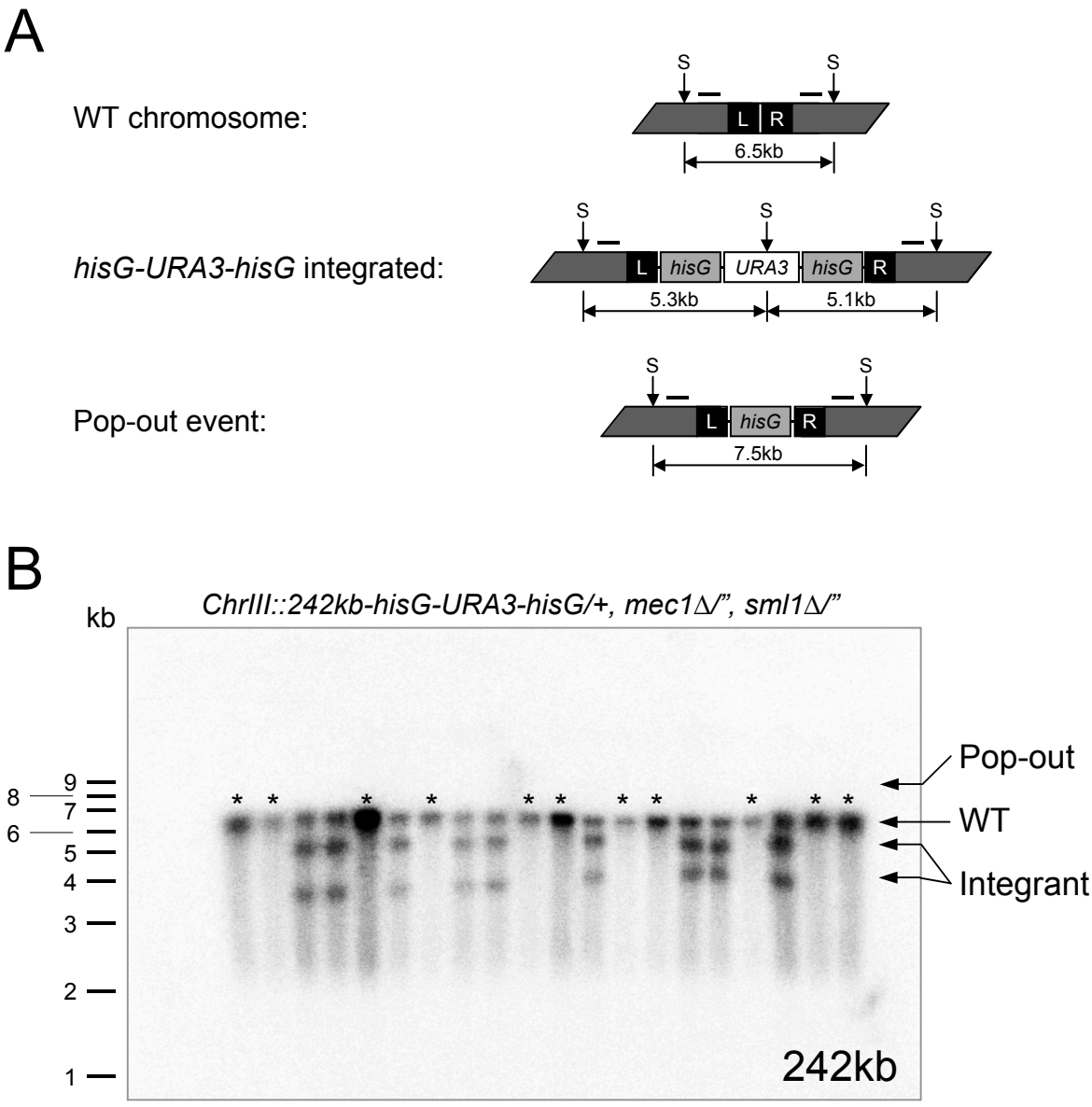

Figure 9.2. Southern blot analysis of JDCY311 (*ChrIII-242kb::hisG-URA3-hisG/+, mec1Δ::LEU2/", sml1Δ::HphMx4/"*) 5-FOA-resistant colonies.

(A) Schematic presentation of DNA structures resolved using probes upstream and downstream (dashed lines) of the integration site. The upper cartoon shows the DNA before insertion of the construct, the middle one shows an integrated *hisG-URA3-hisG* construct and the lower cartoon shows the expected DNA size(s) if a pop-out event has occurred. 'L' and 'R' are the ~500bp sequences that flank the insertion point. Bold lines indicate the position of 0.5kb probes used for the analysis. Vertical arrows mark relevant RE sites. S, *Stu*I. Drawings are not to scale.

(B) Southern blot analysis. The migrating pattern of DNA size markers of indicated sizes (in kb) are shown on the left hand side. Positions of the WT and integrant bands as well as the expected location of DNA resulting from pop-out events are as indicated. The asterix (*) denotes samples that have undergone loss of the entire region of ChrIII containing the construct (Class II mutations). The remaining 5-FOA-resistant colonies analysed here contained a mostly intact integrant construct and likely are the result of small insertions/ deletions within the *URA3* gene (Class I).

in the *URA3* gene are herein referred to as being "Class I" mutants, whilst those arising from loss of the entire region/ chromosome as "Class II" mutants.

Temperature had a small but consistent affect on the ratio of Class I to Class II mutants. Firstly, at 23˚C, more than 90% of the 5-FOA-resistant colonies were the result of small insertions/deletions/point mutations for both the 53kb and 242kb loci (Class I). When 5-FOA-resistant colonies were analysed at 30˚C and 37˚C, however, it was found that the proportion of Class II mutants increased with increasing temperature. For both loci grown at 30˚C the number of Class I mutants was over 80%, and at 37˚C, approximately 75%. Note that the percentage of Class II colonies was very similar between the two loci at all three temperatures tested: a maximum 5% difference existed between the two loci at any one given temperature.

When compared to the WT strains grown at 30˚C in YPD (the conditions defined as being optimal in Chapter 4), an increase in the loss of detection of the *URA3* gene and flanking sequences at the initial insertion point (Class II mutants) was observed when WT strains were grown in conditions of replication stress (10mM HU). Additionally, when the WT copies of the *RRM3*, *SML1*, and *MEC1* genes were separately deleted, the proportion of Class II mutants also increased over those seen for WT strains grown in non-selective conditions. Transient inactivation of *MEC1* or *TOP2* in the *mec1-40* or *top2-1* strain backgrounds did not lead to a significant increase in Class II mutants over non-selective conditions.

9.2.2.2 Conditions that differentially affected loss of URA3 at 53kb and 242kb

As described above, there were several generalizations that could be made for both loci when assessing the proportion of Class II mutants under different conditions/ mutant backgrounds. There were notable differences, however, between the 5-FOA-resistant colonies for the 53kb and 242kb loci.

When diploids strains were grown in the presence of 10mM HU, the number of Class II mutants observed from 5-FOA-resistant colonies was almost double for the 53kb locus than the 242kb one (63% versus 35%, respectively).
A surprising result was seen for the *sml1Δ* diploids. In the 53kb strains 20% of all colonies analysed were Class II mutants, exactly the same proportion observed for colonies derived from non-selective growth conditions at 30˚C. For the 242kb locus, however, 100% of the 5-FOA-resistant colonies were Class II mutants: in comparison, only 15% of colonies derived from non-selective conditions were Class II.

Transient inactivation of the *TOP2* allele (*top2-1* strains) did not lead to an increase in Class II mutants for either location, as stated above in the previous section. For the 53kb locus, 20% of the 5-FOA-resistant colonies analysed were Class II. For the 242kb locus, however, none of the mutant colonies were Class II. This is the opposite result achieved in 242kb *sml1Δ* strains, as noted above.

Finally, as described above, *rrm3Δ* strains led to an increase in the proportion of Class II mutants for both loci tested compared to non-selective conditions. In the 53kb strains, 65% of 5-FOA-resistant colonies were Class II mutants, whilst the 242kb *rrm3Δ* strains had a much higher proportion of 90%.

9.2.3 Potential cis effect on pop-out events

It was surprising to see no pop-out events for either locus. As mentioned in the introduction to this chapter, the original paper describing the *hisG-URA3-hisG* construct stated that all of the 5-FOA colonies examined by Southern analysis had the predicted banding pattern resulting from a deletion of the *URA3* gene and one of the *hisG* sequences (Alani *et al*., 1987). Additionally, earlier studies in my lab found that the majority of transformants containing a single *hisG-URA3-hisG* construct replacing *SPO11* also acquired 5-FOA-resistance by pop-out events (Rita Cha, personal communication).

Two potentially relevant differences between the 5-FOA-resistant cells created in the earlier studies and those created in this study were (i) the growth conditions used and (ii) the loci at which the *hisG-URA3-hisG* construct was introduced. In the other studies, for instance, *URA3* cells were replica-plated from non-selective plates directly onto 5-FOA plates with no growth period in liquid phase: typically, 5-FOA-resistant, ura- colonies emerged after 3-5 days. In this study, specific incubation times were used before cells were plated onto 5-FOA plates. Furthermore, selection for 5-FOA-resistant colonies using *hisG-URA3-hisG* in the past has been used mostly as a means to delete multiple genes in succession repeatedly using *URA3* as a marker. Therefore, most loci examined to date are those containing actively transcribed genes. To see if these factors contributed in determining the incidence of pop-out events, the nature of genetic events associated with 5-FOA-resistance was assessed in all five loci using the same method as in the earlier studies mentioned. Both haploid and diploid strains were used for this purpose, as haploid – rather than diploid cells had also been used in the previous studies.

Diploid and haploid strains stored in -80˚C glycerol stocks were patched onto YPG plates and incubated overnight at 30˚C. These strains were "WT", having no other genotype except one *hisG-URA-hisG* construct inserted at each specific locus within ChrIII. Cells were then replica plated onto non-selective (YPD) media plates, incubated overnight at 30˚C before being replica plated one final time onto 5-FOA agar plates. Colonies emerged after 3-5 days at 30˚C. These colonies were also patched onto ura- dropout media plates to check for false positives. *ura3*, 5-FOA-resistant colonies were processed for Southern analysis in the same manner as those used earlier in this Chapter. Representative results of this analysis for all five loci are shown in Figures 9.3 – 9.7, and detailed below.

No pop-out events were seen for the 53kb locus using this particular approach. All haploids tested were Class I mutants, as was seen with the 5-FOA-resistant colonies produced using the fluctuation analysis growth conditions. The majority of 53kb diploid 5-FOA-resistant colonies were also Class I mutants: one Class II mutant (loss of the entire region/ chromosome) is shown in Figure 9.3B. This was therefore reflective of the results seen for the fluctuation analysis experiments for this

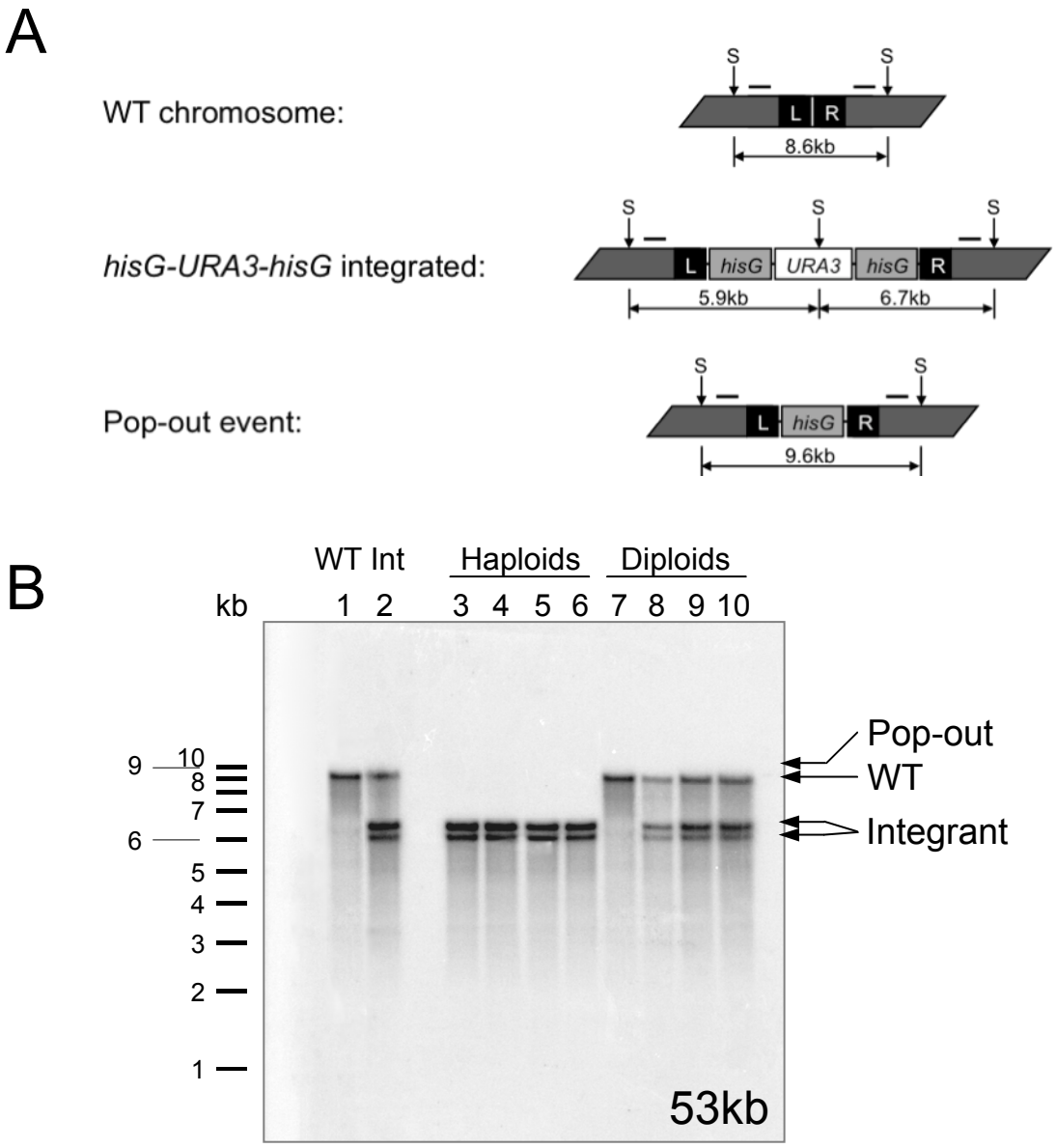

Figure 9.3. Effects of *hisG-URA3-hisG* insertion locations on incidence of pop-out events.

Nature of genetic alterations associated with the acquisition of 5-FOA-resistance in strains containing *hisG-URA3-hisG* at 53kb.

(A) Schematic presentation of DNA structures resolved using probes upstream and downstream (dashed lines) of the integration site. The upper cartoon shows the DNA before insertion of the construct, the middle one shows an integrated *hisG-URA3-hisG* construct and the lower cartoon shows the expected DNA size(s) if a pop-out event has occurred. "L" and "R" are the ~500bp sequences that flank the insertion point. Bold lines indicate the position of 0.5kb probes used for the analysis. Vertical arrows mark relevant RE sites. S, *Stu*I. Drawings are not to scale.

(B) Southern blot analysis. 1, WT diploid strain lacking the *hisG-URA3-hisG* construct; 2, WT diploid strain containing one inserted construct at the specified locus; 3-6 and 7-10, four representative 5-FOA-resistant haploid and diploid mutants, respectively, that resulted from growth conditions described in detail in the text. Known sizes of DNA markers (in kb) are shown on the left hand side and are approximate only.

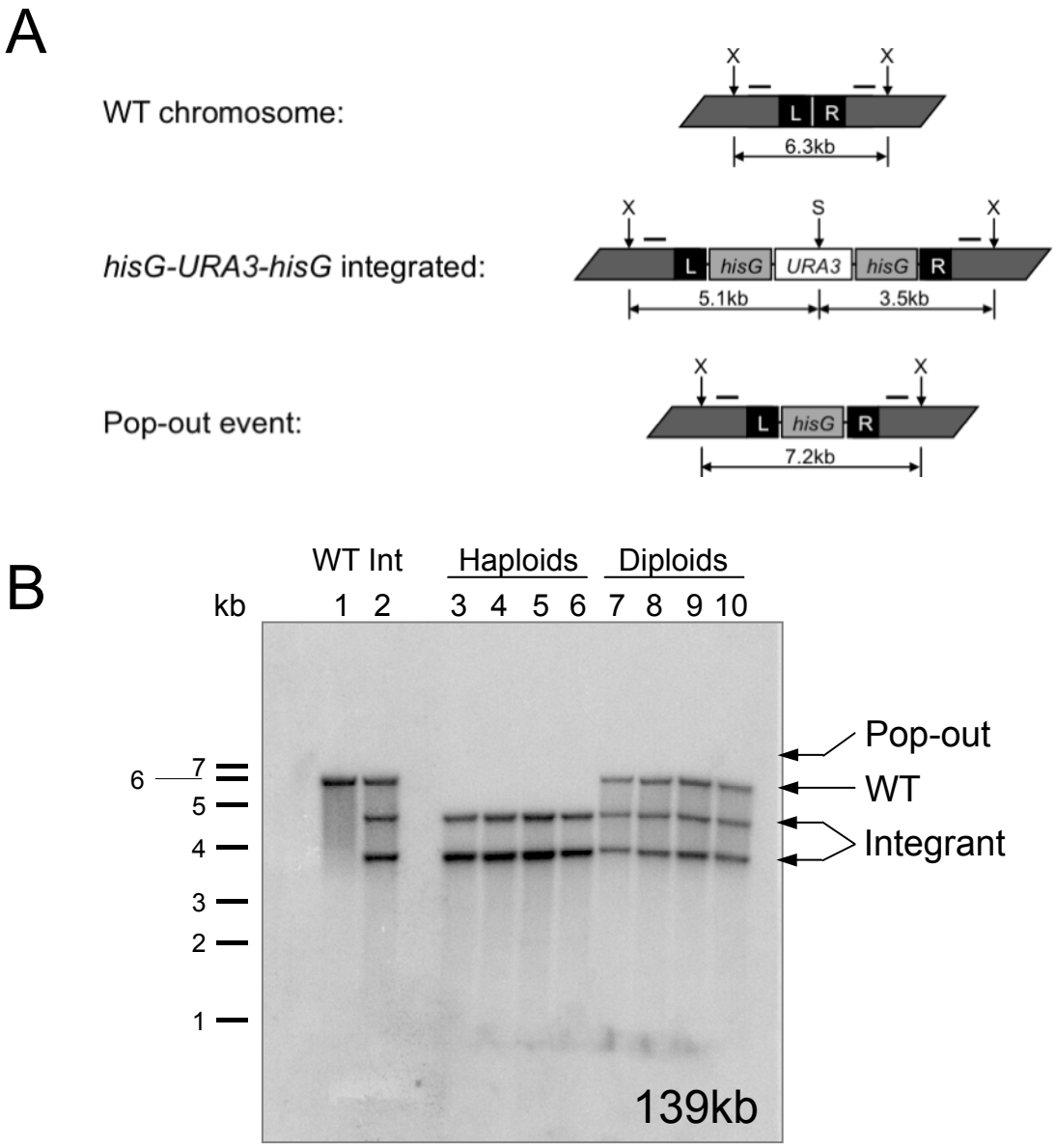

Figure 9.4. Effects of *hisG-URA3-hisG* insertion locations on incidence of pop-out events.

Nature of genetic alterations associated with the acquisition of 5-FOA-resistance in strains containing *hisG-URA3-hisG* at 139kb.

(A) Schematic presentation of DNA structures resolved using probes upstream and downstream (dashed lines) of the integration site. The upper cartoon shows the DNA before insertion of the construct, the middle one shows an integrated *hisG-URA3-hisG* construct and the lower cartoon shows the expected DNA size(s) if a pop-out event has occurred. "L" and "R" are the ~500bp sequences that flank the insertion point. Bold lines indicate the position of 0.5kb probes used for the analysis. Vertical arrows mark relevant RE sites. X, *Xho*I. Drawings are not to scale.

(B) Southern blot analysis. 1, WT diploid strain lacking the *hisG-URA3-hisG* construct; 2, WT diploid strain containing one inserted construct at the specified locus; 3-6 and 7-10, four representative 5-FOA-resistant haploid and diploid mutants, respectively, that resulted from growth conditions described in detail in the text. Known sizes of DNA markers (in kb) are shown on the left hand side and are approximate only.

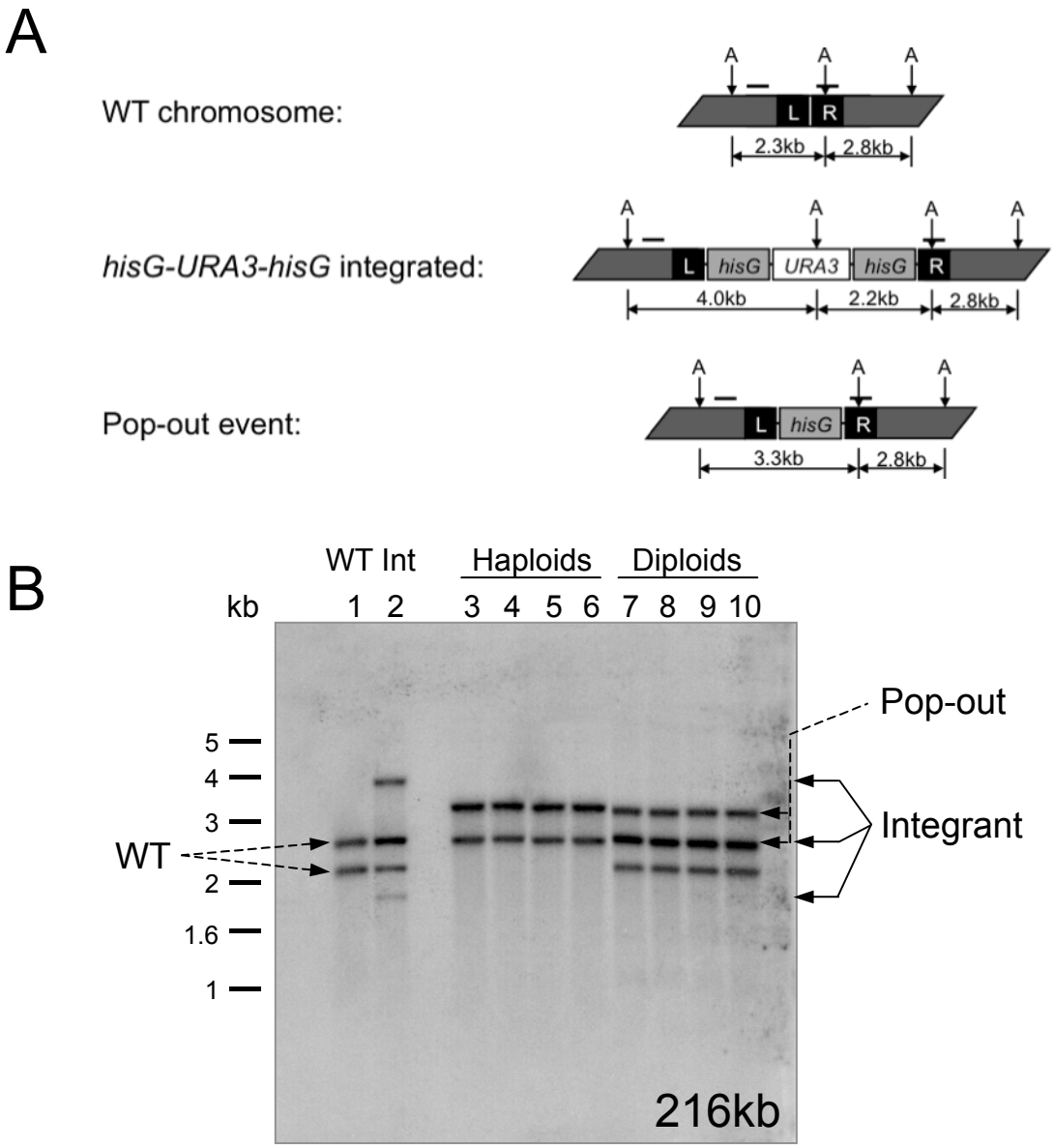

Figure 9.5. Effects of *hisG-URA3-hisG* insertion locations on incidence of pop-out events.

Nature of genetic alterations associated with the acquisition of 5-FOA-resistance in strains containing *hisG-URA3-hisG* at 216kb.

(A) Schematic presentation of DNA structures resolved using probes upstream and downstream (dashed lines) of the integration site. The upper cartoon shows the DNA before insertion of the construct, the middle one shows an integrated *hisG-URA3-hisG* construct and the lower cartoon shows the expected DNA size(s) if a pop-out event has occurred. "L" and "R" are the ~500bp sequences that flank the insertion point. Bold lines indicate the position of 0.5kb probes used for the analysis. Vertical arrows mark relevant RE sites. A, *Apa*I. Drawings are not to scale.

(B) Southern blot analysis. 1, WT diploid strain lacking the *hisG-URA3-hisG* construct; 2, WT diploid strain containing one inserted construct at the specified locus; 3-6 and 7-10, four representative 5-FOA-resistant haploid and diploid mutants, respectively, that resulted from growth conditions described in detail in the text. Known sizes of DNA markers (in kb) are shown on the left hand side and are approximate only.

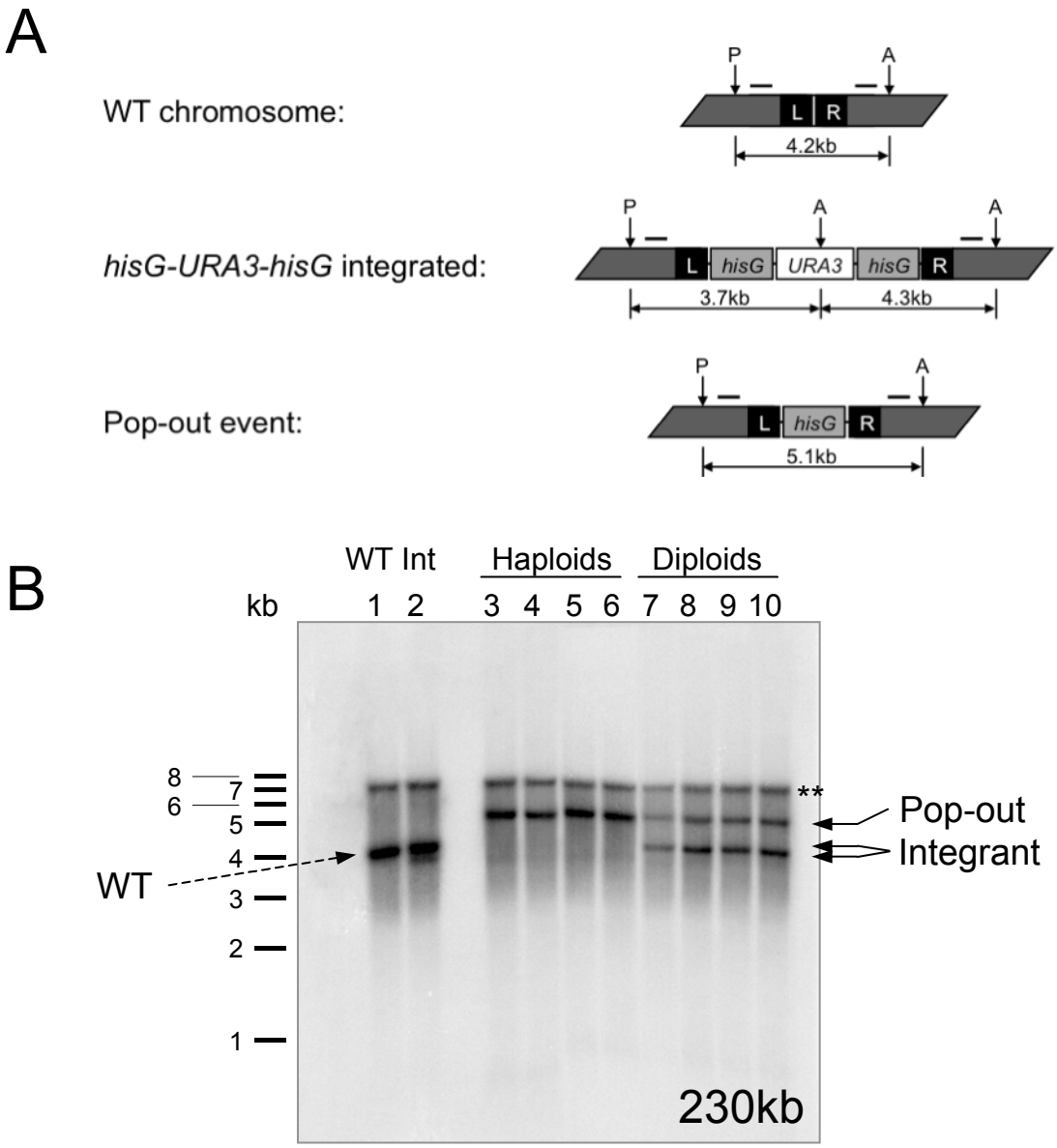

Figure 9.6. Effects of *hisG-URA3-hisG* insertion locations on incidence of pop-out events.

Nature of genetic alterations associated with the acquisition of 5-FOA-resistance in strains containing *hisG-URA3-hisG* at 230kb.

(A) Schematic presentation of DNA structures resolved using probes upstream and downstream (dashed lines) of the integration site. The upper cartoon shows the DNA before insertion of the construct, the middle one shows an integrated *hisG-URA3-hisG* construct and the lower cartoon shows the expected DNA size(s) if a pop-out event has occurred. "L" and "R" are the ~500bp sequences that flank the insertion point. Bold lines indicate the position of 0.5kb probes used for the analysis. Vertical arrows mark relevant RE sites. A, *Apa*I; P, *Pme*I. Drawings are not to scale.

(B) Southern blot analysis. 1, WT diploid strain lacking the *hisG-URA3-hisG* construct; 2, WT diploid strain containing one inserted construct at the specified locus; 3-6 and 7-10, four representative 5-FOA-resistant haploid and diploid mutants, respectively, that resulted from growth conditions described in detail in the text. Known sizes of DNA markers (in kb) are shown on the left hand side and are approximate only. **; non-specific band (Chapter 3).

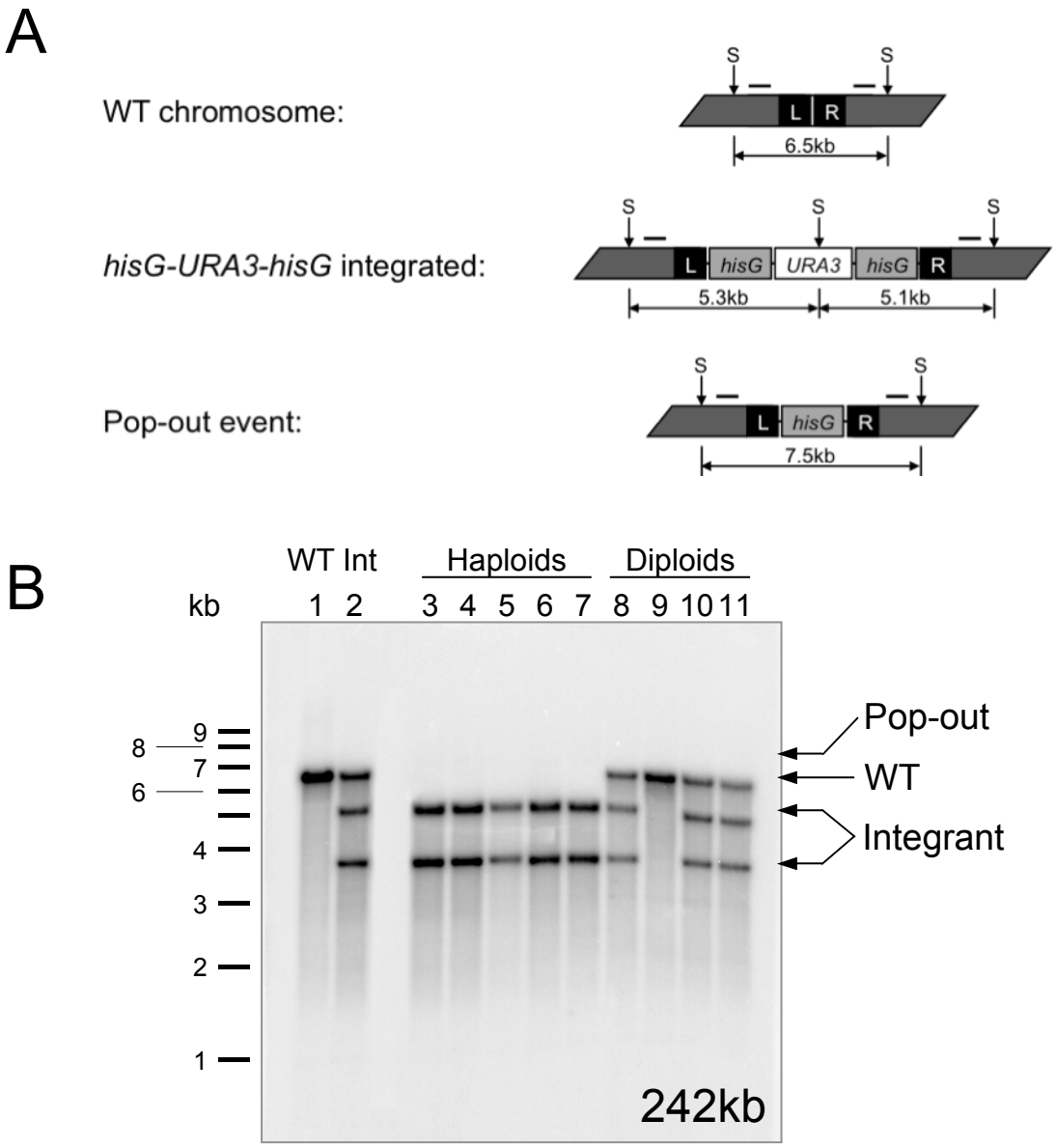

Figure 9.7. Effects of *hisG-URA3-hisG* insertion locations on incidence of pop-out events.

Nature of genetic alterations associated with the acquisition of 5-FOA-resistance in strains containing *hisG-URA3-hisG* at 242kb.

(A) Schematic presentation of DNA structures resolved using probes upstream and downstream (dashed lines) of the integration site. The upper cartoon shows the DNA before insertion of the construct, the middle one shows an integrated *hisG-URA3-hisG* construct and the lower cartoon shows the expected DNA size(s) if a pop-out event has occurred. "L" and "R" are the ~500bp sequences that flank the insertion point. Bold lines indicate the position of 0.5kb probes used for the analysis. Vertical arrows mark relevant RE sites. S, *Stu*I. Drawings are not to scale.

(B) Southern blot analysis. 1, WT diploid strain lacking the *hisG-URA3-hisG* construct; 2, WT diploid strain containing one inserted construct at the specified locus; 3-6 and 7-10, four representative 5-FOA-resistant haploid and diploid mutants, respectively, that resulted from growth conditions described in detail in the text. Known sizes of DNA markers (in kb) are shown on the left hand side and are approximate only.

For the 139kb locus (RSZ, replication termination, Ty2 element) no pop-out events were seen. All 5-FOA-resistant colonies shown in Figure 9.4B were due to Class I mutants in both haploid and diploid 139kb strains.

The 216kb locus showed two migrating bands for all haploid *ura3* colonies analysed. The size of these migrating bands (2.6 and 3.3kb) was predicted if the *URA3* gene and one *hisG* repeat were lost from a pop-out event ('Class III' mutants). Three bands were detected for all 216kb diploids tested, although the middle band was twice as intense as the slower and faster migrating bands. This was expected if the 2.6kb and 2.8kb bands were indistinguishable from each other: the 2.6kb band being from the right hand side of the DNA from a pop-out event, and the 2.8kb band from the right hand side of the WT chromosome. The WT 2.3kb fragment and 3.3kb pop-out fragment were clearly distinguishable. All 5-FOA-resistant colonies analysed for the 216kb locus were therefore the result of a pop-out event for both haploid and diploids. This was in marked contrast to the two previous loci that, incidentally, were also within replication termination zones.

The locus near to an active origin of DNA replication, 230kb, also had 100% of all analysed colonies being the result of pop-out events (Figure 9.6B). The loss of one band and size shift to 5.1kb in these mutants matched exactly with the expected sizes of bands migrating due to the DNA only having one *hisG* sequence left. (Of note is the non-specific band, which, as discussed originally in Chapter 3, was also present in strains not containing a *hisG-URA3-hisG* construct).

Finally, the 242kb locus, which contained no discernable chromosomal features, had no 5-FOA-resistant colonies being the result of pop-out events. All 242kb 5-FOA-resistant haploids were Class I mutants, as was the majority of diploids. One diploid Class II mutant is shown in Figure 9.3E.

Only the *hisG-URA3-hisG* constructs within the 216kb (replication termination) and 230kb (active origin) loci were able, therefore, to undergo pop-out events when grown in non-selective conditions at 30˚C. Constructs integrated within RSZs (53kb and 139kb) and in a region of no discernable chromosomal features (242kb) acquired

particular locus, since diploid strains grown in non-selective media at 30˚C had the majority of 5-FOA-resistant colonies due to small insertions and/or deletions within the *URA3* gene.

5-FOA-resistance either by small insertions/ deletions within the *URA3* gene (Class I mutants), or by loss of the entire region or chromosome containing the construct and flanking 500bp DNA sequences (Class II). One hundred percent of all 5-FOA-resistant haploid strains analysed with the construct integrated at the 53kb, 139kb or 242kb regions were Class I mutants. When 5-FOA-resistant colonies of the corresponding diploids were analysed, the vast majority were Class I mutants, whilst a small proportion were Class II. For the 53kb locus, this was the same result achieved when strains were grown in non-selective conditions at 30˚C using the fluctuation analysis incubation times. As loss of the *URA3* gene and one *hisG* sequence was only possible at two of the five loci, this suggests that, for some reason, pop-out events are regulated at the *cis* level. A summary of both types of Southern blot analysis is shown in Table 9.3.

9.3 Discussion

As one of the aims of this project was to analyse genetic instability within RSZs, the 53kb locus (RSZ, replication termination) was chosen as well as the 242kb locus (containing no discernable chromosomal features) for detailed analysis of their 5-FOA-resistant colonies arising from the specific growth conditions used for fluctuation analysis. It was a surprise result that no pop-out events were observed at either locus under all the conditions tested. This was true regardless of ploidy. Acquisition of 5-FOA-resistance was likely due to small insertions and/or deletions within the *URA3* gene (Class I mutations) for 100% of all haploids tested for both loci. In diploid strains Class I mutations were also evident, yet a notable fraction of 5-FOA-resistant colonies were due to loss of the entire region/ chromosome containing the *hisG-URA3-hisG* construct (Class II mutations). Class II mutations may also have occurred within haploid strains but these would not have been observed due to loss of essential genes that resulted in cell death.

Table 9.3 Summary of Southern blot analyses of haploid and diploid 5-FOA-resistant colonies.

		5-FOA-resistance			
Location	*Ploidy*	*Class I*	*Class II*	*Class III*	*TOTAL*
53kb	Haploid	141 (100%)	0	0	141
	Diploid	123 (69%)	57 (31%)	0	180
139kb	Haploid	4 (100%)	0	0	4
	Diploid	4 (100%)	0	0	4
216kb	Haploid	0	0	4 (100%)	4
	Diploid	0	0	4 (100%)	4
230kb	Haploid	0	0	4 (100%)	4
	Diploid	0	0	4 (100%)	4
242kb	Haploid	145 (100%)	0	0	145
	Diploid	114 (62%)	70 (38%)	0	184

Class I mutants are the likely result of small changes in the *URA3* gene such as point mutations and/or small insertions/deletions that lead to its inactivation. Class II mutants are due to loss of the entire *hisG-URA3-hisG* construct (and flanking sequences) from its original integration point. Class III mutants are those that have acquired 5-FOA-resistance by pop-out events. The *"TOTAL"* column includes the data from Southern blot analyses in Figures 9.3-9.7.

It is possible that pop-out events occurred at a very low frequency (<1%) that was not detected by the Southern analysis. As past studies have observed that greater than 90% of 5-FOA-resistant colonies were due to pop-out events, however, it was evident that this was dramatically different for the 53kb and 242kb strains used in this thesis (Alani *et al*., 1987).

The growth conditions that resulted in pop-out events occurring from the earlier studies were therefore used and all five loci tested rather than just the 53kb and 242kb loci. Using these specific conditions, 100% of all haploid and diploid 216kb (replication termination) and 230kb (active replication origin) 5-FOA-resistant colonies were the result of pop-out events (Class III mutations). Once again, all 5-FOA-resistant haploid colonies from the 53kb and 242kb loci were found to be the result of Class I mutations, and 5-FOA-resistant diploids were the result of Class I and Class II mutations: this was also seen for the 139kb locus (RSZ, replication termination, Ty2 element).

It was interesting to see that when the *hisG-URA3-hisG* construct was inserted into three different replication termination sites (53kb, 139kb, 216kb) the acquisition of 5-FOA-resistance differed, since pop-out events were only observed at the 216kb locus. The construct therefore behaved differently in regions containing RSZs. Additionally, no pop-out events were observed in a region containing no discernable chromosomal features (242kb), but were at an active replication origin (230kb). Taken together, results presented here demonstrate that *cis*- and *trans*-acting factors affect the nature of genetic events leading to acquisition of 5-FOA-resistance from *hisG-URA3-hisG* constructs.

Chapter 10.

General Discussion

10.1 Preface

The overall aim of the project was to identify *cis* and *trans* factors that modulate mutagenesis within *S. cerevisiae*. With respect to *cis* factors, the potential involvement of five loci with notable, differing DNA replication features (RSZ, replication termination, an active origin of replication and no discernable features) was assessed. With respect to *trans* factors, the effects of the DNA processing enzymes Rrm3p and Top2p, and the essential checkpoint protein, Mec1p, were examined. The effects of ploidy, temperature, and the replication inhibitor HU on the mutation rates were also assessed. Specific findings are discussed below.

10.2 *Cis*-regulators of mutagenesis

10.2.1 Mutation rates

In an effort to minimise complications, only the rates of *URA3* inactivation in WT strains grown in optimal growth conditions are analysed here for any *cis*-specific effects. The mutation rates were fairly comparable amongst all five loci in both haploid and diploid strains. Although significant differences were observed in diploid strains, the greatest difference in mutation rate between the loci was still less than 3-fold. As such, no obvious mutational hotspot existed under these experimental conditions. These findings are consistent with work reported by Lichten and Haber (1989), where the rates of interchromosomal exchange at allelic sequences (recombination between sequences at the same location on parental homologues) or from intrachromosomal recombination (pop-out events) both varied less than 3-fold in five different loci, four of which were also within ChrIII. The results of these studies contrast with those of meiotic recombination, where the recombination rates

varied as much as ~40-fold and were highly location-dependent (Lichten *et al*., 1987).

Of particular note was that the highest mutation rates were not observed at loci within RSZs (53kb and 139kb), and thus RSZs are not inherently more mutagenic. This was surprising because it has been widely assumed that fragile sites are mutagenic. The current findings indicate that this is not the case.

RSZs and mammalian fragile sites are regions where replication forks stall and DSBs arise preferentially. The current findings therefore suggest that neither of these two events lead to mutagenesis. How can these results be explained? No one has actually measured the mutation rates at fragile sites either in mammals or in yeast. The fact that many oncogenic mutations are associated with mammalian fragile sites simply means that these mutations had been selected for the growth advantage they had offered, but doesn't say anything about whether they were more mutagenic to begin with. Also, a recent study has shown that not all stalled forks lead to recombination (Pryce *et al*., 2009).

In summary, no obvious *cis*-effects were seen with regards to the rates of *URA3* inactivation.

10.2.2 Mutagenic events

In contrast to the rates of *URA3* inactivation at different loci, the molecular events leading to acquisition of 5-FOA-resistance were strongly influenced by the location of the reporter construct within ChrIII. Pop-out events (loss of one *hisG* repeat and the *URA3* gene) were only observed at the loci at an active origin (230kb) and at a replication termination site not associated with a RSZ (216kb). The reason for this currently remains unknown.

Of note is the fact that, despite the lack of pop-out events at loci within RSZs (53kb and 139kb) and at the locus associated with no discernable chromosomal features (242kb), the mutation rates at these loci are comparable to the other loci. This

suggests that the loci within RSZs and at the no-feature region are more prone to accumulating small genetic changes than the origin or non-RSZ termination regions. A possibility is that the origin and termination regions utilise high fidelity DNA polymerases, whereas the rest of the genome is replicated by alternative DNA polymerases that are more error prone. Studies thus far have focused on the biochemical composition of replication forks at origins and termination sites but little is known about what may happen in between. In the last few years the number of known eukaryotic DNA polymerases has increased to at least 19 (reviewed in Hübscher *et al*., 2002). Many of these genes, when mutated, exhibit defects during normal growth. Perhaps a possibility is that these alternative polymerases are utilised for difficult-to-replicate regions such as RSZs, and, while they are more processive, they are also more error-prone.

10.3 *Trans*-regulators of mutagenesis

10.3.1. Mild replication inhibition by HU

Results showed that incubating both haploid and diploid strains in the presence of HU had the most dramatic fold-increase in mutation rates among all the potential *trans*-regulators examined here. In haploids, a uniform ~3-fold increase was seen with respect to the mutation rates of strains grown in YPD at 30˚C, whilst diploid strains had a higher yet more varied fold-increase. As such, none of the five loci tested in ChrIII were inherently more mutagenic than any other.

It might have been predicted that RSZs were more mutagenic in this growth condition, particularly since they are intrinsically slow-to-replicate regions and any additional inhibition of fork movement may increase fork stalling, potentially leading to an increase in DSBs. The current observations indicate that loci of preferred chromosome breakage do not necessarily correlate with increased mutagenesis.

The extent of mutagenic effects observed for HU in the current study is significantly lower than previously reported, where a 38-fold increase has been observed (Barbera and Petes, 2006). This could be due to the fact that a relatively low concentration of

HU was used here. Other factors such as the specific reporter construct used and/or the location of insertion might have had an effect.

10.3.2 Ploidy

Previous studies have shown that ploidy can modulate mutation rates. In this study ploidy also had differential effects on the rates of *URA3* inactivation, depending on the strain background or growth condition used.

Significantly higher rates of *URA3* inactivation were seen in diploid strains in both the *mec1Δ sml1Δ* and *rrm3Δ* backgrounds, compared to their respective haploids. The mutation rates in diploids were also significantly higher in optimal growth conditions (YPD at 30˚C) for the 230kb (origin) and 242kb (no features) loci, and when treated with 10mM HU for the 53kb (RSZ, termination), 230kb and 242kb loci. Analysis of the types of mutation resulting in *URA3* inactivation (previous section) showed that no Class II (large chromosomal deletion) mutations were observed in haploids. The increase in mutation rate in diploids compared to haploids in these cases may have been partly attributable to this fact alone. It cannot be ruled out that large chromosomal mutations did not occur in haploid strains, but, as discussed above, loss of essential genes would result in cell death and therefore these types of mutation would not be observed. Indeed, analysis of essential genes on ChrIII reveals that loss of just 10kb up- or downstream from any of the five loci studied in this thesis would result in the loss of at least one essential gene (*data not shown*). This thesis therefore confirms the notion that genomic rearrangements and/or deletions resulting from cellular stress are more tolerated in diploids, due to the presence of additional copies of essential genes on the WT chromosome or greater efficiencies of repair (Tourrette *et al*., 2007). Also in agreement with their findings, despite the large opportunity for genomic rearrangements in diploids, the rate of mutation is not necessarily higher than those found in haploids.

10.3.3 Temperature

As well as affecting protein function, temperature can induce several different types of DNA damage; including DNA strand breaks (Bridges *et al*., 1969; Lindahl and Nyberg, 1972; Woodcock and Grigg, 1972; Gomez and Sinskey, 1973). Although past studies have shown that the rates of mitotic recombination increase at higher temperatures at certain genomic loci, little data exists that compares the rates of mutation at different loci within the same strains. The results presented here have revealed that elevated temperatures can increase the mutation rates as much as ~6-fold at 37˚C compared to the rates at 30˚C in WT diploid cells grown in rich media. These increases in mutation rates were not uniform, similar to the result of diploids exposed to 10mM HU, suggesting that different *cis* sequences are more susceptible to elevated temperatures than others. For instance, the highest fold-increase was observed at the 216kb (replication termination) locus, whilst the 139kb (RSZ, termination, Ty2), 230kb (origin) and 242kb (no features) loci all had similar ~2-fold-increases. As well as these findings, certain *cis* effects were seen when WT strains were incubated at high temperature only for specified durations (i.e. using the *mec1-40*- and *top2-1*-specific incubation times), further suggesting that certain *cis* sequences studied in this thesis are more susceptible to changes in temperature than others. Currently the mechanism underlying these observations remains unknown.

10.3.4 MEC1

Inactivation of mammalian ATR leads to expression of CFSs, even in the lack of any other physiological stress (Casper *et al*., 2002). Lack of functional Mec1p, the budding yeast homologue of ATR, also results in fragility at specific regions (RSZs) within the genome. As well as this, replication is intrinsically slow through RSZs even in a *MEC1* background, and replication through CFSs is often hindered compared to replication through non-CFS regions. Together, these findings imply that yeast RSZs could be models for mammalian CFSs, despite the simpler level of organisation that exists in the much smaller yeast genome.

Currently, it is widely believed that fragile site expression leads to mutagenic events. In *mec1-40* strains it might have therefore been expected that the rates of *URA3* inactivation were significantly higher at the loci within RSZs, 53kb and 139kb, than in others. Regardless of ploidy, however, a uniform 2-3-fold increase in mutation rate was seen at all tested loci in *mec1-40* strains compared to WT strains. In conjunction with this, the 53kb (RSZ, termination) and 242kb (no discernible features) *mec1-40* 5-FOA-resistant colonies had near-identical proportions of Class I (small changes) to Class II (gross chromosomal changes) mutants (90:10 and 85:15, respectively). Both of these results suggest that transient inactivation of Mec1p *via* use of the *mec1-40* allele has more genomic-wide repercussions on mutagenesis, rather than solely at RSZs. This agrees with Cha and Kleckner's (2002) original proposal that Mec1p is required for progression of replication forks throughout the genome, but differs somewhat in that higher levels of replication intermediates are seen in RSZs than in non-RSZ regions, and thus higher mutation rates might have been expected for the 53kb locus than the 242kb locus. Regardless of this, however, the results presented here have shown that the increases in mutation rates were modest, being at most only ~3-fold.

One reason for the relative modest effect of *mec1-40* on mutation rates could be due to the fact that the cells were incubated at the restrictive temperature for only four hours, which was perhaps not long enough to confer the full consequence of Mec1p inactivation. Thus, as an independent means of assessing involvement of Mec1p, the rates of *URA3* inactivation were also assessed in *mec1Δ sml1Δ* strains. For diploid *mec1Δ sml1Δ* strains, a uniform 2-3-fold increase in mutation rate was observed for all loci, compared to the rates seen in *sml1Δ* strains. In haploid *mec1Δ sml1Δ* strains, however, no significant increase was seen, and the mutation rates actually decreased for the 216kb (termination) and 230kb (origin) loci, respective to the rates of *sml1Δ* strains. Such reduction in mutation rates associated with Mec1p loss is unexpected – currently the mechanism is unknown. Possibly, Mec1p's role in repair affects mutation rates at certain loci within the genome. In the *mec1Δ sml1Δ*, but not the *mec1-40* background, therefore, ploidy had a significant effect on genomic stability.

The extent of the mutagenic effects of Mec1p inactivation in both *mec1Δ* and *mec1-ts* strains were surprisingly modest. The current observations here differ significantly from previous ones, where inactivation of Mec1p has been linked repeatedly to greatly elevated mutation rates (Myung *et al*., 2001; Craven *et al*., 2002). The difference could be due to the nature of constructs utilised, the location of the genome where the reporter constructs were introduced, and/or other differences in the experimental designs. Note that the current findings suggest that loci within known replication stalling and/or chromosome breakage regions are not necessarily mutation hotspots in a *mec1* background.

10.3.5 SML1

Lack of functional Sml1 protein results in unregulated dNTP production that can result in small increases in mutation rates due to small base pair changes (Chabes *et al*., 1999), though *sml1Δ* does not directly affect replication fork rate progression *per se*. Small increases in mutation rate in the *sml1Δ* strains were also found in this thesis. Unexpectedly, however, small but significant decreases in mutation rate were observed at the 230kb (origin) and 242kb (no features) loci in diploid *sml1Δ* strains. The effect(s) of *sml1Δ* on mutagenesis therefore appears to be location-specific.

Also, the results of earlier studies have shown that increased mutation rates in *sml1Δ* strains are the result of small base changes. It might therefore be reasonable to predict that the majority of *sml1Δ* 5-FOA-resistant colonies would be due to point mutations or small insertions or deletions within the *URA3* gene. Thus, the majority of *ura3* colonies would be Class I mutants, where small changes within the gene (or promoter) inactivated the gene without disrupting the overall gross architecture of the *hisG-URA3-hisG* construct. Although this was true for the 53kb *sml1Δ* diploid strains, where 80% of analysed colonies were Class I mutants (similar to the result seen for WT strains grown at 30˚C), surprisingly, 100% of the 242kb *sml1Δ* diploid 5-FOA-resistant colonies were Class II mutants, and therefore were the result of deletions of the entire region or chromosome containing the reporter construct. The reason for this is unclear, but suggests that the nature of molecular events leading to 5-FOA-resistance is, again, influenced in a *cis*-specific manner.

10.3.6 RRM3

The replicative helicase Rrm3p was of particular interest to my lab since initial experiments found that *rrm3Δ* can suppress DSB formation within RSZs in haploid *mec1-ts* strains at the non-permissive temperature (Nadia Hashash, unpublished results). Thus, *rrm3Δ* may affect the rates of mutation within RSZs if DSBs formation was to correlate with mutagenicity. For diploid strains, the rates of *URA3* inactivation significantly increased at all five loci compared to their respective WT strains. These fold-increases were, like the HU-treated strains, not similar for each locus, and the two loci within RSZs did not have higher mutation rates than the other loci. Thus, RSZs are not inherently more mutagenic than the other loci tested under these experimental conditions. It might have been more prudent to test the rates of *URA3* inactivation in *rrm3Δ mec1-ts* strains as well, yet these strains have very slow growth phenotypes and as such would be unsuitable using the specific incubation times established at the start of this thesis.

In contrast to the results found in diploid strains, the mutation rates were statistically indistinguishable between *rrm3Δ* and WT haploid strains, suggesting that ploidy is an important factor in genomic instability for *rrm3Δ* strains.

10.3.7 TOP2

Top2p is required to relieve topological stress resulting from DNA replication amongst other processes such as transcription, recombination, and chromatin remodelling. Inactivating Top2p significantly reduces the levels of chromosome breakage within RSZs in a *mec1-ts* background at the restrictive temperature (Nadia Hashash, unpublished results). As with the *rrm3Δ mec1-ts* strains, use of *top2-1 mec1-ts* strains was unsuitable for fluctuation analysis due to rapid loss of cell viability of these strains upon exposure to non-permissive temperatures, so it could not be deduced if genetic instability is specifically affected at RSZs in this genetic background. Despite this, transient inactivation of Top2p had no effect on the mutation rates in haploid or diploid strains harbouring the *hisG-URA3-hisG* reporter construct compared to WT strains subjected to the same growth conditions. This is in

direct contrast to previous reports using *top2* strains (Christman *et al*., 1988; Sabourin *et al*., 2003). The lack of mutagenic effect here could be due to the possibility that topological strain and/or DNA damage that occurred from transient inactivation of Top2p may have been efficiently repaired as soon as cells regained WT Top2p function after being returned to the permissive temperature. Also, past studies have implied that loss of Top2p function only results in greatly elevated recombination rates within the repetitive rDNA gene cluster, not at other tandem arrays or dispersed repeats, perhaps suggesting why elevated recombination rates were not observed in this study (Christman *et al*., 1988).

10.4 Integration of all insights

Table 10.1 shows a summary of the mutation rates observed in haploid and diploid strains for all genotypes and/or conditions tested, with the exception of the "WT" strains grown using the *mec1-40* and *top2-1*-specific conditions (all of which were statistically indistinguishable from the mutation rates when grown in optimal conditions at 30˚C). The rates of *URA3* inactivation are normalised for each strain background/condition to the lowest mutation rate of all five loci, and are calculated separately for haploids and diploids.

As mentioned earlier and throughout this thesis, there is no readily identifiable pattern that can be deduced from this information that identifies, for instance, one particular locus being more fragile than any other. Both loci within RSZs, for instance, do not share the majority of the highest mutation rates. One interesting observation, however, is that the 139kb locus (RSZ, termination, Ty2) has the lowest mutation rates for 5/9 conditions at the diploid level, and, at the haploid level, the 230kb locus (origin) has the lowest mutation rates for 4/7 conditions. Perhaps surprisingly, the diploid 242kb (no features) strains have the highest mutation rates for the 10mM HU, *mec1-40* and *rrm3Δ* conditions. To see if loci that contain no identifiable chromosomal features have higher mutation rates than other loci (such as those in RSZs), perhaps it might be prudent to test another locus not associated with any chromosomal features. A locus within another well-studied chromosome, ChrVI, is currently being analysed for this purpose.

Condition/ genotype	53kb		139kb		216kb		230kb		242kb	
	Haploid	Diploid	Haploid	Diploid	Haploid	Diploid	Haploid	Diploid	Haploid	Diploid
WT, 23°C	ND	**1.6** (1.3)	ND	**1.6** (1.3)	ND	**1.2** (1.0)	ND	**1.8** (1.5)	ND	**1.8** (1.5)
WT, 30°C	**2.1** (1.1)	**1.9** (1.7)	**1.9** (1.1)	**1.4** (1.3)	**2.0** (1.1)	**1.1** (1.0)	**1.8** (1.0)	**3.0** (2.7)	**1.9** (1.1)	**3.3** (2.9)
WT, 37°C	ND	ND	ND	**3.7** (1.0)	ND	**6.4** (1.7)	ND	**6.2** (1.7)	ND	**6.9** (1.9)
10mM HU	**5.6** (1.4)	**8.9** (1.6)	**5.3** (1.3)	**5.6** (1.0)	**6.5** (1.6)	**6.2** (1.1)	**4.1** (1.0)	**8.6** (1.5)	**6.6** (1.6)	**9.6** (1.7)
sml1Δ	**2.0** (1.2)	**2.8** (1.8)	**1.8** (1.1)	**1.6** (1.0)	**2.4** (1.4)	**1.7** (1.1)	**2.1** (1.2)	**2.0** (1.3)	**1.7** (1.0)	**1.9** (1.2)
mec1Δ sml1Δ	**2.3** (3.3)	**7.3** (2.4)	**1.2** (1.7)	**3.1** (1.0)	**0.7** (1.0)	**3.9** (1.3)	**0.8** (1.1)	**5.1** (1.6)	**1.4** (2.0)	**6.0** (1.9)
mec1-40	**5.3** (1.4)	**5.1** (1.1)	**6.3** (1.7)	**5.7** (1.2)	ND	**4.7** (1.0)	**3.8** (1.0)	**5.2** (1.1)	**4.8** (1.3)	**9.4** (2.0)
rrm3Δ	**2.1** (1.9)	**5.3** (1.7)	**1.6** (1.5)	**3.2** (1.0)	**1.1** (1.0)	**6.5** (2.0)	**1.5** (1.4)	**1.9** (6.0)	**1.1** (1.0)	**6.7** (2.1)
top2-1	**4.0** (1.8)	**2.9** (1.1)	**3.5** (1.6)	**3.3** (1.2)	ND	**3.8** (1.4)	**2.2** (1.0)	**2.6** (1.0)	**3.0** (1.3)	**3.2** (1.2)

Table 10.1. Summary table of average mutation rates derived from fluctuation analyses.

Numbers in bold represent the average mutation rates (x 10^{-5}) for the genotype/growth condition concerned. Numbers in parentheses represent the *cis*-specific variation, normalised to the lowest mutation rate out of all five loci ("1.0" by definition) . "WT" in this instance refers to strains containing one integrated *hisG-URA3-hisG* reporter construct. All diploid strains are heterozygous for the construct. ND: not determined.

It was unexpected that a locus within a RSZ would have the majority of the lowest mutation rates, since fragile sites are presumed to be inherently more mutagenic than non-fragile site regions. Of note, however, is that Table 10.1 does not indicate the 95% CL values, or if any of the mutation rates differ statistically from each other, so the data presented in Table 10.1 could be misleading. For detailed statistical analysis, see the relevant figures in the previous results chapters.

Also of note is that there is no correlation between the observed mutation rates and the incidence of pop-out events, which only occur at the 216kb and 230kb loci. Currently the reason(s) for why only these two loci are able to undergo pop-out events is unknown.

10.5 Possible mechanisms that can result in fragility

No mechanisms of how fragility was generated at the five different loci have been discussed in this thesis. Comparisons with other known fragile sites do not resemble the situation in the *hisG-URA3-hisG*-containing strains used in this thesis. For instance, expansion of microsatellite repeats in mammalian rare fragile sites is not a representative model of inactivating *URA3*, since the 5-FOA-resistant colonies that emerged from the fluctuation analysis procedure were the result of either a) pop-out events (by SSA or HRR) or b) small insertions and/or deletions that preserve the gross architecture of the *hisG-URA3-hisG* construct. Similarly, proposed models by Lemoine and colleagues (2005) investigating fragility at a site containing inverted repeats, or findings that large deletions are generated within mammalian common sites after replication stress, do not match the situation found here either.

Some of the most dramatic results found from this thesis were that the rates of *URA3* inactivation were only increased significantly in the *rrm3Δ* and *mec1Δ sml1Δ* diploid strains, not haploids. One possible explanation for how ploidy can affect the type of *URA3* inactivation seen in haploids and diploids is the suppression of NHEJ in diploids: *NEJ1* is the haploid-specific gene responsible for limiting the action of NHEJ to haploid cells (Kegel *et al*., 2001; Valencia *et al*., 2001). Repair of DSBs in diploids would therefore occur predominantly by HRR mechanisms. It might

therefore be reasonable to assume that increased levels of ectopic recombination in the *hisG-URA3-hisG* strains may result in loss of the region containing the construct, which – as discussed earlier – would also be tolerated more so in diploids than in haploids. This difference between haploids and diploids cannot, however, account for why using the *mec1-40* temperature sensitive allele resulted in 2-3-fold increases for all five loci in both haploid and diploid strains, or why only the 216kb and 230kb loci were able to undergo pop-out events. Ploidy was therefore an important factor in mutagenesis in some, but not all, cases.

I am therefore proposing that the *cis* sequences at the 216kb and 230kb loci are responsible for pop-out events, either directly (chromosome structure) or indirectly (binding of an as yet unidentified protein, for instance). As no detailed Southern blot analyses were performed in these strains in the *rrm3Δ*, *mec1Δ sml1Δ* or *mec1-40* genetic backgrounds, it remains to be seen if the mode of inactivation of *URA3* is modified in the functional absence of these proteins.

For the other three loci, a simple model of *URA3* inactivation is proposed in Figure 10.1.

10.6 Future directions

There are numerous questions that have not been answered in this thesis that need to be addressed. One important one is if replication through the two studied RSZs (53kb and 139kb) is still slow in the presence of the *hisG-URA3-hisG* cassette: do RSZs still behave the same with the additional ~3.8kb sequence inserted in the middle of them? PFGE (pulsed-field gel electrophoresis) can easily identify DSBs in ChrIII (in *mec1-40* cells grown at the non-permissive temperature, for instance) to ensure breaks still form in the 53kb and 139kb strains. Slow replication through these loci can be detected *via* the use of DNA two-dimensional gel electrophoresis (for detailed methodology, see Brewer and Fangman, 1987 and Nawotka and Huberman, 1988). Another question is if the replication origin at 230kb is still active with the *hisG-URA3-hisG* cassette inserted less than 500bp away, which can also be detected by 2D gel electrophoresis.

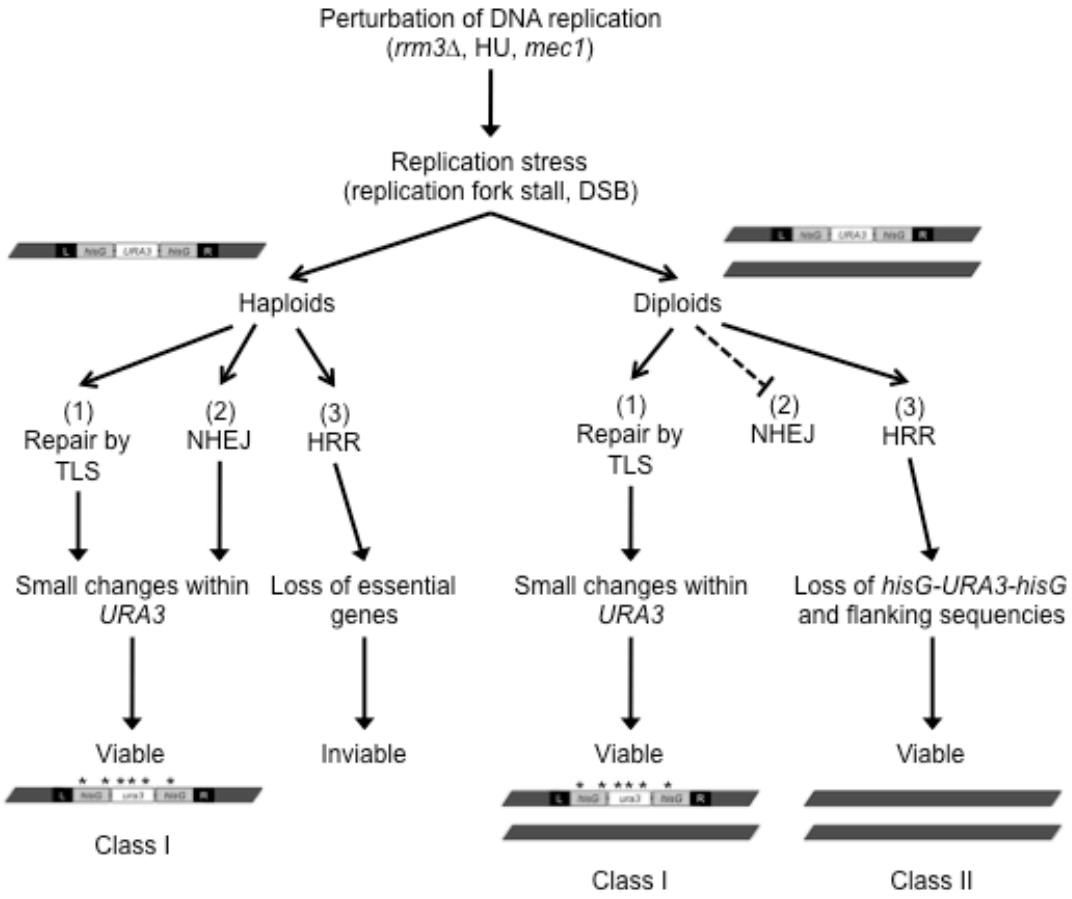

Figure 10.1. Modes of *URA3* inactivation in haploid and diploid strains for the 53kb, 139kb and 242kb loci.

Three primary ways in which *URA3* (within the *hisG-URA3-hisG* cassette) can be inactivated following DNA damage are shown: (1) repair by error-prone polymerases that generate errors within the coding region, including point mutations, frameshifts or small insertions/deletions; (2) repair by NHEJ; and (3) repair by homologous recombination repair (HRR) pathways. Class II mutations are only detected in diploid strains, since additional copies are present on the WT ChrIII. NHEJ is suppressed in diploid strains (see text). TLS: translesion synthesis; NHEJ: non-homologous end joining; HRR: homologous recombination repair. The asterix (*) denotes a small change within the DNA sequence.

Of interest are the different ways in which *URA3* is inactivated in haploids and diploids. In all haploid strains tested, 100% of the 5-FOA-resistant colonies were likely to be the result of small changes within the ORF or silencing of the region (Class I mutations). Currently, 5-FOA-resistant haploid strains are being sequenced to see if *URA3* has been inactivated by, for instance, small insertions or deletions, frameshifts, and so on. If no differences are observed between *ura3* in 5-FOA-resistant strains and *URA3* in 5-FOA-susceptible strains, the 5-FOA-resistant strains will then be examined to see if silencing of the gene (by Sir2p, for instance) is the mechanism of acquiring 5-FOA-resistance. As well as this, Class II 5-FOA-resistant diploid strains will be analysed in more detail to see if loss of the region or entire chromosome was the cause of losing the *URA3* gene and flanking sequences.

To test if ploidy or the expression of both mating type genes are factors contributing to the different classes of mutations observed in haploids verses diploids, haploid strains expressing both mating type loci could be used. These strains will not mate and, although they will not be able to successfully sporulate, will behave essentially as diploid cells. Additionally, if ploidy was exerting its effect *via* its regulation of NHEJ, this may be detected by sequencing of the *ura3* allele in FOA-resistant colonies arising from fluctuation analysis due to small deletions occurring at the initial break point.

The results of Chapter 9 revealed that pop-out events only occurred at the 216kb (termination) and 230kb (origin) loci. Whilst extensive analyses were performed on the 53kb and 242kb loci, they were not for the other three, where strains were only directly patched from non-selective agar media plates onto 5-FOA plates, rather than going through the liquid phase that the fluctuation analysis procedure dictated. The 5-FOA-resistant colonies that have arisen from 139kb, 216kb and 230kb strains subjected to the fluctuation analysis procedure will therefore also be tested to confirm that pop-outs are or are not possible. To see if the type of *URA3* inactivation is the same when colonies are subjected to the liquid phase, 5-FOA-resistant colonies arising from these strains are currently being analysed.

Finally, the mechanism by which pop-out events arise in the 216kb and 230kb strains has not been identified. As SSA occurs independently of Rad51p, assessing the 5-FOA-resistant colonies that arise from these strains in a *rad51Δ* background will determine if the "pop-out" events are the result of a recombination process other than SSA. If pop-out events still occur in the absence of Rad51p, these events would presumably be abolished/reduced in a *rad52Δ* background, as Rad52p is required for all recombination processes.

10.7 Summary

All of the factors studied in this thesis generally had little *cis* effect on the rates of *URA3* inactivation. Certain *trans* factors, such as *rrm3Δ* and *mec1* strains, had stronger effects that were only observed in diploid strains, emphasising the importance of ploidy as a factor in mutagenesis. One of the strong findings of the work presented here is that known sites of DNA fragility, RSZs, do not correlate with increased levels of recombination or mutagenicity.

References

Abraham, R.T. 2001. Cell cycle checkpoint signaling through the ATM and ATR kinases. *Genes Dev* 15(17): 2177-2196.

Admire, A., Shanks, L., Danzl, N., Wang, M., Weier, U., Stevens, W., Hunt, E., and Weinert, T. 2006. Cycles of chromosome instability are associated with a fragile site and are increased by defects in DNA replication and checkpoint controls in yeast. *Genes Dev* 20(2): 159-173.

Alani, E., Cao, L., and Kleckner, N. 1987. A method for gene disruption that allows repeated use of URA3 selection in the construction of multiply disrupted yeast strains. *Genetics* 116(4): 541-545.

Alsbeih, G. and Raaphorst, G.P. 1999. Differential induction of premature chromosome condensation by calyculin A in human fibroblast and tumor cell lines. *Anticancer Res* 19(2A): 903-908.

Arlt, M.F., Durkin, S.G., Ragland, R.L., and Glover, T.W. 2006. Common fragile sites as targets for chromosome rearrangements. *DNA Repair (Amst)* 5(9-10): 1126-1135.

Arlt, M.F., Miller, D.E., Beer, D.G., and Glover, T.W. 2002. Molecular characterization of FRAXB and comparative common fragile site instability in cancer cells. *Genes Chromosomes Cancer* 33(1): 82-92.

Arlt, M.F., Xu, B., Durkin, S.G., Casper, A.M., Kastan, M.B., and Glover, T.W. 2004. BRCA1 is required for common-fragile-site stability via its G2/M checkpoint function. *Mol Cell Biol* 24(15): 6701-6709.

Ashley, C.T., Jr. and Warren, S.T. 1995. Trinucleotide repeat expansion and human disease. *Annu Rev Genet* 29: 703-728.

Atkin, C.L., Thelander, L., Reichard, P., and Lang, G. 1973. Iron and free radical in ribonucleotide reductase. Exchange of iron and Mossbauer spectroscopy of the protein B2 subunit of the Escherichia coli enzyme. *J Biol Chem* 248(21): 7464-7472.

Azvolinsky, A., Dunaway, S., Torres, J.Z., Bessler, J.B., and Zakian, V.A. 2006. The S. cerevisiae Rrm3p DNA helicase moves with the replication fork and affects replication of all yeast chromosomes. *Genes Dev* 20(22): 3104-3116.

Barbera, M.A. and Petes, T.D. 2006. Selection and analysis of spontaneous reciprocal mitotic cross-overs in Saccharomyces cerevisiae. *Proc Natl Acad Sci U S A* 103(34): 12819-12824.

Bartek, J. and Lukas, J. 2003. Chk1 and Chk2 kinases in checkpoint control and cancer. *Cancer Cell* 3(5): 421-429.

Baudat, F. and Nicolas, A. 1997. Clustering of meiotic double-strand breaks on yeast chromosome III. *Proc Natl Acad Sci U S A* 94(10): 5213-5218.

Berger, J.M. 1998a. Structure of DNA topoisomerases. *Biochim Biophys Acta* 1400(1-3): 3-18.

Berger, J.M. 1998b. Type II DNA topoisomerases. *Curr Opin Struct Biol* 8(1): 26-32.

Bermejo, R., Doksani, Y., Capra, T., Katou, Y.M., Tanaka, H., Shirahige, K., and Foiani, M. 2007. Top1- and Top2-mediated topological transitions at replication forks ensure fork progression and stability and prevent DNA damage checkpoint activation. *Genes Dev* 21(15): 1921-1936.

Bierne, H., Ehrlich, S.D., and Michel, B. 1991. The replication termination signal terB of the Escherichia coli chromosome is a deletion hot spot. *Embo J* 10(9): 2699-2705.

Blat, Y. and Kleckner, N. 1999. Cohesins bind to preferential sites along yeast chromosome III, with differential regulation along arms versus the centric region. *Cell* 98(2): 249-259.

Boeke, J.D. and Chapman, K.B. 1991. Retrotransposition mechanisms. *Curr Opin Cell Biol* 3(3): 502-507.

Boeke, J.D., LaCroute, F., and Fink, G.R. 1984. A positive selection for mutants lacking orotidine-5'-phosphate decarboxylase activity in yeast: 5-fluoro-orotic acid resistance. *Mol Gen Genet* 197(2): 345-346.

Boldog, F., Gemmill, R.M., West, J., Robinson, M., Robinson, L., Li, E., Roche, J., Todd, S., Waggoner, B., Lundstrom, R., Jacobson, J., Mullokandov, M.R., Klinger, H., and Drabkin, H.A. 1997. Chromosome 3p14 homozygous deletions and sequence analysis of FRA3B. *Hum Mol Genet* 6(2): 193-203.

Borde, V., Wu, T.C., and Lichten, M. 1999. Use of a recombination reporter insert to define meiotic recombination domains on chromosome III of Saccharomyces cerevisiae. *Mol Cell Biol* 19(7): 4832-4842.

Boule, J.B. and Zakian, V.A. 2006. Roles of Pif1-like helicases in the maintenance of genomic stability. *Nucleic Acids Res* 34(15): 4147-4153.

Brewer, B.J. and Fangman, W.L. 1987. The localization of replication origins in ARS plasmids in S. cerevisiae. *Cell* **51**: 463-471.

Bridges, B.A., Ashwood-Smith, M.J., and Munson, R.J. 1969. Susceptibility of mild thermal and of ionizing radiation damage to the same recovery mechanisms in Escherichia coli. *Biochem Biophys Res Commun* 35(2): 193-196.

Brown, E.J. and Baltimore, D. 2003. Essential and dispensable roles of ATR in cell cycle arrest and genome maintenance. *Genes Dev* 17(5): 615-628.

Caspari, T. 2000. How to activate p53. *Curr Biol* 10(8): R315-317.

Casper, A.M., Durkin, S.G., Arlt, M.F., and Glover, T.W. 2004. Chromosomal instability at common fragile sites in Seckel syndrome. *Am J Hum Genet* 75(4): 654-660.

Casper, A.M., Nghiem, P., Arlt, M.F., and Glover, T.W. 2002. ATR regulates fragile site stability. *Cell* 111(6): 779-789.

Cha, R.S. and Kleckner, N. 2002. ATR homolog Mec1 promotes fork progression, thus averting breaks in replication slow zones. *Science* 297(5581): 602-606.

Chabes, A., Domkin, V., and Thelander, L. 1999. Yeast Sml1, a protein inhibitor of ribonucleotide reductase. *J Biol Chem* 274(51): 36679-36683.

Chabes, A., Georgieva, B., Domkin, V., Zhao, X., Rothstein, R., and Thelander, L. 2003. Survival of DNA damage in yeast directly depends on increased dNTP levels allowed by relaxed feedback inhibition of ribonucleotide reductase. *Cell* 112(3): 391-401.

Chen, C. and Kolodner, R.D. 1999. Gross chromosomal rearrangements in Saccharomyces cerevisiae replication and recombination defective mutants. *Nat Genet* 23(1): 81-85.

Christman, M.F., Dietrich, F.S., and Fink, G.R. 1988. Mitotic recombination in the rDNA of S. cerevisiae is suppressed by the combined action of DNA topoisomerases I and II. *Cell* 55(3): 413-425.

Clarke, A.R., Purdie, C.A., Harrison, D.J., Morris, R.G., Bird, C.C., Hooper, M.L., and Wyllie, A.H. 1993. Thymocyte apoptosis induced by p53-dependent and independent pathways. *Nature* 362(6423): 849-852.

Cliby, W.A., Roberts, C.J., Cimprich, K.A., Stringer, C.M., Lamb, J.R., Schreiber, S.L., and Friend, S.H. 1998. Overexpression of a kinase-inactive ATR protein causes sensitivity to DNA-damaging agents and defects in cell cycle checkpoints. *EMBO J* 17(1): 159-169.

Company, M. and Errede, B. 1987. Cell-type-dependent gene activation by yeast transposon Ty1 involves multiple regulatory determinants. *Mol Cell Biol* 7(9): 3205-3211.

Coppeé, J.Y., Rieger, K.J., Kaniak, A., di Rago, J.P., Groudinsky, O., and Slonimski, P.P. 1996. PetCR46, a gene which is essential for respiration and integrity of the mitochondrial genome. *Yeast* 12(6): 577-582.

Coquelle, A., Pipiras, E., Toledo, F., Buttin, G., and Debatisse, M. 1997. Expression of fragile sites triggers intrachromosomal mammalian gene amplification and sets boundaries to early amplicons. *Cell* 89(2): 215-225.

Corbin, S., Neilly, M.E., Espinosa, R., 3rd, Davis, E.M., McKeithan, T.W., and Le Beau, M.M. 2002. Identification of unstable sequences within the common fragile site at 3p14.2: implications for the mechanism of deletions within fragile histidine triad gene/common fragile site at 3p14.2 in tumors. *Cancer Res* 62(12): 3477-3484.

Cortez, D., Guntuku, S., Qin, J., and Elledge, S.J. 2001. ATR and ATRIP: partners in checkpoint signaling. *Science* 294(5547): 1713-1716.

Cortez, D., Wang, Y., Qin, J., and Elledge, S.J. 1999. Requirement of ATM-dependent phosphorylation of brca1 in the DNA damage response to double-strand breaks. *Science* 286(5442): 1162-1166.

Craven, R.J., Greenwell, P.W., Dominska, M., and Petes, T.D. 2002. Regulation of genome stability by TEL1 and MEC1, yeast homologs of the mammalian ATM and ATR genes. *Genetics* 161(2): 493-507.

Craven, R.J. and Petes, T.D. 2000. Involvement of the checkpoint protein Mec1p in silencing of gene expression at telomeres in Saccharomyces cerevisiae. *Mol Cell Biol* 20(7): 2378-2384.

Denison, S.R., Callahan, G., Becker, N.A., Phillips, L.A., and Smith, D.I. 2003. Characterization of FRA6E and its potential role in autosomal recessive juvenile parkinsonism and ovarian cancer. *Genes Chromosomes Cancer* 38(1): 40-52.

DiNardo, S., Voelkel, K., and Sternglanz, R. 1984. DNA topoisomerase II mutant of Saccharomyces cerevisiae: topoisomerase II is required for segregation of daughter molecules at the termination of DNA replication. *Proc Natl Acad Sci U S A* 81(9): 2616-2620.

Dixon, W.J. and Massey, J., F. J. 1969. Introduction to Statistical Analysis. *McGraw-Hill Book Company*.

Dunham, M.J., Badrane, H., Ferea, T., Adams, J., Brown, P.O., Rosenzweig, F., and Botstein, D. 2002. Characteristic genome rearrangements in experimental evolution of Saccharomyces cerevisiae. *Proc Natl Acad Sci U S A* 99(25): 16144-16149.

Durkin, S.G., Arlt, M.F., Howlett, N.G., and Glover, T.W. 2006. Depletion of CHK1, but not CHK2, induces chromosomal instability and breaks at common fragile sites. *Oncogene* 25(32): 4381-4388.

Durkin, S.G. and Glover, T.W. 2007. Chromosome fragile sites. *Annu Rev Genet* 41: 169-192.

Durkin, S.G., Ragland, R.L., Arlt, M.F., Mulle, J.G., Warren, S.T., and Glover, T.W. 2008. Replication stress induces tumor-like microdeletions in FHIT/FRA3B. *Proc Natl Acad Sci U S A* 105(1): 246-251.

Durocher, D. and Jackson, S.P. 2001. DNA-PK, ATM and ATR as sensors of DNA damage: variations on a theme? *Curr Opin Cell Biol* **13**(2): 225-231.

Eklund, H., Uhlin, U., Farnegardh, M., Logan, D.T., and Nordlund, P. 2001. Structure and function of the radical enzyme ribonucleotide reductase. *Prog Biophys Mol Biol* **77**(3): 177-268.

El Achkar, E., Gerbault-Seureau, M., Muleris, M., Dutrillaux, B., and Debatisse, M. 2005. Premature condensation induces breaks at the interface of early and

late replicating chromosome bands bearing common fragile sites. *Proc Natl Acad Sci U S A* **102**(50): 18069-18074.

Elder, F.F. and Robinson, T.J. 1989. Rodent common fragile sites: are they conserved? Evidence from mouse and rat. *Chromosoma* **97**(6): 459-464.

Elledge, S.J. 1996. Cell cycle checkpoints: preventing an identity crisis. *Science* **274**(5293): 1664-1672.

Elledge, S.J., Zhou, Z., and Allen, J.B. 1992. Ribonucleotide reductase: regulation, regulation, regulation. *Trends Biochem Sci* **17**(3): 119-123.

Elledge, S.J., Zhou, Z., Allen, J.B., and Navas, T.A. 1993. DNA damage and cell cycle regulation of ribonucleotide reductase. *Bioessays* **15**(5): 333-339.

Errede, B., Cardillo, T.S., Sherman, F., Dubois, E., Deschamps, J., and Wiame, J.M. 1980. Mating signals control expression of mutations resulting from insertion of a transposable repetitive element adjacent to diverse yeast genes. *Cell* **22**(2 Pt 2): 427-436.

Evans, W.E. and Parry, J.M. 1972. The cross sensitivity to radiations, chemical mutagens and heat treatment of x-ray sensitive mutants of yeast. *Mol Gen Genet* **118**(3): 261-271.

Evans, W.E. and Parry, J.M. 1975. The genetic effects of elevated temperature in the yeast, Saccharomyces cerevisiae. *Heredity* **35**(3): 347-359.

Fasullo, M., Giallanza, P., Dong, Z., Cera, C., and Bennett, T. 2001. Saccharomyces cerevisiae rad51 mutants are defective in DNA damage-associated sister chromatid exchanges but exhibit increased rates of homology-directed translocations. *Genetics* **158**(3): 959-972.

Ferber, M.J., Eilers, P., Schuuring, E., Fenton, J.A., Fleuren, G.J., Kenter, G., Szuhai, K., Smith, D.I., Raap, A.K., and Brink, A.A. 2004. Positioning of cervical carcinoma and Burkitt lymphoma translocation breakpoints with respect to the human papillomavirus integration cluster in FRA8C at 8q24.13. *Cancer Genet Cytogenet* **154**(1): 1-9.

Ferguson, L.R. 1990. Mutagenic and recombinogenic consequences of DNA-repair inhibition during treatment with 1,3-bis(2-chloroethyl)-1-nitrosourea in Saccharomyces cerevisiae. *Mutat Res* **241**(4): 369-377.

Fishman-Lobell, J. and Haber, J.E. 1992. Removal of nonhomologous DNA ends in double-strand break recombination: the role of the yeast ultraviolet repair gene RAD1. *Science* **258**(5081): 480-484.

Fogel, S. and Welch, J.W. 1982. Tandem gene amplification mediates copper resistance in yeast. *Proc Natl Acad Sci U S A* **79**(17): 5342-5346.

Fu, Y.H., Kuhl, D.P., Pizzuti, A., Pieretti, M., Sutcliffe, J.S., Richards, S., Verkerk, A.J., Holden, J.J., Fenwick, R.G., Jr., Warren, S.T., and et al. 1991. Variation of the CGG repeat at the fragile X site results in genetic instability: resolution of the Sherman paradox. *Cell* **67**(6): 1047-1058.

Gacy, A.M., Goellner, G., Juranic, N., Macura, S., and McMurray, C.T. 1995. Trinucleotide repeats that expand in human disease form hairpin structures in vitro. *Cell* **81**(4): 533-540.

Gale, G.R. 1964. Effect of Hydroxyurea on the Incorporation of Thymidine into Ehrlich Ascites Tumor Cells. *Biochem Pharmacol* **13**: 1377-1382.

Gale, G.R., Kendall, S.M., McLain, H.H., and Dubois, S. 1964. Effect of Hydroxyurea on Pseudomonas Aeruginosa. *Cancer Res* **24**: 1012-1020.

Galli, A. and Schiestl, R.H. 1995. On the mechanism of UV and gamma-ray-induced intrachromosomal recombination in yeast cells synchronized in different stages of the cell cycle. *Mol Gen Genet* **248**(3): 301-310.

Galli, A. and Schiestl, R. H. 1996. Hydroxyurea induces recombination in dividing but not in G1 or G2 cell cycle arrested yeast cells. *Mutat Res* **354**(1): 69-75.

Garcia-Higuera, I., Kuang, Y., Naf, D., Wasik, J., and D'Andrea, A.D. 1999. Fanconi anemia proteins FANCA, FANCC, and FANCG/XRCC9 interact in a functional nuclear complex. *Mol Cell Biol* **19**(7): 4866-4873.

Gatchel, J.R. and Zoghbi, H.Y. 2005. Diseases of unstable repeat expansion: mechanisms and common principles. *Nat Rev Genet* **6**(10): 743-755.

Gatei, M., Zhou, B.B., Hobson, K., Scott, S., Young, D., and Khanna, K.K. 2001. Ataxia telangiectasia mutated (ATM) kinase and ATM and Rad3 related kinase mediate phosphorylation of Brca1 at distinct and overlapping sites. In vivo assessment using phospho-specific antibodies. *J Biol Chem* **276**(20): 17276-17280.

Gerton, J.L., DeRisi, J., Shroff, R., Lichten, M., Brown, P.O., and Petes, T.D. 2000. Inaugural article: global mapping of meiotic recombination hotspots and coldspots in the yeast Saccharomyces cerevisiae. *Proc Natl Acad Sci U S A* **97**(21): 11383-11390.

Giles, F.J. 2007. A new era for ribonucleoside reductase inhibition. *Leuk Res* **31**(9): 1163-1164.

Glover, T.W. 1981. FUdR induction of the X chromosome fragile site: evidence for the mechanism of folic acid and thymidine inhibition. *Am J Hum Genet* **33**(2): 234-242.

Glover, T.W., Berger, C., Coyle, J., and Echo, B. 1984. DNA polymerase alpha inhibition by aphidicolin induces gaps and breaks at common fragile sites in human chromosomes. *Hum Genet* **67**(2): 136-142.

Glover, T.W. and Stein, C.K. 1987. Induction of sister chromatid exchanges at common fragile sites. *Am J Hum Genet* **41**(5): 882-890.

Goda, N., Dozier, S.J., and Johnson, R.S. 2003. HIF-1 in cell cycle regulation, apoptosis, and tumor progression. *Antioxid Redox Signal* **5**(4): 467-473.

Gomez, R.F. and Sinskey, A.J. 1973. Deoxyribonucleic acid breaks in heated Salmonella typhimurium LT-2 after exposure to nutritionally complex media. *J Bacteriol* **115**(2): 522-528.

Goto, T. and Wang, J.C. 1984. Yeast DNA topoisomerase II is encoded by a single-copy, essential gene. *Cell* **36**(4): 1073-1080.

Greenwell, P.W., Kronmal, S.L., Porter, S.E., Gassenhuber, J., Obermaier, B., and Petes, T.D. 1995. TEL1, a gene involved in controlling telomere length in S. cerevisiae, is homologous to the human ataxia telangiectasia gene. *Cell* **82**(5): 823-829.

Grompe, M. and D'Andrea, A. 2001. Fanconi anemia and DNA repair. *Hum Mol Genet* **10**(20): 2253-2259.

Grushcow, J.M., Holzen, T.M., Park, K.J., Weinert, T., Lichten, M., and Bishop, D.K. 1999. Saccharomyces cerevisiae checkpoint genes MEC1, RAD17 and RAD24 are required for normal meiotic recombination partner choice. *Genetics* **153**(2): 607-620.

Gu, Y., Shen, Y., Gibbs, R.A., and Nelson, D.L. 1996. Identification of FMR2, a novel gene associated with the FRAXE CCG repeat and CpG island. *Nat Genet* **13**(1): 109-113.

Haber, J.E. and Leung, W.Y. 1996. Lack of chromosome territoriality in yeast: promiscuous rejoining of broken chromosome ends. *Proc Natl Acad Sci U S A* **93**(24): 13949-13954.

Hammond, E.M., Denko, N.C., Dorie, M.J., Abraham, R.T., and Giaccia, A.J. 2002. Hypoxia links ATR and p53 through replication arrest. *Mol Cell Biol* **22**(6): 1834-1843.

Hecht, F. and Glover, T.W. 1984. Cancer chromosome breakpoints and common fragile sites induced by aphidicolin. *Cancer Genet Cytogenet* **13**(2): 185-188.

Hellman, A., Rahat, A., Scherer, S.W., Darvasi, A., Tsui, L.C., and Kerem, B. 2000. Replication delay along FRA7H, a common fragile site on human chromosome 7, leads to chromosomal instability. *Mol Cell Biol* **20**(12): 4420-4427.

Henderson, S.T. and Petes, T.D. 1992. Instability of simple sequence DNA in Saccharomyces cerevisiae. *Mol Cell Biol* **12**(6): 2749-2757.

Hewett, D.R., Handt, O., Hobson, L., Mangelsdorf, M., Eyre, H.J., Baker, E., Sutherland, G.R., Schuffenhauer, S., Mao, J.I., and Richards, R.I. 1998. FRA10B structure reveals common elements in repeat expansion and chromosomal fragile site genesis. *Mol Cell* **1**(6): 773-781.

Hirao, A., Kong, Y.Y., Matsuoka, S., Wakeham, A., Ruland, J., Yoshida, H., Liu, D., Elledge, S.J., and Mak, T.W. 2000. DNA damage-induced activation of p53 by the checkpoint kinase Chk2. *Science* **287**(5459): 1824-1827.

Hiraoka, M., Watanabe, K., Umezu, K., and Maki, H. 2000. Spontaneous loss of heterozygosity in diploid Saccharomyces cerevisiae cells. *Genetics* **156**(4): 1531-1548.

Horiuchi, T., Nishitani, H., and Kobayashi, T. 1995. A new type of E. coli recombinational hotspot which requires for activity both DNA replication termination events and the Chi sequence. *Adv Biophys* **31**: 133-147.

Howlett, N.G., Taniguchi, T., Durkin, S.G., D'Andrea, A.D., and Glover, T.W. 2005. The Fanconi anemia pathway is required for the DNA replication stress response and for the regulation of common fragile site stability. *Hum Mol Genet* **14**(5): 693-701.

Hubscher, U., Maga, G., and Spadari, S. 2002. Eukaryotic DNA polymerases. *Annu Rev Biochem* **71**: 133-163.

Huebner, K. and Croce, C.M. 2001. FRA3B and other common fragile sites: the weakest links. *Nat Rev Cancer* **1**(3): 214-221.

Hunter, T. 1995. When is a lipid kinase not a lipid kinase? When it is a protein kinase. *Cell* **83**(1): 1-4.

Ivessa, A.S., Lenzmeier, B.A., Bessler, J.B., Goudsouzian, L.K., Schnakenberg, S.L., and Zakian, V.A. 2003. The Saccharomyces cerevisiae helicase Rrm3p facilitates replication past nonhistone protein-DNA complexes. *Mol Cell* **12**(6): 1525-1536.

Durocher, D. and Jackson, S.P. 2001. DNA-PK, ATM and ATR as sensors of DNA damage: variations on a theme? *Curr Opin Cell Biol* **13**(2): 225-231.

Eklund, H., Uhlin, U., Farnegardh, M., Logan, D.T., and Nordlund, P. 2001. Structure and function of the radical enzyme ribonucleotide reductase. *Prog Biophys Mol Biol* **77**(3): 177-268.

El Achkar, E., Gerbault-Seureau, M., Muleris, M., Dutrillaux, B., and Debatisse, M. 2005. Premature condensation induces breaks at the interface of early and late replicating chromosome bands bearing common fragile sites. *Proc Natl Acad Sci U S A* **102**(50): 18069-18074.

Elder, F.F. and Robinson, T.J. 1989. Rodent common fragile sites: are they conserved? Evidence from mouse and rat. *Chromosoma* **97**(6): 459-464.

Elledge, S.J. 1996. Cell cycle checkpoints: preventing an identity crisis. *Science* **274**(5293): 1664-1672.

Elledge, S.J., Zhou, Z., and Allen, J.B. 1992. Ribonucleotide reductase: regulation, regulation, regulation. *Trends Biochem Sci* **17**(3): 119-123.

Elledge, S.J., Zhou, Z., Allen, J.B., and Navas, T.A. 1993. DNA damage and cell cycle regulation of ribonucleotide reductase. *Bioessays* **15**(5): 333-339.

Errede, B., Cardillo, T.S., Sherman, F., Dubois, E., Deschamps, J., and Wiame, J.M. 1980. Mating signals control expression of mutations resulting from insertion

of a transposable repetitive element adjacent to diverse yeast genes. *Cell* **22**(2 Pt 2): 427-436.

Evans, W.E. and Parry, J.M. 1972. The cross sensitivity to radiations, chemical mutagens and heat treatment of x-ray sensitive mutants of yeast. *Mol Gen Genet* **118**(3): 261-271.

Evans, W.E. and Parry, J.M. 1975. The genetic effects of elevated temperature in the yeast, Saccharomyces cerevisiae. *Heredity* **35**(3): 347-359.

Fasullo, M., Giallanza, P., Dong, Z., Cera, C., and Bennett, T. 2001. Saccharomyces cerevisiae rad51 mutants are defective in DNA damage-associated sister chromatid exchanges but exhibit increased rates of homology-directed translocations. *Genetics* **158**(3): 959-972.

Ferber, M.J., Eilers, P., Schuuring, E., Fenton, J.A., Fleuren, G.J., Kenter, G., Szuhai, K., Smith, D.I., Raap, A.K., and Brink, A.A. 2004. Positioning of cervical carcinoma and Burkitt lymphoma translocation breakpoints with respect to the human papillomavirus integration cluster in FRA8C at 8q24.13. *Cancer Genet Cytogenet* **154**(1): 1-9.

Ferguson, L.R. 1990. Mutagenic and recombinogenic consequences of DNA-repair inhibition during treatment with 1,3-bis(2-chloroethyl)-1-nitrosourea in Saccharomyces cerevisiae. *Mutat Res* **241**(4): 369-377.

Fishman-Lobell, J. and Haber, J.E. 1992. Removal of nonhomologous DNA ends in double-strand break recombination: the role of the yeast ultraviolet repair gene RAD1. *Science* **258**(5081): 480-484.

Fogel, S. and Welch, J.W. 1982. Tandem gene amplification mediates copper resistance in yeast. *Proc Natl Acad Sci U S A* **79**(17): 5342-5346.

Fu, Y.H., Kuhl, D.P., Pizzuti, A., Pieretti, M., Sutcliffe, J.S., Richards, S., Verkerk, A.J., Holden, J.J., Fenwick, R.G., Jr., Warren, S.T., and et al. 1991. Variation of the CGG repeat at the fragile X site results in genetic instability: resolution of the Sherman paradox. *Cell* **67**(6): 1047-1058.

Gacy, A.M., Goellner, G., Juranic, N., Macura, S., and McMurray, C.T. 1995. Trinucleotide repeats that expand in human disease form hairpin structures in vitro. *Cell* **81**(4): 533-540.

Gale, G.R. 1964. Effect of Hydroxyurea on the Incorporation of Thymidine into Ehrlich Ascites Tumor Cells. *Biochem Pharmacol* **13**: 1377-1382.

Gale, G.R., Kendall, S.M., McLain, H.H., and Dubois, S. 1964. Effect of Hydroxyurea on Pseudomonas Aeruginosa. *Cancer Res* **24**: 1012-1020.

Galli, A. and Schiestl, R.H. 1995. On the mechanism of UV and gamma-ray-induced intrachromosomal recombination in yeast cells synchronized in different stages of the cell cycle. *Mol Gen Genet* **248**(3): 301-310.

Galli, A. and Schiestl, R.H. 1996. Hydroxyurea induces recombination in dividing but not in G1 or G2 cell cycle arrested yeast cells. *Mutat Res* **354**(1): 69-75.

Garcia-Higuera, I., Kuang, Y., Naf, D., Wasik, J., and D'Andrea, A.D. 1999. Fanconi anemia proteins FANCA, FANCC, and FANCG/XRCC9 interact in a functional nuclear complex. *Mol Cell Biol* **19**(7): 4866-4873.

Gatchel, J.R. and Zoghbi, H.Y. 2005. Diseases of unstable repeat expansion: mechanisms and common principles. *Nat Rev Genet* **6**(10): 743-755.

Gatei, M., Zhou, B.B., Hobson, K., Scott, S., Young, D., and Khanna, K.K. 2001. Ataxia telangiectasia mutated (ATM) kinase and ATM and Rad3 related kinase mediate phosphorylation of Brca1 at distinct and overlapping sites. In vivo assessment using phospho-specific antibodies. *J Biol Chem* **276**(20): 17276-17280.

Gerton, J.L., DeRisi, J., Shroff, R., Lichten, M., Brown, P.O., and Petes, T.D. 2000. Inaugural article: global mapping of meiotic recombination hotspots and coldspots in the yeast Saccharomyces cerevisiae. *Proc Natl Acad Sci U S A* **97**(21): 11383-11390.

Giles, F.J. 2007. A new era for ribonucleoside reductase inhibition. *Leuk Res* **31**(9): 1163-1164.

Glover, T.W. 1981. FUdR induction of the X chromosome fragile site: evidence for the mechanism of folic acid and thymidine inhibition. *Am J Hum Genet* **33**(2): 234-242.

Glover, T.W., Berger, C., Coyle, J., and Echo, B. 1984. DNA polymerase alpha inhibition by aphidicolin induces gaps and breaks at common fragile sites in human chromosomes. *Hum Genet* **67**(2): 136-142.

Glover, T.W. and Stein, C.K. 1987. Induction of sister chromatid exchanges at common fragile sites. *Am J Hum Genet* **41**(5): 882-890.

Goda, N., Dozier, S.J., and Johnson, R.S. 2003. HIF-1 in cell cycle regulation, apoptosis, and tumor progression. *Antioxid Redox Signal* **5**(4): 467-473.

Gomez, R.F. and Sinskey, A.J. 1973. Deoxyribonucleic acid breaks in heated Salmonella typhimurium LT-2 after exposure to nutritionally complex media. *J Bacteriol* **115**(2): 522-528.

Goto, T. and Wang, J.C. 1984. Yeast DNA topoisomerase II is encoded by a single-copy, essential gene. *Cell* **36**(4): 1073-1080.

Greenwell, P.W., Kronmal, S.L., Porter, S.E., Gassenhuber, J., Obermaier, B., and Petes, T.D. 1995. TEL1, a gene involved in controlling telomere length in S. cerevisiae, is homologous to the human ataxia telangiectasia gene. *Cell* **82**(5): 823-829.

Grompe, M. and D'Andrea, A. 2001. Fanconi anemia and DNA repair. *Hum Mol Genet* **10**(20): 2253-2259.

Grushcow, J.M., Holzen, T.M., Park, K.J., Weinert, T., Lichten, M., and Bishop, D.K. 1999. Saccharomyces cerevisiae checkpoint genes MEC1, RAD17 and

RAD24 are required for normal meiotic recombination partner choice. *Genetics* **153**(2): 607-620.

Gu, Y., Shen, Y., Gibbs, R.A., and Nelson, D.L. 1996. Identification of FMR2, a novel gene associated with the FRAXE CCG repeat and CpG island. *Nat Genet* **13**(1): 109-113.

Haber, J.E. and Leung, W.Y. 1996. Lack of chromosome territoriality in yeast: promiscuous rejoining of broken chromosome ends. *Proc Natl Acad Sci U S A* **93**(24): 13949-13954.

Hammond, E.M., Denko, N.C., Dorie, M.J., Abraham, R.T., and Giaccia, A.J. 2002. Hypoxia links ATR and p53 through replication arrest. *Mol Cell Biol* **22**(6): 1834-1843.

Hecht, F. and Glover, T.W. 1984. Cancer chromosome breakpoints and common fragile sites induced by aphidicolin. *Cancer Genet Cytogenet* **13**(2): 185-188.

Hellman, A., Rahat, A., Scherer, S.W., Darvasi, A., Tsui, L.C., and Kerem, B. 2000. Replication delay along FRA7H, a common fragile site on human chromosome 7, leads to chromosomal instability. *Mol Cell Biol* **20**(12): 4420-4427.

Henderson, S.T. and Petes, T.D. 1992. Instability of simple sequence DNA in Saccharomyces cerevisiae. *Mol Cell Biol* **12**(6): 2749-2757.

Hewett, D.R., Handt, O., Hobson, L., Mangelsdorf, M., Eyre, H.J., Baker, E., Sutherland, G.R., Schuffenhauer, S., Mao, J.I., and Richards, R.I. 1998. FRA10B structure reveals common elements in repeat expansion and chromosomal fragile site genesis. *Mol Cell* **1**(6): 773-781.

Hirao, A., Kong, Y.Y., Matsuoka, S., Wakeham, A., Ruland, J., Yoshida, H., Liu, D., Elledge, S.J., and Mak, T.W. 2000. DNA damage-induced activation of p53 by the checkpoint kinase Chk2. *Science* **287**(5459): 1824-1827.

Hiraoka, M., Watanabe, K., Umezu, K., and Maki, H. 2000. Spontaneous loss of heterozygosity in diploid Saccharomyces cerevisiae cells. *Genetics* **156**(4): 1531-1548.

Horiuchi, T., Nishitani, H., and Kobayashi, T. 1995. A new type of E. coli recombinational hotspot which requires for activity both DNA replication termination events and the Chi sequence. *Adv Biophys* **31**: 133-147.

Howlett, N.G., Taniguchi, T., Durkin, S.G., D'Andrea, A.D., and Glover, T.W. 2005. The Fanconi anemia pathway is required for the DNA replication stress response and for the regulation of common fragile site stability. *Hum Mol Genet* **14**(5): 693-701.

Hubscher, U., Maga, G., and Spadari, S. 2002. Eukaryotic DNA polymerases. *Annu Rev Biochem* **71**: 133-163.

Huebner, K. and Croce, C.M. 2001. FRA3B and other common fragile sites: the weakest links. *Nat Rev Cancer* **1**(3): 214-221.

Hunter, T. 1995. When is a lipid kinase not a lipid kinase? When it is a protein kinase. *Cell* **83**(1): 1-4.

Ivessa, A.S., Lenzmeier, B.A., Bessler, J.B., Goudsouzian, L.K., Schnakenberg, S.L., and Zakian, V.A. 2003. The Saccharomyces cerevisiae helicase Rrm3p facilitates replication past nonhistone protein-DNA complexes. *Mol Cell* **12**(6): 1525-1536.

Ivessa, A.S., Zhou, J.Q., Schulz, V.P., Monson, E.K., and Zakian, V.A. 2002. Saccharomyces Rrm3p, a 5' to 3' DNA helicase that promotes replication fork progression through telomeric and subtelomeric DNA. *Genes Dev* **16**(11): 1383-1396.

Ivessa, A.S., Zhou, J.Q., and Zakian, V.A. 2000. The Saccharomyces Pif1p DNA helicase and the highly related Rrm3p have opposite effects on replication fork progression in ribosomal DNA. *Cell* **100**(4): 479-489.

Jackson, J.A., Trevino, A.V., Herzig, M.C., Herman, T.S., and Woynarowski, J.M. 2003. Matrix attachment region (MAR) properties and abnormal expansion of AT island minisatellites in FRA16B fragile sites in leukemic CEM cells. *Nucleic Acids Res* **31**(21): 6354-6364.

Jacobs, P.A., Glover, T.W., Mayer, M., Fox, P., Gerrard, J.W., Dunn, H.G., and Herbst, D.S. 1980. X-linked mental retardation: a study of 7 families. *Am J Med Genet* **7**(4): 471-489.

Jensen, S., Redwood, C.S., Jenkins, J.R., Andersen, A.H., and Hickson, I.D. 1996. Human DNA topoisomerases II alpha and II beta can functionally substitute for yeast TOP2 in chromosome segregation and recombination. *Mol Gen Genet* **252**(1-2): 79-86.

Jessberger, R., Podust, V., Hubscher, U., and Berg, P. 1993. A mammalian protein complex that repairs double-strand breaks and deletions by recombination. *J Biol Chem* **268**(20): 15070-15079.

Joenje, H. and Patel, K.J. 2001. The emerging genetic and molecular basis of Fanconi anaemia. *Nat Rev Genet* **2**(6): 446-457.

Johnson, R.E., Henderson, S.T., Petes, T.D., Prakash, S., Bankmann, M., and Prakash, L. 1992. Saccharomyces cerevisiae RAD5-encoded DNA repair protein contains DNA helicase and zinc-binding sequence motifs and affects the stability of simple repetitive sequences in the genome. *Mol Cell Biol* **12**(9): 3807-3818.

Johnston, J.R. and Mortimer, R. 1967. Influence of temperature on recombination in yeast. *Heredity* **22**(2): 297-303.

Jordan, A. and Reichard, P. 1998. Ribonucleotide reductases. *Annu Rev Biochem* **67**: 71-98.

Kanda, R., Eguchi-Kasai, K., Itsukaichi, H., Mori, M., and Hayata, I. 1999. Chemically induced premature chromosome condensation in human

fibroblast cell lines: fundamental study for applications to the biodosimetry of local exposure. *Somat Cell Mol Genet* **25**(5-6): 317-325.

Kanellis, P., Gagliardi, M., Banath, J.P., Szilard, R.K., Nakada, S., Galicia, S., Sweeney, F.D., Cabelof, D.C., Olive, P.L., and Durocher, D. 2007. A screen for suppressors of gross chromosomal rearrangements identifies a conserved role for PLP in preventing DNA lesions. *PLoS Genet* **3**(8): e134.

Kato, R. and Ogawa, H. 1994. An essential gene, ESR1, is required for mitotic cell growth, DNA repair and meiotic recombination in Saccharomyces cerevisiae. *Nucleic Acids Res* **22**(15): 3104-3112.

Katou, Y., Kanoh, Y., Bando, M., Noguchi, H., Tanaka, H., Ashikari, T., Sugimoto, K., and Shirahige, K. 2003. S-phase checkpoint proteins Tof1 and Mrc1 form a stable replication-pausing complex. *Nature* **424**(6952): 1078-1083.

Kegel, A., Sjostrand, J.O., and Astrom, S.U. 2001. Nej1p, a cell type-specific regulator of nonhomologous end joining in yeast. *Curr Biol* **11**:1611–1617.

Keil, R.L. and McWilliams, A.D. 1993. A gene with specific and global effects on recombination of sequences from tandemly repeated genes in Saccharomyces cerevisiae. *Genetics* **135**(3): 711-718.

Kim, J.M., Vanguri, S., Boeke, J.D., Gabriel, A., and Voytas, D.F. 1998. Transposable elements and genome organization: a comprehensive survey of retrotransposons revealed by the complete Saccharomyces cerevisiae genome sequence. *Genome Res* **8**(5): 464-478.

Kim, S.T., Xu, B., and Kastan, M.B. 2002. Involvement of the cohesin protein, Smc1, in Atm-dependent and independent responses to DNA damage. *Genes Dev* **16**(5): 560-570.

Kitagawa, R., Bakkenist, C.J., McKinnon, P.J., and Kastan, M.B. 2004. Phosphorylation of SMC1 is a critical downstream event in the ATM-NBS1-BRCA1 pathway. *Genes Dev* **18**(12): 1423-1438.

Klein, F., Laroche, T., Cardenas, M.E., Hofmann, J.F., Schweizer, D., and Gasser, S.M. 1992. Localization of RAP1 and topoisomerase II in nuclei and meiotic chromosomes of yeast. *J Cell Biol* **117**(5): 935-948.

Klein, H.L. 2001. Mutations in recombinational repair and in checkpoint control genes suppress the lethal combination of srs2Delta with other DNA repair genes in Saccharomyces cerevisiae. *Genetics* **157**(2): 557-565.

Koc, A., Wheeler, L.J., Mathews, C.K., and Merrill, G.F. 2004. Hydroxyurea arrests DNA replication by a mechanism that preserves basal dNTP pools. *J Biol Chem* **279**(1): 223-230.

Krakoff, I.H., Brown, N.C., and Reichard, P. 1968. Inhibition of ribonucleoside diphosphate reductase by hydroxyurea. *Cancer Res* **28**(8): 1559-1565.

Krakoff, I.H., Savel, H., and Murphy, M.L. 1964. Phase Ii Studies of Hydroxyurea (Nsc-32065) in Adults: Clinical Evaluation. *Cancer Chemother Rep* **40**: 53-55.

Kremer, E.J., Pritchard, M., Lynch, M., Yu, S., Holman, K., Baker, E., Warren, S.T., Schlessinger, D., Sutherland, G.R., and Richards, R.I. 1991. Mapping of DNA instability at the fragile X to a trinucleotide repeat sequence p(CCG)n. *Science* **252**(5013): 1711-1714.

Krokan, H., Wist, E., and Krokan, R.H. 1981. Aphidicolin inhibits DNA synthesis by DNA polymerase alpha and isolated nuclei by a similar mechanism. *Nucleic Acids Res* **9**(18): 4709-4719.

Kronenberg, H.M., Vogel, T., and Goldberger, R.F. 1975. A new and highly sensitive assay for the ATP phosphoribosyltransferase that catalyzes the first step of histidine biosynthesis. *Anal Biochem* **65**(1-2): 380-388.

Kuo, M.T., Vyas, R.C., Jiang, L.X., and Hittelman, W.N. 1994. Chromosome breakage at a major fragile site associated with P-glycoprotein gene amplification in multidrug-resistant CHO cells. *Mol Cell Biol* **14**(8): 5202-5211.

Kupiec, M. and Petes, T.D. 1988. Allelic and ectopic recombination between Ty elements in yeast. *Genetics* **119**(3): 549-559.

Lakin, N.D. and Jackson, S.P. 1999. Regulation of p53 in response to DNA damage. *Oncogene* **18**(53): 7644-7655.

Lang, G.I. and Murray, A.W. 2008. Estimating the per-base-pair mutation rate in the yeast Saccharomyces cerevisiae. *Genetics* **178**(1): 67-82.

Le Beau, M.M., Rassool, F.V., Neilly, M.E., Espinosa, R., 3rd, Glover, T.W., Smith, D.I., and McKeithan, T.W. 1998. Replication of a common fragile site, FRA3B, occurs late in S phase and is delayed further upon induction: implications for the mechanism of fragile site induction. *Hum Mol Genet* **7**(4): 755-761.

Le Beau, M.M. and Rowley, J.D. 1984. Heritable fragile sites in cancer. *Nature* **308**(5960): 607-608.

Lea, D.E. and Coulson, C.A. 1949. The distribution of the numbers of mutants in bacterial populations. *Journal of Genetics* **49**: 264-285.

Lemoine, F.J., Degtyareva, N.P., Lobachev, K., and Petes, T.D. 2005. Chromosomal translocations in yeast induced by low levels of DNA polymerase a model for chromosome fragile sites. *Cell* **120**(5): 587-598.

Lengronne, A., Pasero, P., Bensimon, A., and Schwob, E. 2001. Monitoring S phase progression globally and locally using BrdU incorporation in TK(+) yeast strains. *Nucleic Acids Res* **29**(7): 1433-1442.

Lenski, R.E., Slatkin, M., and Ayala, F.J. 1989. Mutation and selection in bacterial populations: alternatives to the hypothesis of directed mutation. *Proc Natl Acad Sci U S A* **86**(8): 2775-2778.

Lichten, M., Borts, R.H., and Haber, J.E. 1987. Meiotic gene conversion and crossing over between dispersed homologous sequences occurs frequently in Saccharomyces cerevisiae. *Genetics* **115**(2): 233-246.

Lichten, M. and Haber, J.E. 1989. Position effects in ectopic and allelic mitotic recombination in Saccharomyces cerevisiae. *Genetics* **123**(2): 261-268.

Limongi, M.Z., Pelliccia, F., and Rocchi, A. 2003. Characterization of the human common fragile site FRA2G. *Genomics* **81**(2): 93-97.

Lin, F.L., Sperle, K., and Sternberg, N. 1990. Repair of double-stranded DNA breaks by homologous DNA fragments during transfer of DNA into mouse L cells. *Mol Cell Biol* **10**(1): 113-119.

Lindahl, T. and Nyberg, B. 1972. Rate of depurination of native deoxyribonucleic acid. *Biochemistry* **11**(19): 3610-3618.

Liu, Q., Guntuku, S., Cui, X.S., Matsuoka, S., Cortez, D., Tamai, K., Luo, G., Carattini-Rivera, S., DeMayo, F., Bradley, A., Donehower, L.A., and Elledge, S.J. 2000. Chk1 is an essential kinase that is regulated by Atr and required for the G(2)/M DNA damage checkpoint. *Genes Dev* **14**(12): 1448-1459.

Losada, A. and Hirano, T. 2005. Dynamic molecular linkers of the genome: the first decade of SMC proteins. *Genes Dev* **19**(11): 1269-1287.

Louarn, J., Cornet, F., Francois, V., Patte, J., and Louarn, J.M. 1994. Hyperrecombination in the terminus region of the Escherichia coli chromosome: possible relation to nucleoid organization. *J Bacteriol* **176**(24): 7524-7531.

Lovett, S.T., Drapkin, P.T., Sutera, V.A., Jr., and Gluckman-Peskind, T.J. 1993. A sister-strand exchange mechanism for recA-independent deletion of repeated DNA sequences in Escherichia coli. *Genetics* **135**(3): 631-642.

Lowe, S.W., Schmitt, E.M., Smith, S.W., Osborne, B.A., and Jacks, T. 1993. p53 is required for radiation-induced apoptosis in mouse thymocytes. *Nature* **362**(6423): 847-849.

Lowndes, N.F. and Murguia, J.R. 2000. Sensing and responding to DNA damage. *Curr Opin Genet Dev* **10**(1): 17-25.

Luria, S.E. and Delbruck, M. 1943. Mutations of Bacteria from Virus Sensitivity to Virus Resistance. *Genetics* **28**(6): 491-511.

Lydall, D., Nikolsky, Y., Bishop, D.K., and Weinert, T. 1996. A meiotic recombination checkpoint controlled by mitotic checkpoint genes. *Nature* **383**(6603): 840-843.

Lydall, D. and Weinert, T. 1995. Yeast checkpoint genes in DNA damage processing: implications for repair and arrest. *Science* **270**(5241): 1488-1491.

Mailand, N., Falck, J., Lukas, C., Syljuasen, R.G., Welcker, M., Bartek, J., and Lukas, J. 2000. Rapid destruction of human Cdc25A in response to DNA damage. *Science* **288**(5470): 1425-1429.

Maloney, D.H. and Fogel, S. 1987. Gene conversion, unequal crossing-over and mispairing at a non-tandem duplication during meiosis of Saccharomyces cerevisiae. *Curr Genet* **12**(1): 1-7.

Mathews, C.K. 2006. DNA precursor metabolism and genomic stability. *Faseb J* **20**(9): 1300-1314.

Mayer, V.W., Goin, C.J., and Zimmermann, F.K. 1986. Aneuploidy and other genetic effects induced by hydroxyurea in Saccharomyces cerevisiae. *Mutat Res* **160**(1): 19-26.

McAinsh, A.D., Scott-Drew, S., Murray, J.A., and Jackson, S.P. 1999. DNA damage triggers disruption of telomeric silencing and Mec1p-dependent relocation of Sir3p. *Curr Biol* **9**(17): 963-966.

Merrill, B.J. and Holm, C. 1999. A requirement for recombinational repair in Saccharomyces cerevisiae is caused by DNA replication defects of mec1 mutants. *Genetics* **153**(2): 595-605.

Meyn, M.S. 1993. High spontaneous intrachromosomal recombination rates in ataxia-telangiectasia. *Science* **260**(5112): 1327-1330.

Mills, K.D., Sinclair, D.A., and Guarente, L. 1999. MEC1-dependent redistribution of the Sir3 silencing protein from telomeres to DNA double-strand breaks. *Cell* **97**(5): 609-620.

Mishmar, D., Rahat, A., Scherer, S.W., Nyakatura, G., Hinzmann, B., Kohwi, Y., Mandel-Gutfroind, Y., Lee, J.R., Drescher, B., Sas, D.E., Margalit, H., Platzer, M., Weiss, A., Tsui, L.C., Rosenthal, A., and Kerem, B. 1998. Molecular characterization of a common fragile site (FRA7H) on human chromosome 7 by the cloning of a simian virus 40 integration site. *Proc Natl Acad Sci U S A* **95**(14): 8141-8146.

Morrow, D.M., Tagle, D.A., Shiloh, Y., Collins, F.S., and Hieter, P. 1995. TEL1, an S. cerevisiae homolog of the human gene mutated in ataxia telangiectasia, is functionally related to the yeast checkpoint gene MEC1. *Cell* **82**(5): 831-840.

Musio, A., Montagna, C., Mariani, T., Tilenni, M., Focarelli, M.L., Brait, L., Indino, E., Benedetti, P.A., Chessa, L., Albertini, A., Ried, T., and Vezzoni, P. 2005. SMC1 involvement in fragile site expression. *Hum Mol Genet* **14**(4): 525-533.

Myung, K., Chen, C., and Kolodner, R.D. 2001a. Multiple pathways cooperate in the suppression of genome instability in Saccharomyces cerevisiae. *Nature* **411**(6841): 1073-1076.

Myung, K., Datta, A., and Kolodner, R.D. 2001b. Suppression of spontaneous chromosomal rearrangements by S phase checkpoint functions in Saccharomyces cerevisiae. *Cell* **104**(3): 397-408.

Myung, K. and Kolodner, R.D. 2002. Suppression of genome instability by redundant S-phase checkpoint pathways in Saccharomyces cerevisiae. *Proc Natl Acad Sci U S A* **99**(7): 4500-4507.

Nawotka, K.A. and Huberman, J.A. 1988. Two-dimensional gel electrophoretic method for mapping DNA replicons. *Mol Cell Biol* **8**: 1408-1413.

Nghiem, P., Park, P.K., Kim, Y., Vaziri, C., and Schreiber, S.L. 2001. ATR inhibition selectively sensitizes G1 checkpoint-deficient cells to lethal premature chromatin condensation. *Proc Natl Acad Sci U S A* **98**(16): 9092-9097.

Nickoloff, J.A., Singer, J.D., Hoekstra, M.F., and Heffron, F. 1989. Double-strand breaks stimulate alternative mechanisms of recombination repair. *J Mol Biol* **207**(3): 527-541.

Niewmierzycka, A. and Clarke, S. 1999. S-Adenosylmethionine-dependent methylation in Saccharomyces cerevisiae. Identification of a novel protein arginine methyltransferase. *J Biol Chem* **274**(2): 814-824.

Nishitani, H., Hidaka, M., and Horiuchi, T. 1993. Specific chromosomal sites enhancing homologous recombination in Escherichia coli mutants defective in RNase H. *Mol Gen Genet* **240**(3): 307-314.

Nitiss, J.L., Liu, Y.X., and Hsiung, Y. 1993. A temperature sensitive topoisomerase II allele confers temperature dependent drug resistance on amsacrine and etoposide: a genetic system for determining the targets of topoisomerase II inhibitors. *Cancer Res* **53**(1): 89-93.

Nordlund, P. and Reichard, P. 2006. Ribonucleotide reductases. *Annu Rev Biochem* **75**: 681-706.

O'Driscoll, M., Ruiz-Perez, V.L., Woods, C.G., Jeggo, P.A., and Goodship, J.A. 2003. A splicing mutation affecting expression of ataxia-telangiectasia and Rad3-related protein (ATR) results in Seckel syndrome. *Nat Genet* **33**(4): 497-501.

Oberle, I., Rousseau, F., Heitz, D., Kretz, C., Devys, D., Hanauer, A., Boue, J., Bertheas, M., and Mandel, J. 1991. Instability of a 550-base pair DNA segment and abnormal methylation in fragile X syndrome. *Science* **252**(5009): 1097-1102.

Ohta, M., Inoue, H., Cotticelli, M.G., Kastury, K., Baffa, R., Palazzo, J., Siprashvili, Z., Mori, M., McCue, P., Druck, T., Croce, C.M., and Huebner, K. 1996. The FHIT gene, spanning the chromosome 3p14.2 fragile site and renal carcinoma-associated t(3;8) breakpoint, is abnormal in digestive tract cancers. *Cell* **84**(4): 587-597.

Pacek, M., Tutter, A.V., Kubota, Y., Takisawa, H., and Walter, J.C. 2006. Localization of MCM2-7, Cdc45, and GINS to the site of DNA unwinding during eukaryotic DNA replication. *Mol Cell* **21**(4): 581-587.

Palakodeti, A., Han, Y., Jiang, Y., and Le Beau, M.M. 2004. The role of late/slow replication of the FRA16D in common fragile site induction. *Genes Chromosomes Cancer* **39**(1): 71-76.

Pandita, T.K., Pathak, S., and Geard, C.R. 1995. Chromosome end associations, telomeres and telomerase activity in ataxia telangiectasia cells. *Cytogenet Cell Genet* **71**(1): 86-93.

Paques, F. and Haber, J.E. 1999. Multiple pathways of recombination induced by double-strand breaks in Saccharomyces cerevisiae. *Microbiol Mol Biol Rev* **63**(2): 349-404.

Parsell, D.A. and Lindquist, S. 1993. The function of heat-shock proteins in stress tolerance: degradation and reactivation of damaged proteins. *Annu Rev Genet* **27**: 437-496.

Pincheira, J., Bravo, M., Navarrete, M.H., Marcelain, K., Lopez-Saez, J.F., and de la Torre, C. 2001. Ataxia telangiectasia: G2 checkpoint and chromosomal damage in proliferating lymphocytes. *Mutagenesis* **16**(5): 419-422.

Plessis, A., Perrin, A., Haber, J.E., and Dujon, B. 1992. Site-specific recombination determined by I-SceI, a mitochondrial group I intron-encoded endonuclease expressed in the yeast nucleus. *Genetics* **130**(3): 451-460.

Poloumienko, A., Dershowitz, A., De, J., and Newlon, C.S. 2001. Completion of replication map of Saccharomyces cerevisiae chromosome III. *Mol Biol Cell* **12**(11): 3317-3327.

Popescu, N.C. and DiPaolo, J.A. 1989. Preferential sites for viral integration on mammalian genome. *Cancer Genet Cytogenet* **42**(2): 157-171.

Prado, F. and Aguilera, A. 2005. Impairment of replication fork progression mediates RNA polII transcription-associated recombination. *Embo J* **24**(6): 1267-1276.

Pryce, D.W., Ramayah, S., Jaendling, A., and McFarlane, R.J. 2009. Recombination at DNA replication fork barriers is not universal and is differentially regulated by Swi1. *Proc Natl Acad Sci U S A* **106**(12): 4770-4775.

Raghuraman, M.K., Winzeler, E.A., Collingwood, D., Hunt, S., Wodicka, L., Conway, A., Lockhart, D.J., Davis, R.W., Brewer, B.J., and Fangman, W.L. 2001. Replication dynamics of the yeast genome. *Science* **294**(5540): 115-121.

Rassool, F.V., McKeithan, T.W., Neilly, M.E., van Melle, E., Espinosa, R., 3rd, and Le Beau, M.M. 1991. Preferential integration of marker DNA into the chromosomal fragile site at 3p14: an approach to cloning fragile sites. *Proc Natl Acad Sci U S A* **88**(15): 6657-6661.

Ray, A., Siddiqi, I., Kolodkin, A.L., and Stahl, F.W. 1988. Intra-chromosomal gene conversion induced by a DNA double-strand break in Saccharomyces cerevisiae. *J Mol Biol* **201**(2): 247-260.

Reichard, P. 1988. Interactions between deoxyribonucleotide and DNA synthesis. *Annu Rev Biochem* **57**: 349-374.

Rich, T., Allen, R.L., and Wyllie, A.H. 2000. Defying death after DNA damage. *Nature* **407**(6805): 777-783.

Ried, K., Finnis, M., Hobson, L., Mangelsdorf, M., Dayan, S., Nancarrow, J.K., Woollatt, E., Kremmidiotis, G., Gardner, A., Venter, D., Baker, E., and Richards, R.I. 2000. Common chromosomal fragile site FRA16D sequence: identification of the FOR gene spanning FRA16D and homozygous deletions and translocation breakpoints in cancer cells. *Hum Mol Genet* **9**(11): 1651-1663.

Rieger, K.J., Kaniak, A., Coppee, J.Y., Aljinovic, G., Baudin-Baillieu, A., Orlowska, G., Gromadka, R., Groudinsky, O., Di Rago, J.P., and Slonimski, P.P. 1997. Large-scale phenotypic analysis--the pilot project on yeast chromosome III. *Yeast* **13**(16): 1547-1562.

Roca, J. 1995. The mechanisms of DNA topoisomerases. *Trends Biochem Sci* **20**(4): 156-160.

Roeder, G.S. and Fink, G.R. 1980. DNA rearrangements associated with a transposable element in yeast. *Cell* **21**(1): 239-249.

Roelants, F., Potier, S., Souciet, J.L., and de Montigny, J. 1995. Reactivation of the ATCase domain of the URA2 gene complex: a positive selection method for Ty insertions and chromosomal rearrangements in Saccharomyces cerevisiae. *Mol Gen Genet* **246**(6): 767-773.

Rothstein, R., Helms, C., and Rosenberg, N. 1987. Concerted deletions and inversions are caused by mitotic recombination between delta sequences in Saccharomyces cerevisiae. *Mol Cell Biol* **7**(3): 1198-1207.

Rudin, N. and Haber, J.E. 1988. Efficient repair of HO-induced chromosomal breaks in Saccharomyces cerevisiae by recombination between flanking homologous sequences. *Mol Cell Biol* **8**(9): 3918-3928.

Ruiz-Herrera, A., Garcia, F., Fronicke, L., Ponsa, M., Egozcue, J., Caldes, M.G., and Stanyon, R. 2004. Conservation of aphidicolin-induced fragile sites in Papionini (Primates) species and humans. *Chromosome Res* **12**(7): 683-690.

Sabourin, M., Nitiss, J.L., Nitiss, K.C., Tatebayashi, K., Ikeda, H., and Osheroff, N. 2003. Yeast recombination pathways triggered by topoisomerase II-mediated DNA breaks. *Nucleic Acids Res* **31**(15): 4373-4384.

Saibil, H.R. 2008. Chaperone machines in action. *Curr Opin Struct Biol* **18**(1): 35-42.

Sanchez, Y., Desany, B.A., Jones, W.J., Liu, Q., Wang, B., and Elledge, S.J. 1996. Regulation of RAD53 by the ATM-like kinases MEC1 and TEL1 in yeast cell cycle checkpoint pathways. *Science* **271**(5247): 357-360.

Santocanale, C. and Diffley, J.F. 1998. A Mec1- and Rad53-dependent checkpoint controls late-firing origins of DNA replication. *Nature* **395**(6702): 615-618.

Schneider, B.L., Seufert, W., Steiner, B., Yang, Q.H., and Futcher, A.B. 1995. Use of polymerase chain reaction epitope tagging for protein tagging in Saccharomyces cerevisiae. *Yeast* **11**(13): 1265-1274.

Schulz, V.P. and Zakian, V.A. 1994. The saccharomyces PIF1 DNA helicase inhibits telomere elongation and de novo telomere formation. *Cell* **76**(1): 145-155.

Schwartz, M., Zlotorynski, E., Goldberg, M., Ozeri, E., Rahat, A., le Sage, C., Chen, B.P., Chen, D.J., Agami, R., and Kerem, B. 2005. Homologous recombination and nonhomologous end-joining repair pathways regulate fragile site stability. *Genes Dev* **19**(22): 2715-2726.

Seckel, H.P. 1960. Concepts relating the pituitary growth hormone to somatic growth of the normal child. *AMA J Dis Child* **99**: 349-379.

Shiloh, Y. 1997. Ataxia-telangiectasia and the Nijmegen breakage syndrome: related disorders but genes apart. *Annu Rev Genet* **31**: 635-662.

Shiloh, Y. 2001. ATM (ataxia telangiectasia mutated): expanding roles in the DNA damage response and cellular homeostasis. *Biochem Soc Trans* **29**(Pt 6): 661-666.

Shiraishi, T., Druck, T., Mimori, K., Flomenberg, J., Berk, L., Alder, H., Miller, W., Huebner, K., and Croce, C.M. 2001. Sequence conservation at human and mouse orthologous common fragile regions, FRA3B/FHIT and Fra14A2/Fhit. *Proc Natl Acad Sci U S A* **98**(10): 5722-5727.

Sia, E.A., Kokoska, R.J., Dominska, M., Greenwell, P., and Petes, T.D. 1997. Microsatellite instability in yeast: dependence on repeat unit size and DNA mismatch repair genes. *Mol Cell Biol* **17**(5): 2851-2858.

Simchen, G., Idar, D., and Kassir, Y. 1976. Recombination and hydroxyurea inhibition of DNA synthesis in yeast meiosis. *Mol Gen Genet* **144**(1): 21-27.

Siprashvili, Z., Sozzi, G., Barnes, L.D., McCue, P., Robinson, A.K., Eryomin, V., Sard, L., Tagliabue, E., Greco, A., Fusetti, L., Schwartz, G., Pierotti, M.A., Croce, C.M., and Huebner, K. 1997. Replacement of Fhit in cancer cells suppresses tumorigenicity. *Proc Natl Acad Sci U S A* **94**(25): 13771-13776.

Sjogren, C. and Nasmyth, K. 2001. Sister chromatid cohesion is required for postreplicative double-strand break repair in Saccharomyces cerevisiae. *Curr Biol* **11**(12): 991-995.

Skryabin, K.G., Eldarov, M.A., Larionov, V.L., Bayev, A.A., Klootwijk, J., de Regt, V.C., Veldman, G.M., Planta, R.J., Georgiev, O.I., and Hadjiolov, A.A.

1984. Structure and function of the nontranscribed spacer regions of yeast rDNA. *Nucleic Acids Res* **12**(6): 2955-2968.

Smeets, D.F. and van de Klundert, F.A. 1990. Common fragile sites in man and three closely related primate species. *Cytogenet Cell Genet* **53**(1): 8-14.

Smith, P.P., Friedman, C.L., Bryant, E.M., and McDougall, J.K. 1992. Viral integration and fragile sites in human papillomavirus-immortalized human keratinocyte cell lines. *Genes Chromosomes Cancer* **5**(2): 150-157.

Soulie, J. and De Grouchy, J. 1981. A cytogenetic survey of 110 baboons (Papio cynocephalus). *Am J Phys Anthropol* **56**(2): 107-113.

Stone, D.M., Jacky, P.B., Hancock, D.D., and Prieur, D.J. 1991. Chromosomal fragile site expression in dogs: I. Breed specific differences. *Am J Med Genet* **40**(2): 214-222.

Stone, D.M., Stephens, K.E., and Doles, J. 1993. Folate-sensitive and aphidicolin-inducible fragile sites are expressed in the genome of the domestic cat. *Cancer Genet Cytogenet* **65**(2): 130-134.

Strumberg, D., Nitiss, J.L., Dong, J., Kohn, K.W., and Pommier, Y. 1999. Molecular analysis of yeast and human type II topoisomerases. Enzyme-DNA and drug interactions. *J Biol Chem* **274**(40): 28246-28255.

Strunnikov, A.V. and Jessberger, R. 1999. Structural maintenance of chromosomes (SMC) proteins: conserved molecular properties for multiple biological functions. *Eur J Biochem* **263**(1): 6-13.

Stubbe, J., Ge, J., and Yee, C.S. 2001. The evolution of ribonucleotide reduction revisited. *Trends Biochem Sci* **26**(2): 93-99.

Sugawara, N. and Haber, J.E. 1992. Characterization of double-strand break-induced recombination: homology requirements and single-stranded DNA formation. *Mol Cell Biol* **12**(2): 563-575.

Sutherland, G.R. 1977. Fragile sites on human chromosomes: demonstration of their dependence on the type of tissue culture medium. *Science* **197**(4300): 265-266.

Sutherland, G.R. 1979. Heritable fragile sites on human chromosomes I. Factors affecting expression in lymphocyte culture. *Am J Hum Genet* **31**(2): 125-135.

Sutherland, G.R. 2003. Rare fragile sites. *Cytogenet Genome Res* **100**(1-4): 77-84.

Sutherland, G.R. and Baker, E. 2003. Forgotten fragile sites and related phenomena. *Cytogenet Genome Res* **100**(1-4): 89-91.

Sutherland, G.R., Baker, E., and Richards, R.I. 1998. Fragile sites still breaking. *Trends Genet* **14**(12): 501-506.

Szostak, J.W., Orr-Weaver, T.L., Rothstein, R.J., and Stahl, F.W. 1983. The double-strand-break repair model for recombination. *Cell* **33**(1): 25-35.

Takai, H., Tominaga, K., Motoyama, N., Minamishima, Y.A., Nagahama, H., Tsukiyama, T., Ikeda, K., Nakayama, K., Nakanishi, M., and Nakayama, K. 2000. Aberrant cell cycle checkpoint function and early embryonic death in Chk1(-/-) mice. *Genes Dev* **14**(12): 1439-1447.

Taniguchi, T., Garcia-Higuera, I., Andreassen, P.R., Gregory, R.C., Grompe, M., and D'Andrea, A.D. 2002. S-phase-specific interaction of the Fanconi anemia protein, FANCD2, with BRCA1 and RAD51. *Blood* **100**(7): 2414-2420.

Tercero, J.A. and Diffley, J.F. 2001. Regulation of DNA replication fork progression through damaged DNA by the Mec1/Rad53 checkpoint. *Nature* **412**(6846): 553-557.

Thelander, L. and Reichard, P. 1979. Reduction of ribonucleotides. *Annu Rev Biochem* **48**: 133-158.

Thomas, B.J. and Rothstein, R. 1989. The genetic control of direct-repeat recombination in Saccharomyces: the effect of rad52 and rad1 on mitotic recombination at GAL10, a transcriptionally regulated gene. *Genetics* **123**(4): 725-738.

Thompson, D.A., Desai, M.M., and Murray, A.W. 2006. Ploidy controls the success of mutators and nature of mutations during budding yeast evolution. *Curr Biol* **16**(16): 1581-1590.

Thrower, D.A. and Bloom, K. 2001. Dicentric chromosome stretching during anaphase reveals roles of Sir2/Ku in chromatin compaction in budding yeast. *Mol Biol Cell* **12**(9): 2800-2812.

Tibbetts, R.S., Cortez, D., Brumbaugh, K.M., Scully, R., Livingston, D., Elledge, S.J., and Abraham, R.T. 2000. Functional interactions between BRCA1 and the checkpoint kinase ATR during genotoxic stress. *Genes Dev* **14**(23): 2989-3002.

Timson, J. 1975. Hydroxyurea. *Mutat Res* **32**(2): 115-132.

Torres, J.Z., Schnakenberg, S.L., and Zakian, V.A. 2004. Saccharomyces cerevisiae Rrm3p DNA helicase promotes genome integrity by preventing replication fork stalling: viability of rrm3 cells requires the intra-S-phase checkpoint and fork restart activities. *Mol Cell Biol* **24**(8): 3198-3212.

Tourrette, Y., Schacherer, J., Fritsch, E., Potier, S., Souciet, J.L., and de Montigny, J. 2007. Spontaneous deletions and reciprocal translocations in Saccharomyces cerevisiae: influence of ploidy. *Mol Microbiol* **64**(2): 382-395.

Turner, G., Till, R., and Daniel, A. 1978. Marker X chromosomes, mental retardation and macro-orchidism. *N Engl J Med* **299**(26): 1472.

Umezu, K., Amaya, T., Yoshimoto, A., and Tomita, K. 1971. Purification and properties of orotidine-5'-phosphate pyrophosphorylase and orotidine-5'-phosphate decarboxylase from baker's yeast. *J Biochem* **70**(2): 249-262.

Umezu, K., Hiraoka, M., Mori, M., and Maki, H. 2002. Structural analysis of aberrant chromosomes that occur spontaneously in diploid Saccharomyces cerevisiae: retrotransposon Ty1 plays a crucial role in chromosomal rearrangements. *Genetics* **160**(1): 97-110.

Valencia, M., Bentele, M., Vaze, M.B., Herrmann, G., Kraus, E., Lee, S.E., Schar, P., and Haber, J.E. 2001. NEJ1 controls non-homologous end joining in Saccharomyces cerevisiae. *Nature* **414**:666–669.

Vassilev, L. and Russev, G. 1984. Hydroxyurea treatment does not prevent initiation of DNA synthesis in Ehrlich ascites tumour cells and leads to the accumulation of short DNA fragments containing the replication origins. *Biochim Biophys Acta* **781**(1-2): 39-44.

Verkerk, A.J., Pieretti, M., Sutcliffe, J.S., Fu, Y.H., Kuhl, D.P., Pizzuti, A., Reiner, O., Richards, S., Victoria, M.F., Zhang, F.P., and et al. 1991. Identification of a gene (FMR-1) containing a CGG repeat coincident with a breakpoint cluster region exhibiting length variation in fragile X syndrome. *Cell* **65**(5): 905-914.

Voegtli, W.C., Ge, J., Perlstein, D.L., Stubbe, J., and Rosenzweig, A.C. 2001. Structure of the yeast ribonucleotide reductase Y2Y4 heterodimer. *Proc Natl Acad Sci U S A* **98**(18): 10073-10078.

Walter, J. and Newport, J. 2000. Initiation of eukaryotic DNA replication: origin unwinding and sequential chromatin association of Cdc45, RPA, and DNA polymerase alpha. *Mol Cell* **5**(4): 617-627.

Wang, J.C. 1996. DNA topoisomerases. *Annu Rev Biochem* **65**: 635-692.

Wang, X., Watt, P.M., Louis, E.J., Borts, R.H., and Hickson, I.D. 1996. Part1: a topoisomerase II-associated protein required for faithful chromosome transmission in Saccharomyces cerevisiae. *Nucleic Acids Res* **24**(23): 4791-4797.

Warner, J.R. 1989. Synthesis of ribosomes in Saccharomyces cerevisiae. *Microbiol Rev* **53**(2): 256-271.

Weinert, T.A. and Hartwell, L.H. 1990. Characterization of RAD9 of Saccharomyces cerevisiae and evidence that its function acts posttranslationally in cell cycle arrest after DNA damage. *Mol Cell Biol* **10**(12): 6554-6564.

Weinert, T.A., Kiser, G.L., and Hartwell, L.H. 1994. Mitotic checkpoint genes in budding yeast and the dependence of mitosis on DNA replication and repair. *Genes Dev* **8**(6): 652-665.

Wierdl, M., Greene, C.N., Datta, A., Jinks-Robertson, S., and Petes, T.D. 1996. Destabilization of simple repetitive DNA sequences by transcription in yeast. *Genetics* **143**(2): 713-721.

Wilke, C.M., Guo, S.W., Hall, B.K., Boldog, F., Gemmill, R.M., Chandrasekharappa, S.C., Barcroft, C.L., Drabkin, H.A., and Glover, T.W.

1994. Multicolor FISH mapping of YAC clones in 3p14 and identification of a YAC spanning both FRA3B and the t(3;8) associated with hereditary renal cell carcinoma. *Genomics* **22**(2): 319-326.

Wilke, C.M., Hall, B.K., Hoge, A., Paradee, W., Smith, D.I., and Glover, T.W. 1996. FRA3B extends over a broad region and contains a spontaneous HPV16 integration site: direct evidence for the coincidence of viral integration sites and fragile sites. *Hum Mol Genet* **5**(2): 187-195.

Woodcock, E. and Grigg, G.W. 1972. Repair of thermally induced DNA breakage in Escherichia coli. *Nat New Biol* **237**(72): 76-79.

Xu, Y. and Baltimore, D. 1996. Dual roles of ATM in the cellular response to radiation and in cell growth control. *Genes Dev* **10**(19): 2401-2410.

Yang, M.Y. and Long, S.E. 1993. Folate sensitive common fragile sites in chromosomes of the domestic pig (Sus scrofa). *Res Vet Sci* **55**(2): 231-235.

Yazdi, P.T., Wang, Y., Zhao, S., Patel, N., Lee, E.Y., and Qin, J. 2002. SMC1 is a downstream effector in the ATM/NBS1 branch of the human S-phase checkpoint. *Genes Dev* **16**(5): 571-582.

Yunis, J.J. and Soreng, A.L. 1984. Constitutive fragile sites and cancer. *Science* **226**(4679): 1199-1204.

Zakian, V.A. 1995. ATM-related genes: what do they tell us about functions of the human gene? *Cell* **82**(5): 685-687.

Zanesi, N., Fidanza, V., Fong, L.Y., Mancini, R., Druck, T., Valtieri, M., Rudiger, T., McCue, P.A., Croce, C.M., and Huebner, K. 2001. The tumor spectrum in FHIT-deficient mice. *Proc Natl Acad Sci U S A* **98**(18): 10250-10255.

Zhang, C., Roberts, T.M., Yang, J., Desai, R., and Brown, G.W. 2006. Suppression of genomic instability by SLX5 and SLX8 in Saccharomyces cerevisiae. *DNA Repair (Amst)* **5**(3): 336-346.

Zhao, H. and Piwnica-Worms, H. 2001. ATR-mediated checkpoint pathways regulate phosphorylation and activation of human Chk1. *Mol Cell Biol* **21**(13): 4129-4139.

Zhao, X., Muller, E.G., and Rothstein, R. 1998. A suppressor of two essential checkpoint genes identifies a novel protein that negatively affects dNTP pools. *Mol Cell* **2**(3): 329-340.

Zhou, B.B. and Elledge, S.J. 2000. The DNA damage response: putting checkpoints in perspective. *Nature* **408**(6811): 433-439.

Zhou, J.Q., Qi, H., Schulz, V.P., Mateyak, M.K., Monson, E.K., and Zakian, V.A. 2002. Schizosaccharomyces pombe pfh1+ encodes an essential 5' to 3' DNA helicase that is a member of the PIF1 subfamily of DNA helicases. *Mol Biol Cell* **13**(6): 2180-2191.

Zimmermann, F.K. 1971. Induction of mitotic gene conversion by mutagens. *Mutat Res* **11**(3): 327-337.

Zlotorynski, E., Rahat, A., Skaug, J., Ben-Porat, N., Ozeri, E., Hershberg, R., Levi, A., Scherer, S.W., Margalit, H., and Kerem, B. 2003. Molecular basis for expression of common and rare fragile sites. *Mol Cell Biol* **23**(20): 7143-7151.

Acknowledgements

First and foremost, a huge thank you goes to Rita ("The Boss") for not only letting me start this PhD, but also for her time, effort, support and enthusiasm throughout. A lab's not complete without everyone else, though, so many thanks go towards Jesús for his advice, suggestions and farmyard noises in moments of dreariness, Nadia for showing me the ropes, helping me with pretty much every single aspect of the lab throughout the whole duration, especially for not getting fed up with endless "Is that a diploid?" questions and when I was armless for a month, and Tony "The Oracle" Johnson, a fellow Black Countrae lad who understood me from the very start… oh, and also had to put up with endless questions and help (but I think he likes it so I'm not going to worry about it too much). In the Yeast Genetics department, I must say thank you to Marco for helping devise the PCR-based cloning strategy so pivotal to this thesis, to Ad for putting so much time and effort into all those S-phase graphs that never even got into this thesis, and Gosia.

Huge thanks also to the people outside the lab who contributed in other ways, from the ever-present parents for morale (and financial) support, and especially to Marty & Romaana and Colin for allowing me to stay at the very end, without which I wouldn't have been able to finish.

Everyone else, you know who you are, and you all made it easier. Cheers.